UAB

Universitat Autònoma de Barcelona

OPTIMIZATION OF FLOW CYTOMETRY ASSAYS FOR THE DETECTION OF INJURED FOODBORNE PATHOGENIC BACTERIA

Alicia Subires Orenes

UAB

Universitat Autònoma de Barcelona

Facultat de Veterinària

Departament de Ciència Animal i dels Aliments

Doctoral thesis

OPTIMIZATION OF FLOW CYTOMETRY ASSAYS FOR THE DETECTION OF INJURED FOODBORNE PATHOGENIC BACTERIA

Alicia Subires Orenes

Bellaterra (Cerdanyola del Vallès), 2015

Josep Yuste Puigvert, professor agregat, i Marta Capellas Puig, professora titular del Departament de Ciència Animal i dels Aliments de la Universitat Autònoma de Barcelona,

fan constar que la llicenciada en Ciència i Tecnologia dels Aliments Alicia Subires Orenes ha dut a terme, sota la seva direcció, el treball titulat "Optimization of flow cytometry assays for the detection of injured foodborne pathogenic bacteria", que presenta per optar al grau de Doctor.

I perquè així consti, signem el present document a Bellaterra (Cerdanyola del Vallès), el 27 de juliol de 2015.

Josep Yuste Puigvert   Marta Capellas Puig

to find you in infinity of space and time
one must first divide and then combine

J. W. von Goethe

Agraïments

Als meus directors de tesi, la Marta i el Josep, dels qui he après tant durant aquests anys, per confiar en mi i en la meva capacitat per tirar la feina endavant, per la seva paciència i bons consells.

A la Manuela Costa, tècnica del servei de citometria de la UAB, per la seva amabilitat en tot moment i per iniciar-me en la citometria de flux.

I would like to acknowledge Dr. Tjakko Abee, who gave me the chance to work with his research group, and Dr. Maarten Mols, who gave me so many valuable lab tips.

A Manuela Hernández, por acogerme en su despacho estos últimos meses de redacción, por su buen humor, y por enseñarme tanto durante las prácticas del "workshop".

A la resta de gent del Departament: becaris, tècnics, professors. Uns ja han marxat, altres encara hi són, però a tots els agraeixo la seva ajuda quan ho he necessitat, la seva amabilitat, el seu suport i els bons moments, tant dins com fora de la feina.

Als meus pares i a la meva germana. Quina sort tenir-vos...

Publications and presentations related to this thesis

Publications

Title: Flow cytometry immunodetection and membrane integrity assessment of *Escherichia coli* O157:H7 in ready-to-eat pasta salad during refrigerated storage
Authors: A. Subires, J. Yuste, M. Capellas
Reference: International Journal of Food Microbiology, 2014, 168-169: 47-56

Scientific communications

Title: Immunodetection and membrane integrity assessment of *Escherichia coli* O157:H7 by three-colour flow cytometry
Authors: A. Subires, J. Yuste, M. Capellas
Meeting: 5th International Conference on Analysis of Microbial Cells at the Single Cell Level
Place and date: Carry-Le-Rouet, France, 5-8 November, 2011
Type of communication: Poster communication

Title: Assessment of green-fluorescent nucleic acid stains as bacterial viability indicators for flow cytometry analysis
Authors: A. Subires, M. Capellas, S. De Lamo, J. Yuste
Meeting: 22nd International Symposium of the International Committee on Food Microbiology and Hygiene, Food Micro 2010: Microbial behaviour in the food chain
Place and date: Copenhagen, Denmark, 30 August-3 September, 2010
Type of communication: Poster communication

Title: Inactivation-associated reactive oxygen species formation in heat- and acid-stressed bacteria
Authors: A. Subires, M. Mols, M. Capellas, J. Yuste, T. Abee
Meeting: 22nd International Symposium of the International Committee on Food Microbiology and Hygiene, Food Micro 2010: Microbial behavior in the food chain
Place and date: Copenhagen, Denmark, 30 August-3 September, 2010
Type of communication: Oral communication

Title: Flow cytometry for injured pathogen detection

Authors: A. Subires, J. Yuste, M. Capellas

Meeting: 30th Annual Rapid Methods and Automation in Microbiology Workshop/Symposium

Place and date: Manhattan, KS, USA, 11-18 June, 2010

Type of communication: Lecture

Title: Flow cytometry detection of *Escherichia coli* O157:H7 stressed by chemical and physical treatments

Authors: A. Subires, J. Yuste, M. Capellas

Meeting: V European Symposium on Food Safety

Place and date: Berlin, Germany, 7-9 October, 2009

Type of communication: Poster communication

Table of contents

List of figures

List of tables

List of abbreviations

%SI	sublethal injury
a.u.	arbitrary unit
Ab-RPE	R-phycoerythrin-labeled antibody
ADC	analog-to-digital converter
ALOA	agar Listeria according to Ottaviani & Agosti
AM	acetoxymethyl
ANOVA	analysis of variance
BCEcF	2',7'-bis(2-carboxyethyl)-5(6)-carboxyfluorescein
BHI	brain heart infusion
BP	BagPage F blender bag
C	centrifugation
C+S	centrifugation, second dilution
CCCP	carbonyl cyanide m-chlorophenylhydrazone
cDNA	complementary DNA
CECT	*Colección Española de Cultivos Tipo*, Spanish Type Culture Collection
cF	carboxyfluorescein
CF	centrifugal filtration
cFDA AM	acetoxymethyl ester of carboxyfluorescein diacetate
cFDA SE	carboxyfluorescein diacetate succinimidyl ester
cFSE	carboxyfluorescein succinimidyl ester
CFU	colony-forming unit
CLSM	confocal laser scanning microscopy
CNM	*Centro Nacional de Microbiología*, National Microbiology Centre
CR	citric acid + refrigeration
CTC	5-cyano-2,3-ditolyl tetrazolium chloride
CTF	3-cyano-1,5-ditolyl formazan
DA	diacetyl
DMSO	dimethyl sulfoxide
DPSS	diode-pumped solid-state
EB	ethidium bromide
EDTA	ethylene diamine tetraacetic acid
EFM	epifluorescence microscopy
EHEC	enterohemorrhagic *Escherichia coli*
EMA	ethidium monoazide

EthD-1	ethidium homodimer-1
F	freezing
FDA	fluorescein diacetate
FISH	fluorescence *in situ* hybridization
FITC	fluorescein isothiocyanate
FL1	green fluorescence photodetector (530/30 nm)
FL2	yellow-orange fluorescence photodetector (545/82 nm)
FL3	far red fluorescence photodetector (>670 nm)
FL4	red fluorescence photodetector (661/16 nm)
FLIM	lifetime imaging microscopy
FRET	Förster resonance energy transfer
FSC	forward scatter
H	heat
HPP	high pressure processing
ILP	intense light pulses
LOD	limit of detection
LOQ	limit of quantification
LSC	laser scanning cytometry
LSM	laser scanning microscopy
MFI	median fluorescence intensity
NADS	nucleic acid double-staining
NASBA	nucleic acid sequence-based amplification
ND-YAG	neodynium yttrium aluminum garnet
PCR	polymerase chain reaction
PD	photodiode
PE	phycoerythrin
PEF	pulsed electric fields
PI	propidium iodide
PMA	propidium monoazide
PMT	photomultiplier tube
PU	BagFilter Pull-Up blender bag
R	refrigeration
rCV	robust coefficient of variation
RPE	R-phycoerythrin
RTE	ready-to-eat

RT-PCR	reverse-transcription polymerase chain reaction
S	second dilution
S:N	signal-to-noise ratio
SMAC	sorbitol MacConkey
SMAC-CT	SMAC agar supplemented with cefixime tellurite
SR	potassium sorbate + refrigeration
SSC	side scatter
T(χ)	probability binning metric
TAL	thin agar layer
TBS-BSA	Tris buffered saline with bovine serum albumin
TO	tiazole orange
Tris-BSA	Tris with bovine serum albumin
TSAYE	tryptone soya agar supplemented with yeast extract
TSB	tryptone soya broth
VBNC	viable but nonculturable
VR	vinegar + refrigeration
XLD	xylose lysine desoxycholate

Abstract

Nowadays, one of the key factors driving consumer food choice is convenience. This has led to an increase in the ready-to-eat (RTE) meal market, with a consequent emergence of new food safety hazards, since food processing and preservation technologies that may be applied to these food products have a milder effect on microorganisms than traditional food processing strategies (e.g. pasteurization, sterilization). As a result, some of those technologies render injured bacteria, which may lose their ability to multiply and are therefore not detected by conventional plating. However, their presence in food must not be overlooked, due to their potential capacity to recover and pose a hazard to health in the case of pathogens.

Flow cytometry is a culture-independent technique which has been widely used in bacterial research to rapidly assess the physiological state of individual cells, with membrane integrity being one of the most popular parameters due to its essential role in survival. However, flow cytometry results are largely affected by the interference of food particles. In this thesis, several strategies were evaluated to develop a flow cytometry assay, based on the use of the membrane-impermeant dye propidium iodide (PI) combined with a membrane-permeant dye, to accurately detect and enumerate injured pathogenic bacteria. In the first experiment, concentrations and ratios of combinations of PI with SYTO 9, SYTO 24, and SYTO BC were adjusted to improve resolution of healthy and dead *Escherichia coli* O157:H7, *Salmonella* Enteritidis and *Listeria monocytogenes* populations in control suspensions. This allowed detection of injured cells in suspensions exposed to food-related stresses. In the second experiment, optimized stainings were applied to RTE pasta salad samples inoculated with *E. coli* O157:H7. Moreover, eight different salad sample pretreatments based on coarse filtration of homogenates and a dilution/wash step were compared in terms of background particle reduction and *E. coli* O157:H7

recovery. The most advantageous pre-treatment was the combination of a 63-µm filter blender bag and centrifugal filtration through a 5-µm filter, since it was equivalent to sample dilution in reducing background particle concentration. Considering that the ultimate goal of this thesis was to detect specific injured pathogen cells in RTE pasta salad, in the third experiment, optimization was carried out for *E. coli* O157:H7 control suspensions in buffers commonly used in immunoassays and stained with the high-affinity nucleic acid dye SYBR Green I, PI, and an R-phycoerythrin-labeled antibody (Ab-RPE). Addition of Ab-RPE did not remarkably affect population resolution compared with staining only with SYBR Green I and PI, and allowed clear recognition of *E. coli* O157:H7. Finally, in the fourth experiment, a range of signal filtering strategies were evaluated for reduced acquisition of flow cytometry data arising from interfering food particles. Then, optimized salad sample pre-treatment, combined membrane integrity and immunodetection staining, and signal filtering were applied to monitor the changes in membrane integrity of *E. coli* O157:H7 inoculated in pasta salad throughout 14-day refrigerated storage (pH 4.5, 4°C). With this optimized flow cytometry protocol, the limit of detection of the assay was reduced to 5 log CFU/g. Additionally, it was observed that most *E. coli* O157:H7 cells were injured at the beginning of refrigeration, but showed an intact membrane at the end, which suggests that injured cells repaired their membrane during exposure to refrigeration and acid stresses, and therefore survived in RTE pasta salad.

In conclusion, the immunodetection and membrane integrity flow cytometry assay in food samples developed in this thesis is a good tool to monitor the effect of a number of food-related treatments on *E. coli* O157:H7 cell membrane state, a physiological parameter that can be related to the presence of injured cells.

Resumen

Algunos tratamientos de elaboración y conservación de los alimentos lesionan las bacterias, de manera que pierden la capacidad para multiplicarse y no son detectadas por métodos de cultivo convencionales. La citometría de flujo es una técnica de análisis independiente del cultivo de los microorganismos, usada ampliamente para evaluar de manera rápida el estado fisiológico de células bacterianas individuales, siendo la integridad de membrana unos de los indicadores más habituales debido a su importancia en la supervivencia de éstas. Sin embargo, los resultados obtenidos mediante citometría de flujo se ven afectados por la presencia de partículas de las muestras alimentarias.

En esta tesis, se evaluaron estrategias para desarrollar un ensayo por citometría de flujo basado en el uso del yoduro de propidio (YP), fluorocromo que no atraviesa las membranas intactas, combinado con un fluorocromo que penetra las membranas intactas, para detectar y cuantificar con precisión bacterias patógenas lesionadas. En el primer experimento, se ajustaron las concentraciones y las ratios de combinaciones de YP con SYTO 9, SYTO 24 y SYTO BC para mejorar la resolución de poblaciones de células sanas y muertas de *Escherichia coli* O157:H7, *Salmonella* Enteritidis y *Listeria monocytogenes* en suspensiones control. Esto permitió detectar células lesionadas en suspensiones expuestas a estreses relacionados con los alimentos. En el segundo experimento, se aplicaron las tinciones optimizadas a muestras de ensalada de pasta inoculadas con *E. coli* O157:H7. Asimismo, se compararon ocho pre-tratamientos basados en la filtración gruesa de las muestras homogeneizadas y en un paso de dilución/lavado, para evaluar la reducción de partículas interferentes y la recuperación de *E. coli* O157:H7 de la ensalada. El pre-tratamiento más favorable fue la combinación de la bolsa de homogenización con filtro de 63 µm y la filtración centrífuga a través de un filtro de 5 µm, ya que redujo la concentración de partículas interferentes tanto como diluir la muestra. Considerando que el

objetivo principal de esta tesis fue detectar específicamente bacterias patóge-
nas lesionadas, en el tercer experimento, la optimización se llevó a cabo para
suspensiones control de *E. coli* O157:H7 en soluciones tampón comúnmente
usadas en inmunoensayos, y teñidas con SYBR Green I, un fluorocromo con
alta afinidad por los ácidos nucleicos, YP y un anticuerpo marcado con R-
ficoeritrina (Ac-RFE). La adición de Ac-RFE no afectó notablemente la resolu-
ción de las poblaciones en comparación con la resolución conseguida con la
tinción con SYBR Green I y YP, y permitió reconocer claramente las células de
E. coli O157:H7. En el cuarto experimento, se evaluaron estrategias de filtración
de señal analítica para reducir la adquisición de datos procedentes de partícu-
las interferentes. Posteriormente, se aplicó el pre-tratamiento de muestra op-
timizado, la tinción para evaluar la integridad de membrana y la inmunodetec-
ción, y la filtración de señal analítica, para monitorizar los cambios de la inte-
gridad de membrana de *E. coli* O157:H7 inoculada en ensalada de pasta durante
14 días de almacenamiento en refrigeración (pH 4,5; 4°C). Con este protocolo
optimizado, el límite de detección disminuyó a 5 log UFC/g. Además, se ob-
servó que la mayoría de células de *E. coli* O157:H7 estaban lesionadas al princi-
pio del almacenamiento, pero mostraban una membrana intacta al final, lo que
sugiere que las células lesionadas repararon su membrana durante la exposi-
ción a ácido y refrigeración y, por lo tanto, sobrevivieron en la ensalada de
pasta.

En conclusión, el ensayo por citometría de flujo para la evaluación de la inte-
gridad de membrana y la inmunodetección desarrollado en esta tesis es una
buena herramienta para monitorizar el efecto de tratamientos relacionados
con los alimentos sobre el estado de la membrana de *E. coli* O157:H7, parámetro
fisiológico relacionado con la presencia de células lesionadas.

Chapter 1. Literature review

1. Injured bacteria in food

1.1. Minimally processed food as pathogen vectors

Modern consumers ask for convenience, healthy and fresh-looking food. As a result, current trends in food consumption have evolved to minimally processed food, such as some RTE meals or semi-prepared ingredients (e.g. semi-cooked or marinated). This can introduce new food safety hazards into the food supply, since elaboration of these products may not rely on traditional food processing strategies such as pasteurization and sterilization, but on preservation technologies with a milder effect on nutritional value, taste, color and flavor, but also on microorganisms (Quested *et al.*, 2010; Rajkovic *et al.*, 2010). Thus, elucidation of the effect of preservation factors on physiology of foodborne pathogens in minimally processed food is a topic of growing interest, since this provides the basis for the intelligent design of multitarget preservation methods assuring their safety and stability (Leistner, 2000; Delaquis *et al.*, 2007; Luo *et al.*, 2010).

Ingredients of non-animal origin present in minimally processed food, and particularly in RTE meals such as vegetable salads and salad meals, have been increasingly recognized as important vectors of foodborne diseases associated with bacteria, such as *Salmonella* spp., *Campylobacter* spp., *Escherichia coli* O157:H7, and *Listeria monocytogenes* (Little and Gillespie, 2008; Frankel *et al.*, 2009; Berger *et al.*, 2010; EFSA Panel on Biological Hazards, 2013). Contamination of fresh produce and derived RTE meals can occur at any stage from pre-harvest to post-harvest operations (Greig and Ravel, 2009; Berger *et al.*, 2010; Erickson, 2010; Bautista-De León *et al.*, 2013). Thus, crops may be contaminated with animal feces or fecal water, pathogens such as *Salmonella* spp. and *E. coli* O157:H7 can adhere to and survive in them, whereas cross-contamination can occur during food preparation (Little and Gillespie, 2008; Frankel *et al.*, 2009). Minimal or non-existent further processing of contaminated products prior to

consumption and/or inability of chemical treatments to eliminate surface con-
tamination may then lead to the dissemination of the disease (Berger *et al.*,
2010; Erickson, 2010).

1.2. Stress exposure throughout the food chain

A number of stresses (e.g. cold, heat, acids and preservatives) alter homeosta-
sis of foodborne pathogenic bacterial cells throughout the food chain by tar-
geting membranes, enzymes, and nucleic acids, among other cellular compo-
nents (Abee and Wouters, 1999; Brul and Coote, 1999). This may render a phys-
iologically heterogeneous bacterial population, which includes dead, healthy
and also injured cells, the latter being especially found when mild processing
and preservation technologies are used (Rajkovic *et al.*, 2010).

1.2.1. Stress factors and cellular targets

In the case of RTE vegetable salads and salad meals, storage at refrigeration
temperature is the main factor controlling the survival or growth of bacterial
pathogens if present in these products (Little and Gillespie, 2008; Capozzi *et al.*,
2009). Low temperature reduces cell membrane fluidity due to a more ordered
distribution of fatty acids from phospholipids. This results in hampered func-
tionality, namely leakage of intracellular components, disruption of active
transport, and inactivation of membrane-bound redox enzymes. It also reduc-
es solute uptake, enzyme reaction rates, as well as transcription and transla-
tion efficiencies due to stabilization of secondary structures of nucleic acids.
Globally, this leads to restriction of cellular activity, and thus, to growth arrest
and establishment of the survival phase, but not necessarily to cell death
(Phadtare, 2004; Sutherland, 2005; Cavicchioli *et al.*, 2009).

Furthermore, low pH dressings (e.g. vinaigrette, mayonnaise, sour cream, etc.)
are common ingredients in RTE salad meals, since they extend shelf-life by
creating an extra hurdle for the existent microbiota (Heard, 1999; Leistner,

2000). Decrease of intracellular pH due to exposure to weak organic acids interferes with essential metabolic processes, such as the synthesis of ATP, RNA and proteins. It also causes structural damage to DNA, proteins, and cell membranes, and interferes with function of membrane-bound proteins, which reduces nutrient uptake (Brul and Coote, 1999; Cotter and Hill, 2003; Davidson *et al.*, 2013). Moreover, intracellular accumulation of anions resulting from acid dissociation further contributes to perturbation of metabolism by increasing osmolarity (Rajkovic *et al.*, 2010).

Besides low temperature and pH, heat treatments are applied to obtain cooked ingredients, such as pasta, potato or couscous, which are usually present in RTE salad meals (Heard, 1999; Little and Gillespie, 2008). Mechanisms of inactivation by heat include destabilization of a range of cellular components, e.g. nucleic acids, ribosomes, enzymes, other proteins, and membranes, resulting in loss of their functionality and thus the potentially lethal disruption of the cellular metabolism (Abee and Wouters, 1999; Rajkovic *et al.*, 2010). Breakage of DNA strands and degradation of ribosomes have been closely related with cell death following heat exposure. Heat also causes vibration of water molecules in contact with proteins, which are thus denaturated and lose their functionality. Heat first affects membrane-bound proteins and then proteins within ribosomes. Loss of functionality of enzymes, such as catalase, superoxide dismutase and membrane-bound ATPase, upon heat stress is also related with cell death. Finally, heat increases membrane fluidity and causes structural damage, which result in efflux of ions, aminoacids and low molecular weight components (Juneja and Novak, 2005).

Other food processing and preservation strategies to control microbial hazards in minimally processed food include: high pressure processing (HPP), pulsed electric fields (PEF), radiation, or application of chlorine dioxide. HPP has been shown to disrupt the quaternary and tertiary structures of cellular compo-

nents, such as proteins and ribosomes, and therefore their functionality (Juneja and Novak, 2003; Yousef and Courtney, 2003). Cell membrane is also considered a primary target for HPP, which induces compression and decompression of the phospolipid bilayer resulting in membrane malfunction and permeabilization (Abee and Wouters, 1999; Considine *et al.*, 2008; Rajkovic *et al.*, 2010). Moreover, HPP inhibits key enzymes, and protein and DNA synthesis, and causes morphological changes, such as the separation of the cell wall from the cytoplasmic membrane (Yuste *et al.*, 2001; Juneja and Novak, 2003; Considine *et al.*, 2008; Huang *et al.*, 2014). The lethal effect of PEF is believed to be mainly due to alteration and permeabilization of the cell membrane, which disrupts pH homeostasis and ion transport, and induces loss of intracellular components, respectively (Juneja and Novak, 2003; Yousef and Courtney, 2003). Radiation technologies for food preservation include, among others, UV and gamma radiation, and intense light pulses (ILP). UV light alters DNA structure and causes cross-linking between DNA and proteins, which blocks replication and results in cell death. Gamma radiation causes inactivation by altering a range of cell components through the formation of hydroxyl radicals (Yousef and Courtney, 2003). In the case of treatments by ILP, a flash light emitting radiation from the UV to the near-infrared is used. Therefore, damage induced by high intensity UV light is thought to be the key mechanism involved in bacterial inactivation by ILP, although a thermal effect has also been proposed (Yousef and Courtney, 2003; Rajkovic *et al.*, 2010; Ramos-Villarroel *et al.*, 2014). Finally, chlorine dioxide has been used to decontaminate fresh produce due to its powerful oxidizing activity. Although the exact lethal mechanism of this compound is not completely understood, inhibition of protein synthesis, and oxidative damage to proteins and the cell envelope have been observed (Rajkovic *et al.*, 2010).

1.2.2. Stress adaptive responses

Exposure of bacterial cells to stressful conditions, such as heat, cold, or acid, triggers adaptive responses in which metabolic and structural changes take place to counteract the detrimental effects of such stresses (Phadtare, 2004; McClure, 2005). Thus, when bacteria sense alterations in membrane fluidity, proteins, ribosomes or nucleic acids, specific sets of genes encoding regulatory proteins are expressed, which in turn may lead to the synthesis of other proteins to repair damage to cell components and structures.

Stress responses are complex and differ according to the specific stress and bacterial species. Besides a general stress response, which provides protection against a range of stresses, bacteria have evolved responses to specific stresses. Moreover, they can provide immediate or long-term adaptation. At the molecular level, synthesis of stress- related proteins can be regulated at the level of transcription or translation or by adjusting mRNA and protein stability (Yousef and Courtney, 2003). A common regulatory mechanism involves modification of σ factors, which provide promoter binding specificity to RNA polymerase. For example, σ^S, in Gram-negative bacteria, and σ^B, in Gram-positive bacteria, induce expression of genes related with the general stress response (Abee and Wouters, 1999; Yousef and Courtney, 2003).

Upon exposure to cold, bacteria respond by increasing membrane fluidity through modification of phospholipid composition in a process known as homeoviscous adaptation. Increased fluidity is achieved by increasing the proportion of unsaturated fatty acids, reducing fatty acid chain length, or introducing branched fatty acids (Ramos *et al.*, 2001; Sutherland, 2005). Other repair mechanisms include synthesis of cold-shock proteins, including protein chaperones, which ensure proper protein folding and refolding of cold-damaged proteins, and RNA chaperons, which facilitate translation of mRNA by reducing secondary folding of RNA due to low temperature, and therefore promote

protein synthesis (Phadtare, 2004; Nyachuba and Donnelly, 2005; Sutherland, 2005).

Responses to acid stress broadly vary according to growth phase and bacterial species. Mechanisms to counteract the negative effects of low pH include: increased synthesis of the membrane-bound enzyme ATPase, which results in increased proton efflux; increased aminoacid catabolism, which consumes protons and therefore results in alkalinization of the intracellular pH; increased cyclopropane fatty acids in membrane phospholipids, which may affect permeability to protons or activity of membrane-bound proteins; and induction of DNA repair enzymes (Audia *et al.*, 2001; Yousef and Courtney, 2003; McClure, 2005).

Heat exposure rapidly induces the expression of heat-shock proteins, such as protein chaperones, which enable proper folding and assembly of new proteins and refolding of existing misfolded or partially folded proteins; and ATP-dependent proteases, which destroy heat-damaged proteins. Moreover, increased membrane fluidity concomitant to heat exposure is reduced by increasing the ratio of trans-to-cis fatty acids in membrane phospholipids (Abee and Wouters, 1999; Juneja and Novak, 2003; Yousef and Courtney, 2003; Vorob'eva, 2004).

HPP has been shown to induce the synthesis of high levels of cold-shock and heat-shock proteins, as well as other proteins, which suggest that response to this stress is not specific (Abee and Wouters, 1999; Juneja and Novak, 2003; Huang *et al.*, 2014). Little information is available regarding the stress response to PEF treatments, although evidence has been found that damage to the cytoplasmic membrane can be repaired under favorable conditions (Yousef and Courtney, 2003; García *et al.*, 2006). Repair mechanisms of DNA damage induced by radiation include the synthesis of base and nucleotide excision repair enzymes and photoreactivation enzymes. Finally, oxidative stress induces the

synthesis of a number of detoxifying enzymes, such as catalases, peroxidases and superoxide dismutases, as well as other proteins involved in repair of oxidative damage to nucleic acids (Yousef and Courtney, 2003; Capozzi *et al.*, 2009).

1.3. Potential public health hazards posed by injured bacteria

The injured state might be a common physiological state of bacteria in food and food processing environments (Johnson, 2003). Indeed, a range of treatments have been shown to render injured cells, such as heat (Mackey *et al.*, 1994), cold (Fratamico and Bagi, 2007), acid (Liao and Fett, 2005), HPP (Chilton *et al.*, 2001; Somolinos *et al.*, 2008), or PEF (Yaqub *et al.*, 2004; García *et al.*, 2006; Zhao *et al.*, 2011).

Stress responses of food spoilage and pathogenic bacteria have important implications in food quality and safety, since these responses allow injured cells to repair and therefore survive to food processing and preservation methods, and even resume growth and regain virulence (Archer, 1996; Johnson, 2003; Yousef and Courtney, 2003; Wesche *et al.*, 2009). An additional important feature of stress responses is that cells adapted to a certain stress can also show tolerance to other stresses in a phenomenon known as cross-protection (Rodriguez-Romo and Yousef, 2005). Therefore, the application of combinations of stressing factors according to the hurdle technology may be inefficient if cross-protection occurs (Johnson, 2003).

Validation of emerging technologies for food preservation should not therefore omit the detection of potentially harmful injured cells (Rajkovic *et al.*, 2010). However, selective media for pathogen detection and enumeration can fail to evidence the presence of injured cells, which cannot grow due to damage to essential metabolism and/or the structures that otherwise would protect them from selective agents, namely antibiotics, salts, acids, and surface-

active compounds, such as bile salts (Kell *et al.*, 1998; Mackey, 2000; Stephens and Mackey, 2003). For example, sorbitol MacConkey (SMAC) agar, which is the medium commonly used to isolate *E. coli* O157:H7 from foodstuffs, has repeatedly been shown to prevent recovery of stressed cells, whether it is supplemented with cefixime and tellurite or not (McCarthy *et al.*, 1998; Park *et al.*, 2011; Yoshitomi *et al.*, 2012). This may result in overestimation of the efficacy of preservation methods and food safety, since, as previously stated, injured cells can recover from damage (Archer, 1996; Wesche *et al.*, 2009). Another constraint of culture-based methods is that growth of a cell into a colony is necessary for detection and this requires considerable time, especially when injured cells are present. Moreover, these methods do not provide information about the mode of action of a certain treatment (Ueckert *et al.*, 1997; Lemarchand *et al.*, 2001).

2. Detection of injured cells

Viability of bacteria has been traditionally defined in terms of their ability to demonstrate cell division (reproductive growth) by culture methods (Joux and Lebaron, 2000). However, the use of techniques for single-cell analysis in combination with fluorescent compounds (fluorochromes) acting as probes of a variety of physiological functions of cells led to a change in the interpretation of this concept (Nebe-von-Caron *et al.*, 2000). Thus, according to Breeuwer and Abee (2000), "viable cells can be generally defined as those cells which are capable of performing all cell functions necessary for survival under given conditions". Based on such measurable functions, several designations were coined to define the physiological state of cells beyond the "cultivable" (alive, viable) or "noncultivable" (dead) states (Ueckert *et al.*, 1997; Nebe-von-Caron *et al.*, 1998; Joux and Lebaron, 2000). According to their metabolic state, cells can be (i) active or vital, if they show metabolic activity; or (ii) inactive, if they do not show metabolic activity, either because it is not enough to reach a detectable

level or because they are dying cells. Regarding the state of their envelope structures, cells can be (i) intact, if they maintain membrane integrity; or (ii) permeabilized, if they have a damaged membrane. Those cells which have lost their nucleoid, but maintain their envelope are the so-called ghost cells. Moreover, assessment of cell physiology by fluorescence-based assays also contributed to the establishment of the viable but nonculturable (VBNC) state (Oliver, 2005). According to Mackey (2000), this term is "rather loosely applied to (1) organisms that fail to grow on nutrient nonselective media that normally support their growth but which retain cellular metabolic activity measured in one of several different tests and (2) organisms that become nonculturable but can regain the capacity to multiply on their normal growth media following a suitable resuscitation treatment".

2.1. Culture-based methods

2.1.1. Differential plating method

Detection of injured cells by culture methods is based on the assumption that these cells cannot form colonies on a selective medium but can do so in a nonselective medium (Kell *et al.*, 1998). Therefore, quantification of injury in axenic cultures is classically achieved by using the differential plating method, which consists in parallel plating on nonselective and selective media. The nonselective medium allows recovery of injured cells before growth, and so detects both healthy and previously injured cells, whereas the selective medium only detects the healthy fraction, as it is assumed that resistance to selective agents involves having an intact cell envelope. Therefore, the difference between counts on nonselective and selective media gives the sublethally injured cell count (Kell *et al.*, 1998; Wesche *et al.*, 2009). Since sublethally injured cells are culturable in certain conditions, some authors do not consider them as VBNC, at least at the experimental level. Instead, VBNC cells are experimentally defined as those cells which cannot grow on a nonselective medium, but

retain metabolic activity and/or physical integrity (Kell *et al.*, 1998; Mackey, 2000).

Selective media containing bile salts, triphenylmethane dyes, or hydrophobic antibiotics (e.g. MacConkey agar, Brilliant Green agar) is generally used to detect damage to the outer membrane of Gram-negative cells, whereas media containing sodium chloride is used to detect cytoplasmic membrane damage (Mackey, 2000; Chilton *et al.*, 2001). The differential plating method has also been used to monitor recovery of injured cells under specific culture conditions (temperature and time). According to this approach, injured cells are considered completely recovered when counts on selective media are equal to those on nonselective media (Mackey *et al.*, 1994; Mackey, 2000).

The quantification of sublethal injury by the differential plating method largely depends on factors such as the sample handling, media composition, and incubation temperature and time. This implies that optimization of the procedure requires the tedious comparison of different combinations of these factors (Mackey, 2000; Wesche *et al.*, 2009).

2.1.2. Thin agar layer method

The thin agar layer (TAL) method is used to improve recovery of target sublethally injured cells present in food based on the use of a double-layer medium. In this method, a thin layer of nonselective medium is overlaid onto prepoured selective medium. During the first hours of incubation, injured cells, if present, are able to recover and start growing on nonselective medium. Then, selective agents in the bottom layer diffuse to the top layer and react with cells therefore avoiding growth of non-target bacteria and allowing the development of typical colonies of target bacteria (Kang and Fung, 1999, 2000; Wu, 2008). Moreover, since molten media is not used, additional heat injury is avoided. This method has proved suitable to recover injured *E. coli* O157:H7, *L.*

monocytogenes, *Salmonella* Thyphimurium, *Staphylococcus aureus*, and *Yersinia enterocolitica* after heat, acid, cold treatments and HPP (Wu *et al.*, 2001; Yuste *et al.*, 2003, 2004; Wu, 2008). Parallel plating on TAL and selective medium used alone allows the enumeration of sublethally injured cells in food, since TAL recovers both healthy and injured cells and selective medium is supposed to only support growth of healthy cells.

2.2. Culture-independent methods

2.2.1. Molecular methods

Assessment of bacterial viability by molecular methods is based on decay of nucleic acids after cell death. Due to its high stability and therefore long persistence in dead cells, the detection of DNA may not correlate with viability. Conversely, RNA shows lower persistence and is thus proposed as a potential viability marker. Among RNA molecules, rRNA is protected by proteins and shows higher stability than mRNA, which has a very short life-time and is therefore considered a more suitable target to infer about cell viability (Cenciarini-Borde *et al.*, 2009). Nucleic acid decay is generally measured by target amplification methods, namely polymerase chain reaction (PCR) for the detection of DNA, and reverse-transcription PCR (RT-PCR) or nucleic acid sequence-based amplification (NASBA) for RNA (Keer and Birch, 2003; Rodríguez-Lázaro *et al.*, 2006). These methods offer rapid quantitative results with high sensitivity and specificity. In the case of RT-PCR, the target RNA molecule is used as a template for the production of a complementary DNA (cDNA) sequence, which is then amplified by PCR; whereas in NASBA, the target RNA sequence is directly amplified in an isothermal reaction (Cenciarini-Borde *et al.*, 2009).

Reliability of RNA-based viability assessment largely depends on the choice of the target molecule and sensitivity of the detection method itself (Keer and Birch, 2003). Amplification of rRNA targets, such as the 16S rRNA, provides

high sensitivity, since they are present in cells in high copy numbers. However, although it could be used in certain well-defined situations, it has shown to persist for several days after lethal treatments by heat, UV or ethanol. In contrast, mRNA encoding different proteins (ubiquitously expressed, stress regulation, cytotoxicity, surface) have been found to be better candidates for viability assessment (Cenciarini-Borde *et al.*, 2009). In particular, choice of ubiquitously and highly expressed sequences can provide high sensitivity, as well as some certainty that they will be present under most experimental conditions (Keer and Birch, 2003). However, mechanisms of mRNA degradation are complex and therefore analyses have to be optimized for each target, bacterial species and treatment to obtain accurate information about viability. An additional limitation to the mRNA-based viability assessment is the complexity of the analysis procedure due to the high lability of mRNA molecules and the possibility of contamination with DNA, which interferes when using RT-PCR (but not with NASBA). Moreover, VBNC cells may not be detected, since some mRNA sequences are not expressed in this state (Cenciarini-Borde *et al.*, 2009).

The combination of sample pre-treatment with ethidium monoazide (EMA) or propidium monoazide (PMA) and subsequent DNA detection by PCR has been proposed as a good alternative to the previous methods. EMA and PMA are DNA intercalating dyes which can only penetrate into cells with permeabilized membranes. Photoactivation of intercalated dyes prevents subsequent DNA amplification, due to covalent linking. Free EMA or PMA are degraded by photolyzation to inhibit further linking. These pre-treatments decrease the signal from dead cells and therefore allow discrimination of viable cells, with the advantages of DNA detection, which include better tolerance than RNA to extraction and purification steps, presence not dependent on so many factors as with RNA, and presence in VBNC cells. EMA can sometimes affect PCR results, due to a toxic effect or incorporation into viable cells. Such interferences do not occur with PMA, and therefore PMA-PCR is considered a promising tool

to evaluate bacterial viability. However, both EMA-PCR and PMA-PCR may not be efficient when analyzing cells exposed to sublethal stresses (Cenciarini-Borde *et al.*, 2009).

2.2.2. Fluorescence-based techniques

2.2.2.1. *Assessment of physiological parameters by fluorescent probes*

The analysis of multiple cellular functions during exposure to stresses by using fluorescent probes (Figure 1.1) reveals that damage to these functions occurs progressively and sequentially and that different stages can be defined between life and death (Figure 1.2) (Joux *et al.*, 1997; Nebe-von-Caron *et al.*, 1998; Díaz *et al.*, 2010). Thus, reproductive growth is the most demanding proof for viability, since it requires both an intact membrane and metabolic activity, and so it is the first function that is affected upon stress exposure (Vives-Rego *et al.*, 2000; Díaz *et al.*, 2010). However, cells can lose their ability to multiply but still exhibit a range of metabolic activities, which require an intact membrane for their maintenance (Nebe-von-Caron *et al.*, 2000). Some of these metabolic activities additionally require energy supply, whereas others are energy-independent, which implies that the former are more stringent proofs for viability than the latter (Vives-Rego *et al.*, 2000). Measurable energy-dependent metabolic activities include the biosynthesis of macromolecules; the activity of pumps, which in turn involves the efflux of certain compounds and the control of the intracellular pH; and the maintenance of a transmembrane potential gradient (Nebe-von-Caron *et al.*, 2000). The synthesis of enzymes such as dehydrogenases and esterases requires energy, but their activities are energy-independent (Vives-Rego *et al.*, 2000). Thus, detection of these enzymatic activities only shows the past ability of a cell to synthesize the enzymes and maintain them active. Irreversible membrane permeabilization is usually the last stage in cell damage and death, since cells can no longer generate and maintain the electrochemical gradients necessary to be functional and the exposed

internal structures finally break down (Hewitt *et al.*, 1999; Nebe-von-Caron *et al.*, 2000).
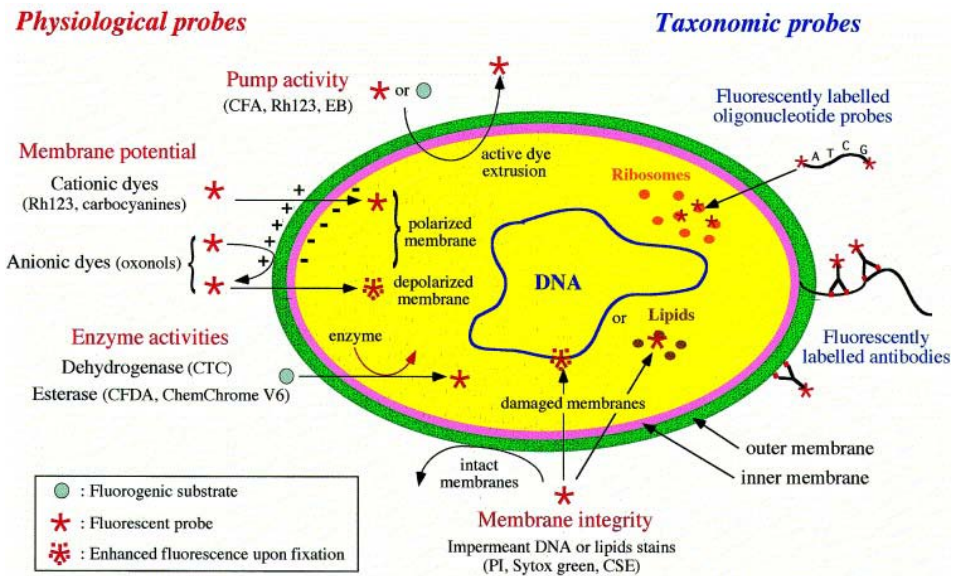
Figure 1.1 Different cellular target sites for physiological and taxonomic fluorescent dyes. Reprinted from Microbes and Infection, 2, F. Joux and P. Lebaron, Use of fluorescent probes to assess physiological functions of bacteria at single-cell level, 1523–1535, Copyright (2000),with permission from Éditions scientifiques et médicales Elsevier SAS.

The presence of an intact membrane indicates that cell constituents are protected and that metabolic activity is possible (Vives-Rego *et al.*, 2000). However, these characteristics are only presumptive evidences for reproductive growth, and as such, they cannot be used to conclude about the reproductive viability of cells (Nebe-von-Caron *et al.*, 2000). Indeed, discrepancy between cell counts obtained from staining with fluorescent probes and culture methods is usually found, especially when dealing with cells exposed to stress, which is partly due to the limitations of both methods (Nebe-von-Caron *et al.*, 1998). Thus, a cell may fail to grow as a result of irreversible DNA damage or the inability to repair under suboptimal culture conditions (Nebe-von-Caron *et al.*, 2000). Fluorescent staining of living cells may be affected by the presence of the outer
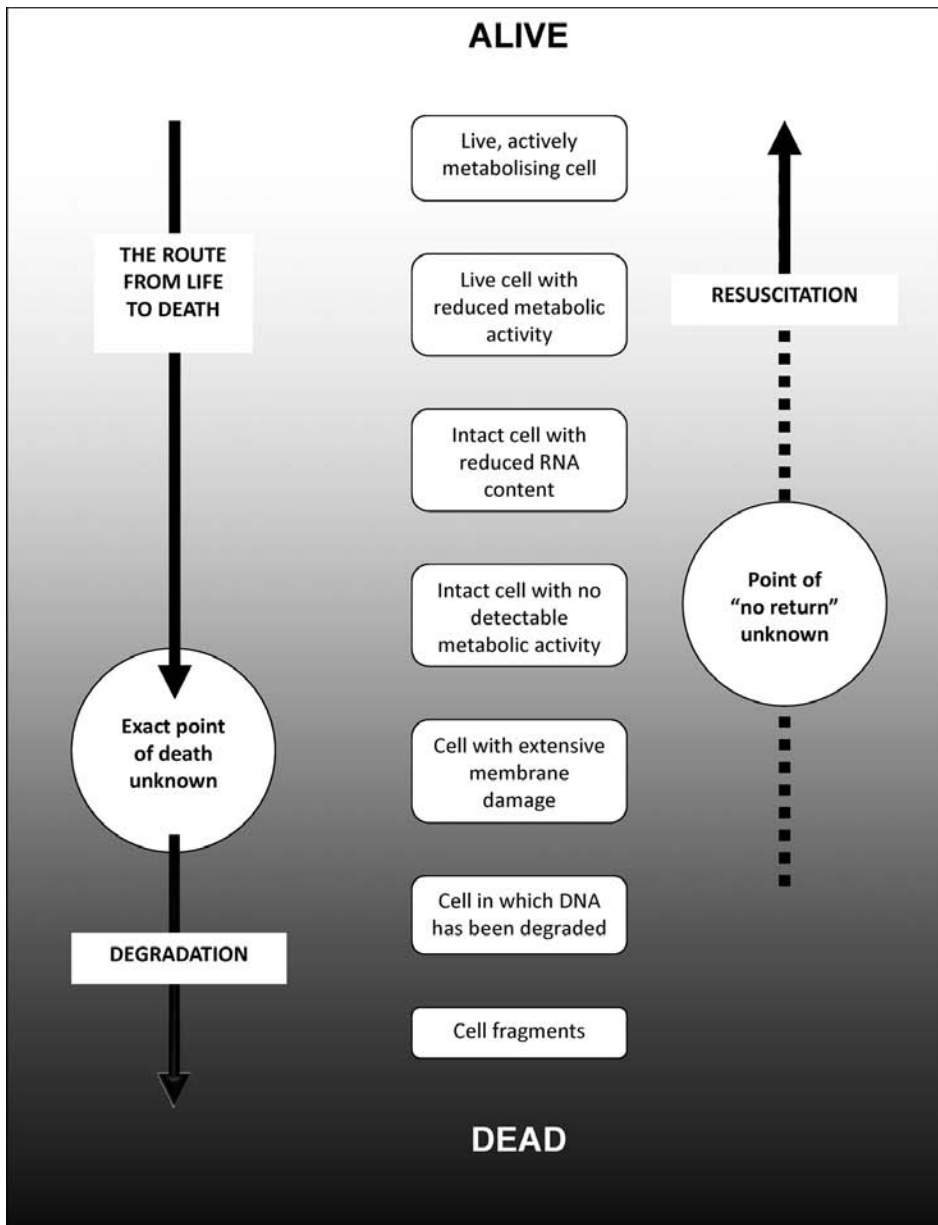
Figure 1.2 The route from "live" to "dead". From "Life, death and in-between: meanings and methods in microbiology", by H.M. Davey. Copyright © American Society for Microbiology, [Applied and Environmental Microbiology, 77, 2011, 5571–5576].

membrane in Gram-negative cells, dye efflux pumps, and weak or absent metabolic activity (Nebe-von-Caron *et al.*, 1998). The outer membrane acts as a barrier to hydrophobic fluorochromes and therefore requires permeabilization prior to staining (Berney *et al.*, 2007; Hammes *et al.*, 2012). Ethylene diamine tetraacetic acid (EDTA) may be used for this purpose (Vaara, 1992), but this treatment is controversial, since it needs extensive optimization to minimize its adverse effect on cell functionality (Shapiro, 2000b; Doherty *et al.*, 2010; Sträuber and Müller, 2010). Additionally, sodium azide, verapamil, NaN_3 or *m*-chlorophenylhydrazone can be used to uncouple efflux pumps and avoid dye extrusion (Nebe-von-Caron *et al.*, 1998, 2000; Müller and Nebe-von-Caron, 2010).

2.2.2.1.1. Membrane integrity

Bacterial cells possess complex envelope structures which modulate the uptake of fluorochromes. Thus, envelope permeation to specific fluorochromes depends on their respective hydrophobic or hydrophilic natures and this principle can be used to obtain information about its integrity state (Sträuber and Müller, 2010). The cytoplasmic membrane or inner membrane encompasses the cytoplasm and contains phospholipids fairly evenly arranged in a bilayer which has therefore a major hydrophobic nature. The cell wall is the structure outside the cytoplasmic membrane and, in the case of Gram-positive bacteria, is composed of 10 to 20 peptidoglycan layers. Conversely, the cell wall of Gram-negative bacteria contains 1 to 3 peptidoglycan layers and an additional structure known as the outer membrane, with phospholipids mainly found in its inner leaflet, whereas in the outer leaflet, some phospholipids are present but also lipopolysaccharides and proteins. As a result of this asymmetric arrangement of phospholipids, the outer membrane has a hydrophilic nature. Therefore, for a cell with an intact membrane, only small uncharged (or with delocalized charge) hydrophobic molecules can diffuse through the peptidoglycan layers and the cytoplasmic membrane (Sträuber and Müller, 2010). However,

for Gram-negative bacteria, the outer membrane constitutes a significant barrier for the penetration of such molecules (Cao-Hoang *et al.*, 2008). This implies that Gram-positive cells are more permeable to hydrophobic compounds than Gram-negative ones, and that the latter are more permeable to hydrophilic compounds than the former (Sträuber and Müller, 2010). In both cases, the presence of porin channels and transporter proteins allows selective permeability to small charged hydrophilic molecules.

According to these foundations, the entry of charged hydrophilic fluorochromes into a cell is assumed to be due to the loss of its membrane integrity (Cao-Hoang *et al.*, 2008). This is the basis for the so-called dye-exclusion assays, which usually rely on the use of nucleic acid dyes, i.e. dyes whose fluorescence significantly increases when bound to nucleic acids (Joux and Lebaron, 2000; Nebe-von-Caron *et al.*, 2000). Propidium iodide (PI) is one of the most popular dyes to detect membrane damage (Endo *et al.*, 2001; Ananta *et al.*, 2005; Hayouni *et al.*, 2008; Tong *et al.*, 2009). Due to its large molecular weight (668.4), double positive charge and hydrophilic nature, this red-fluorescent nucleic acid dye can only penetrate and stain cells with permeabilized membranes, which are therefore considered as dead (Manini and Danovaro, 2006; Sträuber and Müller, 2010). Moreover, to simultaneously detect those cells with intact membranes, PI is usually combined with a membrane-permeable green-fluorescent nucleic acid dye, such as SYTO 9, SYTO BC, SYTO 24 (Gunasekera *et al.*, 2000, 2003b; Bunthof *et al.*, 2001; Bunthof and Abee, 2002; Jang and Rhee, 2009; Zhou *et al.*, 2010; Corbitt *et al.*, 2011) or SYBR Green I (Barbesti *et al.*, 2000; Berney *et al.*, 2007, 2008).

Other nucleic acid dyes which posses more than one positive charge and are thus membrane-impermeant are the cyanine dyes from the SYTOX, TOTO and TO-PRO families, or the phenanthridine dye ethidium homodimer-1 (EthD-1) (Shapiro, 2000b; Haugland, 2010a). Membrane permeation to these

fluorochromes varies according to their chemical structures and this has im-plications on the kind of information that they provide (Cao-Hoang *et al.*, 2008; Müller and Nebe-von-Caron, 2010).

The main limitation of the dye-exclusion approach is the appearance of false positive results as a consequence of a transient membrane permeabilization. Thus, a transient disturbance of cell envelope integrity can occur during cell wall reconstruction concomitant to cell elongation and subsequent division (Shi *et al.*, 2007; Sträuber and Müller, 2010). This would explain the increased-red fluorescence emission in PI-stained viable cells reported for Gram-negative and Gram-positive bacteria in the exponential and stationary growth phases (Herrero *et al.*, 2006; Shi *et al.*, 2007; Quirós *et al.*, 2009). False positives may also arise from the induction of porins due to increased abundance of nutrients (Müller and Nebe-von-Caron, 2010). Moreover, transient membrane permeabilization can be also induced by some treatments, such as heat, osmot-ic stress, ultrasound, and electro- and chemoporation, which implies that ade-quate time for membrane repair has to be allowed before integrity assessment (Nebe-von-Caron *et al.*, 1998, 2000). Assay validation according to the bacterial species under study is therefore necessary to reliably obtain information about their membrane integrity, and should include the assessment of PI uptake in different growth states and conditions, including the effect of the diluents used for staining (Müller and Nebe-von-Caron, 2010; Sträuber and Müller, 2010).

In spite of these limitations, results obtained by validated membrane integrity measurements provide a bigger security margin than culture methods or met-abolic activity measurements, due to the existent uncertainty in the optimal growth conditions for the diverse bacterial species and physiological states (e.g. injured, dormant or starved cells), as well as in the reliable detection of

metabolic activity in cells with active efflux pumps or injured cells (Nebe-von-Caron *et al.*, 1998; Vives-Rego *et al.*, 2000).

2.2.2.1.2. Metabolic activity

Efflux pump activity

Bacterial cells possess multidrug transport systems to remove toxic compounds from their inside. Such excretion systems are energy-dependent and act on a broad range of compounds (Müller and Nebe-von-Caron, 2010). For example, efflux of fluorochromes such as ethidium bromide (EB), Rhodamine 123, carboxyfluorescein (cF) or 2',7'-bis(2-carboxyethyl)-5(6)-cF (BCEcF) from energized cells has been observed, resulting in false negative results (Nebe-von-Caron *et al.*, 1998; Bunthof, 2002). However, active dye efflux suggests the capacity of a cell to generate energy and can therefore be assessed as an indicator of its functionality. Since cessation of dye efflux in metabolically compromised cells occurs before membrane depolarization, pump activity is considered a very sensitive parameter to assess cell stress (Nebe-von-Caron *et al.*, 2000). EB, a nucleic acid dye with a single delocalized positive charge, which can thus penetrate intact membranes, has been successfully used for this purpose (Nebe-von-Caron *et al.*, 1998; Shapiro, 2000b).

Intracellular pH

A constant intracellular pH is necessary for a number of vital functions, e.g. DNA transcription, protein synthesis and enzyme activities. Therefore, bacteria have mechanisms to maintain their cytoplasmic pH, such as the active extrusion of protons to the extracellular environment, which results in the generation of a pH gradient (Davidson *et al.*, 2013). The ability to sustain this pH gradient under suboptimal conditions is thus considered an indication of cell viability (Ueckert *et al.*, 1995; Chitarra *et al.*, 2000). Measurement of the intracellular pH is necessary to assess the pH gradient and this can be done by using

fluorescent probes with pH-dependent ionic equilibriums which display different fluorescence emission spectra according to their protonation state (Cao-Hoang *et al.*, 2008; Haugland, 2010b). Since the pK_a of the probe has to match the pH of the experimental system, probes with different pK_a values are available to measure different pH ranges. Fluorescein derivatives are most commonly used for intracellular pH measurements by fluorescence techniques since they are useful at physiological pH values (Haugland, 2010b). These probes are taken up by cells in a nonfluorescent form (fluorogenic substrate) and then cleaved by nonspecific esterases to a more polar fluorescent product, which is therefore retained if the membrane is intact. Fluorogenic substrates are frequently modified with diacetyl (DA) and acetoxymethyl (AM) ester groups to obtain uncharged compounds and therefore improve cell uptake (Breeuwer *et al.*, 1996). However, the leakage of the fluorescent product to the external environment occurs in a varying degree according to its polarity. This results in increased background fluorescence and therefore in the potential inability to exclusively measure the intracellular pH. For example, the fluorescent product of fluorescein diacetate (FDA), fluorescein, rapidly leaks out of the cells. This problem is only partially addressed with the fluorescent product of the AM ester of carboxyfluorescein diacetate (cFDA AM), cF, which bears an extra negative charge. Improved retention is achieved with BCEcF (taken up in the form of its AM ester), which has 4 to 5 negative charges (Haugland, 2010b). Additionally, (Breeuwer *et al.*, 1996) proposed carboxyfluorescein succinimidyl ester (cFSE) (taken up in the form of its DA ester) as an alternative to the more widely used BCEcF, since succinimidyl ester groups bind to intracellular aliphatic amines and this results in better retention. An alternative option to fluorescein derivatives is the cSNARF-1 dye, which does not require enzymatic cleavage and is suggested to be more sensitive to pH changes than BCEcF (Leyval *et al.*, 1997; Haugland, 2010b).

To calibrate the fluorescence signal, cells are loaded with the fluorescent probe and suspended in different buffers of known pH values (Cao-Hoang *et al.*, 2008). Cells are then treated with an ionophore, such as valinomycin or nigericin, to dissipate the pH gradient, i.e. to equilibrate the intracellular and the extracellular pH, so that the intracellular pH can be known. The fluorescence signal is then measured at two different wavelengths: one at which intensity depends on probe concentration and pH, and another at which intensity only depends on the concentration (isosbestic point). A ratio is calculated between fluorescence intensities at the pH-dependent wavelength and those at the pH-independent wavelength to obtain a concentration-independent measure. The ratios of unknown samples can then be used to calculate the intracellular pH.

Membrane potential

Selective permeability of the cell membrane to different cations and anions, such as Na^+, K^+, H^+ and Cl^-, generates ion concentration gradients between opposite sides of the membrane, which in turn results in the presence of an electrical potential gradient of typically –100 mV, with negative charge inside the cell (Nebe-von-Caron *et al.*, 2000; Shapiro, 2000a). The membrane potential, along with the pH gradient, is a component of the proton motive force, which has important functions in cell physiology, such as the uptake of aminoacids and glucose, chemotaxis, ATP synthesis, and survival at low pH (Sträuber and Müller, 2010). The magnitude of membrane potential therefore reflects the state of energy metabolism. Thus, membrane potential decreases due to cessation of energy metabolism under stressing conditions (Hewitt *et al.*, 1999; Shapiro, 2000a). However, it should be noted that membrane depolarization, i.e. the collapse or reduction in the magnitude of membrane potential, is not a good indication of cell death in itself, but rather an evidence of cell damage (Nebe-von-Caron *et al.*, 1998).

Estimation of membrane potential by fluorescence techniques is based on the use of lipophilic dyes with a delocalized positive or negative charge which therefore distribute across the membrane according to the electrical charge gradient (distributional probes) (Shapiro, 2000a). Carbocyanines, such as $DiOC_6(3)$, $DiOC_2(3)$, and $DiSC_3(5)$, are dyes with a delocalized positive charge which are attracted by cells with membrane potential; whereas oxonols, such as $DiBAC_4(3)$, are anionic dyes which can only penetrate cells when they are depolarized (Breeuwer and Abee, 2000; Cao-Hoang *et al.*, 2008). Once inside the cell, carbocyanines accumulate in the inner side of the membrane, where they initially bind to negatively charged phospholipid heads, and then also to the nonpolar fatty acid chains; whereas oxonols bind to positively charged proteins (Sträuber and Müller, 2010). However, at high dye concentrations, both carbocyanines and oxonols can nonspecifically bind to other hydrophobic regions of the cell due to their lipophilic nature (Müller and Nebe-von-Caron, 2010). Dye accumulation in cell structures results in enhanced fluorescence intensity, sometimes accompanied with a shift in the emission spectrum, which depends on the magnitude of the membrane potential (Ueckert *et al.*, 1995; Cao-Hoang *et al.*, 2008). Generally, only actively growing cells generate a membrane potential that is large enough to be measured (Sträuber and Müller, 2010).

However, fluorescence intensity not only depends on membrane potential, but also on the amount of binding sites present in the cell and therefore on the total membrane surface (Müller and Nebe-von-Caron, 2010). This implies that cells with different sizes will exhibit different fluorescence intensity levels regardless their respective membrane potentials. To eliminate the measurement variance due to cell size heterogeneity, a ratio can be calculated between fluorescence intensity and a parameter directly related with cell size (ratiometric method), such as forward scatter light (FSC) in flow cytometry. In this method, dye concentrations in the nanomolar range are used to avoid

nonspecific binding (Sträuber and Müller, 2010). However, broad fluorescence distributions are obtained which do not allow the calibration of membrane potential (Novo *et al.*, 1999). To overcome this problem, (Novo *et al.*, 1999) proposed a ratiometric method based on the use of DiOC$_2$(3) at a concentration in the micromolar range. At this rather high concentration, cells are overloaded and intracellular fluorescent aggregates are formed, which show a shift from the green fluorescence emission of the monomeric form to red fluorescence emission (Sträuber and Müller, 2010). Red fluorescence depends both on membrane potential and cell size, whereas green fluorescence, which is still emitted, depends on cell size but not on membrane potential. The resulting ratiometric parameter gives narrow distributions and this allows calibration of membrane potential of Gram-positive bacteria, and optimum differentiation of membrane potential heterogeneity in Gram-negative bacteria (Shapiro, 2000a).

Nonspecific binding of dyes to hydrophobic regions of the cell may interfere with the accurate measurement of membrane potential. In the absence of such artifactual fluorescence, dyes should respond to depolarization and hyperpolarization of the cells. This is usually tested by using control samples of cells treated with different concentrations of ionophores, such as carbonyl cyanide *m*-chlorophenylhydrazone (CCCP), gramicidin and valinomycin (Shapiro, 2000a; Müller and Nebe-von-Caron, 2010). Other factors which may have an impact on results are the ionic strength and pH of the suspending medium and the presence of active efflux pumps (Cao-Hoang *et al.*, 2008). For example, high ionic strength may increase staining of active cells with anionic dyes or decrease staining with cationic dyes. If pH of the suspending medium is lower than the intracellular pH, the electrical gradient will be negligible.

Esterase activity

Esterases are present in all living organisms and their activity can be assessed by using the fluorogenic substrates previously described for the measurement

of intracellular pH. In these assays, fluorescence emission is related to both the presence of functional enzymes, which cleave the nonfluorescent substrate to a fluorescent product, and an intact membrane capable of retaining this polar fluorescent product (Sträuber and Müller, 2010). Thus, detection of esterase activity is also considered a dye-retention assay (Nebe-von-Caron *et al.*, 2000). Cells with damaged membranes are therefore unable to retain the fluorescent product even if they posses residual metabolic activity (Joux and Lebaron, 2000). However, since esterase activity is energy-independent, it can persist for long periods and be detected after cell death (Vives-Rego *et al.*, 2000).

Limitations to this approach include poor substrate uptake, leakage of the fluorescent product and active extrusion, which result in weak fluorescence signals, increased background fluorescence, and consequently in false negative results. Thus, the fluorogenic substrate selected to test a specific bacterial strain has to meet the requirements of optimum uptake and retention, which are dependent on its chemical characteristics. As previously stated, fluorescein (the flurorescent product of FDA) rapidly leaks out of the cells, whereas its derivative cF (the fluorescent product of cFDA) is better retained due to an additional negative charge. Moreover, Gram-negative bacteria show a relatively low permeability to FDA and therefore require permeabilization of the outer membrane (Joux and Lebaron, 2000; Takeuchi and Frank, 2001). Other fluorescein derivatives show improved retention, such as calcein AM, due to the presence of two imino-diacetic acid groups, and cFDA succinimidyl ester (cFDA SE), which binds to positively charged proteins and so additionally overcomes the problem with active extrusion (Breeuwer and Abee, 2000; Sträuber and Müller, 2010). Due to its better uptake and reduced extrusion and leakage, the ChemChrome V6 staining kit has been claimed to provide a more accurate assessment of esterase activity in a wide variety of Gram-positive and Gram-negative bacteria (Joux and Lebaron, 2000). This kit contains a buffer which supposedly contains ionophores to reduce dye extrusion (Parthuisot *et al.*,

2000). A different strategy to inhibit active extrusion systems consists in sealing the cells with glutaraldehyde after incubation with the probe (Sträuber and Müller, 2010). An additional factor affecting esterase activity measurements is the pH-dependent fluorescence emission of most of these probes, which results in weak signals at certain pH values. Mild acidification of the staining buffer can be used to reduce background fluorescence and therefore improve detection of cell-associated fluorescence (Müller and Nebe-von-Caron, 2010).

Dehydrogenase activity

The tetrazolium salt 5-cyano-2,3-ditolyl tetrazolium chloride (CTC) acts as an electron acceptor. The reduction of this soluble, colorless salt results in the formation of insoluble, fluorescent crystals (3-cyano-1,5-ditolyl formazan, CTF), which are retained if the cell has an intact membrane (Breeuwer and Abee, 2000; Joux and Lebaron, 2000; Shapiro, 2000b). The bulk of redox reactions occurring in bacterial cells are responsible for CTC reduction, but this has been primarily linked to the activity of dehydrogenases present in the electron transport chain (Smith and Mcfeters, 1997; Joux and Lebaron, 2000; Yoshida and Hiraishi, 2004). Therefore, CTC reduction is used as an indication of respiration either under aerobic or anaerobic conditions.

Incubation of cells with CTC needs optimization, since several factors affect its reduction. Thus, Yoshida and Hiraishi (2006) found that high staining efficiency was obtained at pH 6.5. The composition of the staining buffer has also an important role, since presence of phosphate at concentrations higher than 10 mM inhibits CTC reduction, whereas presence of reducing substances can lead to the abiotic reduction of CTC (Smith and Mcfeters, 1997). The addition of exogenous substrates, such as yeast extract, peptone and glucose, to the staining buffer allows the detection of cells which do not have enough endogenous carbon sources for CTC reduction and would otherwise be neglected (Yoshida and Hiraishi, 2004). This strategy has the additional advantage of increasing

the fluorescence signal, but care has to be taken to ensure that growth does not occur during incubation and that CTC reduction associated to the substrate is limited (Smith and Mcfeters, 1997; Joux and Lebaron, 2000). Staining efficiency is further improved by the addition of Meldola's Blue, which acts as an intermediate electron carrier, thus increasing the possibilities of CTC reduction in the electron transport chain (Yoshida and Hiraishi, 2004).

At the commonly used concentrations, CTC suppresses aerobic growth, hence its suggested toxicity (Ullrich *et al.*, 1996). However, Yoshida and Hiraishi (2004) showed that, rather than being a toxic effect, reduced growth is due to the competition of CTC with oxygen as the terminal electron acceptor, which reduces the synthesis of ATP and therefore the synthesis of proteins and transport of solutes, but not the respiratory activity itself. Another issue with the CTC reduction assay is the low staining efficiency reported for some bacterial species, which may derive from the varied configurations of their respiratory chains, with some species having low proton motive force or lacking a complete Kreb's cycle (Smith and Mcfeters, 1997).

2.2.2.2. *Fluorescence detection*

Technologies for fluorescence detection share many properties, but also have their own advantages and limitations, which determine their suitability for specific biological applications (Shapiro, 2000b; Wang *et al.*, 2010). Important selection criteria for bacterial physiology assessment include, for example: the detection limit, the counting accuracy in a given cell concentration range, the duration of the analysis, the type of sample, and the fluorescent probes which can be effectively excited and detected (Joux and Lebaron, 2000; Lemarchand *et al.*, 2001).

Fluorescence techniques can be broadly classified into (i) image-based techniques, which include fluorescence microscopy and solid-phase cytometry,

and (ii) non-image-based techniques, which include fluorescence spectroscopy and flow cytometry.

Fluorescence microscopy resolves fluorescence as a function of two (epifluorescence microscopy, EFM) or three (confocal laser scanning microscopy, CLSM; two-photon LSM) spatial coordinates and therefore allows direct visualization of cells and distribution of fluorescence over time. EFM is a standard technique to enumerate bacterial cells, especially from environmental samples. To obtain accurate microscopy counts, several microscopic fields with a sufficient number of homogeneously distributed cells have to be evaluated (Lemarchand *et al.*, 2001; Lisle *et al.*, 2004). Moreover, the detection of rare cells is difficult due to its low detection limit (1 cell per microscopic field). Therefore, obtaining microscopy counts is a time-consuming task, even when using automated systems (Joux and Lebaron, 2000; Lisle *et al.*, 2004). EFM provides limited information about the localization of fluorescence, as well as about fine details due to interferences from out-of-focus and scattered light. Conversely, CLSM is a higher resolution technique, which gives precise information about fluorescence localization, and therefore about cell structure and distribution of cells in solid samples (Joux and Lebaron, 2000; Shapiro, 2000b; Roche *et al.*, 2012). For that purpose, a laser beam rapidly scans the sample to section it optically and a computerized image is then built. However, CLSM has limitations in the detection of rare events and in some applications, such as the analysis of thick samples, due to strong light scattering from the laser which result in contrast reduction (Joux and Lebaron, 2000; Roche *et al.*, 2012). Two-photon LSM is considered an alternative to CLSM for the analysis of thick samples, since it improves sample excitation and fluorescence collection for a better spatial resolution and penetration at greater depths. The aforementioned microscopy techniques can be combined with spectroscopy analysis to obtain multiparametric fluorescence data. For example, in the case of fluorescence emission spectral imaging, a stack of images recorded at different wave-

lengths is obtained, whereas fluorescence lifetime imaging microscopy (FLIM) measures the kinetics of the de-excitation process of a fluorochrome, rather than fluorescence intensity, since the former provides an absolute quantity, i.e. it is not affected by factors such as fluorochrome concentration (Roche *et al.*, 2012).

Solid-phase cytometry combines the attributes of image and flow cytometry, and includes the analyses performed with a microscope-based laser scanning cytometer, or with the Chemunex ScanRDI system (Darzynkiewicz *et al.*, 1999; Joux and Lebaron, 2000). Laser scanning cytometry (LSC) allows the rapid and accurate detection of scattered light and fluorescence of several wavelengths from individual cells on a membrane filter or microscope slide, with a detection limit of 1 cell per surface (Darzynkiewicz *et al.*, 1999). The ScanRDI system is not a microscope-based instrument but has equivalent analytical capabilities to that of a laser scanning cytometer and improved performance, although its use is restricted to the analysis of filterable samples (Joux and Lebaron, 2000). It scans, detects and counts cells on the entire membrane filter in three minutes. Moreover, the laser scanning pattern is fully overlapping to ensure the detection of all cells, which are automatically discriminated from particles based on their optical and electronic properties (Yvon, 2006a). This system proved to be superior to EFM in the analysis of water in terms of accuracy, repeatability, and detection of rare cells (Lemarchand *et al.*, 2001; Lisle *et al.*, 2004).

Fluorescence spectroscopy measures the average fluorescence of samples, with high sensitivity and selectivity (Cao-Hoang *et al.*, 2008; Haugland, 2010c). Fluorescence emission can be measured in steady-state conditions or continuously to obtain time-resolved information. Moreover, multiple wavelengths can be detected at the same time, and multiple samples can be analyzed when using microtiter plate readers (Royer, 1995).

In contrast to bulk fluorescence measurements provided by fluorescence spectroscopy, flow cytometry analyzes multiple fluorescence and light scatter characteristics of single cells with high speed (thousands of cells per second) and accuracy (less than 5% of instrument error), which allows revealing the heterogeneity of physiological state of cells in a sample (Haugland, 2010c; Wang *et al.*, 2010). Moreover, cells with characteristics of interest can be physically separated for further analysis (cell sorting). Limitations of this technique include the inability to analyze the same cell over time, and a somewhat high detection limit (*ca.* 10^4 cells/mL) for some applications (Joux and Lebaron, 2000; Shapiro, 2000b).

3. Basic principles of flow cytometry

The term "cytometry" refers to any analytical method used to obtain quantitative information on the physical and chemical characteristics of individual cells and cellular constituents, mostly by optical means (Shapiro, 2003a). In the case of flow cytometry, the measurement of optical characteristics is done while cells suspended in a liquid stream pass individually through a beam of light (Givan, 2001a). The intersection of a cell with the illuminating beam results in light scattering and fluorescence emission, which can be intrinsic (autofluorescence) or associated with staining with fluorochromes (Carter and Ormerod, 2000; Veal *et al.*, 2000).

Due to the very nature of flow cytometry, it offers many advantages over other cytometry techniques. First, since the intensities of multiple parameters are simultaneously analyzed for each individual cell, it is possible to differentiate several cell types or populations based on correlation of such parameters, and thus to obtain a quantitative measure of sample heterogeneity. Additionally, a large number of cells are analyzed in few seconds, with measurement rates ranging from 1,000 to 100,000 cells per second, depending on the model of the instrument (Davey, 2002; Díaz *et al.*, 2010). This facilitates the rapid acquisition

of statistically meaningful data and increases the chances of detecting rare cell populations (Davey and Kell, 1996). Finally, some flow cytometers have the ability to physically separate selected cell populations for further analysis, a process known as cell sorting (Carter and Ormerod, 2000).

3.1. Instrumentation

A flow cytometer is typically composed of three major systems: (i) the fluidics, which transports the suspended cells to the analysis point; (ii) the optics, which includes one or more light sources with focusing lenses to illuminate the cells, and a system of lenses and optical filters to collect, separate and select light of specific wavelengths emerging from cells and direct it to the photodetectors; and (iii) the signal processing electronics, which converts the optical signals into electrical pulses proportional to light intensity and, in turn, into digital values.

3.1.1. Fluidics

The sheath fluid, usually a buffer suitable to preserve the physiological state of the cells, is used to transport the sample to the analysis point, i.e. the place where cells intersect the light beam. It flows continuously through a fluid line from a pressurized reservoir to the inlet of the flow cell, which is the unit where it joins the sample. After it leaves the reservoir, a filter eliminates suspended coarse particles to avoid clogging of the fluid circuit, whereas a purge line allows clearing of air bubbles. Moreover, a pressure regulator allows the setting of optimal flow conditions.

The sample tube is installed onto the sample port which delivers the sample into the flow cell by means of a manifold or a motor-driven syringe (Givan, 2001a). In the former design, the sample tube is tightly sealed around an O-ring, and air is introduced to force the sample through the injection tube; whereas, in the latter, a volume of sample is removed from the tube and in-

jected into the system, for a more precise control of the sample flow rate (Carter and Ormerod, 2000).

Thus, the fluidic system of a flow cytometer is composed of two fluid lines which feed the flow cell: the sheath fluid line and the sample line. The flow cell has a wide inlet for the sheath fluid and a smaller tube, placed in the center of this wide inlet, for the sample. This allows the sample to be slowly injected (typically at 10-60 μL/min) into the center of the faster sheath fluid stream (approximately, 20 km/h) (Veal *et al.*, 2000). The combination of sample and sheath fluid is then accelerated due to the presence of a narrowing channel known as the flow channel. Here is where the cells, which were in a random three-dimensional arrangement, are precisely aligned so that they will be uniformly illuminated one at a time by the light beam. This process is known as hydrodynamic focusing and, in most flow cytometers, is a consequence of the liquid stream circulating in laminar flow (Carter and Ormerod, 2000).

According to the principle of laminar flow, the velocity of the liquid front at the inlet is the same for the center and the walls. However, as it moves forward, the velocity of the liquid front at the walls is slowed down due to viscous drag. This creates a velocity gradient between the center and the outer layers of the liquid stream, with the center showing the highest velocity, which results in the formation of a parabola. As a result, the sample (with the suspended cells) is pulled towards the center and confined to a core within the sheath fluid stream (coaxial flow) (Carter and Ormerod, 2000). This occurs with no significant mixing due to pressure differences (Díaz *et al.*, 2010). Passing through the flow channel narrows this core (5-20 μm) and forces the cells to progress in single file while they are illuminated by the light beam (Givan, 2001a). After illumination, the liquid stream is directed to the waste tank.

The described flow cell design corresponds to that of most analytical flow cytometers, that is, those instruments that have no sorting capability. In these

cases, the flow cell is typically a flat-sided quartz cuvette, which is placed perpendicularly to the light beam (Carter and Ormerod, 2000; Sharpe, 2006).

The configuration of the fluidic system has important implications on the optimal operation of the flow cytometer. Thus, perturbations of the stream profile alter the alignment between the cells and the illuminating beam, and this results in broadening and fluctuation of the optical signals (Givan, 2001a). Such perturbations occur, for example, when the pressure in the fluid lines is modified due to partial clogging or the presence of air bubbles, or when the sample flow rate is too fast. In this case, the sample core within the sheath fluid stream widens and cells deviate from the central position. This may result in non uniform illumination and coincidence of more than one cell in the analysis point. Coincidence may also occur when analyzing a too concentrated cell suspension, since cells will flow too close to each other through the light beam.

3.1.2. Optics

3.1.2.1. *Excitation optics*

The excitation optics includes one or more light sources, and lenses to focus and shape the light into a narrow beam.

3.1.2.1.1. Light sources

Arc lamps, lasers and light emitting diodes can be used as light sources, but most flow cytometers currently available use an assortment of lasers (Telford *et al.*, 2009). Lasers produce intense and coherent light, i.e. light that is monochromatic and focused to a tight spot. These characteristics make them the ideal light sources for flow cytometry (Carter and Ormerod, 2000), since high intensity light is required to efficiently illuminate the (very small) cells in very short time. Moreover, optimal excitation of fluorochromes occurs at specific light wavelengths.

Early analytical flow cytometers incorporated gas lasers, typically an air-cooled argon ion laser emitting blue light (488 nm) (Shapiro, 2000b; Telford *et al.*, 2003). Other gas lasers were less common, such as helium-neon lasers emitting red light (633 nm), and helium-cadmium lasers emitting UV light (325 nm). Advances in laser technology have led to the replacement of gas lasers by solid-state lasers (diode and diode-pumped solid-state, DPSS), which are small, inexpensive and have low maintenance requirements (Telford *et al.*, 2003; Telford, 2011). In diodes, electricity is pumped into a solid medium to generate light, rather than into a gas plasma tube (Telford, 2004). Red (635 nm) diode lasers were introduced in commercial cytometers many years ago, whereas UV (355 nm), violet (405 nm) and blue (488 nm) diode lasers were made current later on (Kapoor *et al.*, 2008). In DPSS lasers, light is generated by using a diode to pump a crystalline material, generally neodymium yttrium aluminum garnet (ND-YAG) (Telford, 2004). Currently available DPSS lasers include green (532 nm), blue (488 nm), and, more recently, yellow (561 nm) and orange (594 nm) sources (Telford *et al.*, 2009). Thus, solid-state laser technology has greatly expanded the availability of excitation wavelengths to virtually the complete visible light spectrum, and so the use of the increasing array of commercial fluorochromes for biological analysis (Telford, 2011).

Recently, Telford *et al.* (2009) evaluated supercontinuum white light lasers as multiwavelength sources for flow cytometry analysis. These solid-state lasers emit a light mixture from the near-UV to the infrared with relatively high intensity levels. When combined with selective filtering of specific wavelengths, it proved comparable to single wavelength lasers. Thus, this is a promising advance in terms of cost, space and more efficient excitation of fluorochromes by precisely matching their excitation maxima.

3.1.2.1.2. Light shaping

The cross-sectional profile of a laser beam is a symmetrical spot of 1-2 mm in diameter, where intensity decreases across its radius (Givan, 2001a). However, for flow cytometry analysis, the laser beam should be higher in width than the sample core, and lower in height than the smallest particle in the sample (Carter and Ormerod, 2000). To approach these characteristics, that is, to produce an elliptical spot (*ca.* 20 by 60 μm), combinations of cylindrical lenses are used. This provides optimal tolerance to deviation of the cells from the sample core center (width dimension), and resolution of the optical signals generated by each cell (height dimension) (Givan, 2001a).

3.1.2.2.   *Collection optics*

Cells scatter light as a result of the intersection with the laser beam in the analysis point. Light that is scattered with two different angles from the laser beam is used to obtain information on the physical characteristics of cells. The light scattered to a small angle (generally, 0.5°) is known as FSC light, whereas the light scattered to a 90° angle is known as side scatter (SSC) light (Givan, 2001a). The biological significance of these parameters will be discussed later in this section. Moreover, if fluorescent compounds are present, cells will emit light of colors different from that of the excitation source (fluorescent light).

The collection optics is located around the analysis point and includes collection lenses and optical filters. A forward collection lens is used to gather the FSC light cone, whereas a right-angle collection lens is used to gather the SSC and fluorescent light cones (Sharpe, 2006). The obscuration bar is a metallic strip which is placed between the analysis point and the photodetector for the FSC light to prevent the excitation light beam from reaching it. This allows only the light scattered by cells to 0.5° to be detected (Givan, 2001a). Additionally, a neutral density filter can be also found in front of the FSC photodetector to attenuate the light arising from large particles (Shapiro, 2003b).

Optical filters, generally interference filters, are used to separate the mixture of SSC and fluorescent light and direct selected wavelengths to specific photodetectors. Three types of filters can be defined in terms of their light transmission behavior: (i) short-pass filters, which transmit light below a defined wavelength; (ii) long-pass filters, which transmit light longer than a defined wavelength; and (iii) band-pass filters, which transmit light over a narrow range of wavelengths. Short-pass and long-pass filters are generally used in the form of dichroic filters, which are placed after the right-angle collection lens to simultaneously split light into different specific wavelengths and direct it to specific directions where the photodetectors are located (Carter and Ormerod, 2000). Conversely, band-pass filters are placed in front of a photodetector to further restrict the light wavelengths it registers to a defined color.

The number of fluorescence detectors varies according to the model of the flow cytometer. Although more complex optical layouts can be found in modern flow cytometers, the standard layout for the benchtop flow cytometer FACSCalibur (BD Biosciences, San Jose, CA, USA) used in this thesis is presented in Figure 1.3.

3.1.3. Signal processing electronics

3.1.3.1. *Analog signal processing*

Photodetectors produce a current of electrons in response to the light photons reaching their surface and convert this current into voltage pulses (Snow, 2004). Two types of photodetectors can be found in most flow cytometers: photodiodes (PD) and photomultiplier tubes (PMT). PMT, which have an internal low-noise gain, are more sensitive to dim light signals than PD, which lack gain (Snow, 2004). Thus, gains applied to PMT allow the user to increase the response to light of these devices to make the signal large enough to be measured (Givan, 2001a). PMT are used to detect the weak SSC and fluorescence

signals, whereas use of PD is restricted to the detection of the strong FSC signal (Sharpe, 2006).
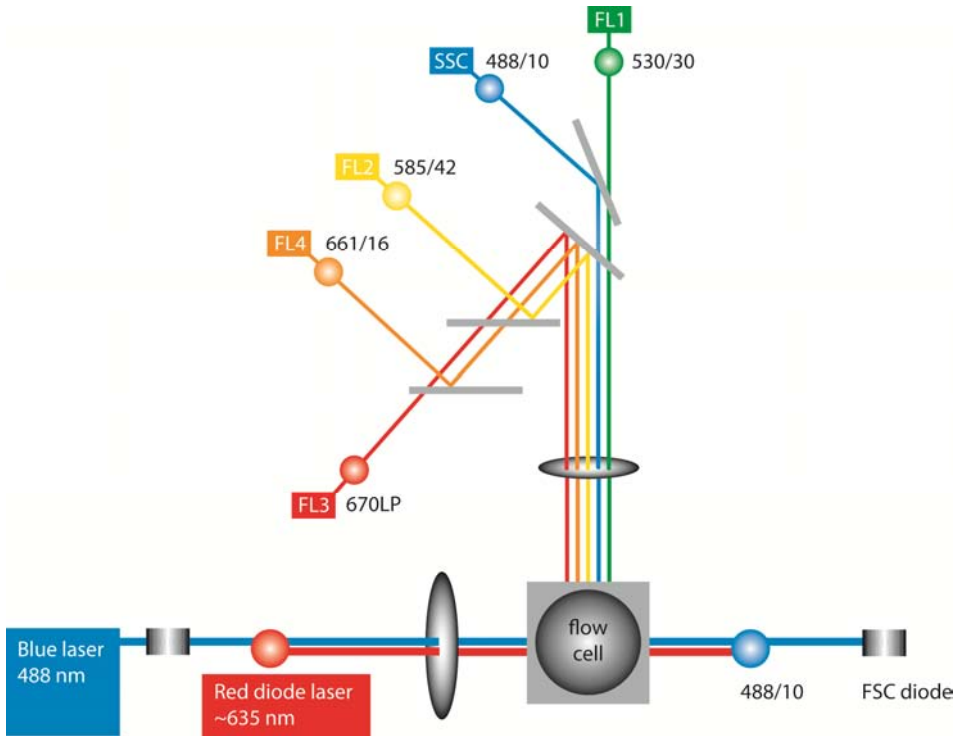
Figure 1.3   BD FACSCalibur optical path configuration. FL1: green fluorescence photodetector; FL2: yellow-orange fluorescence photodetector; FL3: far red fluorescence photodetector; FL4: red fluorescence photodetector; SSC: side scatter light photodetector; FSC: forward scatter light photodetector; DM: dichroic mirror; SP: short-pass filter; BP: band-pass filter. Courtesy and © by Becton, Dickinson and Company. Reprinted with permission.

Electrical signals can be further modulated after they leave the photodetectors by means of amplifiers, which operate at programmable gains. However, it is important to point out that inherent noise levels of such amplifiers increase at high gain values. This makes more advisable to increase the PMT gains first, since they have lower noise levels (Snow, 2004). Early flow cytometers incorporated both linear and logarithmic amplifiers. Logarithmic amplification in-

creases the dynamic range of the measurements, so that both cells with very weak signals and cells with very strong signals can be visualized on the same scale. However, logarithmic amplifiers introduce a significant error in the measurements, especially in the lower and upper decades of the signal intensity scale (Snow, 2004). Therefore, linear-to-logarithmic transformation is currently performed by the data acquisition and analysis software.

Thus, the PMT gains (commonly known as voltages), amplification type and amplifier gains are user-configurable settings which need to be adjusted according to the range of signal intensities in a certain analysis to make the cells with the weakest and the strongest signals appear in the bottom and the top of the intensity scale, respectively (Givan, 2001a).

When present in high proportions, background signals, i.e. light signals not associated with cells, interfere with the accurate acquisition of the signals of interest (Steen, 2000; Snow, 2004). Sources of such unwanted signals are the sample matrix and optical and electronic noise arising from some components of the flow cytometer (Sharpe and Wulff, 2006). By defining an electronic threshold for a specific trigger parameter (FSC, SSC or fluorescences), the user can limit the amount of background signals registered by the instrument, since only signals exceeding a pre-set intensity value will be further processed (Carter and Ormerod, 2000). If necessary, multiple trigger parameters can be defined in most flow cytometers (Sharpe and Wulff, 2006).

Additional circuits present in the analog signal processing system are the fluorescence compensation circuits. Fluorescence wavelengths transmitted by the optical filters fitting PMT are selected according to a narrow wavelength range where a fluorochrome emits with high efficiency. However, fluorescence emission of fluorochromes usually expands over a wider range of wavelengths. This results in the spillover of a part of the fluorescence signal emitted by a fluorochrome into PMT which are not dedicated to measuring that

fluorochrome. Compensation allows to mathematically correct for this effect (Roederer, 2002). For each pair of fluorochromes presenting overlap of their emission spectra, two analog subtraction circuits are necessary for compensation of such overlap. The simultaneous analysis of an ever-increasing number of colors and the use of fluorochromes that can be excited by multiple lasers, which require cross-beam compensation, have made analog compensation very disadvantageous. Therefore, and similarly to logarithmic transformation, most modern flow cytometers collect uncompensated data and compensation is performed by using the data acquisition and analysis software (Snow, 2004).

3.1.3.2. *Digital signal processing*

The last stage in signal processing is the conversion of analog voltage values (continuous distribution) into digital values (discrete distribution), which allow faster data processing by computer systems (Carter and Ormerod, 2000; Snow, 2004). Digitalization is performed by an analog-to-digital converter (ADC) chip, which groups the electrical signals into a defined number of ranges or channels (250; 1,014 or 65,536). Thus, each channel represents a certain range of light intensities and electrical signals are assigned accordingly. Light intensity ranges represented by each channel can be modified through the voltage and amplification settings, allowing proper resolution of the displayed data. This fact implies that light intensity values provided by the flow cytometer are relative and user-adjustable (Givan, 2001a).

3.2. Data display and analysis

Specific software packages for flow cytometry data analysis are used to display the measurements in one-, two- and three-dimensional plots, and extract statistics for selected groups of events (generic name referring to the output associated with either cells or background signals). Frequency histograms are one-dimensional plots commonly used when the distribution of only one fluorescence parameter has to be evaluated, e.g. to obtain the proportion of cells

positive for that fluorescence or their degree of positivity (fluorescence intensity). Moreover, comparison of several samples is possible by using the histogram overlay option present in most software packages (Lugli *et al.*, 2010). The measured parameters can also be correlated in any of the possible directions (e.g. FSC *vs.* SSC, fluorescence *vs.* SSC, fluorescence *vs.* FSC, etc.) by using different types of two-dimensional plots (Weaver, 2000; Givan, 2001b). In these plots, events are represented according to their pair of values for the displayed parameters. Dot plots have been the most widely used two-dimensional plots (Lugli *et al.*, 2010). However, in this monochromatic display, events with the same light intensities pile up, thus hiding information regarding the event frequency for certain intensities (Givan, 2001b). This limitation is overcome by using density-based plots. One such option is the contour plot, where zones with equal event density are joined by lines (Carter and Ormerod, 2000). Another option is the pseudocolor dot plot, which assigns a color to each level of event density (Lugli *et al.*, 2010). Moreover, event density can be represented by using different shades of grey in the so-called density plots. Three-dimensional isometric plots can also be used to obtain information about the frequency of the two-parameter correlated events, which is represented in the *z*-axis (Carter and Ormerod, 2000). Finally, three-dimensional plots can also be used to correlate three different parameters (Sharpe, 2006).

Once the data are suitably displayed, statistics (e.g. mean, mode or median light intensity, event frequency, event count, etc.) for a group of events of interest can be obtained by selecting them according to their defining characteristics. To accomplish this task, different types of regions encompassing such events can be drawn, such as markers in histograms, or ellipses, and polygons in two-dimensional plots (Carter and Ormerod, 2000). In some instances, the creation of a gate is necessary to fully define the cells of interest, i.e. several regions have to be sequentially drawn on the data displayed in two-dimensional plots of different parameter combinations. Thus, only cells ful-

filling all the specified characteristics will be included for statistical analysis (Givan, 2001b). This procedure is known as sequential gating and is the classical method for the analysis of flow cytometry data.

However, sequential gating has some limitations, especially when dealing with modern polychromatic flow cytometry data, which can include up to 20 parameters. Analysis of such complex data sets by sequential gating is very time-consuming and influenced by subjectivity, as well as prone to miss important information since only two- or three-dimensional data are understandable to the human brain. Therefore, effort is being recently devoted to the development of bioinformatic tools based both on supervised and unsupervised analysis methods (Lugli *et al.*, 2010).

3.3. Cell parameters measured by flow cytometry

3.3.1. Scattering signals

It is generally assumed that the intensity of FSC light is correlated to cell size, particularly to its cross-sectional area; whereas SSC light intensity is correlated to the cell surface characteristics, with rough surfaces scattering more light, and the presence of granular material in the cytoplasm (e.g. inclusion bodies), which increases the chances of incident light to be scattered to the side (Davey and Kell, 1996; Givan, 2001a; Shapiro, 2003c; Müller and Nebe-von-Caron, 2010). However, the relationship between light scatter and cell morphology is far more complex, since many other factors are involved. Thus, light scattered at forward and side angles also depend on the difference in refractive index between the cell and the surrounding medium, and the optical configuration of the flow cytometer, namely the geometry of the lasers and optical components and the excitation wavelength (Shapiro, 2003c; Müller and Nebe-von-Caron, 2010).

Intensity of FSC light increases with the difference between the refractive in-dex of a cell and its surrounding medium (Givan, 2001a). A well-known exam-ple of this effect is found when comparing the FSC signals of living and dead cells. Thus, even when dead cells are usually larger, they show lower FSC in-tensity than living cells, since their refractive index is similar to that of the surrounding medium due to permeabilization of their membranes (Shapiro, 2003c). Similarly, the refractive index of cells is modified by treatments with fixative agents, such as formaldehyde or formalin, and this results in decreased scattering (Vives-Rego *et al.*, 2000). Therefore, size comparison among cells with different refractive indices should be avoided. However, even in the case of refractive index-matched cells or particles, FSC does not always correlate monotonically with size, i.e. a 5-μm latex bead may give a stronger FSC signal than a 6-μm bead, due to the specific optical configuration of the instrument (Shapiro, 2000b; Müller and Nebe-von-Caron, 2010). Moreover, most flow cy-tometers show poor performance in the detection of FSC from small particles, and this makes them unsuitable to evaluate small differences in signal intensi-ty for this parameter.

Regarding the SSC light, it also depends on the cross-sectional area (or shape) of a cell. Thus, rod-shaped cells show a unimodal distribution of FSC intensi-ties, but a bimodal distribution of SSC intensities; whereas coccoid cells show unimodal distributions for both parameters (Hewitt and Nebe-von-caron, 2004). These characteristic light scatter profiles result from the sensitivity of the SSC light to the cross-sectional area of cells, i.e. the SSC bimodal distribu-tion for rod-shaped cells is attributed to changes in the orientation of the cells relative to the illuminating beam, whereas this effect is not observed in coccoid cells due to their symmetrical cross-sectional area.

Nevertheless, even if the exact biological meaning of light scattering might be not known for a specific experimental set-up, FSC and SSC (or light scatter and

fluorescence) usually allow to distinguish the cells from the background particles, and thus are used as gating parameters (Davey and Kell, 1996). Moreover, light scatter profiles have proved valuable to characterize microbial populations to a certain extent, e.g. species differentiation or assessment of intracellular product synthesis (see Müller and Nebe-von-Caron, 2010, for a review).

3.3.2. Fluorescence signals

A variety of functional parameters of cells can be evaluated by staining them with fluorochromes, i.e. molecules which are susceptible of emitting fluorescence (Figure 1.4). For this phenomenon to occur, the illuminating light beam provides photons ($h\upsilon_{EX}$) which are absorbed by such molecules, and as a result, electrons are raised from their ground state to high-energy orbitals (Givan, 2001c). This stage in the fluorescence emission process is called excitation. In this unstable excited electronic state (S_1'), the fluorochrome undergoes conformational changes and interacts with its molecular environment, resulting in partial dissipation of energy in the form of heat, and thus in the establishment of a semi-stable excited state (S_1) (Ormerod, 2000; Haugland, 2010c). Finally, the fluorochrome returns to its ground state (S_0) by releasing the energy excess in the form of light (radiative transition), i.e. fluorescence ($h\upsilon_{EM}$). Since thousands of photons are emitted by a single fluorochrome molecule, fluorescence techniques are highly sensitive (Haugland, 2010c). Due to partial energy loss during the excited-state lifetime, the emitted light has lower energy, and therefore higher wavelength (and different color), than the excitation light (Ormerod, 2000). The difference between the excitation and emission wavelengths is known as the Stokes shift. Unless the excited fluorochrome molecule is irreversibly destroyed due to high-intensity illumination (photobleaching), it can undergo the fluorescence process cyclically (Haugland, 2010c). This allows the fluorochrome to be excited and detected repeatedly during the short time that a cell is illuminated in the analysis point (Ormerod, 2000), thus in-

creasing the analytical signal and further improving the sensitivity of the technique.
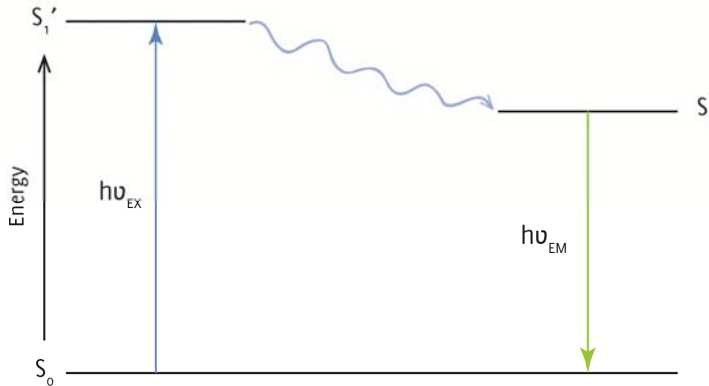
Figure 1.4 Jablonski diagram illustrating the transition between fluorochrome electronic states during absorption of light and fluorescence emission. $h\upsilon_{EX}$: photon of light emitted by the light source; $h\upsilon_{EM}$: photon of light emitted by the fluorochrome (fluorescence); S_0: ground state of the fluorochrome; S_1': singlet excited state of the fluorochrome; S_1: relaxed singlet excited state of the fluorochrome.

Since fluorochrome molecules are usually polyatomic, they absorb and emit light in a broad range of wavelengths, known as the excitation and emission spectra, respectively (Haugland, 2010c). These spectra are specific to each fluorochrome, since the particular light wavelengths that its constituent atoms can absorb and then emit are determined by the difference between the energy levels of their orbitals (Givan, 2001c). The wavelengths at which excitation and fluorescence emission are more efficient are the excitation and emission maxima, respectively. This explains why it is important to match as closely as possible the wavelength of the illuminating beam with the excitation maximum of a given fluorochrome, and the light wavelengths transmitted by an optical filter with its emission maximum. Thus, when several fluorescence parameters are simultaneously analyzed, the selected fluorochromes should be optimally excited by the same illuminating source, and have sufficiently sepa-

rated or minimally overlapped fluorescence emission spectra, that is, different Stokes shifts (Ormerod, 2000; Haugland, 2010c).

Other spectroscopic properties of fluorochromes are important to characterize its fluorescence output, such as the extinction coefficient and the fluorescence quantum yield. The extinction coefficient is a measure of the efficiency of a fluorochrome to absorb light at a given excitation wavelength, which usually corresponds to the excitation maximum. The fluorescence quantum yield is the amount of fluorescent light emitted by a fluorochrome over its entire emission spectrum relative to the amount of absorbed light. Brightness of a fluorochrome is proportional to the product of these two properties. Fluorescence signal is also quantitatively dependent on the fluorochrome concentration, the intensity of the excitation light, the length of the optical path, and the sensitivity of the flow cytometer (Haugland, 2010c). Additionally, background fluorescence signals, which may arise from intrinsic sample constituents (autofluorescence) or from unbound or nonspecifically bound fluorochrome molecules (reagent background), interfere with the sensitivity of the flow cytometry analysis.

Fluorescence emission spectra and quantum yields are dependent on environmental factors. One such factor is the interaction between fluorochrome molecules occurring during the excited-state lifetime, which results in a non-radiative transition to the ground state, i.e. no light is emitted (Givan, 2001c; Haugland, 2010c). Collisional quenching and Förster resonance energy transfer (FRET) are examples of non-radiative transitions. Fluorescence quenching refers to any process that causes a reduction in the quantum yield of a fluorochrome without a change in its emission spectrum (Haugland, 2010c). Collisional quenching occurs when an excited fluorochrome molecule contacts with another molecule, the quencher (e.g. oxygen, iodide) (Albani, 2004). In the case of FRET, light emitted by one fluorochrome (donor) is coupled to the exci-

tation of another fluorochrome (acceptor). As a result, fluorescence of the donor is quenched, whereas the acceptor emits fluorescence. The occurrence of this process depends on the spectral overlap of the emission spectrum of the donor and the excitation spectrum of the acceptor, as well as on the distance between these molecules (Haugland, 2010c). Other environmental factors include the solvent polarity and the pH of the aqueous medium, which cause shifts in the fluorescence emission spectrum of particular fluorochromes.

3.4. Flow cytometers for bacterial analysis

The instrument considered as the first flow cytometer was developed in 1947 for the analysis of dust particles and bacterial spores in aerosols (Winson and Davey, 2000). However, early commercial flow cytometers were originally designed for the analysis of eukaryotic, mainly mammalian, cells (Shapiro, 2000b). Since the volume of bacterial cells is 1,000-times lower than that of mammalian cells, and so it is the amount of stainable cellular components and derived optical signals (Davey, 2002; Müller and Davey, 2009), such instruments lacked sensitivity for the suitable analysis of bacteria, especially in the detection of light scatter signals, mainly as a consequence of significant optical noise (Steen, 2000). As a result, the use of flow cytometry in bacterial analysis has been traditionally limited by the difficulty in discriminating the cells from background particles, due to their small size and the presence of background fluorescence, especially in environmental samples (Veal *et al.*, 2000).

Limitations were progressively reduced due to technological advances (Winson and Davey, 2000). Although still designed for the analysis of mammalian cells, optimization of the instrument set-up made commercial instruments useful for a number of microbial applications. Thus, strategies to increase the collection of FSC light from bacterial cells include the adjustment of the angle of the photodetector, the manipulation of the obscuration bar, and the reduction or removal of the neutral density filter. Additionally, the FSC PD may be replaced

with a PMT, since, as stated before, PMT are more sensitive than PD. If this is not possible, it is advisable to set the trigger parameter to SSC rather than FSC (Sharpe and Wulff, 2006). Moreover, the sample flow rate can be reduced to increase the excitation time, and thus the emitted light (Steen, 2000). Finally, the sheath fluid, the solution used to suspend the cells, and other reagents, such as fluorochrome diluents, should be filtered through a 0.2-μm filter (Hewitt and Nebe-von-caron, 2004).

Steen and Lindmo first developed an instrument especially designed for bacterial analysis in 1979. It was an arc lamp-based instrument with a microscope-based flow cell, which was commercialized as the Skraton Argus, and updated during the mid-nineties by Bio-Rad Laboratories as the Bryte HS (Winson and Davey, 2000). However, this flow cytometer was discontinued many years ago. Nowadays, highly sensitive instruments have been developed for the analysis of small particles, i.e. particles within a size range from tens of nanometers to few micrometers, in which bacterial cells are included (1-5 μm) (Sharpe and Wulff, 2006). Examples of such flow cytometers are the BD Accuri C6, the Apogee A50 Micro, and the Partec CyFlow models Space, Cube 6 or Cube 8. Features in these improved instrument designs include, depending on the model: three (custom) detection angles for light scatter, light scatter resolution lower than 0.01 μm, improved fluorescence sensitivity, custom sample flow rates and so custom core diameters, higher acquisition rates (up to 100,000 event/s), and true volumetric absolute counting. With this, the minimum detectable particle size for these flow cytometers ranges from 0.05 to 0.50 μm.

Moreover, some flow cytometers have been specifically designed for routine quality control analysis in the food, pharmaceutical, or cosmetics industries, among others, to provide more rapid microbiological results than other methods and allow reducing the production cycle. The Chemunex D-Count and BactiFlow systems use (i) a pre-labeling buffer to recover injured cells and ac-

tivate spores, (ii) a proprietary fluorescein-derived non-fluorescent substrate to label viable cells and provide a total viable count, or other reagents especially developed to identify specific microorganisms for presence/absence testing, and (iii) counterstain agents that reduce background fluorescence. In the case of the D-Count analyzer, the cell labeling step is fully automated for up to 64 samples per batch, whereas BactiFlow is a compact analyzer which requires manual labeling. In either case, data are automatically analyzed and results are directly displayed as total cell counts per sample volume or a presence/absence statement, without the need for user interpretation. During data acquisition, a computerized process automatically distinguishes cells from background signals based on their optical and electronic characteristics, e.g. signal width, amplitude and area, fluorescence ratio, and channel-to-channel signal correlation. Examples of analytical applications for the food industry include the detection of yeasts in fermented milk products, bacteria and yeasts in fruit juices and soft drinks, and the specific detection of *Salmonella* spp. (Yvon, 2006b). The BD FACSMicroCount is also a fully automated flow cytometer with a load capacity of 42 samples per batch, which uses nucleic acid dyes for a membrane integrity-based viability assessment and performs both qualitative and quantitative tests. In contrast with the D-Count system, it allows some user customization of analysis, with pre-defined tests (which can be optimized) or user-defined tests, and graphical or tabular data display options (Steger, 2006).

4. Flow cytometry measurements of food-related bacteria

4.1. Challenges of flow cytometry detection of bacteria in food

Flow cytometry detection of bacterial cells in food is hindered by the release of a large number of food particles in the same size range during pre-analytical sample processing (Raybourne and Tortorello, 2003; Wilkes *et al.*, 2012). When

present in high counts, these background particles compromise the limit of detection (LOD) of flow cytometry and the reliability of the resulting data (Givan, 2001d; Shapiro, 2003b). Firstly, because cells will not form a visible cluster within the much larger cluster of background particles in a light scatter plot (Nebe-von-Caron *et al.*, 2000). Additionally, conferring fluorescence emission to cells may not be enough to make them detectable among background particles, since these particles can nonspecifically bind to fluorescent dyes (Gunasekera *et al.*, 2000; Cao-Hoang *et al.*, 2008; Doherty *et al.*, 2010). For example, nonspecific staining has been linked to the presence of protein and fat in food matrices such as milk (Gunasekera *et al.*, 2000), yoghurt and whey protein isolates (Doherty *et al.*, 2010), surimi-based products (Endo *et al.*, 2001), and non-dairy probiotic drinks (Maukonen *et al.*, 2006). Thus, if background fluorescence and cell fluorescence are similar, background particles may be mistakenly scored as cells (Comas-Riu and Rius, 2009). Therefore, only rather high cell concentrations can be reliably analyzed (Wilkes *et al.*, 2012). Secondly, a large amount of background particles will probably result in acquisition rates (event/s) exceeding the processing capability of the flow cytometer, which in turn will result in loss of data both from background and cells (Sharpe and Wulff, 2006). To address these limitations, it is necessary to separate bacterial cells from food particulate and optionally concentrate them before flow cytometry analysis, by using methods which, ideally, should be simple, rapid and inexpensive, and provide high recoveries while maintaining viability. Moreover, careful instrument set-up optimization, including adequate signal filtering strategies, can be of great help in reducing food matrix interference.

4.2. Sample preparation

A conventional sample preparation procedure for the microbiological analysis of foods can include dilution, homogenization and an enrichment step. Enrichment allows recovering and growing target pathogens, which are usually present in much lower counts than other microbiota. Moreover, it dilutes in-

terfering components of the food matrix. However, it does not allow enumeration of the initial bacterial load and is not generally compatible with rapid detection required in quality control in food industries (Stevens and Jaykus, 2004; Wilkes *et al.*, 2012; Rohde *et al.*, 2015).

Centrifugation and filtration are the most commonly used methods in pre-analytical sample processing for flow cytometry analysis, and meet the criteria of simplicity, rapidity, and cheapness. In simple high-speed centrifugation (8,000-60,000 × g), sedimentation of both bacterial cells and particles with densities equal to or higher than those from cells occurs. This is an efficient method to harvest cells from liquid culture media and some liquid foods, but in solid and semi-solid foods, a large quantity of food particles is also deposited. In the case of differential centrifugation, a low-speed centrifugation (< 1,000 × g) step is first applied for large food particle sedimentation while cells remain in the supernatant, and a subsequent high-speed centrifugation step is then used for cell sedimentation. However, some food particles may still sediment with the latter centrifugation step (Stevens and Jaykus, 2004). Large particles can also be removed from food homogenates by coarse filtration, which is generally performed using filter blender bags with a pore diameter ranging from 250 to 500 μm (Tortorello *et al.*, 1997; Stevens and Jaykus, 2004; Wilkes *et al.*, 2012; Buzatu *et al.*, 2013). Moreover, coarse filtration may be used as a pre-filtration step in order to facilitate further filtration through smaller pore size filters (e. g. 5 μm).

A decrease in bacterial recovery may occur during centrifugation and filtration, due to adsorption of cells to food particles and filters via nonspecific and reversible physicochemical interactions (e.g. hydrophobic and electrostatic interactions). Regarding centrifugation, fat globules may trap bacteria and avoid their sedimentation, whereas attachment to other food components can cause their sedimentation at low-speed centrifugation. In the case of filtration,

cells can be adsorbed to retained food particles or the filter (Stevens and Jaykus, 2004). To improve desorption of bacterial cells and increase sample filterability, food homogenates may be treated with enzymes (Tortorello *et al.*, 1997; Yamaguchi *et al.*, 2006) or detergents (Buzatu *et al.*, 2013), or subjected to changes in pH or ionic strength (Wilkes *et al.*, 2012). Addition of detergents, such as Triton X-100 or hydrochloric acid, can also serve the purpose of protein and fat flocculation, which results in increased centrifugation efficiency (Bunthof and Abee, 2002; Stevens and Jaykus, 2004; Wilkes *et al.*, 2012). However, the aforementioned treatments tend to impair cell viability (Stevens and Jaykus, 2004).

Bacterial cells can also be separated from food particles by density gradient centrifugation. In this case, the food homogenate is centrifuged in a medium capable of forming density gradients upon centrifugation, such as Percoll and Bact-Xtractor, which are nontoxic and low osmotic strength colloidal suspensions of polyvinylpyrrolidone-coated silica particles with a range of diameters (Lindqvist, 2000). This results in the migration of cells to the region with their same density and the formation of a band that is removed for further sample processing. Limitations of this approach include its high cost, difficult procedure, and decreased cell recovery when cells are trapped by fat at the gradient medium interfaces or when several wash steps are necessary to remove the gradient medium (Stevens and Jaykus, 2004).

Immunomagnetic separation has also been used in pre-analytical sample processing for flow cytometry analysis of enrichment broths from food, such as ground beef, apple juice and milk (Seo *et al.*, 1998a). Target bacteria in the food homogenate are specifically caught onto paramagnetic beads coated with antibodies. The complexes of bacteria and beads are recovered by using a magnet placed on the side of the sample-containing tube and washed several times to remove food particles and other microorganisms. Then, target bacteria can be

stained and analyzed by flow cytometry (Hibi *et al.*, 2007). However, as previously stated, some cells may be adsorbed to food particles and also paramagnetic beads may nonspecifically bind to food particles. Moreover, efficient detection requires relatively high cell concentrations (Stevens and Jaykus, 2004).

Background fluorescence interference due to food particle autofluorescence arising from pigments such as chlorophylls, carotenoids or flavonoids can be reduced by using chemical photosensitizers and light exposure. Wilkes *et al.* (2012) used sodium carbonate to photobleach spinach autofluorescence, but found that this treatment caused membrane permeabilization of cells. Buzatu *et al.* (2013, 2014) improved this approach by using Phloxine B and brief light exposure, which successfully reduced spinach and carrot autofluorescence without an impact on cell membrane integrity.

Pre-analytical sample processing for flow cytometry analysis usually combines several of the aforementioned separation methods according to the specific food physicochemical characteristics.

4.2.1. Liquid foods

As previously stated, milk lipid globules and protein micelles nonspecifically bind with fluorochromes and therefore interfere with detection of bacteria by flow cytometry (Gunasekera *et al.*, 2000). Partial removal of these interferences has been achieved by using a proteolytic treatment consisting in Triton X-100 and Proteinase K followed by high-speed centrifugation. Digested proteins and the upper lipid layer can then be removed and the bacterial pellet resuspended for flow cytometry analysis (McClelland and Pinder, 1994; Gunasekera *et al.*, 2000, 2003b; Bunthof and Abee, 2002; Yamaguchi *et al.*, 2003, 2006). Pre-treatment of other liquid foods, such as apple juice, cider, wine, beer or juice-based probiotic drinks, generally consists in high-speed centrifugation alone

or in combination with previous filtration (Yamaguchi *et al.*, 2003; Maukonen *et al.*, 2006; Quirós *et al.*, 2009; Díaz *et al.*, 2010; Wilkes *et al.*, 2012; Takahashi *et al.*, 2015). Wilkes *et al.* (2012) proposed gradient density centrifugation followed by filtration through a 5-μm filter for pre-treatment of viscous liquid foods, such as mayonnaise, horseradish, cheese and tartar sauces.

4.2.2. Semi-solid and solid foods

Wilkes *et al.* (2012) proposed a pre-treatment for high-fat content food, such as peanut butter, consisting in fat flocculation with hydrochloric acid, followed by low-speed centrifugation, recovery of the lower layer and high-speed cen- trifugation. These authors also applied this pre-treatment to high-fat content liquid foods, such as milk and half and half. For flow cytometry analysis of ba- by food purees, homogenates were coarse filtered, further filtered through a 5- μm filter and then treated by density gradient centrifugation. The same re- search group used this approach for the analysis of spinach, but also included detachment of bacterial cells from leaves with Tween 20 during homogeniza- tion in filter blender bags, a background fluorescence photobleaching step with Phloxine B, and a high-speed centrifugation step before 5-μm filtration and density gradient centrifugation (Buzatu *et al.*, 2013). A common ground beef pre-treatment consists in coarse filtration of homogenates, an optional proteolytic treatment with Triton X-100 and trypsin, and further filtration through a 5-μm filter, followed by centrifugation to pellet the cells (Tortorello *et al.*, 1997; Wilkes *et al.*, 2012).

4.3. Applications

4.3.1. Identification of bacteria

Flow cytometry detection of specific bacteria in foods has been achieved by using fluorescently labeled antibodies or oligonucleotide rRNA probes. In both cases, the most commonly used fluorescent label is fluorescein isothiocyanate

(FITC). Other common labels include phycobiliproteins, such as phycoerythrin (PE), indocarbocyanines, such as Cy3, Cy5 or Cy7, and Alexa dyes, such as Alexa Fluor 488 (Shapiro, 2000b; Vives-Rego *et al.*, 2000).

Immunofluorescence labeling of surface antigens is the preferred method for bacterial identification by flow cytometry in food, since this assay does not require permeabilization of cell membranes and therefore allows combination with fluorescent probes of physiological parameters (Nebe-von-Caron *et al.*, 2000; Hammes and Egli, 2010). For example, a FITC-labeled antibody in combination with CTC or PI has been used for detection of respiring or viable *E. coli* O157:H7 in ground beef, milk, and juice (Yamaguchi *et al.*, 2003) or spinach leaves (Buzatu *et al.*, 2013), respectively (Table 1.1). Another example is the detection of viable *Bifidobacterium animalis* spp. *lactis* in fermented milk products by using an Alexa Fluor 647-tagged antibody and cFDA (Geng *et al.*, 2014). Either indirect or direct immunostaining methods have been used. In the case of indirect staining methods, a fluorescently labeled secondary antibody is directed against a non-fluorescent primary antibody; whereas a fluorescently labeled primary antibody is used in direct staining methods to avoid extensive sample processing. The availability of improved kits for the conjugation of antibodies with fluorescent labels has enabled researchers to increasingly use this straightforward approach (Vives-Rego *et al.*, 2000; Müller and Nebe-von-Caron, 2010). Key factors in the reliability of an immunodetection assay include the careful generation and purification of antibodies and the assessment of absence of cross-reactivity in particular experimental conditions (Müller and Nebe-von-Caron, 2010). For example, Buzatu *et al.* (2013) used spinach inoculated with *E. coli* O157:H7 and a non-O157 *E. coli* strain or *Enterobacter cloacae* to assess cross-reactivity of an anti-*E. coli* O157:H7 antibody; whereas Geng *et al.* (2014) tested cross-reactivity of an antibody specific for *B. animalis* spp. *lactis* with lactic acid bacteria (*Lactobacillus delbrueckii* spp. *bulgaricus*, *Streptococcus thermophilus*, *Lactococcus lactis*) present in fermented milks. In both studies, the

absence of cross-reactivity was confirmed. Reliability of immunodetection assays is also affected by the fact that epitopes may be partially masked, more exposed or altered depending on the characteristics of the environment where the antigen-antibody reaction takes place, as well as on the physiological state of cells and cultivation conditions (Miller and Levinson, 1996; Hammes and Egli, 2010; Müller and Nebe-von-Caron, 2010; McCarthy and Culloty, 2011).

Alternatively, fluorescence *in situ* hybridization (FISH) of oligonucleotide rRNA probes in combination with flow cytometry detection has also proved a highly specific and sensitive assay for the detection of specific bacteria among the microbiota of food matrices (Rohde *et al.*, 2015). Thus, selection of target 16S or 23S rRNA sequences can either be based on the identification of specific bacterial species or groups, whereas the presence of thousands of copies of these targets provides intrinsic amplification of the fluorescence signal (Shapiro, 2000b; Hammes and Egli, 2010). FISH assays relying on the detection of 23S rRNA sequences are increasingly replacing the previously common targeted 16S rRNA sequences, since the former are longer and offer similar capacity for species differentiation (Rohde *et al.*, 2015). However, FISH assays do not allow simultaneous assessment of the physiological state of cells, since hybridization of rRNA probes requires fixation and membrane permeabilization (Joux and Lebaron, 2000; Nebe-von-Caron *et al.*, 2000; Hammes and Egli, 2010).

Table 1.1 Flow cytometry studies in food.

Reference	Food	Microorganism	Stress	Identification probe	Functional probe	Counterstain	Count type	LOD
Donnelly and Baigent, 1986	Milk	*Listeria monocytogenes*	None	Ab-Ab-FITC, Ab-FITC	None	PI	Total	6
Patchett *et al.*, 1991	Milk	*Escherichia coli*	None	None	None	EB	Total	ND
McClelland and Pinder, 1994	Milk	*Salmonella* Typhimurium	None	Ab-FITC	None	EB	Total	3
Seo *et al.*, 1998a	Milk	*E. coli* O157:H7	None	Ab-FITC	None	None	Total	NS
Gunasekera *et al.*, 2000	Milk	Total bacteria	None	None	None	SYTO BC	Total	4
Bunthof and Abee, 2002	Milk	*Lactobacillus plantarum*	None	None	None	SYTO 9	Total	5
		Total bacteria	None	None	None	SYTO 9	Total	NS
		Total bacteria	None	None	cFDA+TOTO	cFDA+TOTO	Intact active/ permeabilized; total	5

Reference	Food	Microorganism	Stress	Identifica-tion probe	Functional probe	Coun-terstain	Count type	LOD
Gunasekera et al., 2003b	Milk	*E. coli, Staphylococcus aureus, Pseudomonas fluorescens*	None	FISH-FITC	None	None	Total	3
			None	None	None	SYTO BC	Total	4
			None	None	CTC+DiBAC, SYTO 9+PI	None	Respiring/depolarized, live/dead	NS
Gunasekera et al., 2003a	Milk	*Pseudomonas* spp.	None	FISH-FITC	None	None	Total	NS
Yamaguchi et al., 2003	Milk	*E. coli* O157:H7	None	Ab-FITC	CTC	None	Respiring	3
Jang and Rhee, 2009	Milk	*Cronobacter* spp.	Caprylic acid and mild heat	None	SYTO 9+PI, PI	None	Viable/disrupted membrane, disrupted membrane	6[a]
Laflamme et al., 2008	Milk	*Bacillus cereus*	None	FISH-Alexa 488	None	None	Total	NS
Cassoli et al., 2010	Milk	Total bacteria	Refrigeration	None	None	EB	Total	NS
Lavilla et al., 2010	Milk	*Clostridium tyrobutyricum* spores	None	Ab-FITC, Ab-Alexa Fluor 488	None	None	Total	3

Reference	Food	Microorganism	Stress	Identification probe	Functional probe	Counterstain	Count type	LOD
Bunthof and Abee, 2002	Probiotic yoghurt drink	Lactic acid bacteria	None	None	cFDA+TOTO	cFDA+TOTO	Intact active/permeabilized; total	NS
Doherty *et al.*, 2010	Whey protein isolate, yoghurt	*Lactobacillus rhamnosus*	None, heat, acid, storage	None	TO+PI	None	Live/injured/dead	7[a]
Geng *et al.*, 2014	Fermented milk products	*Bifidobacterium animalis* ssp. *lactis*	None	Ab-Ab-Alexa Fluor 647	cFDA	None	Viable	5[a]
Seo *et al.*, 1998a	Apple juice	*E. coli* O157:H7	None	Ab-FITC	None	None	Total	NS
Yamaguchi *et al.*, 2003	Apple juice	*E. coli* O157:H7	None	Ab-FITC	CTC	None	Respiring	3
Quirós *et al.*, 2009	Apple juice, cider	*Lactobacillus hilgardii*	Freezing, freeze-drying	None	PI, ChemChrome V6	None	Dead, active	6[a]
Maukonen *et al.*, 2006	Probiotic juice-based drinks	Lactic acid bacteria	None	None	SYTO 9+PI, ChemChrome V6	None	Viable, viable	5

Reference	Food	Microorganism	Stress	Identification probe	Functional probe	Counterstain	Count type	LOD
Rodriguez and Thornton, 2008	Wine	Yeast	None	Ab-Ab-Alexa Fluor 488	PI	None	Viable	NS
		Oenococcus oeni	None	Ab-Alexa Fluor 488	PI	None	Viable	NS
Takahashi *et al.*, 2015	Beer	Total bacteria	None	FISH-FITC	None	None	Total	3
		Eukaryotic microorganisms	None	FISH-FITC	None	None	Total	NS
McClelland and Pinder, 1994	Egg	*S.* Typhimurium	None	Ab-FITC	None	EB	Total	3
Wilkes *et al.*, 2012	Spinach	*E. coli* O157:H7	None	Ab-FITC	PI	None	Viable	NS
Buzatu *et al.*, 2013	Spinach	*E. coli* O157:H7	None	Ab-FITC	PI	None	Viable	NS
Bisha and Brehm-Stecher, 2009a	Tomato	*S.* Typhimurium, *Salmonella* Newport	None	FISH-Cy5	None	None	Total	3[b]

Reference	Food	Microorganism	Stress	Identification probe	Functional probe	Counterstain	Count type	LOD
Bisha and Brehm-Stecher, 2009b	Alfalfa sprouts	*S.* Typhimurium	None	FISH-Cy5	None	None	Total	NS
Tamburini *et al.*, 2014	Carrot	*E. coli*	High pressure carbon dioxide	None	SYBR+PI, BCEcF AM	None	Intact/permeabilized/partially permeabilized, active	7[a]
Raymond and Champagne, 2015	Chocolate, cereal bar	*L. rhamnosus*	Freeze-drying, microencapsulation	None	SYTO 9+PI	SYTO 9+PI	Dead/viable; total	6[a]
Patchett *et al.*, 1991	Meat	*E. coli*	None	None	None	EB	Total	4
Tortorello *et al.*, 1997	Ground beef	*E. coli* O157:H7	None	Ab-FITC	None	None	Total	4
Seo *et al.*, 1998a	Ground beef	*E. coli* O157:H7	None	Ab-FITC	None	None	Total	NS
Seo *et al.*, 1998b	Ground beef	*E. coli* O157:H7	None	Ab-FITC	None	None	Total	3
Yamaguchi *et al.*, 2003	Ground beef	*E. coli* O157:H7	None	Ab-FITC	CTC	None	Respiring	3
Patchett *et al.*, 1991	Paté	*E. coli*	None	None	None	EB	Total	6

Reference	Food	Microorganism	Stress	Identification probe	Functional probe	Counterstain	Count type	LOD
Ferrentino *et al.*, 2015	Dry cured ham	*L. monocytogenes*	High pressure carbon dioxide	None	SYBR+PI	None	Intact/permeabilized/partially permeabilized	6[a]
Endo *et al.*, 2001	Surimi	*E. coli*	None	None	None	PI	Total	5

Ab: antibody

LOD: limit of detection (log CFU/mL)

ND: not detected

NS: not stated

[a]: when analysis for LOD determination was not conducted, cell concentration in flow cytometry sample is indicated.

[b]: log CFU/cm^2

Typically, the LOD of flow cytometry-based identification assays is 3 log colo-ny-forming unit (CFU)/mL, which corresponds to 4 log CFU/g in solid foods (Table 1.1). By way of illustration, this LOD has been reported for the patho-gens *E. coli* O157:H7 (Yamaguchi *et al.*, 2003), *S.* Typhimurium (McClelland and Pinder, 1994), and *S. aureus*, or the spoilage bacteria *Pseudomonas* spp. (Gunasekera *et al.*, 2003b) and *Clostridium tyrobutyricum* spores (Lavilla *et al.*, 2010) in milk. The LOD for *E. coli* O157:H7 in apple juice (Yamaguchi *et al.*, 2003) and ground beef (Seo *et al.*, 1998b; Yamaguchi *et al.*, 2003), for *S.* Typhimurium in egg (McClelland and Pinder, 1994), and for total bacteria in beer (Takahashi *et al.*, 2015) was also 3 log CFU/mL. Some authors have reported higher LOD. For example, Tortorello *et al.* (1997) reported a 4-log CFU/mL LOD for the de-tection of *E. coli* O157:H7 in ground beef pretreated by proteolysis and filtra-tion. Therefore, this high LOD was attributed to the presence of autofluorescent meat particles. A 6-log CFU/mL LOD was found for the detec-tion of *L. monocytogenes* in milk, with dilution being the only pre-treatment (Donnelly and Baigent, 1986). On the whole, the LOD of flow cytometry is ra-ther high for the detection of specific foodborne pathogens, since they are usually found in low concentrations in naturally contaminated food. As a re-sult, most studies intended for pathogen detection in quality control include enrichment steps of variable length, both for immunofluorescence (Donnelly and Baigent, 1986; McClelland and Pinder, 1994; Tortorello *et al.*, 1997; Seo *et al.*, 1998a; b; Wilkes *et al.*, 2012; Buzatu *et al.*, 2013) and FISH (Yamaguchi *et al.*, 2006; Laflamme *et al.*, 2008; Bisha and Brehm-Stecher, 2009a) assays.

4.3.2. Enumeration of bacteria

Enumeration of bacterial cells is required in food microbiology applications, such as the determination of growth, survival, or inactivation. Flow cytometry can rapidly accomplish this task when a calibrated suspension of microspheres with adequate concentration, fluorescence and size is added to samples. For higher precision and accuracy, modern flow cytometers allow direct meas-

urement of sample volume (Hammes and Egli, 2010; Müller and Nebe-von-Caron, 2010). Staining with nucleic acid dyes is particularly useful to discriminate bacterial cells from food particles and other background signals and therefore obtain accurate cell counts (Raybourne and Tortorello, 2003; Hammes and Egli, 2010; Müller and Nebe-von-Caron, 2010). As previously stated, fluorescence of such dyes is significantly increased when bound to nucleic acids, whereas they are virtually non-fluorescent when unbound. For this purpose, membrane-permeant dyes, such as SYTO 9 and SYTO BC, are commonly used (Table 1.1). Membrane-impermeant dyes, such as PI and EB, have also been used, but a membrane permeabilization treatment of the sample is required prior to staining if all cells need to be enumerated. Moreover, nonspecific staining of food particles can occur with these dyes and should be therefore evaluated (Gunasekera *et al.*, 2000; Doherty *et al.*, 2010).

Plating is the standard technique for comparison with flow cytometry cell counts during method development. A summary of regression analyses of cell counts in inoculated food obtained by these techniques is presented in Table 1.2. The strongest correlations were found for *S.* Typhimurium in milk and egg (McClelland and Pinder, 1994), and *Lactobacillus plantarum* in milk (Bunthof, 2002). The poorest fit of the linear model was found for respiring cells of *E. coli* O157:H7 in meat (Yamaguchi *et al.*, 2003). However, it should be reminded that discrepancy between plating and flow cytometry counts may be a consequence of the different physiological parameters being measured by each method, as well as to counting artifacts due to the presence of interfering signals in flow cytometry data.

Table 1.2 Studies including regression analyses of cell counts in food obtained by plating and flow cytometry.

Reference	Food	Microorganism	Staining	Concentration range (log CFU/mL)	Regression analysis
McClelland and Pinder, 1994	Milk	*Salmonella* Typhimurium	Ab-FITC+EB	3 - 7	$r = 0.999$
Bunthof and Abee, 2002	Milk	*Lactobacillus plantarum*	SYTO 9	5 - 9	$r = 0.9974$
Yamaguchi *et al.*, 2003	Milk	*Escherichia coli* O157:H7	Ab-FITC+CTC	2 - 8	$r^2 = 0.988$
Geng *et al.*, 2014	Milk	*Bifidobacterium animalis* ssp. *lactis*	Ab-Ab-Alexa	7 - 8	$r = 0.954$
Doherty *et al.*, 2010	Milk	*Lactobacillus rhamnosus*	PI+TO	1 - 10	$r = 0.93$
Gunasekera *et al.*, 2000	Milk	Total bacteria	SYTO BC	4 - 6	$r = 0.91$
Cassoli *et al.*, 2010	Milk	Total bacteria	EB	4 - 7.5	$r^2 = 0.8235$
Yamaguchi *et al.*, 2003	Apple juice	*E. coli* O157:H7	Ab-FITC+CTC	2 - 8	$r^2 = 0.972$
McClelland and Pinder, 1994	Egg	*S.* Typhimurium	EB	3 - 7	$r = 0.998$
Patchett *et al.*, 1991	Meat	*E. coli*	EB	3 - 8	$r = 0.95$
Yamaguchi *et al.*, 2003	Meat	*E. coli* O157:H7	Ab-FITC+CTC	2 - 8	$r^2 = 0.538$

Ab: antibody.

r: Pearson correlation coefficient, measure of linear correlation.

r^2: coefficient of determination, measure of fit of linear model.

4.3.3. Physiological state assessment

Flow cytometry detection of fluorescence associated with probes of cell physiological parameters has been used to assess the effect of processing and preservation methods on pathogens, fecal indicators, spoilage bacteria, and lactic acid bacteria in food matrices (Table 1.1). Examples include the analysis of *Cronobacter* spp. in reconstituted infant formula treated by a combination of caprylic acid and mild heat (Jang and Rhee, 2009), and of *L. monocytogenes* and *E. coli* on the surface of sliced cured ham (Ferrentino *et al.*, 2015) and carrots (Tamburini *et al.*, 2014), respectively, treated by high pressure carbon dioxide. The physiological state of lactic acid bacteria has been evaluated in commercial probiotic drinks (Bunthof and Abee, 2002; Maukonen *et al.*, 2006), and following the application of probiotic preservation processes, such as freeze-drying and microencapsulation (Raymond and Champagne, 2015), or environmental stresses found during food processing and the passage through the gastro-intestinal tract, such as heat and acid (Doherty *et al.*, 2010). Moreover, the effect of freezing and freeze-drying preservation treatments has also been assessed in lactic acid bacteria starter cultures for cider fermentation (Quirós *et al.*, 2009).

In these studies, membrane integrity is the most commonly assessed parameter, mainly by using combinations of PI and SYTO 9 (Gunasekera *et al.*, 2003b; Maukonen *et al.*, 2006; Jang and Rhee, 2009; Raymond and Champagne, 2015) or SYBR Green I (Tamburini *et al.*, 2014; Ferrentino *et al.*, 2015). PI has also been used alone (Jang and Rhee, 2009; Quirós *et al.*, 2009) or in combination with the membrane-permeant nucleic acid dye thiazole orange (TO) (Doherty *et al.*, 2010); whereas the membrane-impermeant dye TOTO has been combined with esterase activity assessment by cFDA (Bunthof and Abee, 2002). When combinations of PI and SYBR Green I or TO were used, researchers were able to detect cells with partially damaged membranes apart from cells with intact or damaged membranes (Tamburini *et al.*, 2014; Ferrentino *et al.*, 2015). In addi-

tion to cFDA, esterase activity has been determined by using ChemChrome V6 (Maukonen *et al.*, 2006; Quirós *et al.*, 2009) and BCEcF AM (Tamburini *et al.*, 2014). Assessment of multiple physiological parameters by using combinations of fluorescent probes provides a more accurate picture of the state of cells beyond culturability (Joux and Lebaron, 2000).

5. References

Abee, T., and J.A. Wouters. 1999. Microbial stress response in minimal processing. *International Journal of Food Microbiology*. 50:65–91.

Albani, J.R. 2004. Fluorescence quenching. *In* Structure and dynamics of macromolecules: absorption and fluorescence studies. Elsevier, Amsterdam. 141–192.

Ananta, E., D. Voigt, M. Zenker, V. Heinz, and D. Knorr. 2005. Cellular injuries upon exposure of *Escherichia coli* and *Lactobacillus rhamnosus* to high-intensity ultrasound. *Journal of Applied Microbiology*. 99:271–278.

Archer, D.L. 1996. Preservation microbiology and safety: evidence that stress enhances virulence and triggers adaptive mutations. *Trends in Food Science & Technology*. 7:91–95.

Audia, J.P., C.C. Webb, and J.W. Foster. 2001. Breaking through the acid barrier: an orchestrated response to proton stress by enteric bacteria. *International Journal of Medical Microbiology*. 291:97–106.

Barbesti, S., S. Citterio, M. Labra, M.D. Baroni, M.G. Neri, and S. Sgorbati. 2000. Two and three-color fluorescence flow cytometric analysis of immunoidentified viable bacteria. *Cytometry Part A*. 40:214–218.

Bautista-De León, H., C.A. Gómez-Aldapa, E. Rangel-Vargas, E. Vázquez-Barrios, and J. Castro-Rosas. 2013. Frequency of indicator bacteria, *Salmonella* and diarrhoeagenic *Escherichia coli* pathotypes on ready-to-eat cooked vegetable salads from Mexican restaurants. *Letters in Applied Microbiology*. 56:1–8.

Berger, C.N., S. V Sodha, R.K. Shaw, P.M. Griffin, D. Pink, P. Hand, and G. Frankel. 2010. Fresh fruit and vegetables as vehicles for the transmission of human pathogens. *Environmental Microbiology*. 12:2385–2397.

Berney, M., F. Hammes, F. Bosshard, H.-U. Weilenmann, and T. Egli. 2007. Assessment and interpretation of bacterial viability by using the

LIVE/DEAD BacLight kit in combination with flow cytometry. *Applied and Environmental Microbiology*. 73:3283–3290.

Berney, M., M. Vital, I. Hülshoff, H.-U. Weilenmann, T. Egli, and F. Hammes. 2008. Rapid, cultivation-independent assessment of microbial viability in drinking water. *Water Research*. 42:4010–4018.

Bisha, B., and B.F. Brehm-Stecher. 2009a. Simple adhesive-tape-based sampling of tomato surfaces combined with rapid fluorescence in situ hybridization for *Salmonella* detection. *Applied and Environmental Microbiology*. 75:1450–1455.

Bisha, B., and B.F. Brehm-Stecher. 2009b. Flow-through imaging cytometry for characterization of *Salmonella* subpopulations in alfalfa sprouts, a complex food system. *Biotechnology Journal*. 4:880–887.

Breeuwer, P., and T. Abee. 2000. Assessment of viability of microorganisms employing fluorescence techniques. *International Journal of Food Microbiology*. 55:193–200.

Breeuwer, P., J.L. Drocourt, F.M. Rombouts, and T. Abee. 1996. A novel method for continuous determination of the intracellular pH in bacteria with the internally conjugated fluorescent probe 5 (and 6-)-carboxyfluorescein succinimidyl ester. *Applied and Environmental Microbiology*. 62:178–183.

Brul, S., and P. Coote. 1999. Preservative agents in foods. Mode of action and microbial resistance mechanisms. *International Journal of Food Microbiology*. 50:1–17.

Bunthof, C.J. 2002. Flow cytometry, fluorescent probes, and flashing bacteria. Wageningen University.

Bunthof, C.J., and T. Abee. 2002. Development of a flow cytometric method to analyze subpopulations of bacteria in probiotic products and dairy starters. *Applied and Environmental Microbiology*. 68:2934–2942.

Bunthof, C.J., S. van Schalkwijk, W. Meijer, T. Abee, and J. Hugenholtz. 2001. Fluorescent method for monitoring cheese starter permeabilization and lysis. *Applied and Environmental Microbiology*. 67:4264–4271.

Buzatu, D.A., W.M. Cooper, C. Summage-West, J.B. Sutherland, A.J. Williams, D.A. Bass, L.L. Smith, R.S. Woodruff, J.M. Christman, S. Reid, R.K. Tucker, C.J. Haney, A. Ahmed, F. Rafii, and J.G. Wilkes. 2013. Photobleaching with phloxine B sensitizer to reduce food matrix interference for detection of *Escherichia coli* serotype O157:H7 in fresh spinach by flow cytometry. *Food Microbiology*. 36:416–425.

Buzatu, D.A., T.J. Moskal, A.J. Williams, W.M. Cooper, W.B. Mattes, and J.G. Wilkes. 2014. An integrated flow cytometry-based system for real-time, high sensitivity bacterial detection and identification. *PLoS ONE*. 9:e94254.

Cao-Hoang, L., P.A. Marechal, M. Lê-Thanh, P. Gervais, and Y. Waché. 2008. Fluorescent probes to evaluate the physiological state and activity of microbial biocatalysts: a guide for prokaryotic and eukaryotic investigation. *Biotechnology Journal*. 3:890–903.

Capozzi, V., D. Fiocco, M.L. Amodio, A. Gallone, and G. Spano. 2009. Bacterial stressors in minimally processed food. *International Journal of Molecular Sciences*. 10:3076–3105.

Carter, N.P., and M.G. Ormerod. 2000. Introduction to the principles of flow cytometry. *In* Flow cytometry. A practical approach. M.G. Ormerod, editor. Oxford University Press, Oxford. 1–22.

Cassoli, L.D., G. Francischetti, P.F. Machado, and G.B. Mourão. 2010. The relationship of flow cytometry results with classical measures of bacterial counts in raw refrigerated milk. *International Journal of Dairy Technology*. 63:297–300.

Cavicchioli, R., N. Saunders, and T. Thomas. 2009. Cold-shock response in microorganisms. *In* Extremophiles. C. Gerday and N. Glandsdorff, editors. Encyclopedia of Life Support Systems Publishers, Oxford. http://www.eolss.net.

Cenciarini-Borde, C., S. Courtois, and B. La Scola. 2009. Nucleic acids as viability markers for bacteria detection using molecular tools. *Future Microbiology*. 4:45–64.

Chilton, P., N.S. Isaacs, P. Manias, and B.M. Mackey. 2001. Biosynthetic requirements for the repair of membrane damage in pressure-treated *Escherichia coli*. *International Journal of Food Microbiology*. 71:101–104.

Chitarra, L.G., P. Breeuwer, R.W. van den Bulk, and T. Abee. 2000. Rapid fluorescence assessment of intracellular pH as a viability indicator of *Clavibacter michiganensis* subsp. *michiganensis*. *Journal of applied microbiology*. 88:809–816.

Comas-Riu, J., and N. Rius. 2009. Flow cytometry applications in the food industry. *Journal of Industrial Microbiology & Biotechnology*. 36:999–1011.

Considine, K.M., A.L. Kelly, G.F. Fitzgerald, C. Hill, and R.D. Sleator. 2008. High-pressure processing – effects on microbial food safety and food quality. *FEMS Microbiology Letters*. 281:1–9.

Corbitt, T.S., Z. Zhou, Y. Tang, S.W. Graves, and D.G. Whitten. 2011. Rapid evaluation of the antibacterial activity of arylene-ethynylene compounds. *ACS Applied Materials & Interfaces*. 3:2938–2943.

Cotter, P.D., and C. Hill. 2003. Surviving the acid test: responses of Gram-positive bacteria to low pH. *Microbiology and Molecular Biology Reviews*. 67:429–453.

Darzynkiewicz, Z., E. Bedner, X. Li, W. Gorczyca, and M.R. Melamed. 1999. Laser-scanning cytometry: a new instrumentation with many applications. *Experimental Cell Research*. 249:1–12.

Davey, H.M. 2002. Flow cytometric techniques for the detection of microorganisms. *Methods in Cell Science*. 24:91–97.

Davey, H.M. 2011. Life, death and in-between: meanings and methods in microbiology. *Applied and Environmental Microbiology*. 77:5571–5576.

Davey, H.M., and D.B. Kell. 1996. Flow cytometry and cell sorting of heterogeneous microbial populations: the importance of single-cell analyses. *Microbiological Reviews.* 60:641–696.

Davidson, M.P., T.M. Taylor, and S.E. Schmidt. 2013. Chemical preservatives and natural antimicrobial compounds. *In* Food microbiology: fundamentals and frontiers. M.P. Doyle and R.L. Buchanan, editors. ASM Press, Washington DC. 765–781.

Delaquis, P., S. Bach, and L.D. Dinu. 2007. Behavior of *Escherichia coli* O157:H7 in leafy vegetables. *Journal of Food Protection.* 70:1966–1974.

Díaz, M., M. Herrero, L.A. García, and C. Quirós. 2010. Application of flow cytometry to industrial microbial bioprocesses. *Biochemical Engineering Journal.* 48:385–407.

Doherty, S.B., L. Wang, R.P. Ross, C. Stanton, G.F. Fitzgerald, and A. Brodkorb. 2010. Use of viability staining in combination with flow cytometry for rapid viability assessment of *Lactobacillus rhamnosus* GG in complex protein matrices. *Journal of Microbiological Methods.* 82:301–310.

Donnelly, C.W., and G.J. Baigent. 1986. Method for flow cytometric detection of *Listeria monocytogenes* in milk. *Applied and Environmental Microbiology.* 52:689–695.

EFSA Panel on Biological Hazards. 2013. Scientific opinion on the risk posed by pathogens in food of non-animal origin. Part 1 (outbreak data analysis and risk ranking of food/pathogen combinations). *EFSA Journal.* 11:3025–3163.

Endo, H., Y. Nagano, H. Ren, and T. Hayashi. 2001. Rapid enumeration of bacteria grown on surimi-based products by flow cytometry. *Fisheries Science.* 67:969–974.

Erickson, M.C. 2010. Microbial risks associated with cabbage, carrots, celery, onions, and deli salads made with these produce items. *Comprehensive Reviews in Food Science and Food Safety.* 9:602–619.

Ferrentino, G., S. Tamburini, K. Bath, P. Foladori, S. Spilimbergo, and O. Jousson. 2015. Application of culture-independent methods for monitoring *Listeria monocytogenes* inactivation on food products. *Process Biochemistry*. 50:188–193.

Frankel, G., R.K. Shaw, D. Pink, C.N. Berger, and P. Hand. 2009. Fresh produce as a potential vector for bacterial human pathogens. *Microbial Biotechnology*. 2:595–597.

Fratamico, P.M., and L.K. Bagi. 2007. Comparison of methods for detection and isolation of cold- and freeze-stressed *Escherichia coli* O157:H7 in raw ground beef. *Journal of Food Protection*. 70:1663–1669.

García, D., P. Mañas, N. Gómez, J. Raso, and R. Pagán. 2006. Biosynthetic requirements for the repair of sublethal membrane damage in *Escherichia coli* cells after pulsed electric fields. *Journal of Applied Microbiology*. 100:428–435.

Geng, J., C. Chiron, and J. Combrisson. 2014. Rapid and specific enumeration of viable Bifidobacteria in dairy products based on flow cytometry technology: a proof of concept study. *International Dairy Journal*. 37:1–4.

Givan, A.L. 2001a. Instrumentation: into the black box. *In* Flow cytometry. First principles. Wiley-Liss, New York, NY. 15–39.

Givan, A.L. 2001b. Information: harnessing the data. *In* Flow cytometry. First principles. Wiley-Liss, New York, NY. 42–57.

Givan, A.L. 2001c. Seeing the light: lasers, fluorochromes, and filters. *In* Flow cytometry. First principles. Wiley-Liss, New York, NY. 59–80.

Givan, A.L. 2001d. Cells from without: leukocytes, surface proteins, and the strategy of gating. *In* Flow cytometry. First principles. Wiley-Liss, New York, NY. 81–113.

Greig, J.D., and A. Ravel. 2009. Analysis of foodborne outbreak data reported internationally for source attribution. *International Journal of Food Microbiology*. 130:77–87.

Gunasekera, T.S., P. V Attfield, and D.A. Veal. 2000. A flow cytometry method for rapid detection and enumeration of total bacteria in milk. *Applied and environmental microbiology*. 66:1228–1232.

Gunasekera, T.S., M.R. Dorsch, M.B. Slade, and D.A. Veal. 2003a. Specific detection of *Pseudomonas* spp. in milk by fluorescence *in situ* hybridization using ribosomal RNA directed probes. *Journal of Applied Microbiology*. 94:936–945.

Gunasekera, T.S., D.A. Veal, and P. V Attfield. 2003b. Potential for broad applications of flow cytometry and fluorescence techniques in microbiological and somatic cell analyses of milk. *International Journal of Food Microbiology*. 85:269–279.

Hammes, F., and T. Egli. 2010. Cytometric methods for measuring bacteria in water: advantages, pitfalls and applications. *Analytical and Bioanalytical Chemistry*. 397:1083–1095.

Hammes, F., T. Broger, H.-U. Weilenmann, M. Vital, J. Helbing, U. Bosshart, P. Huber, R.P. Odermatt, and B. Sonnleitner. 2012. Development and laboratory-scale testing of a fully automated online flow cytometer for drinking water analysis. *Cytometry Part A*. 81:508–516.

Haugland, R.P. 2010a. Assays for cell viability, proliferation and function. *In* The Molecular Probes handbook. A guide to fluorescent probes and labelling technologies. M.T.Z. Spence, editor. Invitrogen, Carlsbad, CA. 665–738.

Haugland, R.P. 2010b. pH indicators. *In* The Molecular Probes handbook. A guide to fluorescent probes and labelling technologies. M.T.Z. Spence, editor. Invitrogen, Carlsbad, CA. 883–902.

Haugland, R.P. 2010c. Introduction of fluorescence techniques. *In* The Molecular Probes handbook. A guide to fluorescent probes and labelling technologies. M.T.Z. Spence, editor. Invitrogen, Carlsbad, CA. 2–9.

Hayouni, E.A., M. Bouix, M. Abedrabba, J.-Y. Leveau, and M. Hamdi. 2008. Mechanism of action of *Melaleuca armillaris* (Sol. Ex Gaertu) Sm. essential

oil on six LAB strains as assessed by multiparametric flow cytometry and automated microtiter-based assay. *Food Chemistry*. 111:707–718.

Heard, G. 1999. Microbial safety of ready-to-eat salads and minimally processed vegetables and fruits. *Food Australia*. 51:414–420.

Herrero, M., C. Quirós, L.A. García, and M. Díaz. 2006. Use of flow cytometry to follow the physiological states of microorganisms in cider fermentation processes. *Applied and EnvironmentalMicrobiology*. 72:6725–6733.

Hewitt, C.J., and G. Nebe-von-Caron. 2004. The application of multi-parameter flow cytometry to monitor individual microbial cell physiological state. *Advances in Biochemical Engineering/Biotechnology*. 89:197–223.

Hewitt, C.J., G. Nebe-von-Caron, A.W. Nienow, and C.M. McFarlane. 1999. The use of multi-parameter flow cytometry to compare the physiological response of *Escherichia coli* W3110 to glucose limitation during batch, fed-batch and continuous culture cultivations. *Journal of Biotechnology*. 75:251–264.

Hibi, K., K. Mitsubayashi, H. Fukuda, H. Ushio, T. Hayashi, H. Ren, and H. Endo. 2007. Rapid direct determination using combined separation by prepared immunomagnetic and flow cytometry of *Flavobacterium psychrophilum*. *Biosensors & Bioelectronics*. 22:1916–1919.

Huang, H.-W., H.-M. Lung, B.B. Yang, and C.-Y. Wang. 2014. Responses of microorganisms to high hydrostatic pressure processing. *Food Control*. 40:250–259.

Jang, H.I., and M.S. Rhee. 2009. Inhibitory effect of caprylic acid and mild heat on *Cronobacter* spp. (*Enterobacter sakazakii*) in reconstituted infant formula and determination of injury by flow cytometry. *International Journal of Food Microbiology*. 133:113–120.

Johnson, E.A. 2003. Microbial adaptation and survival of foods. *In* Microbial stress adaptation and food safety. A.E. Yousef and V.K. Juneja, editors. CRC Press, Boca Raton, FL. 75–103.

Joux, F., and P. Lebaron. 2000. Use of fluorescent probes to assess physiological functions of bacteria at single-cell level. *Microbes and infection.* 2:1523–1535.

Joux, F., P. Lebaron, and T. Marc. 1997. Succession of cellular states in a *Salmonella typhimurium* population during starvation in artificial seawater microcosms. *FEMS Microbiology Ecology.* 22:65–76.

Juneja, V., and J. Novak. 2003. Adaptation of foodborne pathogens to stress from exposure to physical intervention strategies. *In* Microbial stress adaptation and food safety. A.E. Yousef and V. Juneja, editors. CRC Press, Boca Raton, FL. 31–53.

Juneja, V., and J. Novak. 2005. Pathogen resistance and adaptation to heat stress. *In* Understanding pathogen behaviour: virulence, stress response and resistance. M. Griffiths, editor. Woodhead Publishing, Cambridge. 422–441.

Kang, D.-H., and D.Y.C. Fung. 1999. Thin agar layer method for recovery of heat-injured *Listeria monocytogenes. Journal of Food Protection.* 62:1346–1349.

Kang, D.-H., and D.Y.C. Fung. 2000. Application of thin agar layer method for recovery of injured *Salmonella typhimurium. International Journal of Food Microbiology.* 54:127–132.

Kapoor, V., V. Karpov, C. Linton, F.V. Subach, V.V. Verkhusha, and W.G. Telford. 2008. Solid state yellow and orange lasers for flow cytometry. *Cytometry Part A.* 73:570–577.

Keer, J., and L. Birch. 2003. Molecular methods for the assessment of bacterial viability. *Journal of Microbiological Methods.* 53:175–183.

Kell, D.B., A.S. Kaprelyants, D.H. Weichart, C.R. Harwood, and M.R. Barer. 1998. Viability and activity in readily culturable bacteria: a review and discussion of the practical issues. *Antonie van Leeuwenhoek.* 73:169–187.

Laflamme, C., L. Gendron, N. Turgeon, G. Filion, J. Ho, and C. Duchaine. 2008. Rapid detection of germinating *Bacillus cereus* cells using fluorescent *in*

situ hybridization. *Journal of Rapid Methods and Automation in Microbiology.* 17:80–102.

Lavilla, M., I. Marzo, R. de Luis, M.D. Perez, M. Calvo, and L. Sánchez. 2010. Detection of *Clostridium tyrobutyricum* spores using polyclonal antibodies and flow cytometry. *Journal of Applied Microbiology.* 108:488–498.

Leistner, L. 2000. Basic aspects of food preservation by hurdle technology. *International Journal of Food Microbiology.* 55:181–186.

Lemarchand, K., N. Parthuisot, P. Catala, and P. Lebaron. 2001. Comparative assessment of epifluorescence microscopy, flow cytometry and solid-phase cytometry used in the enumeration of specific bacteria in water. *Aquatic Microbial Ecology.* 25:301–309.

Leyval, D., F. Debay, J.-M. Engasser, and J.-L. Goergen. 1997. Flow cytometry for the intracellular pH measurement of glutamate producing *Corynebacterium glutamicum*. *Journal of Microbiological Methods.* 29:121–127.

Liao, C.H., and W.F. Fett. 2005. Resuscitation of acid-injured *Salmonella* in enrichment broth, in apple juice and on the surfaces of fresh-cut cucumber and apple. *Letters in Applied Microbiology.* 41:487–492.

Lindqvist, R. 2000. Food microorganisms: buoyant density centrifugation. *In* Encyclopedia of separation science. M. Cooke and C.F. Poole, editors. Elsevier, Amsterdam. 2843–2849.

Lisle, J.T., M.A. Hamilton, A.R. Willse, and G.A. McFeters. 2004. Comparison of fluorescence microscopy and solid-phase cytometry methods for counting bacteria in water. *Applied and Environmental Microbiology.* 70:5343–5348.

Little, C.L., and I.A. Gillespie. 2008. Prepared salads and public health. *Journal of Applied Microbiology.* 105:1729–1743.

Lugli, E., M. Roederer, and A. Cossarizza. 2010. Data analysis in flow cytometry: the future just started. *Cytometry Part A.* 77:705–713.

Luo, Y., Q. He, and J.L. McEvoy. 2010. Effect of storage temperature and duration on the behavior of *Escherichia coli* O157:H7 on packaged fresh-

cut salad containing romaine and iceberg lettuce. *Journal of Food Science.* 75:390–397.

Mackey, B.M. 2000. Injured bacteria. *In* Microbiological safety and quality of food. B.M. Lund, T. Baird-Parker, and G.W. Gould, editors. Springer-Verlag, Gaithersburg, MD. 315–341.

Mackey, B.M., E. Boogard, C.M. Hayes, and J. Baranyi. 1994. Recovery of heat-injured *Listeria monocytogenes. International Journal of Food Microbiology.* 22:227–237.

Manini, E., and R. Danovaro. 2006. Synoptic determination of living/dead and active/dormant bacterial fractions in marine sediments. *FEMS Microbiology Ecology.* 55:416–423.

Maukonen, J., H.-L. Alakomi, L. Nohynek, K. Hallamaa, J.M. Leppämäki, and M. Saarela. 2006. Suitability of the fluorescent techniques for the enumeration of probiotic bacteria in commercial non-dairy drinks and in pharmaceutical products. *Food Research International.* 39:22–32.

McCarthy, M., and S.C. Culloty. 2011. Optimization of two immunofluorescent antibodies for the detection of *Escherichia coli* using immunofluorescent microscopy and flow cytometry. *Current Microbiology.* 62:402–408.

McCarthy, J., R. Holbrook, and P.J. Stephens. 1998. An improved direct plate method for the enumeration of stressed *Escherichia coli* O157:H7 from food. *Journal of Food Protection.* 61:1093–1097.

McClelland, R.G., and A.C. Pinder. 1994. Detection of *Salmonella typhimurium* in dairy products with flow cytometry and monoclonal antibodies. *Applied and environmental microbiology.* 60:4255–4262.

McClure, P. 2005. *Escherichia coli*: virulence, stress response, and resistance. *In* Understanding pathogen behaviour: virulence, stress response and resistance. M. Griffiths, editor. Woodhead Publishing, Cambridge. 240–278.

Miller, J.J., and S.S. Levinson. 1996. Interferences in immunoassays. *In* Immunoassay. E.P. Diamandis and T.K. Christopoulos, editors. Academic Press, Burlington, VT. 165–190.

Müller, S., and H.M. Davey. 2009. Recent advances in the analysis of individual microbial cells. *Cytometry Part A*. 75:83–85.

Müller, S., and G. Nebe-von-Caron. 2010. Functional single-cell analyses: flow cytometry and cell sorting of microbial populations and communities. *FEMS Microbiology Reviews*. 34:554–587.

Nebe-von-Caron, G., P.J. Stephens, and R.A. Badley. 1998. Assessment of bacterial viability status by flow cytometry and single cell sorting. *Journal of Applied Microbiology*. 84:988–998.

Nebe-von-Caron, G., P.J. Stephens, C.J. Hewitt, J.R. Powell, and R.A. Badley. 2000. Analysis of bacterial function by multi-colour fluorescence flow cytometry and single cell sorting. *Journal of Microbiological Methods*. 42:97–114.

Novo, D., N.G. Perlmutter, R.H. Hunt, and H.M. Shapiro. 1999. Accurate flow cytometric membrane potential measurement in bacteria using diethyloxacarbocyanine and a ratiometric technique. *Cytometry*. 35:55–63.

Nyachuba, D., and C. Donnelly. 2005. Sublethal injury, pathogen virulence and adaptation. *In* Understanding pathogen behaviour: virulence, stress response and resistance. M.W. Griffiths, editor. Woodhead Publishing, Cambridge. 152–198.

Oliver, J.D. 2005. The viable but nonculturable state in bacteria. *Journal of Microbiology*. 43:93–100.

Ormerod, M.G. 2000. Fluorescence and fluorochromes. *In* Flow cytometry. A practical approach. M.G. Ormerod, editor. Oxford University Press, Oxford. 23–34.

Park, S.-H., S. Ryu, and D.H. Kang. 2011. Improved selective and differential medium for isolation of *Escherichia coli* O157:H7. *Journal of Clinical Microbiology.* 49:405–408.

Parthuisot, N., P. Catala, K. Lemarchand, J. Baudart, and P. Lebaron. 2000. Evaluation of ChemChrome V6 for bacterial viability assessment in waters. *Journal of Applied Microbiology.* 89:370–380.

Patchett, R.A., J.P. Back, A.C. Pinder, and R.G. Kroll. 1991. Enumeration of bacteria in pure cultures and in foods using a commercial flow cytometer. *Food Microbiology.* 8:119–125.

Phadtare, S. 2004. Recent developments in bacterial cold-shock response. *Current Issues in Molecular Biology.* 6:125–136.

Quested, T.E., P.E. Cook, L.G.M. Gorris, and M.B. Cole. 2010. Trends in technology, trade and consumption likely to impact on microbial food safety. *International Journal of Food Microbiology.* 139:29–42.

Quirós, C., M. Herrero, L.A. García, and M. Díaz. 2009. Taking advantage of the flow cytometry technique for improving malolactic starters production. *European Food Research and Technology.* 228:543–552.

Rajkovic, A., N. Smigic, and F. Devlieghere. 2010. Contemporary strategies in combating microbial contamination in food chain. *International Journal of Food Microbiology.* 141:29–42.

Ramos, J.L., M.-T. Gallegos, S. Marqués, M.-I. Ramos-González, M. Espinosa-Urgel, and A. Segura. 2001. Responses of Gram-negative bacteria to certain environmental stressors. *Current opinion in microbiology.* 4:166–171.

Ramos-Villarroel, A., N. Aron-Maftei, O. Martín-Belloso, and R. Soliva-Fortuny. 2014. Bacterial inactivation and quality changes of fresh-cut avocados as affected by intense light pulses of specific spectra. *International Journal of Food Science and Technology.* 49:128–136.

Raybourne, R.B., and M.L. Tortorello. 2003. Microscopy techniques: DEFT and flow cytometry. *In* Detecting pathogens in food. T. McMeekin, editor. Woodhead Publishing, Cambridge. 186–216.

Raymond, Y., and C.P. Champagne. 2015. The use of flow cytometry to accurately ascertain total and viable counts of *Lactobacillus rhamnosus* in chocolate. *Food Microbiology*. 46:176–183.

Roche, Y., L. Cao-Hoang, J.M. Perrier-Cornet, and Y. Waché. 2012. Advanced fluorescence technologies help to resolve long-standing questions about microbial vitality. *Biotechnology Journal*. 7:608–619.

Rodriguez, S.B., and R.J. Thornton. 2008. Use of flow cytometry with fluorescent antibodies in real-time monitoring of simultaneously inoculated alcoholic-malolactic fermentation of Chardonnay. *Letters in Applied Microbiology*. 46:38–42.

Rodríguez-Lázaro, D., M. Hernández, M. D'Agostino, and N. Cook. 2006. Application of nucleic acid sequence-based amplification for the detection of viable foodborne pathogens: progress and challenges. *Journal of Rapid Methods and Automation in Microbiology*. 14:218–236.

Rodriguez-Romo, L., and A.E. Yousef. 2005. Cross-protective effects of bacterial stress. *In* Understanding pathogen behaviour: virulence, stress response and resistance. M. Griffiths, editor. Woodhead Publishing, Cambridge. 128–151.

Roederer, M. 2002. Compensation in flow cytometry. *Current Protocols in Cytometry*. 22:1.14.1–1.14.20.

Rohde, A., J.A. Hammerl, B. Appel, R. Dieckmann, and S. Al Dahouk. 2015. FISHing for bacteria in food – A promising tool for the reliable detection of pathogenic bacteria? *Food Microbiology*. 46:395–407.

Royer, C.A. 1995. Approaches to teaching fluorescence spectroscopy. *Biophysical Journal*. 68:1191–1195.

Seo, K.H., R.E. Brackett, and J.F. Frank. 1998a. Rapid detection of *Escherichia coli* O157:H7 using immuno-magnetic flow cytometry in ground beef, apple juice, and milk. *International Journal of Food Microbiology*. 44:115–123.

Seo, K.H., R.E. Brackett, J.F. Frank, and S. Hilliard. 1998b. Immunomagnetic separation and flow cytometry for rapid detection of *Escherichia coli* O157:H7. *Journal of Food Protection*. 61:812–816.

Shapiro, H.M. 2000a. Membrane potential estimation by flow cytometry. *Methods*. 21:271–279.

Shapiro, H.M. 2000b. Microbial analysis at the single-cell level: tasks and techniques. *Journal of Microbiological Methods*. 42:3–16.

Shapiro, H.M. 2003a. Overture. *In* Practical flow cytometry. John Wiley & Sons, Hoboken, NJ. 1–60.

Shapiro, H.M. 2003b. How flow cytometers work. *In* Practical flow cytometry. John Wiley & Sons, Hoboken, NJ. 101–224.

Shapiro, H.M. 2003c. Parameters and probes. *In* Practical flow cytometry. John Wiley & Sons, Hoboken, NJ. 273–410.

Sharpe, J. 2006. Flow cytometry instrumentation. *In* Guide to flow cytometry. S. Wulff, editor. Dako, Carpinteria, CA. 9–16.

Sharpe, J., and S. Wulff. 2006. Small-particle analysis. *In* Guide to flow cytometry. S. Wulff, editor. Dako, Carpinteria, CA. 69–75.

Shi, L., S. Günther, T. Hübschmann, L.Y. Wick, H. Harms, and S. Müller. 2007. Limits of propidium iodide as a cell viability indicator for environmental bacteria. *Cytometry Part A*. 71:592–598.

Smith, J.J., and G.A. Mcfeters. 1997. Mechanisms of INT and CTC reduction in *Escherichia coli* K-12. *Journal of Microbiological Methods*. 29:161–175.

Snow, C. 2004. Flow cytometer electronics. *Cytometry Part A*. 57:63–69.

Somolinos, M., D. García, R. Pagán, and B.M. Mackey. 2008. Relationship between sublethal injury and microbial inactivation by the combination of high hydrostatic pressure and citral or tert-butyl hydroquinone. *Applied and Environmental Microbiology*. 74:7570–7577.

Steen, H.B. 2000. Flow cytometry of bacteria: glimpses from the past with a view to the future. *Journal of Microbiological Methods*. 42:65–74.

Steger, A.M. 2006. Rapid enumeration of microorganisms using advanced analytical's RBD 3000. *In* Encyclopedia of rapid microbiological methods. M.J. Miller, editor. PDA, Bethesda, MD. 379–396.

Stephens, P.J., and B.M. Mackey. 2003. Recovery of stressed microorganisms. *In* Handbook of culture media for food microbiology. J.E.L. Corry, G.D.W. Curtis, and R.M. Baird, editors. Elsevier. 25–48.

Stevens, K.A., and L.-A. Jaykus. 2004. Bacterial separation and concentration from complex sample matrices: a review. *Critical Reviews in Microbiology*. 30:7–24.

Sträuber, H., and S. Müller. 2010. Viability states of bacteria. Specific mechanisms of selected probes. *Cytometry Part A*. 77:623–634.

Sutherland, J.P. 2005. Pathogen resistance and adaptation to low temperature. *In* Understanding pathogen behaviour: virulence, stress response and resistance. M. Griffiths, editor. Woodhead Publishing, Cambridge. 507–523.

Takahashi, M., Y. Kita, K. Kusaka, A. Mizuno, and N. Goto-Yamamoto. 2015. Evaluation of microbial diversity in the pilot-scale beer brewing process by culture-dependent and culture-independent method. *Journal of Applied Microbiology*. 118:454–469.

Takeuchi, K., and J.F. Frank. 2001. Confocal microscopy and microbial viability detection for food research. *Jounal of Food Protection*. 64:2088–2102.

Tamburini, S., P. Foladori, G. Ferrentino, S. Spilimbergo, and O. Jousson. 2014. Accurate flow cytometric monitoring of *Escherichia coli* subpopulations on solid food treated with high pressure carbon dioxide. *Journal of Applied Microbiology*. 117:440–450.

Telford, W.G. 2004. Small lasers in flow cytometry. *Methods in Molecular Biology*. 263:399–418.

Telford, W.G. 2011. Lasers in flow cytometry. *Methods in Cell Biology.* 102:375–409.

Telford, W.G., T.S. Hawley, and R.G. Hawley. 2003. Analysis of violet-excited fluorochromes by flow cytometry using a violet laser diode. *Cytometry Part A.* 54:48–55.

Telford, W.G., F. V Subach, and V.V Verkhusha. 2009. Supercontinuum white light lasers for flow cytometry. *Cytometry Part A.* 75:450–459.

Tong, S., A.P. Bos, and S. Brul. 2009. Assessing freeze-thaw and high pressure low temperature induced damage to *Bacillus subtilis* cells with flow cytometry. *Innovative Food Science & Emerging Technologies.* 10:9–15.

Tortorello, M.L., D.S. Stewart, and R.B. Raybourne. 1997. Quantitative analysis and isolation of *Escherichia coli* O157:H7 in a food matrix using flow cytometry and cell sorting. *FEMS immunology and medical microbiology.* 19:267–274.

Ueckert, J., P. Breeuwer, T. Abee, P.J. Stephens, G. Nebe-von-Caron, and P.F. ter Steeg. 1995. Flow cytometry applications in physiological study and detection of foodborne microorganisms. *International Journal of Food Microbiology.* 28:317–326.

Ueckert, J., G. Nebe-von-Caron, A.P. Bos, and P.F. ter Steeg. 1997. Flow cytometric analysis of *Lactobacillus plantarum* to monitor lag times, cell division and injury. *Letters in Applied Microbiology.* 25:295–299.

Ullrich, S., B. Karrasch, H. Hoppe, K. Jeskulke, and M. Mehrens. 1996. Toxic effects on bacterial metabolism of the redox dye 5-cyano-2,3-ditolyl tetrazolium chloride. *Applied and Environmental Microbiology.* 62:4587–4593.

Vaara, M. 1992. Agents that increase the permeability of the outer membrane. *Microbiological Reviews.* 56:395–411.

Veal, D.A., D. Deere, B. Ferrari, J. Piper, and P. V Attfield. 2000. Fluorescence staining and flow cytometry for monitoring microbial cells. *Journal of Immunological Methods.* 243:191–210.

Vives-Rego, J., P. Lebaron, and G. Nebe-von-Caron. 2000. Current and future applications of flow cytometry in aquatic microbiology. *FEMS Microbiology Reviews*. 24:429–448.

Vorob'eva, L.I. 2004. Stressors, stress reactions, and survival of bacteria: a review. *Applied Biochemistry and Microbiology*. 40:261–269.

Wang, Y., F. Hammes, K. De Roy, W. Verstraete, and N. Boon. 2010. Past, present and future applications of flow cytometry in aquatic microbiology. *Trends in Biotechnology*. 28:416–424.

Weaver, J.L. 2000. Introduction to flow cytometry. *Methods*. 21:199–201.

Wesche, A.M., J.B. Gurtler, B.P. Marks, and E.T. Ryser. 2009. Stress, sublethal injury, resuscitation, and virulence of bacterial foodborne pathogens. *Journal of Food Protection*. 72:1121–1138.

Wilkes, J.G., R.K. Tucker, J.A. Montgomery, W.M. Cooper, J.B. Sutherland, and D.A. Buzatu. 2012. Reduction of food matrix interference by a combination of sample preparation and multi-dimensional gating techniques to facilitate rapid, high sensitivity analysis for *Escherichia coli* serotype O157 by flow cytometry. *Food Microbiology*. 30:281–288.

Winson, M.K., and H.M. Davey. 2000. Flow cytometric analysis of microorganisms. *Methods*. 21:231–240.

Wu, V.C.H. 2008. A review of microbial injury and recovery methods in food. *Food Microbiology*. 25:735–744.

Wu, V.C.H., D.Y.C. Fung, D.H. Kang, and L.K. Thompson. 2001. Evaluation of thin agar layer method for recovery of acid-injured foodborne pathogens. *Journal of Food Protection*. 64:1067–1071.

Yamaguchi, N., M. Sasada, M. Yamanaka, and M. Nasu. 2003. Rapid detection of respiring *Escherichia coli* O157:H7 in apple juice, milk, and ground beef by flow cytometry. *Cytometry Part A*. 54:27–35.

Yamaguchi, N., H. Ohba, and M. Nasu. 2006. Simple detection of small amounts of *Pseudomonas* cells in milk by using a microfluidic device. *Letters in Applied Microbiology*. 43:631–636.

Yaqub, S., J.G. Anderson, S.J. MacGregor, and N.J. Rowan. 2004. Use of a fluorescent viability stain to assess lethal and sublethal injury in food-borne bacteria exposed to high-intensity pulsed electric fields. *Letters in Applied Microbiology*. 39:246–251.

Yoshida, N., and A. Hiraishi. 2004. An improved redox dye-staining method using 5-cyano-2,3-ditoryl tetrazolium chloride for detection of metabolically active bacteria in activated sludge. *Microbes and Environments.* 19:61–70.

Yoshida, N., and A. Hiraishi. 2006. A modified cyanoditolyl tetrazolium reduction method for differential detection of metabolically active Gram-positive and Gram-negative bacteria. *Microbes and Environments.* 21:272–277.

Yoshitomi, K.J., R. Zapata, K.C. Jinneman, S.D. Weagant, and W. Fedio. 2012. Recovery of *E. coli* O157 strains after exposure to acidification at pH 2. *Letters in Applied Microbiology.* 54:499–503.

Yousef, A.E., and P.D. Courtney. 2003. Basics of stress adaptation and implications in new-generation foods. *In* Microbial stress adaptation and food safety. A.E. Yousef and V. Juneja, editors. CRC Press, Boca Raton, FL. 1–30.

Yuste, J., M. Capellas, R. Pla, and D.Y.C. Fung. 2001. High pressure processing for food safety and preservation: a review. *Journal of Rapid Methods & Automation in Microbiology*. 9:1–10.

Yuste, J., M. Capellas, R. Pla, S. Llorens, D.Y.C. Fung, and M. Mor-Mur. 2003. Use of conventional media and thin agar layer method for recovery of foodborne pathogens from pressure-treated poultry products. *Journal of Food Science*. 68:2321–2324.

Yuste, J., M. Capellas, D.Y.C. Fung, and M. Mor-Mur. 2004. Inactivation and sublethal injury of foodborne pathogens by high pressure processing: evaluation with conventional media and thin agar layer method. *Food Research International*. 37:861–866.

Yvon, P. 2006a. Viability-based technologies: solid-phase cytometry using Chemunex ScanRDI. *In* Encyclopedia of rapid microbiological methods. M.J. Miller, editor. PDA, Bethesda, MD. 291–313.

Yvon, P. 2006b. Viability-based technologies: digital flow cytometry using Chemunex D-count and BactiFlow. *In* Encyclopedia of rapid microbiological methods. M.J. Miller, editor. PDA, Bethesda, MD. 357–378.

Zhao, W., R. Yang, H.Q. Zhang, W. Zhang, X. Hua, and Y. Tang. 2011. Quantitative and real time detection of pulsed electric field induced damage on *Escherichia coli* cells and sublethally injured microbial cells using flow cytometry in combination with fluorescent techniques. *Food Control.* 22:566–573.

Zhou, Z., T.S. Corbitt, A. Parthasarathy, Y. Tang, L.K. Ista, K.S. Schanze, and D.G. Whitten. 2010. "End-Only" functionalized oligo(phenylene ethynylene)s: synthesis, photophysical and biocidal activity. *The Journal of Physical Chemistry Letters.* 1:3207–3212.

Chapter 2. Introduction

1. Statement of the problem

Current trends in food consumption have evolved to minimally processed food, such as some ready-to-eat (RTE) meals. This can introduce new food safety hazards into the food supply, since elaboration of these products may not rely on traditional food processing strategies such as pasteurization and sterilization, but on preservation technologies with a milder effect on nutritional value, taste, color and flavor, but also on microorganisms. Indeed, ingredients of non-animal origin, which are present in RTE meals such as vegetable salads and salad meals, have been increasingly recognized as important vectors of foodborne diseases associated with bacteria, such as *Escherichia coli* O157:H7, *Salmonella* spp., *Campylobacter* spp., and *Listeria monocytogenes*. Moreover, some mild processing and preservation technologies have shown to render injured bacteria, which may lose their ability to multiply and are therefore not detected by conventional plate count procedures. However, injured bacteria may still retain a certain level of metabolic activity and structural integrity, recover in food and pose a hazard to health in the case of pathogenic bacteria. As a consequence, culture-based methods can overestimate effectiveness of processing and preservation treatments. Additionally, they require long time to result and do not provide information about the mode of action of treatments.

Flow cytometry, a rapid high throughput technique, coupled with fluorescent staining allows physiological state assessment beyond culturability. Due to its essential role in bacterial survival, membrane integrity is the physiological parameter most commonly assessed. Combined staining with a membrane-impermeant nucleic acid dye and a membrane-permeant nucleic acid dye reveals the presence of cells with damaged membranes, considered as dead, and cells with intact membranes. Intermediate cellular states, which are attributed to partial membrane damage typical of injured cells, can also be differentiated. Nevertheless, there is lack of consensus about a procedure to optimize the

staining protocol and results are often difficult to interpret, especially when it comes to unequivocally identifying injured cells. Moreover, the use of flow cytometry in bacterial analysis has been traditionally limited by the difficulty in discriminating the cells from interfering particles, due to their small size and the presence of background fluorescence, especially in food samples. Therefore, evaluation of pre-analytical sample processing methods to effectively reduce food particle interference is necessary to address this limitation.

2. Objectives

2.1. General objective

The general objective of the present thesis was to develop a flow cytometry assay based on cell membrane integrity assessment to accurately detect and enumerate injured pathogenic bacteria in RTE meals.

2.2. Specific objectives

a) To determine the staining conditions (i.e. dye concentrations, dye ratio, dye combination, and staining medium) and flow cytometer set up providing enhanced separation between populations of cells with intact and damaged membranes to optimally set a gate for cells with partially damaged membranes (injured cells).

b) To adapt the improved membrane integrity assay to specifically detect *E. coli* O157:H7 by immunofluorescence.

c) To evaluate the performance of centrifugal filtration during sample preparation for background particle reduction and recovery of *E. coli* O157:H7 cells from pasta salad, in comparison with other simple centrifugation- and filtration-based protocols.

d) To compare several signal filtering strategies in terms of their ability to reduce acquisition of data arising from background signals in salad sam-

ples, and therefore increase the signal-to-noise ratio and reduce the limit of detection of the assay.

e) To evaluate the efficacy of the improved protocols for injured cell detection by applying them to bacterial suspensions exposed to a range of food-related stresses and to refrigerated pasta salad containing a vinaigrette dressing.

3. Work plan

These objectives were met in the following experiments:

1. Improvement of flow cytometry assays for membrane integrity assessment using nucleic acid dyes to detect injured *Escherichia coli* O157:H7, *Salmonella* Enteritidis and *Listeria monocytogenes* (Figure 2.1): objectives **a** and **e**.

2. Sample preparation based on centrifugal filtration for flow cytometry membrane integrity assessment of *Escherichia coli* O157:H7 in RTE pasta salad (Figure 2.2): objectives **c** and **e**.

3. Improvement of a protocol for flow cytometry immunodetection and membrane integrity assessment of *Escherichia coli* O157:H7 (Figure 2.3): objectives **a** and **b**.

4. Flow cytometry immunodetection and membrane integrity assessment of *Escherichia coli* O157:H7 in RTE pasta salad during refrigerated storage (Figure 2.4 and 2.5): objectives **a**, **d** and **e**.

Staining optimization

Healthy and dead bacterial control suspensions (~10^7 CFU/mL)

Green-fluorescent dye concentration
- Unstained
- SYTO 9 (10-1,000 nM)
- SYTO 24 (20-95 nM)
- SYTO BC (0.5:10^5-1.0:10^5)

→ Green FI histogram overlay

SYTO concentration selection

Green-fluorescent dye-to-PI ratio
- SYTO 9 + PI (0.6-40.0 µM)
- SYTO 24 + PI (0.6-40.0 µM)
- SYTO BC + PI (0.6-40.0 µM)

→ Green FI *vs.* red FI plot

PI concentration selection
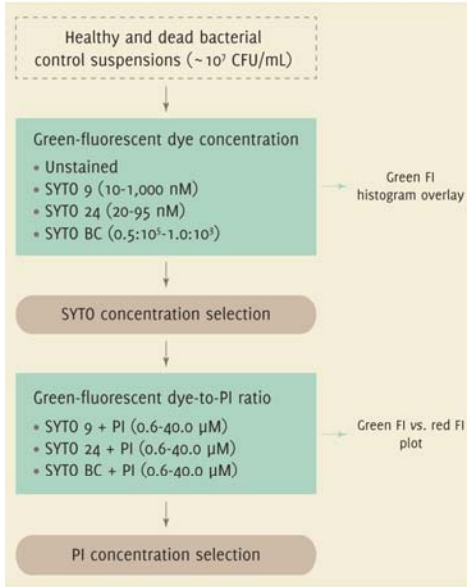
Screening of stress conditions inducing significant sublethal injury

Untreated bacterial suspensions (~10^7 CFU/mL)

Differential plating

→ mean %SI + SD = threshold value for significant %SI

Stress exposure time
- F (5, 10, 15 days)
- R (5, 10, 15, 21 days)
- H (5, 10, 15, 20 min)
- SR (5, 10, 15, 21 days)
- VR (5, 10, 15 days)
- CR (5, 10, 15 days)

Differential plating → %SI

Exposure time selection
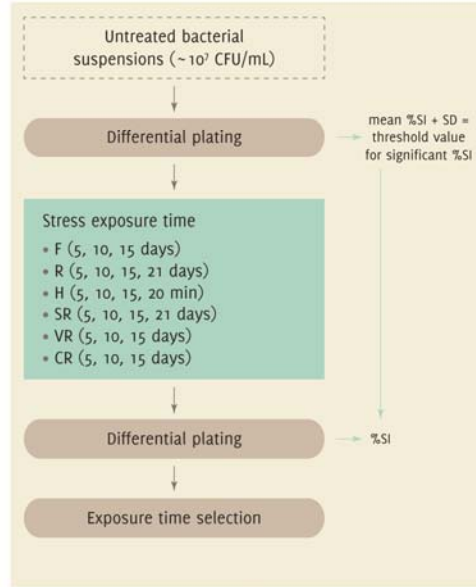
Evaluation of selected conditions in problem samples

Untreated bacterial suspensions (~10^7 CFU/mL)

Stress exposure

Dye combination
- SYTO 9 + PI
- SYTO 24 + PI
- SYTO BC + PI

Flow cytometry analysis

Fluorescence microscopy

Differential plating

Healthy cell count
Injured cell count

%SI
Healthy cell count
Injured cell count

Dye combination selection
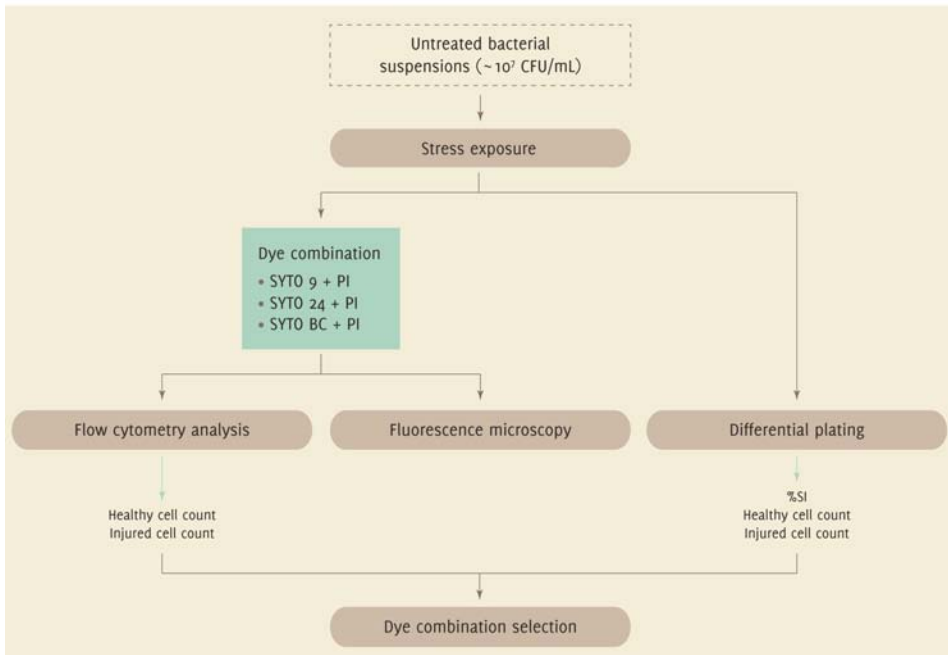
Figure 2.1 Work plan corresponding to experiment 1. FI: fluorescence intensity; PI: propidium iodide; %SI: sublethal injury; SD: standard deviation; F: freezing; R: refrigeration; H: heat; SR: potassium sorbate + refrigeration; VR: vinegar + refrigeration; CR: citric acid + refrigeration.
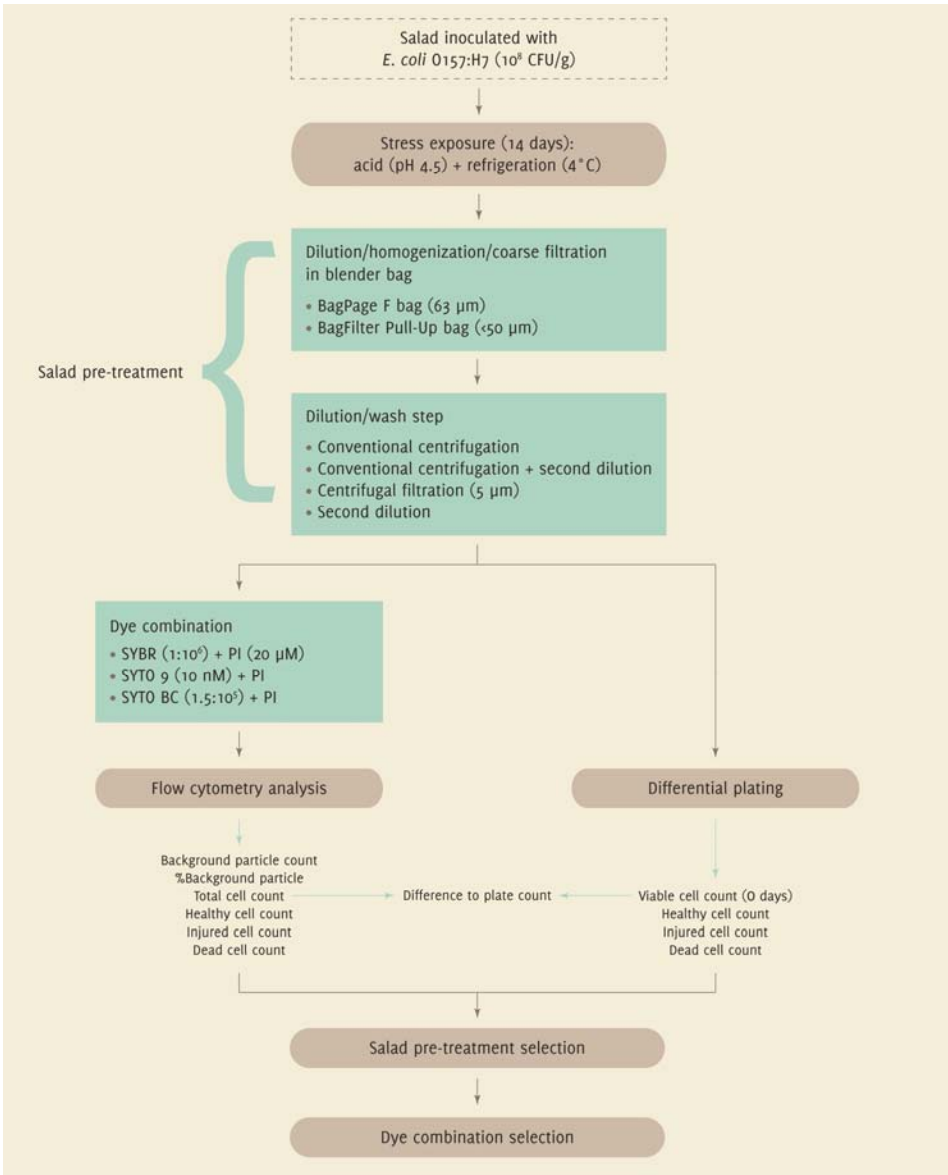
Figure 2.2 Work plan corresponding to experiment 2. SYBR: SYBR Green I; PI: propidium iodide.
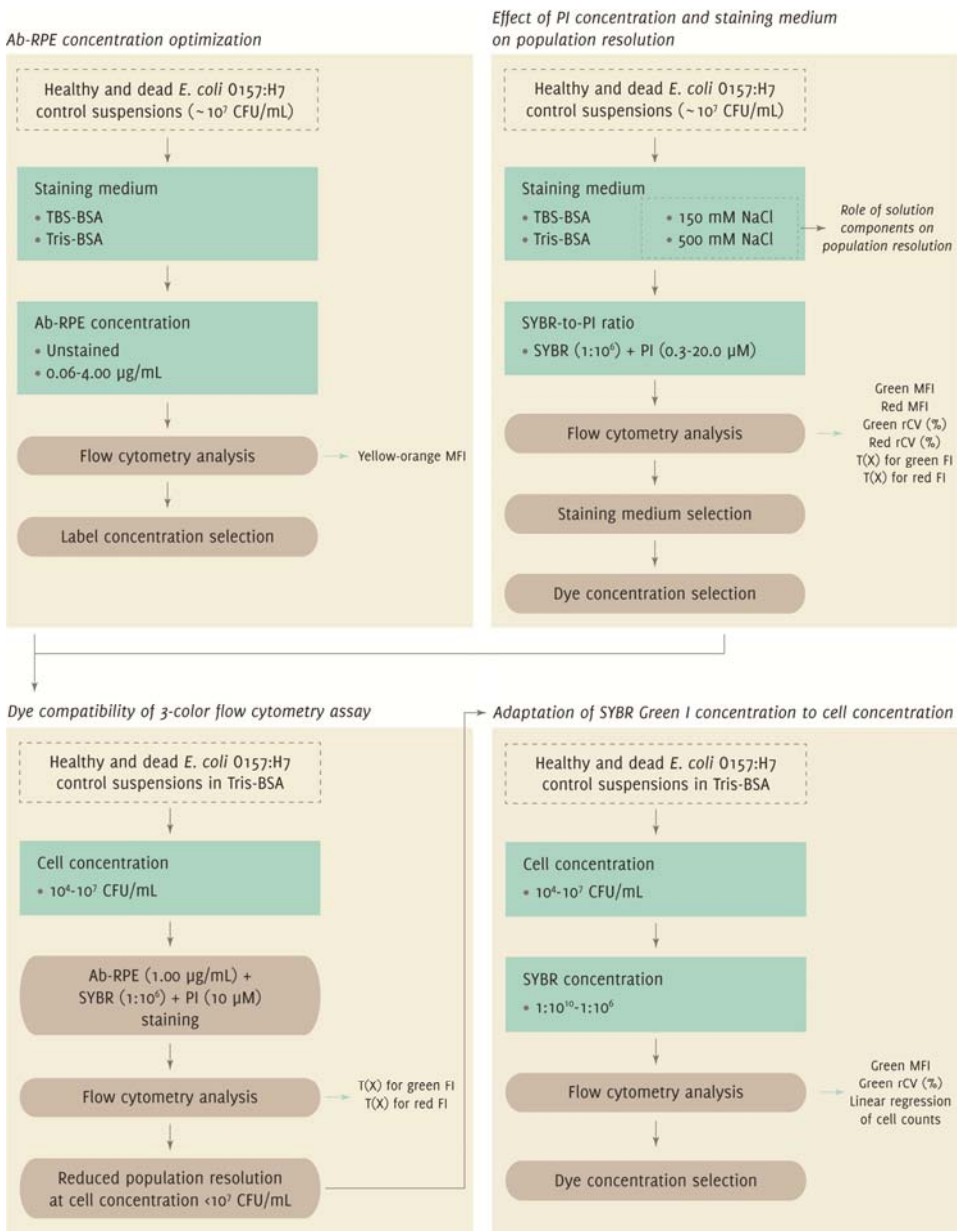
Figure 2.3 Work plan corresponding to experiment 3. Ab-RPE: antibody anti-*E. coli* O157:H7 conjugated to R-phycoerythrin; TBS-BSA: Tris buffered saline with bovine serum albumin; Tris-BSA: Tris with BSA; MFI: median fluorescence intensity; SYBR: SYBR Green I; PI: propidium iodide; rCV: robust coefficient of variation; T(χ): probability binning metric.
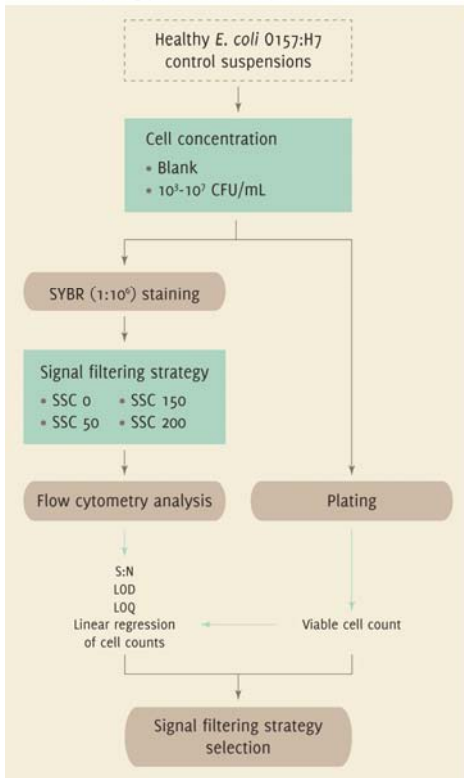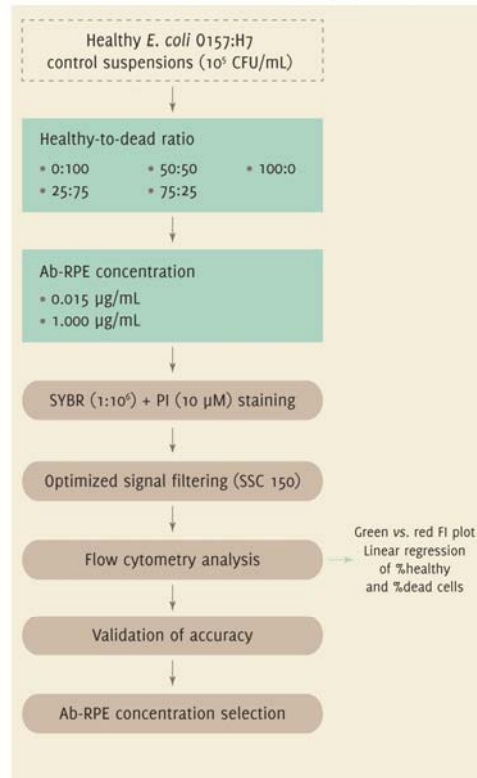
Figure 2.4 Work plan corresponding to experiment 4: protocol validation for control samples. SYBR: SYBR Green I; SSC: side scatter; S:N: signal-to-noise ratio; LOD: limit of detection; LOQ: limit of quantification; Ab-RPE: antibody anti-*E. coli* O157:H7 conjugated to R-phycoerythrin; FI: fluorescence intensity.
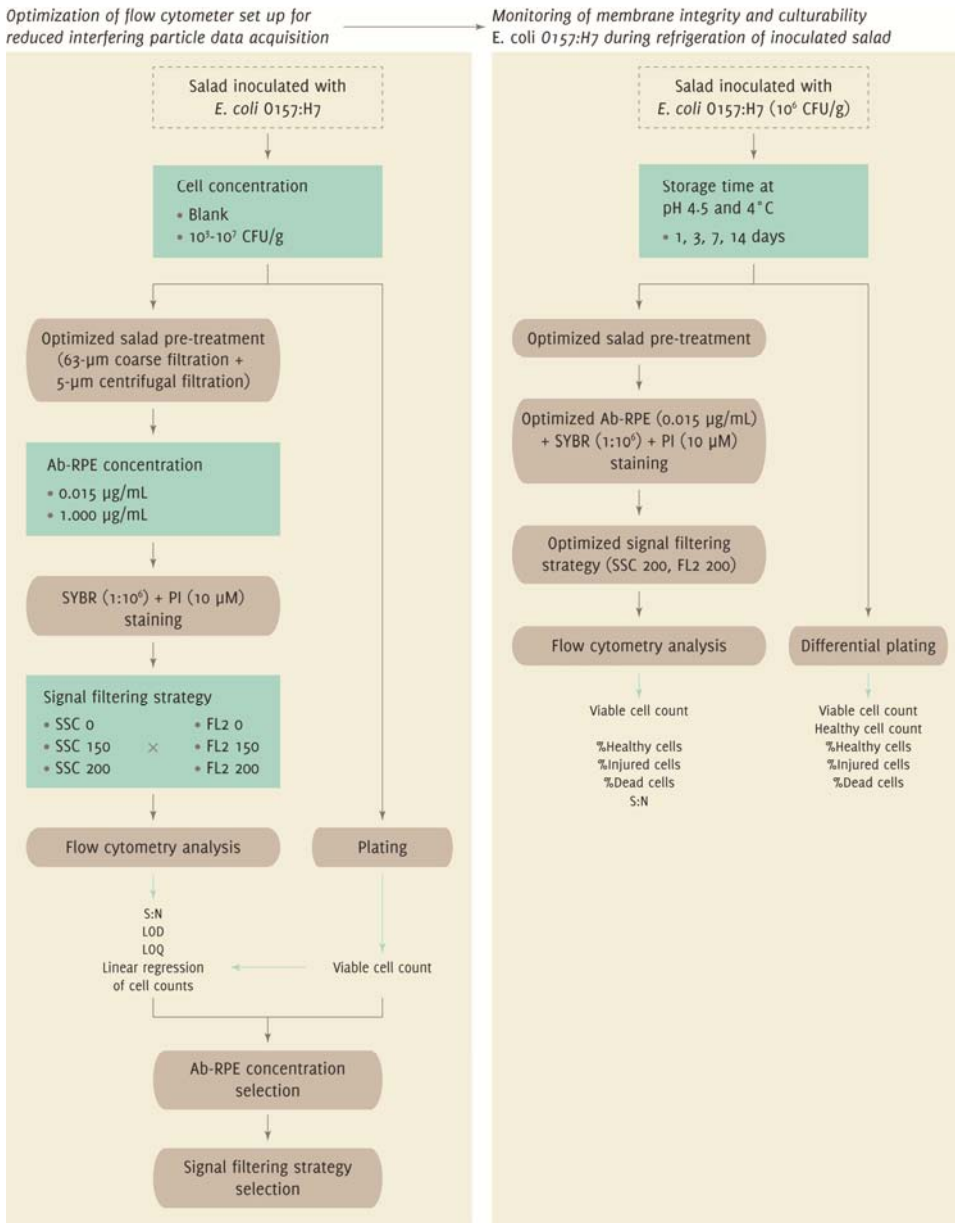
Figure 2.5 Work plan corresponding to experiment 4: protocol validation for salad samples and assessment of membrane integrity during refrigerated storage. Ab-RPE: antibody anti-*E. coli* O157:H7 conjugated to R-phycoerythrin; SYBR: SYBR Green I; PI: propidium iodide; SSC: side scatter; FL2: yellow-orange fluorescence; S:N: signal-to-noise ratio; LOD: limit of detection; LOQ: limit of quantification.

Chapter 3. Improvement of flow cytometry assays for membrane integrity assessment using nucleic acid dyes to detect injured *Escherichia coli* O157:H7, *Salmonella* Enteritidis and *Listeria monocytogenes*

Abstract

Food processing and preservation technologies can render injured microorganisms, which may not be detected by conventional plate count procedures. Flow cytometry combined with membrane-integrity fluorescent indicators has been widely used to rapidly infer the presence of healthy and dead bacterial cells. In the present study, *Escherichia coli* O157:H7, *Salmonella* Enteritidis and *Listeria monocytogenes* were exposed to food-related stresses (freezing, refrigeration, heat, potassium sorbate + refrigeration, vinegar + refrigeration, and citric acid + refrigeration) inducing sublethal injury as assessed by parallel plating on nonselective and selective media (differential plating method). Membrane integrity was then investigated by flow cytometry coupled to dual staining consisting of the red-fluorescent nucleic acid dye propidium iodide (PI) and the green-fluorescent nucleic acid dyes SYTO 9, SYTO 24 or SYTO BC. Optimization of staining protocols allowed detecting cells with partially damaged membranes. Injured cell counts tended to be higher with SYTO 24 and PI than with SYTO 9 or SYTO BC and PI. However, these results may have arisen from an artifact since atypically high red fluorescence was also observed. Adjusted staining protocols for PI and SYTO 9 or SYTO BC proved reliable for the detection of cells with partially damaged membranes. This approach can help to relate the effectiveness of a number of treatments to their effect on cell membranes.

1. Introduction

Current trends in food consumption have evolved to minimally processed food, such as ready-to-eat meals or semi-prepared ingredients (e. g. semi-cooked or marinated), which may introduce new food safety hazards into the food supply (Quested *et al.*, 2010). Throughout the food chain, a number of stresses (e.g. cold, heat, acids and preservatives) alter homeostasis of food-borne pathogenic bacterial cells by targeting membranes, enzymes, and nucleic acids, among other cellular components (Abee and Wouters, 1999; Brul and Coote, 1999). This may render a physiologically heterogeneous bacterial population, which includes dead, healthy and also sublethally injured cells, the latter being especially found when mild processing and preservation technologies are used (Rajkovic *et al.*, 2010). In such instances, selective media for pathogen detection and enumeration will probably fail to evidence the presence of sublethally injured cells, which cannot grow due to damage to essential metabolism and/or the structures that otherwise would protect them from selective agents, namely antibiotics, salts, acids, and surface-active compounds, such as bile salts (Kell *et al.*, 1998; Mackey, 2000; Stephens and Mackey, 2003). This may result in overestimation of the efficacy of preservation methods and food safety, as sublethally injured cells can recover from damage, provided that suitable conditions are present, and subsequently grow and regain virulence (Archer, 1996; Wesche *et al.*, 2009). Validation of emerging technologies for food preservation should not therefore omit the detection of potentially harmful injured cells (Rajkovic *et al.*, 2010). In this regard, quantification of sublethal injury in axenic cultures is classically achieved by using the differential plating method, which consists in parallel plating on nonselective and selective media. The nonselective medium allows recovery of sublethally injured cells before growth, and so enumerates both healthy and previously injured cells, whereas the selective medium only recovers the healthy fraction, as it is

assumed that resistance to selective agents involves having intact cell membranes (Kell *et al.*, 1998; Wesche *et al.*, 2009).

In addition, a large number of flow cytometry assays with fluorescent dyes measuring structural or functional attributes of bacterial cells have been described for rapid assessment of physiological state beyond culturability (Comas-Riu and Rius, 2009; Müller and Nebe-von-Caron, 2010). Among these attributes, membrane integrity is generally accepted as a good predictor of cell viability, since an intact cell membrane is crucial to maintain metabolic activity and permit multiplication. In addition, cell membrane is the most common target of food processing and preservation technologies (Wu, 2008). However, interpretation of this parameter should be carefully considered. Firstly, because inactive cells may conceivably retain an intact membrane (Davey *et al.*, 2004; Berney *et al.*, 2007). Secondly, because membrane permeabilization may be only transient, as observed following exposure to stresses such as electroporation (Mackey, 2000), or during fast growth (Müller and Nebe-von-Caron, 2010). Thus, setting the limit between lethal and sublethal membrane damage is not always straightforward. In spite of this, irreversible membrane damage is likely to occur if bacterial cells are exposed to simultaneous stressing factors (e.g. high salinity or low pH) (Mackey, 2000).

Cytoplasmic membrane integrity has been extensively assessed in bacterial research using propidium iodide (PI) (Endo *et al.*, 2001; Ananta *et al.*, 2005; Hayouni *et al.*, 2008; Tong *et al.*, 2009), a membrane-impermeant red-fluorescent nucleic acid dye that is therefore excluded by cells with intact membranes but stains permeabilized cells. In order to simultaneously analyze cells with intact and damaged membranes, PI has been combined with membrane-permeant green-fluorescent nucleic acid dyes, such as SYTO 9, SYTO BC, SYTO 24 (Gunasekera *et al.*, 2000, 2003; Bunthof *et al.*, 2001; Bunthof and Abee, 2002; Jang and Rhee, 2009; Zhou *et al.*, 2010; Corbitt *et al.*, 2011) or SYBR Green I

(Barbesti *et al.*, 2000; Berney *et al.*, 2007, 2008). In these assays, cells with intact membranes are expected to display very low red fluorescence and high green fluorescence. When SYTO 9 and PI are inside a cell at the same time, that is, when membrane is damaged, cells should emit high red fluorescence and very low green fluorescence due to a combined mechanism (Stocks, 2004): (i) displacement of SYTO 9 from its binding to nucleic acids due to a stronger nucleic acid affinity of PI, which causes a decrease in green fluorescence, and (ii) PI fluorescence enhancement by energy transfer from SYTO 9 (Förster resonant energy transfer – FRET – phenomenon). Displacement and energy transfer are also likely to occur when PI is combined with SYTO BC, SYTO 24 or SYBR Green I (Barbesti *et al.*, 2000; Ben-Amor *et al.*, 2005; Corbitt *et al.*, 2011). Interestingly, cells emitting both high green and red fluorescence have been found after exposure of Gram-negative and Gram-positive bacteria to some stresses, including bacteriocin leucocin B-TA11a (Swarts *et al.*, 1998), glycerol (Saegeman *et al.*, 2007), and irradiation (Berney *et al.*, 2007), or in fecal bacteria (Ben-Amor *et al.*, 2005). In these cells, considered as injured, partially damaged membranes might prevent the entrance of enough quantity of PI to displace the green-fluorescent nucleic acid dye (Barbesti *et al.*, 2000; Saegeman *et al.*, 2007).

The fluorescent staining combining SYTO 9 and PI is one of the most popular cytochemical assays to assess the physiological state of microbial cells by flow cytometry. Nevertheless, there is lack of consensus about a procedure to adjust the staining protocol so that the aforementioned fluorescence pattern is attained. In practice, not optimally reaching this pattern does not usually preclude the identification and separation of cells with intact membranes from cells with damaged membranes. However, these results are often difficult to interpret, especially when it comes to unequivocally identifying the cells having incorporated both dyes, i.e. cells with partially damaged membranes or injured cells. Thus, the aim of this study was to establish a reliable and accurate protocol for improvement of flow cytometry-based detection of injured

Escherichia coli O157:H7, *Salmonella* Enteritidis and *Listeria monocytogenes*. First, we sought to adjust the staining concentrations and the instrumental set up for best resolution of control populations, according to the expected fluorescence patterns. These improved methods were then evaluated in bacterial suspensions exposed to food-related physical and physicochemical treatments inducing sublethal injury, as assessed by the differential plating method.

2. Materials and methods

2.1. Bacterial strains and culture conditions

Three strains were used: *Escherichia coli* O157:H7 CECT 5947 and *Listeria monocytogenes* CECT 4032, provided by the Spanish Type Culture Collection (Colección Española de Cultivos Tipo, CECT), and *Salmonella enterica* serovar Enteritidis F4, provided by the National Microbiology Centre (Centro Nacional de Microbiología, CNM).

Lyophilized cultures were reconstituted and subcultured for stock culture preparation. Stock cultures were stored at –65°C in cryovials containing beads (AES Chemunex, Bruz, France). Pre-cultures were prepared by transferring one bead from the stock culture to a 100 mL Erlenmeyer flask containing 20 mL of tryptone soya broth (TSB; Oxoid, Basingstoke, UK), to grow *E. coli* O157:H7 and *S.* Enteritidis, or brain heart infusion (BHI; Oxoid) to grow *L. monocytogenes*, and then, incubated overnight at 37°C in a shaking water bath at 86 rpm. To obtain stationary phase cultures, 50 μL of the corresponding overnight culture were inoculated into 20 mL of TSB or BHI and incubated at 37°C for 20 h. Growth time to reach stationary phase was previously determined by measuring the optical density at 600 nm (Bioscreen C; Oy Growth Curves AB, Helsinki, Finland).

2.2. Optimization of flow cytometry protocols

2.2.1. Cell preparation

To prepare *E. coli* O157:H7, *S.* Enteritidis and *L. monocytogenes* control samples, untreated cells and heat-killed cells (80°C/30 min) were pelleted (13,000 × *g*, 30 s, 20°C), resuspended, and diluted to *ca.* 7.5 log colony-forming unit (CFU)/mL in filtered (0.22 μm, polyethersulfone; Millipore, Cork, Ireland) 2 mM potassium citrate solution (pH 7.4).

2.2.2. Staining procedures

To assess cytoplasmic membrane integrity, the red-fluorescent nucleic acid dye propidium iodide (PI; Invitrogen, Eugene, OR, USA) was used in combination with the green-fluorescent nucleic acid dyes SYTO 9, SYTO 24 or SYTO BC (Invitrogen). Firstly, several concentrations of green-fluorescent dyes were tested in heat-killed controls (Table 3.1). Since unstained cells were used as the reference to set voltage amplifications and compensation values, for each green-fluorescent dye, the selected concentration was that allowing visualization of both the unstained and single stained populations (Table 3.2). Secondly, as previously described by Barbesti *et al.* (2000), discrimination between intact- and compromised-membrane populations and their fluorescence pattern were evaluated as a function of PI concentration. To that end, mixtures of healthy and heat-killed cells (1:1) were stained with SYTO 9, SYTO 24 or SYTO BC, at the previously set concentration, and a range of PI concentrations (Table 3.1). Once optimal concentration ratios were established (Table 3.2), proper staining of cells taking up PI was verified by the analysis of controls containing heat-killed cells, alone or mixed with healthy cells (1:1). Dye stock solutions were prepared in filtered (0.20 μm, nylon; Millipore) dimethyl sulfoxide (DMSO) and stored at 4°C. Concentrations of such stock solutions were chosen to minimize the presence of DMSO in the sample (1-1.5 μL stock solution/mL). After addi-

tion of nucleic acid dyes, cells were incubated at 20°C for 30 min, protected from light.

Table 3.1 Tested dye concentrations.

Pathogen	Dye			
	SYTO 9 (nM)	SYTO 24 (nM)	SYTO BC[a]	PI (µM)
E. coli O157:H7	10; 25; 50; 100, 500; 1,000	20; 30; 40; 50; 60; 70; 80; 90; 95	$0.5:10^5$; $1.5:10^5$; $0.5:10^4$; $0.5:10^3$; $1:10^3$	0.6; 1.3; 2.5; 5; 10; 20; 40
S. Enteritidis	10; 25	40; 50; 60; 70; 80; 95	$1:10^5$; $1.5:10^5$	0.6; 1.3; 2.5; 5; 10; 20; 40
L. monocytogenes	10; 25	60; 70; 80	$1:10^5$; $1.5:10^5$	0.6; 1.3; 2.5; 5; 6; 7; 8; 9; 10; 20; 40

[a] Final dilution of the stock solution.

Table 3.2 Selected dye concentrations.

Pathogen	Dye combination		
	SYTO 9 (nM) + PI (µM)	SYTO 24 (nM) + PI (µM)	SYTO BC[a] + PI (µM)
E. coli O157:H7	10.0 + 20.0	80.0 + 20.0	$1.5:10^5$ + 20.0
S. Enteritidis	10.0 + 2.5	55.0 + 2.5	$1.0:10^5$ + 2.5
L. monocytogenes	10.0 + 7.0	60.0 + 7.0	$1.0:10^5$ + 7.0

[a] Final dilution of the stock solution.

2.3. Evaluation of flow cytometry protocols

To evaluate the applicability of improved protocols, the pathogens were exposed to food-related treatments inducing a significant level of sublethal injury and were then analyzed by differential plating and flow cytometry.

2.3.1. Sample preparation for stress exposure

Cultures were diluted to *ca.* 7.5 log CFU/mL in TSB, for *E. coli* O157:H7 and *S.* Enteritidis, or in BHI, for *L. monocytogenes*, and then exposed to physical (freezing [F], refrigeration [R], heat [H]) and physicochemical stresses (potassium sorbate + refrigeration [SR], vinegar + refrigeration [VR], citric acid + refrigeration [CR]) in 50 mL polypropylene centrifuge tubes, or 100 mL Erlenmeyer flasks for H (Table 3.3 and 3.4). Potassium sorbate (Cargill, Rubí, Spain), vinegar (purchased at a local retail), and citric acid (Cargill) were aseptically added before dilution.

2.3.2. Differential plating method

Parallel plating on nonselective and selective media was used to estimate:

(i)   *viable cells* or *survivor cells*: count on nonselective medium;
(ii) *healthy cells*: count on selective medium;
(iii) *sublethally injured cells*: count on nonselective medium – count on selective medium;
(iv) sublethal injury: $\%SI = \dfrac{\text{count nonselective media} - \text{count selective media}}{\text{count nonselective media}} \times 100$

Untreated and treated samples were serially diluted in peptone physiological salt solution (1 g/L neutralized bacteriological peptone [Oxoid] and 8.5 g/L NaCl, in water). Prior to dilution, cells exposed to physicochemical stresses were pelleted (13,000 × *g*, 30 s, 20°C) and resuspended in peptone physiological salt solution. Appropriate dilutions were spiral-plated (Eddy Jet; IUL, Barcelona, Spain) on tryptone soya agar supplemented with 0.6% (w/v) yeast extract (TSAYE; Oxoid) as the nonselective medium. Samples were also plated on selective media: sorbitol MacConkey (SMAC) agar (Oxoid) for *E. coli* O157:H7, xylose lysine desoxycholate (XLD) agar (Oxoid) for *S.* Enteritidis, and agar Listeria according to Ottaviani & Agosti (ALOA; AES Chemunex) for *L. monocytogenes.* Plates were incubated at 37°C for 24 h, except for ALOA plates, which were incubated for 48 h.

Table 3.3 Tested treatment conditions.

Treatment	Pathogen	Tested conditions
Freezing	*E. coli* O157:H7	–18°C; 5, 10, 15 days
	S. Enteritidis	–18°C; 5, 10, 15 days
	L. monocytogenes	–18°C; 5, 10, 15 days
Refrigeration	*E. coli* O157:H7	4°C; 5, 10, 15 days
	S. Enteritidis	4°C; 5, 10, 15, 21 days
	L. monocytogenes	-
Heat	*E. coli* O157:H7	55°C; 5, 10 min
	S. Enteritidis	55°C; 10, 15, 20 min
	L. monocytogenes	55°C; 10, 15, 20 min. 60°C; 5, 10, 15, 20 min. 65°C; 5, 10 min
Potassium sorbate + refrigeration	*E. coli* O157:H7	0.15 % w/v; 4°C; 5, 10, 15 days
	S. Enteritidis	0.15 % w/v; 4°C; 5, 10, 15, 21 days
	L. monocytogenes	0.15 % w/v; 4°C; 5, 10, 15, 21 days
Vinegar + refrigeration	*E. coli* O157:H7	14 % v/v (pH 4.0); 4°C; 5, 10, 15 days
	S. Enteritidis	6 % v/v (pH 4.5), 14 % v/v (pH 4.0); 4°C; 5, 10, 15 days
	L. monocytogenes	3.5 % v/v (pH 5.0), 6 % v/v (pH 4.5), 16 % v/v (pH 4.0); 4°C; 5, 10, 15 days
Citric acid + refrigeration	*E. coli* O157:H7	0.4 % w/w (pH 4.5), 0.7 % w/v (pH 4.0); 4°C; 5, 10, 15 days
	S. Enteritidis	0.4 % w/w (pH 4.5), 0.7 % w/v (pH 4.0); 4°C; 5, 10, 15 days
	L. monocytogenes	0.3 % w/w (pH 5.0), 0.6 % w/w (pH 4.5), 0.9 % w/v (pH 4.0); 4°C; 5, 10, 15 days

Differential plating of untreated cultures allowed to evaluate the ability of selective media to sustain growth of unstressed cells, and to determine a threshold value for %SI (mean + standard deviation) (Jasson *et al.*, 2007), above which %SI calculated for a treated sample is surely a consequence of the stress. Threshold values were then used to select, from the tested range, the treatment conditions inducing significant %SI (Table 3.3 and 3.4).

2.3.3. Sample preparation for flow cytometry

Cells exposed to selected stress conditions were harvested (13,000 × g, 30 s, 20°C) from 1 mL aliquots, resuspended in potassium citrate solution, stained at the selected dye concentrations, and incubated as previously stated. To calculate cell concentration, a microsphere standard (Invitrogen) was used according to the manufacturer protocol.

2.4. Flow cytometry

Samples were analyzed with a FACScalibur flow cytometer (BD, Franklin Lakes, NJ, USA) equipped with a 15-mW 488-nm air-cooled argon-ion laser. Band-pass filter for SYTO 9, SYTO 24 and SYTO BC light emission was 530/30 (FL1), whereas long-pass filter for PI light emission was 670 nm (FL3). Voltage amplification was applied at logarithmic scale. Thresholds were set to the lowest value (0) to ensure that the entire population was analyzed, as the different stresses were previously seen to change cell scatter properties. This did not prevent from clearly distinguishing the bacterial cluster from background particles and electronic noise. Use of a FL1 threshold was ruled out, since green fluorescence of damaged cells was reduced to such extent as to miss them out from analysis. Filtered double distilled water was used as sheath fluid, since preliminary results using sterile phosphate buffered saline showed poor distinction between cell populations. Dual-stained untreated cell controls evaluation showed that double distilled water did not affect cell physiology. Data were obtained from 20,000 cells gated in the forward scatter (FSC) *vs.* SSC plot at low flow rate (12 μL/min) using CellQuest Pro software (version 4.0.2; BD).

Table 3.4 Selected stress conditions inducing sublethal injury (%SI).

Pathogen	Treatment	Stress conditions	%SI
E. coli O157:H7	Untreated	-	6.64± 7.55[b]
	Freezing	–18°C, 10 days	66.83± 1.91[*y]
	Refrigeration	4°C, 15 days	69.08± 3.63[*y]
	Heat	55°C, 10 min	65.83± 1.76[*y]
	Potassium sorbate + refrigeration	0.15% w/v, 4°C, 10 days	27.52± 0.83[*z]
	Vinegar + refrigeration	14% v/v, pH 4.0, 4°C, 15 days	99.74± 0.40[*w]
	Citric acid + refrigeration	0.7% w/v, pH 4.0, 4°C, 15 days	85.28± 9.80[*x]
S. Enteritidis	Untreated	-	3.20± 3.99[c]
	Freezing	–18°C, 10 days	97.71± 1.03[*w]
	Refrigeration	4°C, 10 days	19.85±13.15[z]
	Heat	55°C, 15 min	68.20±10.26[*xy]
	Potassium sorbate + refrigeration	0.15% w/v, 4°C, 10 days	29.96±10.30[*z]
	Vinegar + refrigeration	6% v/v, pH 4.5, 4°C, 10 days	78.60± 4.14[*wx]
	Citric acid + refrigeration	0.7% w/v, pH 4.0, 4°C, 5 days	88.95± 8.59[*wx]
L. monocytogenes	Untreated	-	5.94± 6.22[d]
	Freezing	–18°C, 10 days	21.60± 7.63[y]
	Refrigeration	na[a]	na
	Heat	60°C, 5 min	94.83± 4.49[*x]
	Potassium sorbate + refrigeration	0.15% w/v, 4°C, 21 days	21.80±11.10[y]
	Vinegar + refrigeration	6% v/v, pH 4.5, 4°C, 10 days	31.60±20.01[y]
	Citric acid + refrigeration	0.9% w/v, pH 4.0, 4°C, 5 days	86.01±23.96[*x]

[a] Stress not applied.

[b] Test value for one sample t-test = 14%.

[c] Test value for one sample t-test = 7%.

[d] Test value for one sample t-test = 12%.

* For each pathogen, %SI significantly higher than the test value (P < 0.05).

[w-z] For each pathogen, %SI lacking a common superscript differ significantly (P < 0.05).

2.5. Analysis of flow cytometry data

When using the present dye combinations, compensation is not strictly necessary to discriminate between healthy cells and cells with damaged membranes, but this procedure was applied in order to correctly visualize double positive cells, that is, cells with partially damaged membranes. FlowJo software (version 7.6.1; Tree Star, Ashland, OR, USA) was used for data compensation and analysis. Data acquired from unstained untreated cells were used as a negative control in software compensation, whereas heat-killed single-stained cells were used as positive controls to correct SYTO and PI spillovers. Dual-stained untreated and heat-killed cells (1:1) were used as a reference to define the regions encompassing cells with intact (SYTO$^+$), damaged (PI$^+$) and partially damaged (SYTO$^+$/PI$^+$) membranes. Both compensation and dual-stained controls always accompanied acquisition of experimental samples.

Raw data were first evaluated by displaying all parameter combinations in pseudocolor bivariate plots to detect interferences and find the best gating strategy, as suggested by Nebe-von-Caron (2009). Debris and noise were sufficiently low to define and gate bacterial cells by their scatter characteristics (Figure 3.1). Gated events were then displayed according to their green and red fluorescence, and regions were set to discriminate bacterial populations. Microspheres were also gated in the FSC *vs.* SSC plot.

To verify proper cell staining and dye specificity, samples were analyzed with a BX51 fluorescence microscope (Olympus, Tokyo, Japan) equipped with a 100-W mercury arc lamp, and a mirror unit (U-M51004 F/R-V2) for simultaneous visualization of green and red fluorescence. Images were captured using a CCD camera (DP50-CU, Olympus) and analySIS software (version 3.1; Soft Imaging System, Münster, Germany). For cell observation, flow cytometry samples were centrifuged (13,000 × *g*, 30 s, 20°C) and 10-times concentrated by removing 900 μL of the supernatant. To immobilize cells, 1-μL aliquot was dispensed

on an agar layer prepared onto a glass slide and covered with a coverslip (Tran *et al.*, 2004).
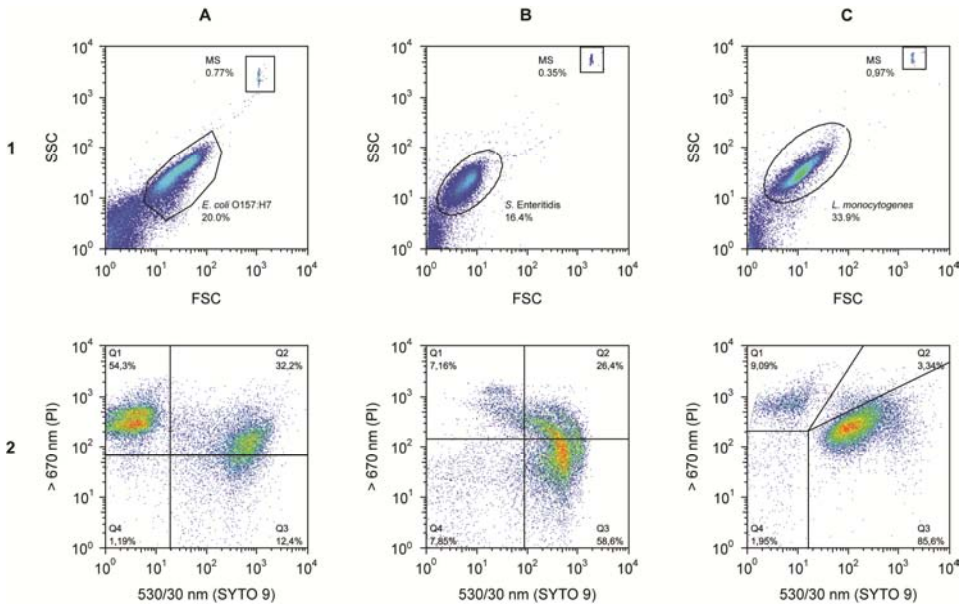
Figure 3.1 Gating strategy and gate boundaries for *Escherichia coli* O157:H7 exposed to sorbate + refrigeration (A), *Salmonella* Enteritidis exposed to vinegar + refrigeration (B), and *Listeria monocytogenes* exposed to freezing (C), stained with propidium iodide (PI) and SYTO 9. (1) Gating of bacterial cells according to their light scatter characteristics. (2) Bivariate SYTO 9 *vs.* PI plot of cells gated in the scatter plot and gating for subpopulation discrimination (Q1: dead; Q2: injured; Q3: healthy; Q4: negative).

2.6. Statistical analysis

Counts were log-transformed, except for the calculation of %SI, and means and standard deviations of three biologically independent replicates were calculated. A one-tailed one-sample *t*-test was used to compare %SI from treated samples with the corresponding threshold value. Analysis of variance was used to compare treatment or counting method groups. For this purpose, the General Linear Models procedure of SAS software (the SAS System for Windows, version 9.1; SAS Institute, Cary, NC, USA) was used. When the analysis was signifi-

cant ($P < 0.05$), Tukey's test was used to separate means. Dunett's test was used to compare healthy or injured cell counts obtained by flow cytometry with those obtained by (differential) plating. Representative pseudocolor bivariate plots are shown in figures.

3. Results

3.1. Enhancement of separation between populations with intact and compromised membranes

When combinations of PI with SYTO are used, cells with intact membranes are expected to display very low red fluorescence and high green fluorescence, whereas cells with damaged membranes are those displaying high red fluorescence and very low green fluorescence. This fluorescence pattern was the requisite to increase resolution of cells with partially damaged membranes and therefore to improve their detection. To this end, enough quantity of PI is necessary to ensure the displacement of bound SYTO molecules in cells with damaged membranes, which results in the desired decrease in green fluorescence. Thus, a range of PI concentrations were tested in combination with a fixed SYTO concentration. For all pathogens, green fluorescence resolution of untreated (healthy) and heat-killed cell populations increased with PI concentration, whereas red fluorescence resolution decreased (Figure 3.2). Distances between healthy and heat-killed cell populations at most of PI concentrations were enough to clearly distinguish them, but better population shifts and thus fluorescence patterns were achieved at 20.0, 2.5 and 7.0 µM PI, for *E. coli* O157:H7, *S.* Enteritidis and *L. monocytogenes*, respectively. Pathogen-specific dye concentrations were then used to stain control and experimental samples (Figure 3.3, 3.4, and 3.5). At the selected dye concentration ratios, the expected green fluorescence decrease and red fluorescence increase in dead cells was achieved for *E. coli* O157:H7 stained with SYTO 9 + PI and SYTO BC + PI (Figure 3.3A). Similar green fluorescence decrease was achieved in *L. monocytogenes*

stained with SYTO 9 + PI (Figure 3.5). However, green fluorescence decrease for *S.* Enteritidis was low with all dye combinations (Figure 3.4). Propidium iodide concentrations higher than the selected ones, increased green fluorescence loss in dead cells, but it concomitantly increased red background fluorescence in healthy cells, which was already high, especially for *L. monocytogenes* (Figure 3.2). Staining of heat-killed cell controls at the selected dye concentrations was adequate, as cells displayed similar fluorescence levels to those in mixed controls (Figure 3.6).
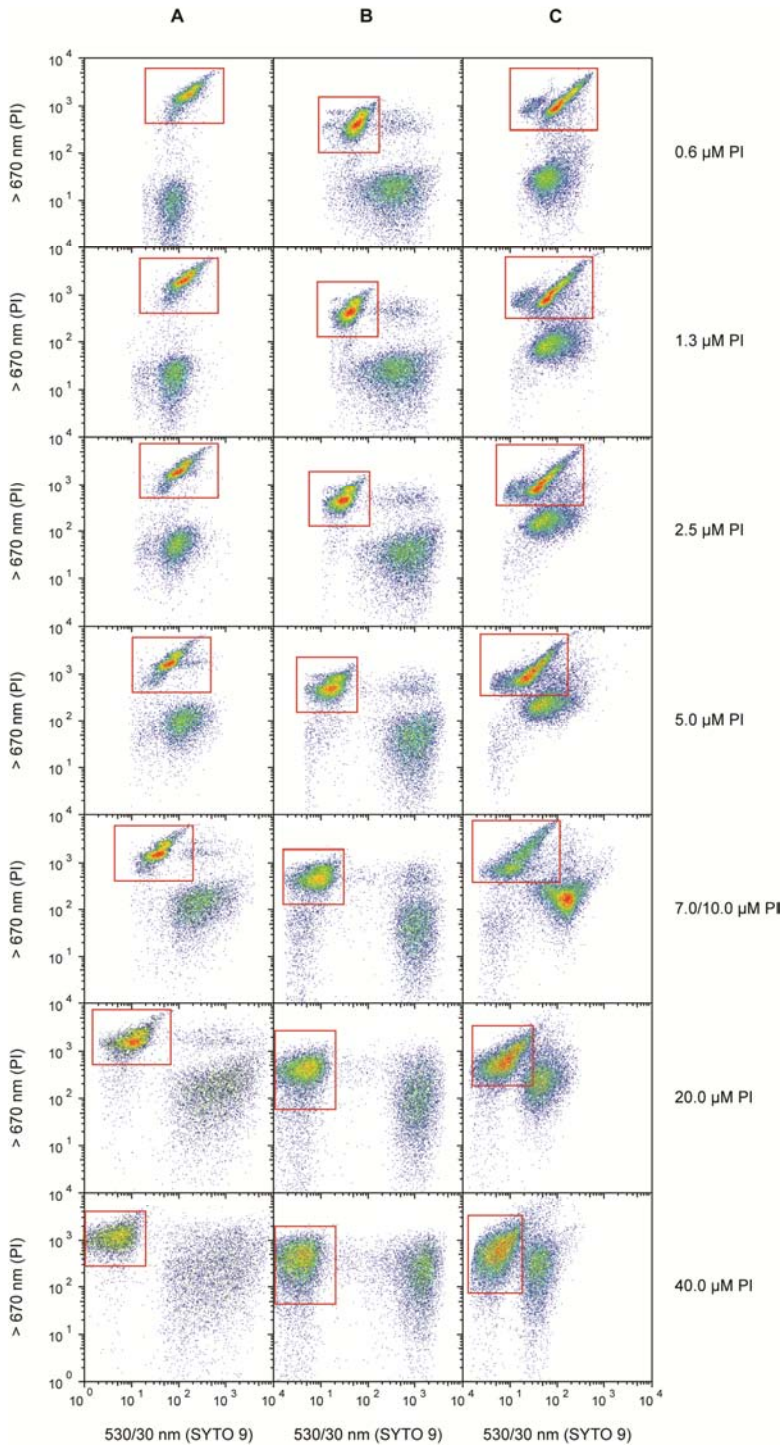
Figure 3.2 Effect of propidium iodide (PI) concentration on discrimination between cells with intact and damaged membranes. Healthy and heat-killed (1:1) *Escherichia coli* O157:H7 (A), *Salmonella* Enteritidis (B), and *Listeria monocytogenes* (C) were stained with 10 nM SYTO 9 and different PI concentrations (rows). For *L. monocytogenes*, a PI concentration range between 5 and 10 μM PI was also evaluated, thus, 7 μM PI is presented for this pathogen. A region is drawn around damaged cell populations.
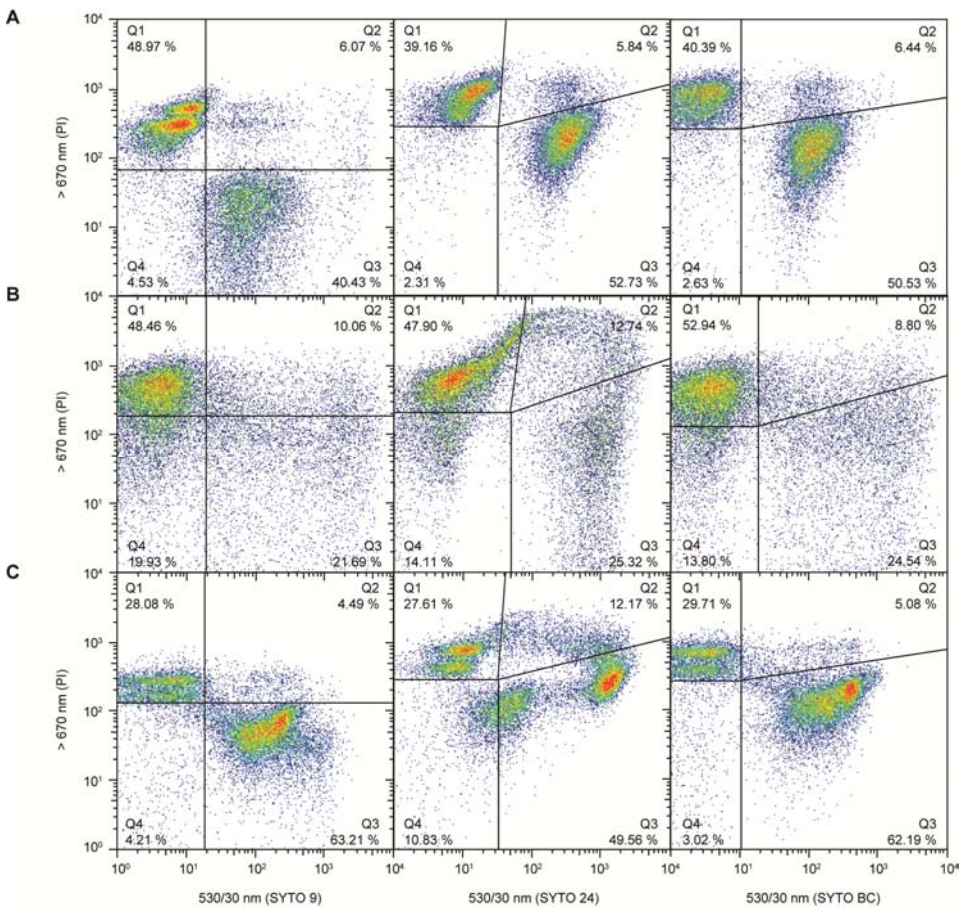
Figure 3.3 *Escherichia coli* O157:H7 exposed to heat (B) and citric acid + refrigeration (C) and stained with membrane integrity indicators. Control (A): heat-killed and healthy cells. Q1: dead; Q2: injured; Q3: healthy; Q4: negative.
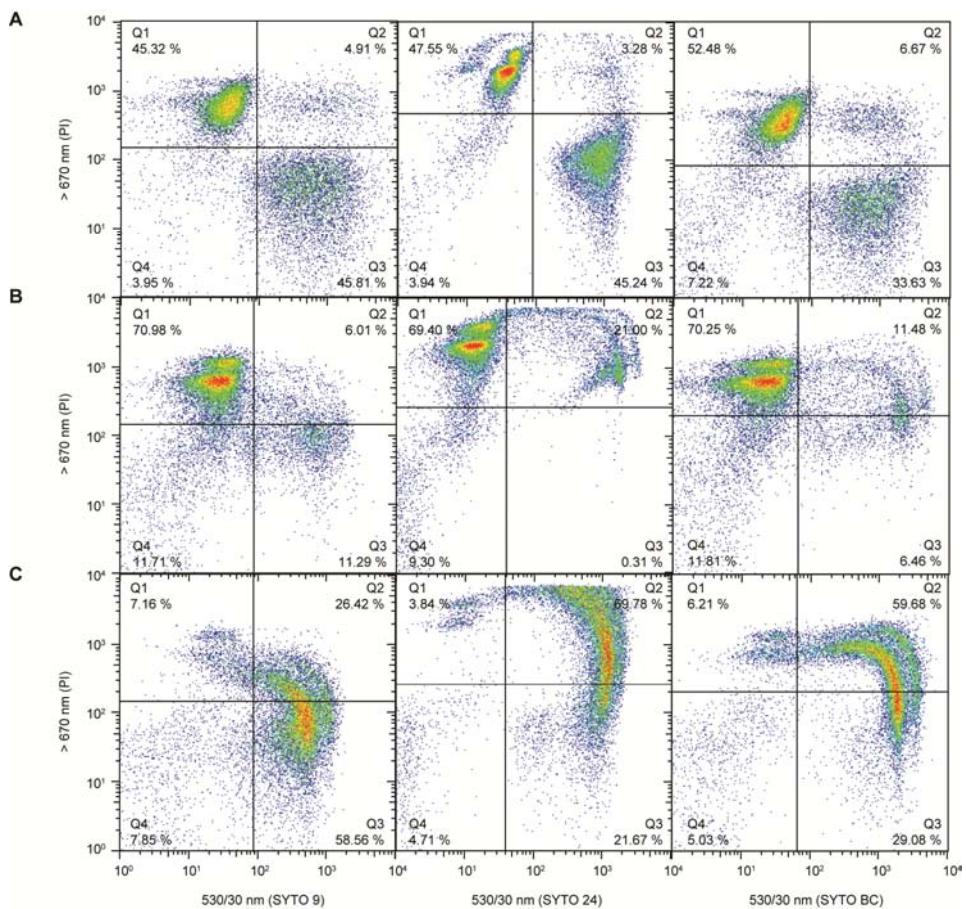
Figure 3.4 *Salmonella* Enteritidis exposed to freezing (B) and vinegar + refrigeration (C) and stained with membrane integrity indicators. Control (A): heat-killed and healthy cells. Q1: dead; Q2: injured; Q3: healthy; Q4: negative.
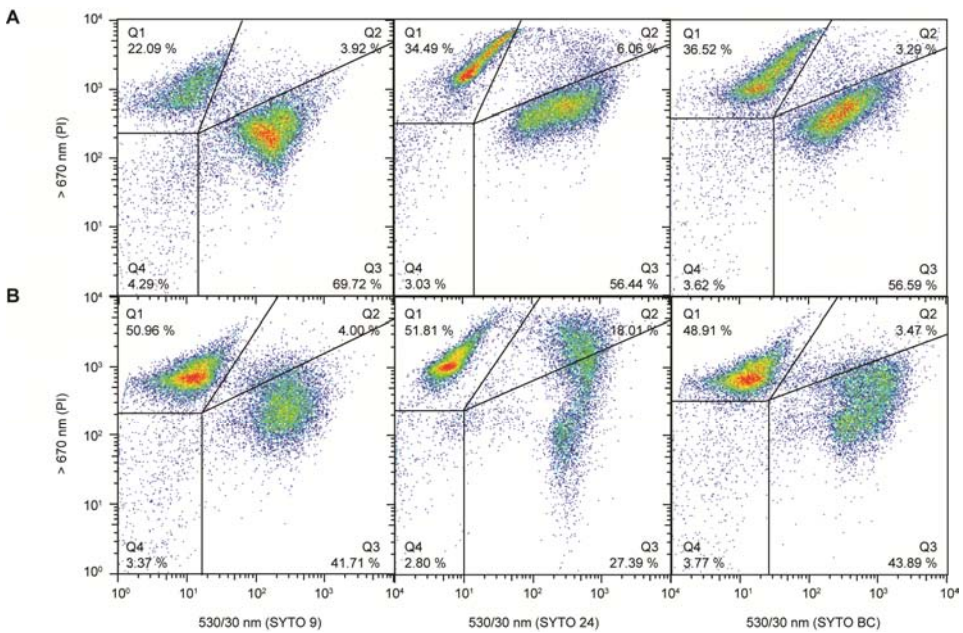
Figure 3.5 *Listeria monocytogenes* exposed to vinegar + refrigeration (B) and stained with membrane integrity indicators. Control (A): heat-killed and healthy cells. Q1: dead; Q2: injured; Q3: healthy; Q4: negative.
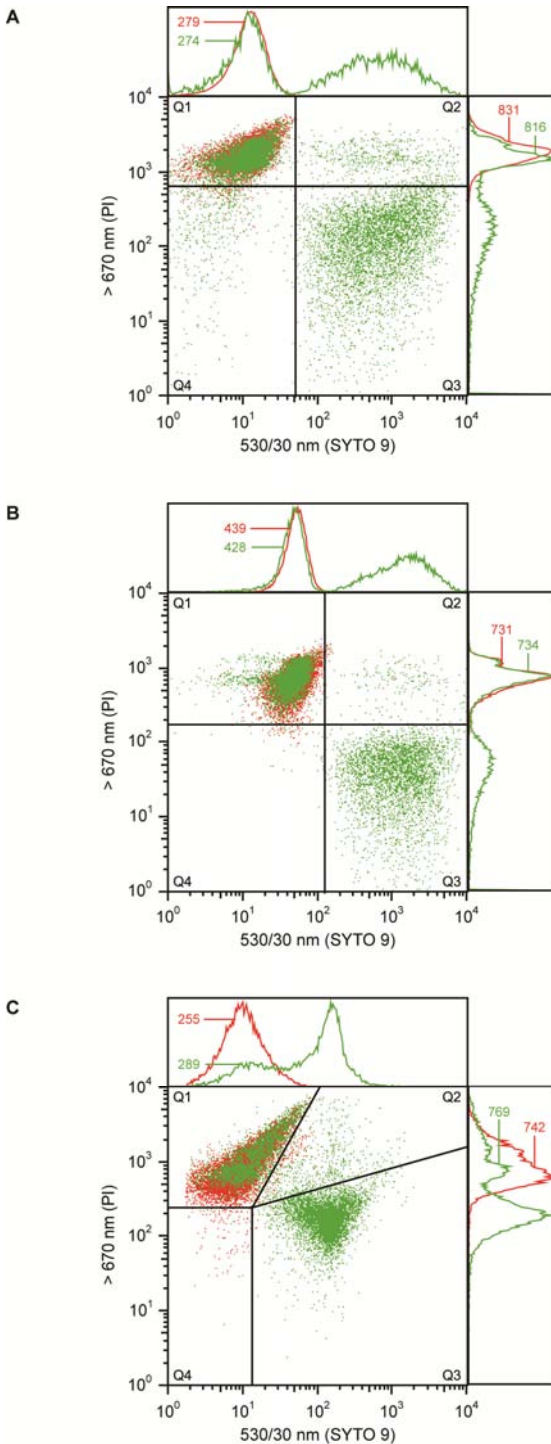
Figure 3.6 Effect of healthy-to-damaged cell ratio on fluorescence intensities of damaged cells. Control samples containing heat-killed cells and healthy cells (1:1) (green) or only heat-killed cells (red) were stained with 10 nM SYTO 9 and 20.0 μM, 2.5 μM and 7.0 μM PI, for *Escherichia coli* O157:H7 (A), *Salmonella* Enteritidis (B), and *Listeria monocytogenes* (C), respectively. Median channel numbers for green and red fluorescence of damaged cell populations (Q1) are shown in adjunct histograms. Q1: dead; Q2: injured; Q3: healthy; Q4: negative.

3.2. Plate count assessment of sublethal injury

For all pathogens, no differences ($P > 0.05$) were found between counts on non-selective and selective media before treatment (data not shown). These counts were used to calculate threshold values for sublethal injury in each selective medium: 14% for *E. coli* O157:H7 on SMAC agar, 7% for *S.* Enteritidis on XLD agar, and 12% for *L. monocytogenes* on ALOA (Table 3.4). Except for *L. monocytogenes*, %SI after treatment was significantly higher than the corresponding threshold value for most of the selected treatment conditions.

3.3. Performance of membrane integrity indicators to detect heterogeneous physiological states

After exposure to stresses, use of flow cytometry with all combinations of membrane integrity indicators revealed a large increase in the number of double positive cells (showing high green and high red fluorescence), that is, cells with partially damaged membranes or injured cells, which were in the minority in control samples (Figure 3.3, 3.4, and 3.5).

3.3.1. Flow cytometry counts

Flow cytometry counts obtained by using three dye combinations were compared (Table 3.5). Few experimental conditions showed significant differences among counts, which were mainly observed for the injured population. For all pathogens and treatments, viable counts (cells with intact or partially damaged membranes) did not differ significantly using any dye combination (data not shown). The same result was obtained for the healthy populations of *E. coli* O157:H7 and *L. monocytogenes* (Table 3.5). Conversely, SYTO 24 + PI gave significantly lower healthy cell counts for *S.* Enteritidis exposed to F, compared with SYTO 9 + PI and SYTO BC + PI; and exposed to VR, compared with SYTO 9 + PI. Moreover, injured cell count obtained with SYTO 24 + PI was higher than that obtained with SYTO 9+ PI and SYTO BC + PI for *E. coli* O157:H7 treated with H

and CR, and *L. monocytogenes* treated with VR (Table 3.5). For *S.* Enteritidis exposed to F, injured cell counts obtained with SYTO 9 + PI were significantly lower than those obtained with SYTO 24 + PI, but when exposed to VR, counts were lower than SYTO24 + PI and SYTO BC + PI. Regarding dead cell counts, no differences were found among dye combinations for *L. monocytogenes*, whereas for *E. coli* O157:H7 and *S.* Enteritidis, SYTO 24 + PI gave lower counts than SYTO 9 + PI or SYTO BC + PI in a few cases (Table 3.6).

3.3.2. Flow cytometry profiles

As mentioned previously, for treated samples, flow cytometry injured cell (SYTO$^+$/PI$^+$) count was the parameter with more significant differences among dye combinations. In such cases, shown in Figure 3.3, 3.4, and 3.5, differences between profiles were apparent in the bivariate plots. For H- and CR-treated *E. coli* O157:H7 stained with SYTO 24 + PI, median red fluorescence of the injured cell population was higher than that of the dead cell population, and also than that of the injured cell population of SYTO 9 + PI- and SYTO BC + PI-stained samples (Figure 3.3B and 3.3C). Red fluorescence of some F- and VR-injured *S.* Enteritidis cells stained with SYTO 24 + PI was higher than that of the dead cells, although the median was lower (Figure 3.4B and 3.4C). Moreover, most of the cells (especially for F) in the quadrant encompassing healthy cells in SYTO 9 + PI plot were detected as injured cells in the SYTO 24 + PI-stained sample. This was less pronounced in the SYTO BC + PI-stained sample. For VR-treated *L. monocytogenes*, almost all the SYTO-positive cells appeared in the healthy cell quadrant when using SYTO 9 + PI and SYTO BC + PI, whereas in the SYTO 24 + PI-stained sample, a larger part appeared as injured cells (Figure 3.5B).

Injured *E. coli* O157:H7 and *S.* Enteritidis populations from F-, R-, SR- and CR-treated samples displayed higher green fluorescence than healthy populations in control samples (e.g. Figure 3.3A, 3.3C, 3.4A, and 3.4B), whereas this did not occur for the injured *L. monocytogenes* populations.

Table 3.5 Healthy and injured counts assessed by flow cytometry combined with membrane integrity indicators (log cell number/mL) and by plating (log CFU/mL) after exposure to stresses.

Pathogen	Method	Stress					
		Freezing	Refrigeration	Heating	Sorbate + refrigeration	Vinegar + refrigeration	Citric acid + refrigeration
Healthy							
E. coli O157:H7	SMAC agar	5.29±0.04	5.27±0.03	4.59±0.15	6.85±0.11	3.32±0.82	5.80±0.45
	SYTO 9 + PI	5.77±0.27^{x}*	6.50±0.08^{x}*	7.08±0.05^{x}*	6.26±0.27^{x}*	7.04±0.27^{x}*	7.28±0.04^{x}*
	SYTO 24 + PI	5.44±0.18^{x}	6.46±0.10^{x}*	6.98±0.04^{x}*	5.79±0.16^{x}*	7.27±0.06^{x}*	7.27±0.07^{x}*
	SYTO BC + PI	5.64±0.10^{x}	6.43±0.09^{x}*	7.00±0.05^{x}*	6.16±0.32^{x}*	7.28±0.06^{x}*	7.35±0.05^{x}*
S. Enteritidis	XLD agar	4.78±0.19	7.31±0.04	6.58±0.19	7.15±0.19	4.18±0.97	4.29±1.36
	SYTO 9 + PI	6.28±0.52^{x}*	7.68±0.19^{x}*	6.75±0.31^{x}	7.67±0.15^{x}*	7.39±0.04^{x}*	6.43±0.19^{x}*
	SYTO 24 + PI	4.95±0.50^{y}	7.42±0.15^{x}	6.68±0.06^{x}	7.48±0.14^{x}*	6.96±0.18^{y}*	5.92±0.49^{x}
	SYTO BC + PI	6.15±0.28^{x}*	7.64±0.18^{x}*	6.73±0.20^{x}	7.61±0.14^{x}*	7.24±0.08^{x,y}*	6.02±0.44^{x}
L. monocytogenes	ALOA	7.26±0.09	na[a]	5.81±0.34	7.48±0.16	5.79±0.54	2.67±1.28
	SYTO 9 + PI	7.21±0.40^{x}	na	7.36±0.14^{x}*	7.45±0.38^{x}	6.98±0.32^{x}*	7.19±0.44^{x}*
	SYTO 24 + PI	7.42±0.05^{x}	na	7.06±0.36^{x}*	7.61±0.44^{x}	6.79±0.45^{x}*	7.25±0.53^{x}*
	SYTO BC + PI	7.39±0.16^{x}	na	7.29±0.25^{x}*	7.48±0.40^{x}	7.01±0.26^{x}*	6.67±0.18^{x}*

Pathogen	Method	Stress					
		Freezing	**Refrigeration**	**Heating**	**Sorbate + refrigeration**	**Vinegar + refrigeration**	**Citric acid + refrigeration**
Injured							
E. coli O157:H7	Differential plating	5.60±0.04	5.62±0.06	4.87±0.12	6.43±0.10	6.04±0.01	6.40±0.02
	SYTO 9 + PI	5.88±0.31[x]	6.14±0.08[x*]	6.55±0.04[y*]	6.86±0.10[x*]	6.16±0.21[x]	6.16±0.07[y*]
	SYTO 24 + PI	6.06±0.22[x]	5.99±0.05[x*]	6.75±0.04[x*]	6.68±0.10[x]	6.14±0.11[x]	6.54±0.06[x]
	SYTO BC + PI	6.03±0.15[x]	6.12±0.08[x*]	6.60±0.04[y*]	6.91±0.18[x*]	6.45±0.11[x*]	6.23±0.08[y]
S. Enteritidis	Differential plating	6.44±0.32	6.63±0.38	6.93±0.08	6.69±0.19	4.75±0.87	5.28±1.17
	SYTO 9 + PI	6.10±0.39[y]	6.49±0.22[x]	6.23±0.32[x*]	6.49±0.18[x]	7.09±0.09[y*]	6.51±0.11[x]
	SYTO 24 + PI	6.71±0.19[x]	6.73±0.08[x]	6.53±0.02[x]	6.54±0.13[x]	7.49±0.07[x*]	6.59±0.19[x]
	SYTO BC + PI	6.42±0.27[x,y]	6.53±0.13[x]	6.41±0.13[x*]	6.39±0.27[x]	7.41±0.06[x*]	6.64±0.10[x]
L. monocytogenes	Differential plating	4.80±3.22	na	7.20±0.28	6.88±0.39	3.47±3.01	5.19±1.13
	SYTO 9 + PI	6.00±0.43[x]	na	6.26±0.58[x*]	5.90±0.60[x]	5.77±0.12[y]	6.25±0.50[x]
	SYTO 24 + PI	6.62±0.48[x]	na	7.09±0.21[x]	6.58±0.56[x]	6.49±0.09[x*]	6.35±0.60[x]
	SYTO BC + PI	6.29±0.40[x]	na	6.53±0.54[x]	5.76±0.44[x]	5.84±0.06[y]	6.79±0.42[x]

[a] Stress not applied.

[x-y] For each pathogen and stress, flow cytometry counts lacking a common superscript differ significantly ($P < 0.05$).

* For each pathogen and stress, flow cytometry counts differ significantly from the corresponding plate count ($P < 0.05$).

Table 3.6 Dead (PI⁺) population (log cell number/mL) detected by flow cytometry combined with membrane integrity indicators after exposure to stresses.

Pathogen	Method	Stress					
		Freezing	Refrigeration	Heating	Sorbate + refrigeration	Vinegar + refrigeration	Citric acid + refrigeration
E. coli O157:H7	SYTO 9 + PI[a]	7.38 ± 0.14^x	7.23 ± 0.05^x	7.39 ± 0.04^x	7.16 ± 0.04^{xy}	6.84 ± 0.22^x	6.94 ± 0.08^x
	SYTO 24 + PI	7.51 ± 0.05^x	7.19 ± 0.05^x	7.32 ± 0.02^x	7.04 ± 0.10^y	7.18 ± 0.06^x	6.93 ± 0.02^x
	SYTO BC + PI	7.53 ± 0.02^x	7.20 ± 0.06^x	7.36 ± 0.05^x	7.30 ± 0.09^x	7.10 ± 0.08^x	7.03 ± 0.09^x
S. Enteritidis	SYTO 9 + PI	7.55 ± 0.16^x	6.71 ± 0.09^x	6.26 ± 0.36^x	6.63 ± 0.10^x	6.76 ± 0.22^x	5.77 ± 0.07^{xy}
	SYTO 24 + PI	7.51 ± 0.08^x	6.56 ± 0.08^{xy}	6.27 ± 0.09^x	6.40 ± 0.10^x	6.23 ± 0.24^y	5.50 ± 0.18^y
	SYTO BC + PI	7.52 ± 0.20^x	6.51 ± 0.06^y	6.20 ± 0.23^x	6.36 ± 0.22^x	6.36 ± 0.11^{xy}	5.86 ± 0.10^x
L. monocytogenes	SYTO 9 + PI	6.02 ± 0.57^x	na[a]	6.39 ± 0.77^x	5.99 ± 0.25^x	7.00 ± 0.06^x	7.27 ± 0.08^x
	SYTO 24 + PI	6.46 ± 0.12^x	na	6.71 ± 0.45^x	6.12 ± 0.36^x	6.91 ± 0.15^x	7.12 ± 0.02^x
	SYTO BC + PI	6.37 ± 0.11^x	na	6.54 ± 0.56^x	5.93 ± 0.29^x	6.91 ± 0.13^x	7.20 ± 0.14^x

[a] Stress not applied.

[x-y] For each pathogen and stress, means within a column lacking a common superscript differ significantly ($P < 0.05$).

An unexpected subpopulation with lower green and red fluorescence compared with the control populations appeared in the SYTO 24 + PI plot for CR-treated *E. coli* O157:H7 (Figure 3.3A, and 3.3C). Due to its light scatter characteristics, it was computed as healthy cells. A similar subpopulation was also found for *S.* Enteritidis exposed to R and SR and stained with SYTO 9 + PI and SYTO BC + PI (data not shown).

3.3.3. Healthy and injured cell detection by flow cytometry and (differential) plating

Flow cytometry counts significantly higher than plate counts were mostly found for healthy cells (Table 3.5). Only for *E. coli* O157:H7 exposed to SR, flow cytometry healthy cell counts were lower than plate counts.

Flow cytometry injured cell counts were mostly equal to those obtained by differential plating for *S.* Enteritidis and *L. monocytogenes.* For *E. coli* O157:H7, a similar number of cases showed no differences and positive differences (flow cytometry counts significantly higher than plate counts). For all pathogens, significantly lower flow cytometry injured cell counts were found mostly when using SYTO 9 + PI. This was the case of H-injured *S.* Enteritidis and *L. monocytogenes*, and CR-injured *E. coli* O157:H7. Using SYTO BC + PI, H-injured *S.* Enteritidis counts were also lower than differential plating counts. For all pathogens, no significant differences were observed between F-injured cell counts obtained by flow cytometry and differential plating.

4. Discussion

Interpretation of flow cytometry profiles from cells stained with SYTO 9 and PI is susceptible to be hindered by a number of artifacts (Stocks, 2004). In general, poor tuning of absolute and relative dye concentrations has led to confusing profiles where healthy and dead bacteria appeared to emit both green and red

fluorescence with a varying degree of distinctiveness (Lehtinen *et al.*, 2004; Stocks, 2004; Jang and Rhee, 2009). Reduction of the SYTO 9:PI ratio has shown to decrease green fluorescence level of dead cells, thus improving population resolution (Hoefel *et al.*, 2003). However, healthy cells exhibited the characteristic red fluorescence level of dead cells. As a result, identification of true double positive cells (injured cells), which was the main goal in the present study, was problematic in those previous experimental setups. Barbesti *et al.* (2000) proposed a procedure to find the optimum dye concentration ratio for another combination of membrane integrity indicators, in which a fixed SYBR Green I concentration was combined with increasing amounts of PI. In the present study, the adjustment of SYTO 9, SYTO 24 and SYTO BC concentrations to reduce signal intensity and Barbesti's approach allowed us to optimize population resolution and create a region for double positive cells, free of the interference of fluorescence spillover from green-fluorescent nucleic acid dyes. Besides for SYTO 9, green fluorescence quenching in the presence of PI was observed for SYTO BC, as also reported by Ben-Amor *et al.* (2005), and for SYTO 24. Fluorescence microscopy allowed discarding cell aggregation and/or incomplete cell division (Figure 3.7), which may appear as double positive cells by flow cytometry (Müller and Nebe-von-Caron, 2010; Want *et al.*, 2011).

Furthermore, complete displacement of green-fluorescent dyes bound to nucleic acids in dead cells requires a relatively high PI concentration. This resulted in increased red fluorescence in healthy cells, which might be related to the presence of transport proteins, and/or the disturbance of cell wall integrity during cell wall reconstruction concomitant to cell growth and division (Shi *et al.*, 2007; Sträuber and Müller, 2010). Several authors have reported this effect for cells in the exponential phase. For example, Herrero *et al.* (2006) and Quirós *et al.* (2009) found malolactic bacteria to faintly emit red fluorescence. Similarly, Shi *et al.* (2007) reported positive PI staining for a Gram-negative and a Gram-positive soil bacteria, and although less pronounced, this was also
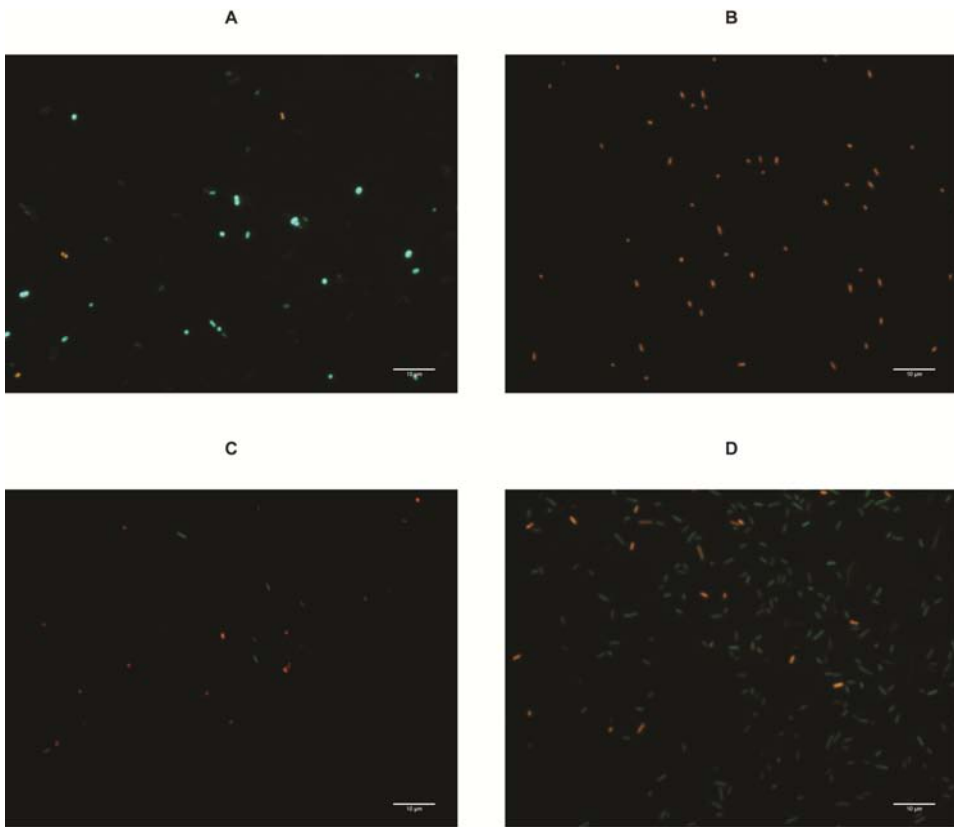
Figure 3.7 Fluorescence microscopy images of healthy (untreated, A), dead (heat-killed, B), heat-treated (C), and refrigeration + citric acid-treated (D) *Escherichia coli* O157:H7 stained with SYTO BC (1.5:10^5 final dilution of the stock solution) and PI (20.0 μM). Images (original magnification × 60) were obtained using a green and red filter. Each image contains a scale bar representing 10 μm.

observed for cells in the stationary phase. We found this effect to be more marked for healthy *L. monocytogenes*, even though they were not stained with the highest PI concentration. This increased PI-uptake, compared with *E. coli* O157:H7 and *S.* Enteritidis, and the fact that complete separation from dead cells by red fluorescence was not possible for *L. monocytogenes* may be explained by the difference in dye permeability between Gram-positive and

Gram-negative bacteria, with *L. monocytogenes* lacking the additional barrier coming from the outer membrane.

The SYTO green-fluorescent nucleic acid stains are cyanine dyes that differ in polarity, target (SYTO 9 and SYTO BC bind to DNA and RNA, whereas SYTO 24 binds to DNA), binding affinity, fluorescence enhancement upon binding, and excitation and emission spectra (Haugland, 2010). Thus, although dye concentrations were selected to meet similar flow cytometry patterns, comparison between SYTO 9 + PI and SYTO 24 + PI counts revealed their different behavior. When using SYTO 24 + PI (the combination with the highest SYTO:PI ratio), injured cell counts tended to be higher for all pathogens, which coincided with these cells emitting increased red fluorescence compared with dead cells. Stocks (2004) showed that PI emission was enhanced after addition of SYTO 9 and related this fact to the FRET phenomenon, consisting in energy being transferred nonradiatively from the excited donor fluorophore to the acceptor fluorophore due to overlapping between the emission spectrum of one and the excitation spectrum of the other (Laib and Seeger, 2004). Then, in injured cells, SYTO 24 and PI would be bound to nucleic acids and close to each other, making it possible for SYTO 24 to transfer energy to PI, as shown by the enhanced red fluorescence, although inefficient transfer is corroborated by the retained green fluorescence. This may result in cells in the transition from the healthy to the injured state emitting high red fluorescence due to FRET rather than to an actual high degree of membrane permeabilization. Notably, when significant differences were found, SYTO BC + PI behavior was similar to that of SYTO 9 + PI for *E. coli* O157:H7 and *L. monocytogenes,* but it was similar to that of SYTO 24 + PI for *S.* Enteritidis. Enhanced PI emission in SYTO BC + PI-stained injured *S.* Enteritidis was also observed, although less pronounced than that found with SYTO 24 + PI. As the FRET effect should be independent from the particular bacteria, distinct results obtained for *S.* Enteritidis might be related to the use of high SYTO BC:PI and SYTO 24:PI ratios, which suggests a donor (SYTO)

concentration dependent FRET effect, as that previously reported for other cyanine dyes (Laib and Seeger, 2004). The intermediate behavior of SYTO BC might be explained by the fact that, as stated by the manufacturer, it is a mixture of the best SYTO dyes for bacterial staining. Additionally, a high SYTO 24:PI ratio may cause dead cells to appear as double positive cells, due to insufficient amount of PI, as observed by Barbesti *et al.* (2000) using SYBR Green I and PI. However, in the present study, dead cell controls showed that selected PI concentrations were enough to properly stain them.

The increased green fluorescence observed in injured Gram-negative bacteria is in agreement with the results of Berney *et al.* (2007), who found the same effect in *E. coli* stained with SYTO 9 and PI after exposure to UVA light. According to this, they proposed an outer membrane dependent diffusion mechanism for SYTO 9, which makes it possible to assess not only cytoplasmic membrane permeabilization but also outer membrane disruption. This might partly explain the fact that injured *L. monocytogenes* populations did not showed increased green fluorescence. In some cold-treated samples, a subpopulation of the healthy *E. coli* O157:H7 and *S.* Enteritidis cells displayed lower green fluorescence intensity compared with control samples. This fact may be due to heterogeneity in the outer membrane integrity of healthy cells exposed to low temperatures, a stress factor which alters permeability of the cell envelope (Denich *et al.*, 2003; Trevors, 2003; Sträuber and Müller, 2010). This effect was not observed for the psychrotrophic *L. monocytogenes*, which has a cold-adapted cell envelope.

For some experimental conditions, flow cytometry injured cell counts were higher than those obtained by differential plating. Since an intact membrane is a requisite for reproductive growth, injured cells need to repair their membrane before starting division (Kell *et al.*, 1998; Mackey, 2000). Thus, lower injured cell counts obtained by differential plating may indicate that culture

conditions did allow the repair of the extensive membrane damage of some injured cells (Wu, 2008). Indeed, Kennedy *et al.* (2011) proved that, after sorting, some red fluorescent SYTO 9 + PI-stained *E. coli* cells were able to grow on solid media. Moreover, in the present study, flow cytometry healthy cell counts were higher than counts on selective media. This fact may be explained by the presence of cells with intact membranes but unable to grow on solid media (e.g. damaged-DNA cells) (Davey *et al.*, 2004). On the whole, differences may imply a different nature of the injury reported by each method.

5. Conclusions

In this study, we proved that it is possible to approach the expected fluorescence pattern when using not only SYTO 9 + PI, but also SYTO 24 + PI or SYTO BC + PI. Notably, the highest cell population resolution by both green and red fluorescence did not occur at the same PI concentration. Thus, a compromise has to be reached when selecting the adequate PI concentration. Moreover, the procedure for the optimization of the staining protocol gave better results for the Gram-negative pathogens *E. coli* O157:H7 and *S.* Enteritidis. Protocol optimization also contributed to the detection of cells with partially damaged membranes after stress exposure, which likely depended on the interaction between dye combination and dye concentration ratio. Thus, SYTO 9 + PI and SYTO BC + PI, unlike SYTO 24 + PI, proved suitable to detect cells with partially damaged membranes for the pathogens and stresses tested. In summary, protocol adjustment allowed us to reliably detect three different membrane integrity states, and thus to obtain a useful and rapid tool to investigate the effect of a range of food processing and preservation treatments on this important cellular target. The relation between partial membrane damage and ability to resume growth could then be ascertained by sorting.

6. References

Abee, T., and J.A. Wouters. 1999. Microbial stress response in minimal processing. *International Journal of Food Microbiology*. 50:65–91.

Ananta, E., D. Voigt, M. Zenker, V. Heinz, and D. Knorr. 2005. Cellular injuries upon exposure of *Escherichia coli* and *Lactobacillus rhamnosus* to high-intensity ultrasound. *Journal of Applied Microbiology*. 99:271–278.

Archer, D.L. 1996. Preservation microbiology and safety: evidence that stress enhances virulence and triggers adaptive mutations. *Trends in Food Science & Technology*. 7:91–95.

Barbesti, S., S. Citterio, M. Labra, M.D. Baroni, M.G. Neri, and S. Sgorbati. 2000. Two and three-color fluorescence flow cytometric analysis of immunoidentified viable bacteria. *Cytometry Part A*. 40:214–218.

Ben-Amor, K., H. Heilig, H. Smidt, E.E. Vaughan, T. Abee, and W.M. de Vos. 2005. Genetic diversity of viable, injured, and dead fecal bacteria assessed by fluorescence-activated cell sorting and 16S rRNA gene analysis. *Applied and Environmental Microbiology*. 71:4679–4689.

Berney, M., F. Hammes, F. Bosshard, H.-U. Weilenmann, and T. Egli. 2007. Assessment and interpretation of bacterial viability by using the LIVE/DEAD BacLight kit in combination with flow cytometry. *Applied and Environmental Microbiology*. 73:3283–3290.

Berney, M., M. Vital, I. Hülshoff, H.-U. Weilenmann, T. Egli, and F. Hammes. 2008. Rapid, cultivation-independent assessment of microbial viability in drinking water. *Water Research*. 42:4010–4018.

Brul, S., and P. Coote. 1999. Preservative agents in foods. Mode of action and microbial resistance mechanisms. *International Journal of Food Microbiology*. 50:1–17.

Bunthof, C.J., and T. Abee. 2002. Development of a flow cytometric method to analyze subpopulations of bacteria in probiotic products and dairy starters. *Applied and Environmental Microbiology*. 68:2934–2942.

Bunthof, C.J., S. van Schalkwijk, W. Meijer, T. Abee, and J. Hugenholtz. 2001. Fluorescent method for monitoring cheese starter permeabilization and lysis. *Applied and Environmental Microbiology.* 67:4264–4271.

Comas-Riu, J., and N. Rius. 2009. Flow cytometry applications in the food industry. *Journal of Industrial Microbiology & Biotechnology.* 36:999–1011.

Corbitt, T.S., Z. Zhou, Y. Tang, S.W. Graves, and D.G. Whitten. 2011. Rapid evaluation of the antibacterial activity of arylene-ethynylene compounds. *ACS Applied Materials & Interfaces.* 3:2938–2943.

Davey, H.M., D.B. Kell, D.H. Weichart, and A.S. Kaprelyants. 2004. Estimation of microbial viability using flow cytometry. *Current Protocols in Cytometry.* 29:11.3.1–11.3.21.

Denich, T.J., L.A. Beaudette, H. Lee, and J.T. Trevors. 2003. Effect of selected environmental and physico-chemical factors on bacterial cytoplasmic membranes. *Journal of Microbiological Methods.* 52:149–182.

Endo, H., Y. Nagano, H. Ren, and T. Hayashi. 2001. Rapid enumeration of bacteria grown on surimi-based products by flow cytometry. *Fisheries Science.* 67:969–974.

Gunasekera, T.S., P. V Attfield, and D.A. Veal. 2000. A flow cytometry method for rapid detection and enumeration of total bacteria in milk. *Applied and Environmental Microbiology.* 66:1228–1232.

Gunasekera, T.S., D.A. Veal, and P. V Attfield. 2003. Potential for broad applications of flow cytometry and fluorescence techniques in microbiological and somatic cell analyses of milk. *International Journal of Food Microbiology.* 85:269–279.

Haugland, R.P. 2010. Nucleic acid detection and genomics technology. *In* The Molecular Probes handbook. A guide to fluorescent probes and labelling technologies. M.T.Z. Spence, editor. Invitrogen, Carlsbad, CA. 302–360.

Hayouni, E.A., M. Bouix, M. Abedrabba, J.-Y. Leveau, and M. Hamdi. 2008. Mechanism of action of *Melaleuca armillaris* (Sol. Ex Gaertu) Sm. essential

oil on six LAB strains as assessed by multiparametric flow cytometry and automated microtiter-based assay. *Food Chemistry.* 111:707–718.

Herrero, M., C. Quirós, L.A. García, and M. Díaz. 2006. Use of flow cytometry to follow the physiological states of microorganisms in cider fermentation processes. *Applied and Environmental Microbiology.* 72:6725–6733.

Hoefel, D., W.L. Grooby, P.T. Monis, S. Andrews, and C.P. Saint. 2003. Enumeration of water-borne bacteria using viability assays and flow cytometry: a comparison to culture-based techniques. *Journal of Microbiological Methods.* 55:585–597.

Jang, H.I., and M.S. Rhee. 2009. Inhibitory effect of caprylic acid and mild heat on *Cronobacter* spp. (*Enterobacter sakazakii*) in reconstituted infant formula and determination of injury by flow cytometry. *International Journal of Food Microbiology.* 133:113–120.

Jasson, V., M. Uyttendaele, A. Rajkovic, and J. Debevere. 2007. Establishment of procedures provoking sub-lethal injury of *Listeria monocytogenes*, *Campylobacter jejuni* and *Escherichia coli* O157 to serve method performance testing. *International Journal of Food Microbiology.* 118:241–249.

Kell, D.B., A.S. Kaprelyants, D.H. Weichart, C.R. Harwood, and M.R. Barer. 1998. Viability and activity in readily culturable bacteria: a review and discussion of the practical issues. *Antonie van Leeuwenhoek.* 73:169–187.

Kennedy, D., U.P. Cronin, and M.G. Wilkinson. 2011. Responses of *Escherichia coli*, *Listeria monocytogenes*, and *Staphylococcus aureus* to simulated food processing treatments, determined using fluorescence-activated cell sorting and plate counting. *Applied and Environmental Microbiology.* 77:4657–4668.

Laib, S., and S. Seeger. 2004. FRET studies of the interaction of dimeric cyanine dyes with DNA. *Journal of Fluorescence.* 14:187–191.

Lehtinen, J., J. Nuutila, and E.-M. Lilius. 2004. Green fluorescent protein-propidium iodide (GFP-PI) based assay for flow cytometric measurement of bacterial viability. *Cytometry Part A*. 60:165–172.

Mackey, B.M. 2000. Injured bacteria. *In* Microbiological safety and quality of food. B.M. Lund, T. Baird-Parker, and G.W. Gould, editors. Springer-Verlag, Gaithersburg, MD. 315–341.

Müller, S., and G. Nebe-von-Caron. 2010. Functional single-cell analyses: flow cytometry and cell sorting of microbial populations and communities. *FEMS Microbiology Reviews*. 34:554–587.

Nebe-von-Caron, G. 2009. Standardization in microbial cytometry. *Cytometry Part A*. 75:86–89.

Quested, T.E., P.E. Cook, L.G.M. Gorris, and M.B. Cole. 2010. Trends in technology, trade and consumption likely to impact on microbial food safety. *International Journal of Food Microbiology*. 139:29–42.

Quirós, C., M. Herrero, L.A. García, and M. Díaz. 2009. Taking advantage of the flow cytometry technique for improving malolactic starters production. *European Food Research and Technology*. 228:543–552.

Rajkovic, A., N. Smigic, and F. Devlieghere. 2010. Contemporary strategies in combating microbial contamination in food chain. *International Journal of Food Microbiology*. 141:29–42.

Saegeman, V.S., R. De Vos, N.D. Tebaldi, J.M. van der Wolf, J.H. Bergervoet, J. Verhaegen, D. Lismont, B. Verduyckt, and N.L. Ectors. 2007. Flow cytometric viability assessment and transmission electron microscopic morphological study of bacteria in glycerol. *Microscopy and Microanalysis*. 13:18–29.

Shi, L., S. Günther, T. Hübschmann, L.Y. Wick, H. Harms, and S. Müller. 2007. Limits of propidium iodide as a cell viability indicator for environmental bacteria. *Cytometry Part A*. 71:592–598.

Stephens, P.J., and B.M. Mackey. 2003. Recovery of stressed microorganisms. *In* Handbook of culture media for food microbiology. J.E.L. Corry, G.D.W. Curtis, and R.M. Baird, editors. Elsevier, Amsterdam. 25–48.

Stocks, S.M. 2004. Mechanism and use of the commercially available viability stain, *Bac*Light. *Cytometry Part A*. 61:189–195.

Sträuber, H., and S. Müller. 2010. Viability states of bacteria. Specific mechanisms of selected probes. *Cytometry Part A*. 77:623–634.

Swarts, A.J., J.W. Hastings, R.F. Roberts, and A. von Holy. 1998. Flow cytometry demonstrates bacteriocin-induced injury to *Listeria monocytogenes*. *Current Microbiology*. 36:266–270.

Tong, S., A.P. Bos, and S. Brul. 2009. Assessing freeze-thaw and high pressure low temperature induced damage to *Bacillus subtilis* cells with flow cytometry. *Innovative Food Science & Emerging Technologies*. 10:9–15.

Tran, P.T., A. Paoletti, and F. Chang. 2004. Imaging green fluorescent protein fusions in living fission yeast cells. *Methods*. 33:220–225.

Trevors, J.T. 2003. Fluorescent probes for bacterial cytoplasmic membrane research. *Journal of Biochemical and Biophysical Methods*. 57:87–103.

Want, A., H. Hancocks, C.R. Thomas, S.M. Stocks, G. Nebe-von-Caron, and C.J. Hewitt. 2011. Multi-parameter flow cytometry and cell sorting reveal extensive physiological heterogeneity in *Bacillus cereus* batch cultures. *Biotechnology Letters*. 33:1395–1405.

Wesche, A.M., J.B. Gurtler, B.P. Marks, and E.T. Ryser. 2009. Stress, sublethal injury, resuscitation, and virulence of bacterial foodborne pathogens. *Journal of Food Protection*. 72:1121–1138.

Wu, V.C.H. 2008. A review of microbial injury and recovery methods in food. *Food Microbiology*. 25:735–744.

Zhou, Z., T.S. Corbitt, A. Parthasarathy, Y. Tang, L.K. Ista, K.S. Schanze, and D.G. Whitten. 2010. "End-Only" functionalized oligo(phenylene ethynylene)s: synthesis, photophysical and biocidal activity. *The Journal of Physical Chemistry Letters*. 1:3207–3212.

Chapter 4. Sample preparation based on centrifugal filtration for flow cytometry membrane integrity assessment of *Escherichia coli* O157:H7 in ready-to-eat pasta salad

Abstract

Ready-to-eat vegetable salads and salad meals are potential vectors of food-borne pathogens, such as enterohemorrhagic *Escherichia coli* O157:H7. Elucidation of the physiological effects of the stresses found in such minimally processed food products is necessary to design safe preservation methods. Flow cytometry is an efficient tool for the analysis of a variety of physiological parameters at the single-cell level, but it is largely affected by the presence of food particles. The present study compared eight different salad sample pre-treatments, based on coarse filtration of food homogenates and a dilution/wash step, for flow cytometry analysis of inoculated *E. coli* O157:H7 in terms of background particle reduction and cell recovery. The most advantageous pre-treatment was the combination of a 63-μm filter blender bag and centrifugal filtration through a 5-μm filter, since it was equivalent to sample dilution in reducing background particle concentration. Although bacterial recovery was reduced after centrifugal filtration, only a 0.2 log CFU/g difference was found compared with the standard plating method. Resolution of *E. coli* O157:H7 populations with intact, partially damaged and damaged membranes was evaluated in samples pre-treated by centrifugal filtration and stained with combinations of SYBR Green I, SYTO 9 or SYTO BC with propidium iodide. These assays revealed an increase in cells with partially damaged membranes, conceivably as a consequence of exposure to refrigeration and acetic acid in the salad. Therefore, the proposed sample pre-treatment based on centrifugal filtration was suitable for the flow cytometry detection of bacterial cells in a complex food matrix and the assessment of their membrane integrity.

1. Introduction

Foodborne diseases caused by the enterohemorrhagic pathogen *Escherichia coli* O157:H7 have been increasingly linked to products of non-animal origin over the past years (Berger *et al.*, 2010). Indeed, in 2011, produce, fruits, and products thereof were involved in half of the enterohemorrhagic *Escherichia coli* (EHEC) foodborne outbreaks occurred in the EU (European Food Safety Authority and European Centre for Disease Prevention and Control, 2013). Special concern has been raised in relation to those products of non-animal origin which are consumed raw or minimally processed, such as ready-to-eat (RTE) vegetable salads and salad meals, since safety may be compromised (Little and Gillespie, 2008; EFSA Panel on Biological Hazards, 2013). Storage of RTE vegetable salads at refrigeration temperature is the main factor controlling the growth of *E. coli* O157:H7 if present in these products (Delaquis *et al.*, 2007; Luo *et al.*, 2010). Moreover, low pH dressings (e. g. vinaigrette, mayonnaise, sour cream, etc.) are common ingredients in RTE salad meals, since shelf-life is extended by creating an extra hurdle for the existent microbiota (Heard, 1999; Leistner, 2000). However, *E. coli* O157:H7 is an unusually acid tolerant pathogen, fact shown by its ability to withstand the passage through the stomach, and to survive in acidic foods, such as fruit juices, fermented sausages, yogurt or mayonnaise (Buchanan and Doyle, 1997; Robinson and McKillip, 2010). Thus, elucidation of the effect of food preservation factors on physiology of *E. coli* O157:H7 in RTE salad meals is a topic of growing interest, since this provides the basis for the intelligent design of multitarget preservation methods assuring the safety and stability of such minimally processed products (Leistner, 2000; Delaquis *et al.*, 2007; Luo *et al.*, 2010).

Bacterial viability has been traditionally assessed using the plate count technique, but it has recognized limitations despite its widespread use (Davey, 2011). Actually, sorbitol MacConkey (SMAC) agar, which is the medium com-

monly used to isolate *E. coli* O157:H7 from foodstuffs, has repeatedly been shown to prevent recovery of stressed cells, whether it is supplemented with cefixime and tellurite or not (McCarthy *et al.*, 1998; Park *et al.*, 2011; Yoshitomi *et al.*, 2012). Moreover, *E. coli* O157:H7 has demonstrated to enter into the viable but nonculturable (VBNC) state when exposed to acid, cold or starvation conditions (Zhao and Matthews, 2000; Dinu and Bach, 2011). This fact is of special concern since VBNC *E. coli* O157:H7 cells have the ability to retain virulence, and thus the potential capacity to initiate infection once they resuscitate from that state (Liu *et al.*, 2010; Oliver, 2010). Consequently, nonculture-based techniques should be used to avoid underestimation of *E. coli* O157:H7 viability.

Membrane integrity and metabolic activity are physiological parameters related with cell viability that can be estimated using a wide range of fluorochromes (Breeuwer and Abee, 2000; Müller and Nebe-von-Caron, 2010). Cell-associated fluorescence may then be detected by flow cytometry, a high-throughput technique which gives quantitative information on heterogeneity of population physiology in few seconds (Davey, 2011). However, flow cytometry detection of bacterial cells in food is hindered by the release of a large number of food particles in the same size range during pre-analytical sample processing (Raybourne and Tortorello, 2003; Wilkes *et al.*, 2012). In such cases, conferring fluorescence emission to cells may not be enough to make them detectable among background particles, since these particles can non-specifically bind to fluorescent dyes (Gunasekera *et al.*, 2000; Cao-Hoang *et al.*, 2008; Doherty *et al.*, 2010). To address these limitations, it is necessary to separate and concentrate bacterial cells before flow cytometry analysis, by using methods which, ideally, should be simple, rapid and inexpensive, and provide high cell recoveries while maintaining cell viability.

Centrifugation and filtration are the most commonly used methods in pre-analytical sample processing for flow cytometry analysis, and meet the criteria

of simplicity, rapidity, and cheapness. In simple high-speed centrifugation (8,000-60,000 × *g*), sedimentation of both bacterial cells and particles with densities equal to or higher than those from cells occur (Stevens and Jaykus, 2004). This is an efficient method to harvest cells from liquid culture media and some liquid foods, but in solid and semi-solid foods, a large quantity of food particles is also deposited. To minimize this effect, large particles can be removed from food homogenates by coarse filtration, which is generally performed using filter blender bags with a pore diameter ranging from 250 to 500 μm (Tortorello *et al.*, 1997; Stevens and Jaykus, 2004; Wilkes *et al.*, 2012; Buzatu *et al.*, 2013). More recently, low porosity filter blender bags with approximately 10-time smaller pores have been commercialized. Moreover, coarse filtration may be used as a pre-filtration step in order to facilitate further filtration through smaller pore size filters (e. g. 5 μm). Such an approach has been previously applied to processing of meat, spinach and baby food puree samples for flow cytometry analysis (Tortorello *et al.*, 1997; Wilkes *et al.*, 2012; Buzatu *et al.*, 2013). Centrifugation and filtration may be combined in one step to increase filtration efficiency and reduce labor. In centrifugal filtration, sample filtration is driven by centrifugal force rather than by pressure difference, which results in reduced hold-up volume, while particles in the filtrate settle (Svarovsky, 2001). This method is commonly applied to biological sample preparation, but its suitability for flow cytometry analysis of food samples has not been reported. Thus, the goal of this study was to assess the efficacy of centrifugal filtration for sample preparation and subsequent membrane integrity flow cytometry analysis of *E. coli* O157:H7 cells in a RTE salad meal. The performance of centrifugal filtration in background particle reduction and bacterial recovery was compared to that from other simple centrifugation- and filtration-based protocols. The ability of the experimental set-up to resolve cell populations showing different membrane integrity states was also evaluated.

2. Materials and methods

2.1. Bacterial strain and culture conditions

Escherichia coli O157:H7 CECT 5947, provided by the Spanish Type Culture Collection (Colección Española de Cultivos Tipo, CECT), was used for all the experiments. A lyophilized culture was reconstituted and cultured for stock culture preparation. The stock culture was stored at –65°C in cryovials containing beads (AES Chemunex, Bruz, France). Pre-cultures were prepared by transferring one bead from the stock culture to a 100-mL Erlenmeyer flask containing 20 mL of tryptone soya broth (TSB; Oxoid, Basingstoke, UK), and then, incubated overnight at 37°C in a shaking water bath at 86 rpm. To obtain stationary phase cultures, 50 μL of the overnight culture were inoculated into 20 mL of TSB and incubated at 37°C for 20 h. Growth time to reach stationary phase was previously determined by measuring the optical density at 600 nm (Bioscreen C; Oy Growth Curves AB, Helsinki, Finland).

2.2. Cell preparation

Escherichia coli O157:H7 suspensions obtained from stationary phase cultures were used as flow cytometry controls (instrument set up, compensation and gating) and as inocula for RTE pasta salad samples. To prepare flow cytometry controls, untreated cells or heat-killed cells (80°C/30 min) were pelleted (13,000 × g, 30 s, 20°C), resuspended, and diluted to *ca.* 7.5 log colony-forming unit (CFU)/mL in filtered (0.22 μm, polyethersulfone; Millipore, Cork, Ireland) 2 mM potassium citrate solution (pH 7.4). For inoculum preparation, untreated cells were harvested (4,000 × g, 10 min, 20°C), and resuspended in potassium citrate solution.

2.3. Ready-to-eat pasta salad sample preparation

Non-pasteurized RTE pasta salad (Central de Cocinados Catar, Mollet del Vallès, Spain) contained cooked fusilli, green and red pepper, onion, water, sunflower oil, vinegar, salt, sodium benzoate, garlic powder, basil, parsley, and xanthan gum. Salad pH was 4.5. Salad was transferred to a sterile glass container, autoclaved (121°C, 15 min), and inoculated with *E. coli* O157:H7 to *ca.* 8 log CFU/g (2.5 mL of inoculum in 25 g of salad). This allowed to specifically test the experimental set-up for *E. coli* O157:H7 detection. After inoculation, samples were vacuum-packaged in low porosity filter blender bags (Interscience, Saint-Nom-la-Bretêche, France): BagPage F (BP; micro-perforated full-surface filter, 63 μm) or BagFilter Pull-Up (PU; nonwoven side filter, <50 μm), and stored at 4°C for 14 days, which was the shelf-life of the salad. At day 14, salad samples were ten times diluted in potassium citrate solution and blended for 30 s (Pulsifier, Microgen Bioproducts, Camberley, UK). Dilution/wash steps included in pre-analytical sample processing methods were: conventional centrifugation (C), conventional centrifugation and second dilution (C+S), centrifugal filtration (CF), or second dilution alone (neither centrifugation nor centrifugal filtration) (S). For C and C+S, 1-mL aliquots were centrifuged at 13,000 × *g* for 30 s at 20°C, and resuspended in potassium citrate solution. For CF, 2-mL aliquots were clarified (5,000 × *g*, 10 min, 20°C) by means of a centrifugal filter device (5 μm, polyvinylidene difluoride, Ultrafree-CL; Millipore), and the pellets were resuspended in 2 mL of potassium citrate solution. For S, second dilution was made in potassium citrate solution. An overview of these pre-treatments is presented in Figure 4.1.
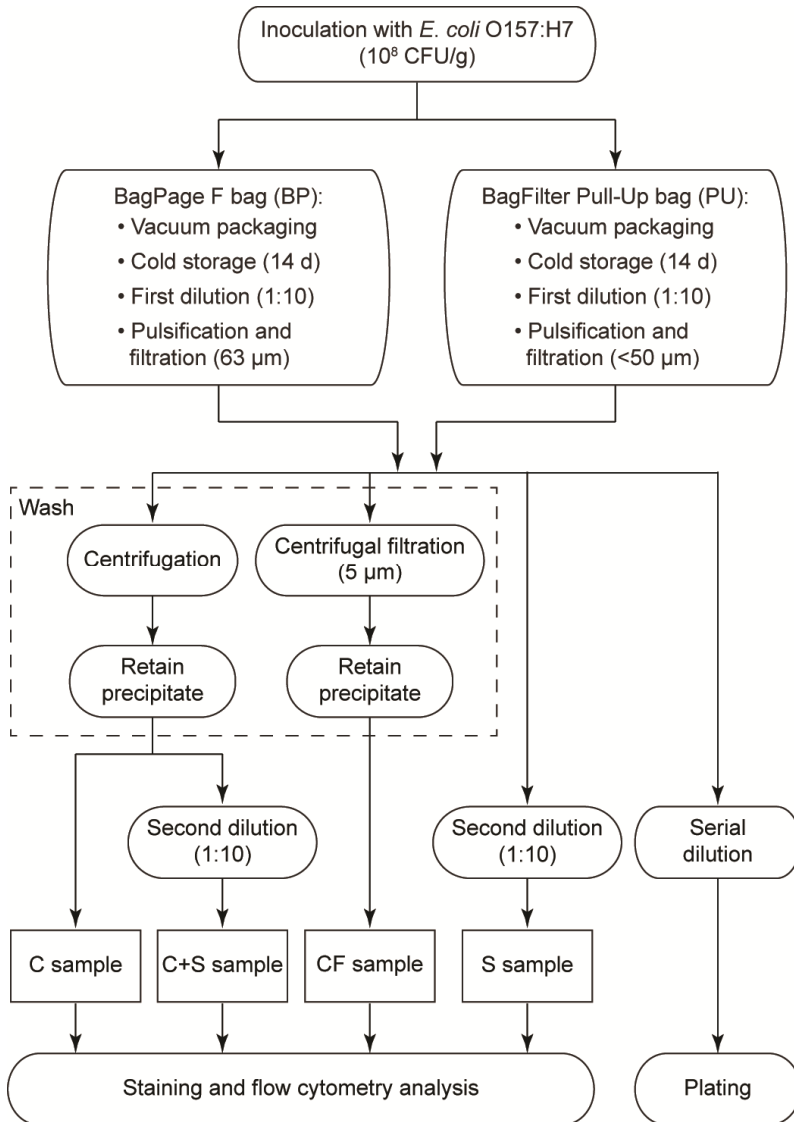
Figure 4.1 Pre-analytical pasta salad sample processing methods for flow cytometry analysis. C: centrifugation; C+S: centrifugation, second dilution; CF: centrifugal filtration; S: second dilution.

2.4. Staining

Cells contained in 1-mL aliquots were stained with one of the following combinations of nucleic acid dyes (Invitrogen, Eugene, OR, USA): SYBR Green I (1:10^6 dilution of the stock solution) with propidium iodide (PI; 20 µM), SYTO 9 (10 nM) with PI, and SYTO BC (1.5:10^5 dilution of the stock solution) with PI. Propidium iodide is a red-fluorescent dye that stains permeabilized cells, whereas SYBR Green I, SYTO 9 and SYTO BC are green-fluorescent dyes that stain both permeabilized cells and cells with intact membranes (Barbesti *et al.*, 2000; Stocks, 2004; Ben-Amor *et al.*, 2005). Thus, cells with intact membranes display very low red fluorescence and high green fluorescence, whereas cells with damaged membranes emit high red fluorescence and very low green fluorescence. To achieve such fluorescence profiles, dye concentrations in samples were selected from preliminary work (data not shown). Dye stock solutions were prepared in filtered (0.20 µm, nylon; Millipore) dimethyl sulfoxide (DMSO) and stored at 4°C. Concentrations of such stock solutions were chosen to minimize the presence of DMSO in the sample (1-1.5 µL stock solution/mL). After dye addition, samples were incubated at 20°C for 30 min, protected from light. To calculate cell concentrations, a microsphere standard (Invitrogen) was used according to manufacturer's instructions. This calibrated suspension contained 10^8 polysterene microspheres/mL with a 6.0-µm diameter and green and red fluorescence emission.

Flow cytometry controls consisted in unstained untreated cells (instrument set up), single-stained heat-killed cells (compensation of spectral overlap between fluorescence emission of red and green fluorescent dyes), and a dual-stained mixture (1:1) of untreated and heat-killed cells (population gating). For flow cytometry data analysis purposes (backgating), one salad sample aliquot was stained only with SYBR Green I.

2.5. Flow cytometry and data analysis

Samples were analyzed with a FACScalibur flow cytometer (BD, Franklin Lakes, NJ, USA) equipped with a 15-mW 488-nm air-cooled argon-ion laser. Data were acquired for forward scatter (FSC), side scatter (SSC), green fluorescence (FL1), yellow-orange fluorescence (FL2) and red fluorescence (FL3) parameters. Band-pass filter for SYBR Green I, SYTO 9 and SYTO BC light emission was 530/30 nm, whereas PI light emission was collected with a 545/82-nm band-pass filter and a 670-nm long-pass filter. Voltage amplification was applied at logarithmic scale. Filtered double-distilled water was used as sheath fluid and sample flow rate was kept at 12 μL/min. CellQuest Pro software (version 4.0.2; BD) was used for acquisition of multiparametric data from 20,000 cells gated in the FSC *vs.* SSC plot, with thresholds set on FSC (primary threshold) and SSC parameters. Flow cytometry controls always accompanied acquisition of salad samples.

FlowJo software (version 7.6.1; Tree Star, Ashland, OR, USA) was used for data compensation and analysis. Data acquired from unstained untreated cells were used as negative control in software compensation, whereas single-stained heat-killed cells were used as positive controls. Raw data from salad samples were first evaluated by displaying all parameter combinations in pseudocolor bivariate plots to detect interferences and find the best gating strategy (Nebe-von-Caron, 2009). Microspheres were gated in the FSC *vs.* SSC plot. Cells in SYBR Green I-stained salad samples were gated in the FSC *vs.* FL1 plot. Gated cells were then displayed according to FSC and SSC parameters (backgating) and a region was drawn loosely encompassing them. This region was applied to dual-stained salad samples to reduce the presence of background particles during data analysis, and thus to facilitate the visualization of the bacterial cluster. Then, a second gate was set in the FSC *vs.* FL2 plot, and gated cells were displayed according to their green and red fluorescence. Finally, regions were set to discriminate bacterial populations with different degrees of membrane integrity. These regions were previously defined using controls containing

dual-stained untreated and heat-killed cells. After gating, counts were estimated for:

(i)   *healthy cells*: cells with intact membranes (SYBR Green I$^+$/PI$^-$ or SYTO$^+$/PI$^-$);

(ii) *injured cells*: cells with partially damaged membranes (SYBR Green I$^+$/PI$^+$ or SYTO$^+$/PI$^+$);

(iii) *dead cells*: cells with damaged membranes (SYBR Green I$^-$/PI$^+$ or SYTO$^-$/PI$^+$);

(iv) *total cells*: healthy cells + injured cells + dead cells;

(v) *background particles*: total events – (total cells + microsphere count)

Cell concentrations were expressed as log cell/g of inoculated salad, whereas background particle concentrations were expressed as log background particle/mL of flow cytometry sample. Referring background particle counts to the weight of salad sample would have led to mistakenly inferring that salads initially contained different amounts of background particles and would have masked the effect of the second dilution.

2.6. Plate count

At day 14, salad samples were homogenized, as previously described, and serially diluted in peptone physiological salt solution (1 g/L neutralized bacteriological peptone [Oxoid] and 8.5 g/L NaCl, in water). Appropriate dilutions were spiral-plated (Eddy Jet; IUL, Barcelona, Spain) on the nonselective medium tryptone soya agar supplemented with 0.6% (w/v) yeast extract (TSAYE; Oxoid), and the *E. coli* O157:H7-selective medium sorbitol MacConkey (SMAC) agar (Oxoid). Plates were incubated at 37°C for 24 h.

According to the so called differential plating method, that is, parallel plating on nonselective and selective medium (Wesche *et al.*, 2009), both healthy and injured cells are able to grow on TSAYE, whereas only healthy cells grow on SMAC. Since salad was sterilized before pathogen inoculation, only *E. coli* O157:H7 grew on TSAYE. This principle was used to estimate counts of:

(i)   *viable cells*: count on TSAYE;

(ii) *healthy cells*: count on SMAC;

(iii) *sublethally injured cells*: count on TSAYE – count on SMAC;

(iv) *dead cells*: initial count on TSAYE – count on TSAYE.

Initial count on TSAYE was taken as the reference to evaluate recovery of *E. coli* O157:H7 cells from salad, after sample preparation, reported by flow cytometry. Healthy, injured and dead cell counts from plating were also compared with those obtained by flow cytometry.

2.7. Statistical analysis

Counts were logarithmically transformed, except for the calculation of % background particles, and means and standard deviations of three biologically independent replicates were calculated. Analysis of variance (ANOVA) was used to compare pre-treatments (bag and dilution/wash step), methods (plating and flow cytometry), or cell population (healthy, injured and dead). When the analysis was significant ($p < 0.05$), Tukey's test was used to separate means. Dunett's test was used to compare flow cytometry total cell counts with the initial plate count. For these purposes, the Stats (R Core Team, 2013) and Multcomp (Hothorn *et al.*, 2008) packages of R software (version 3.0.1; R Foundation for Statistical Computing, Vienna, Austria) were used. R software was run in the user interface RStudio IDE (version 0.97.551; RStudio, Boston, MA). Representative bivariate plots are shown in figures.

3. Results and discussion

3.1. Effect of pre-analytical sample processing methods on background particles detected by flow cytometry

Background particles, i.e. unwanted events, come both from the instrument (optical and electronic noise) and the sample (debris) and, when present in

high counts, they compromise the limit of detection of flow cytometry and the reliability of the resulting data (Givan, 2001; Shapiro, 2003). Firstly, because cells will not form a visible cluster within the much larger cluster of background events in a light scatter plot, nor in a fluorescence plot, if background fluorescence (autofluorescence, nonspecific binding, free fluorochrome) and cell fluorescence are similar (Nebe-von-Caron *et al.*, 2000). Secondly, a large amount of background events will probably result in acquisition rates (event/s) exceeding the processing capability of the instrument, which in turn will result in loss of data both from background and cells (Sharpe and Wulff, 2006). To assess the efficacy of the tested sample pre-treatments (blender bag and dilution/wash step) in facilitating the analysis of flow cytometry data, background particle counts in flow cytometry samples were compared (Table 4.1).

Background particle counts were also expressed as a percentage from the total number of events, since this parameter strongly influences discrimination from cells (Nebe-von-Caron *et al.*, 2000). The interaction between bag and dilution/wash step was kept in the 3-way ANOVA model. However, significance of the interaction term, $F(3, 62) = 2.91$, $p = 0.0416$, was marginal compared with those from bag, $F(1, 62) = 37.95$, $p < 0.001$, and dilution/wash step, $F(3, 62) = 12.68$, $p < 0.001$, main effects. Dye combination had no significant effect on variability of percentages, $F(2, 62) = 0.01$, $p = 0.9880$. In general, percentages of background particles were higher for pre-treatments with PU bags or with the dilution/wash step S. Therefore, the highest percentage of background particles was observed for PU-S (84.14±8.31%) and PU-CF (72.65±8.63%). Conversely, a lower percentage was observed for BP-CF (49.07±12.46%) and BP-C (55.13±7.76%). No differences were found after applying C and C+S strategies, regardless the blender bag. Therefore, the observed high percentage for S could be attributed to lack of washing, and combination with PU bag may worsen this effect. This is corroborated by the fact that a significantly lower

Table 4.1 Background particles in flow cytometry samples after different salad pre-treatments.

Pre-treatment	log background particle/mL			Percentage from total events		
	SYBR + PI	SYTO 9 + PI	SYTO BC + PI	SYBR + PI	SYTO 9 + PI	SYTO BC + PI
BP bag						
C	7.82±0.30	7.80±0.24	7.87±0.28	53.65± 9.13	56.93± 7.72	54.79± 9.47
CF	7.36±0.23	7.18±0.42	7.17±0.34	48.97±15.07	49.03±14.35	49.19±13.69
S	7.34±0.30	7.28±0.19	7.34±0.26	68.69± 8.99	68.76± 7.98	70.97± 9.10
C+S	7.07±0.32	7.03±0.15	7.10±0.30	60.43±11.25	61.15± 7.33	63.08± 9.06
PU bag						
C	8.01±0.34	8.03±0.28	8.03±0.37	66.63± 9.66	62.93±11.75	63.33±11.27
CF	7.43±0.13	7.51±0.21	7.54±0.18	72.36±11.27	72.39± 9.50	73.19± 8.94
S	7.66±0.30	7.65±0.29	7.74±0.40	84.65± 9.93	83.83± 8.78	83.94±10.01
C+S	7.17±0.32	7.28±0.44	7.17±0.38	67.36±10.61	69.80±11.51	67.55±11.45

Mean ± standard deviation; n = 3.

BP: BagPage F bag; PU: BagFilter Pull-Up bag.

C: centrifugation; CF: centrifugal filtration; S: second dilution; C+S: centrifugation, second dilution.

percentage was found for BP-S (69.47±7.66%) and PU-C+S (68.24±9.77%) compared with PU-S. Since an acceptable discrimination of cells is achieved when the percentage of cells exceeds the percentage of background particles, the best pre-treatment was BP-CF. Additionally, lower density of background particles with scatter properties similar to those from bacterial cells was observed after CF compared with pre-treatments that did not include the centrifugal filtration step (Figure 4.2). A slightly higher background particle density in the scatter range of cells was observed for samples homogenized in PU blender bag. This finding supports the suggestion of the filter shedding particles to the filtrate in PU bags.

3.2. Recovery of *Escherichia coli* O157:H7 cells from pasta salad for flow cytometry analysis

Total *E. coli* O157:H7 flow cytometry counts obtained after applying different salad pre-treatments were also compared (Table 4.2). Three-way ANOVA showed a significant effect for the interaction between blender bag and dilution/wash step, $F(3, 62) = 9.01$, $p < 0.001$, whereas dye combination, $F(2, 62) = 0.22$, $p = 0.8049$, did not have an impact on results. Significant differences were found for pre-treatments including the dilution/wash step CF, which gave lower total cell counts than other pre-treatments. This result indicates that some cells are lost during centrifugal filtration, probably as a result of filter clogging, and cell adsorption to the filter and retained food particles (Payne and Kroll, 1991; Jaykus, 2003). To improve desorption of bacterial cells from food particles, food homogenates may be treated with enzymes (Tortorello *et al.*, 1997; Yamaguchi *et al.*, 2006), detergents (Buzatu *et al.*, 2013), or subjected to changes in pH and ionic strength (Wilkes *et al.*, 2012). However, such treatments were not considered in this study, since they tend to impair cell viability (Stevens and Jaykus, 2004). Decrease in bacterial recovery was of especial biological relevance when centrifugal filtration was combined with PU bag. This might be due to the presence of higher background particle counts in samples
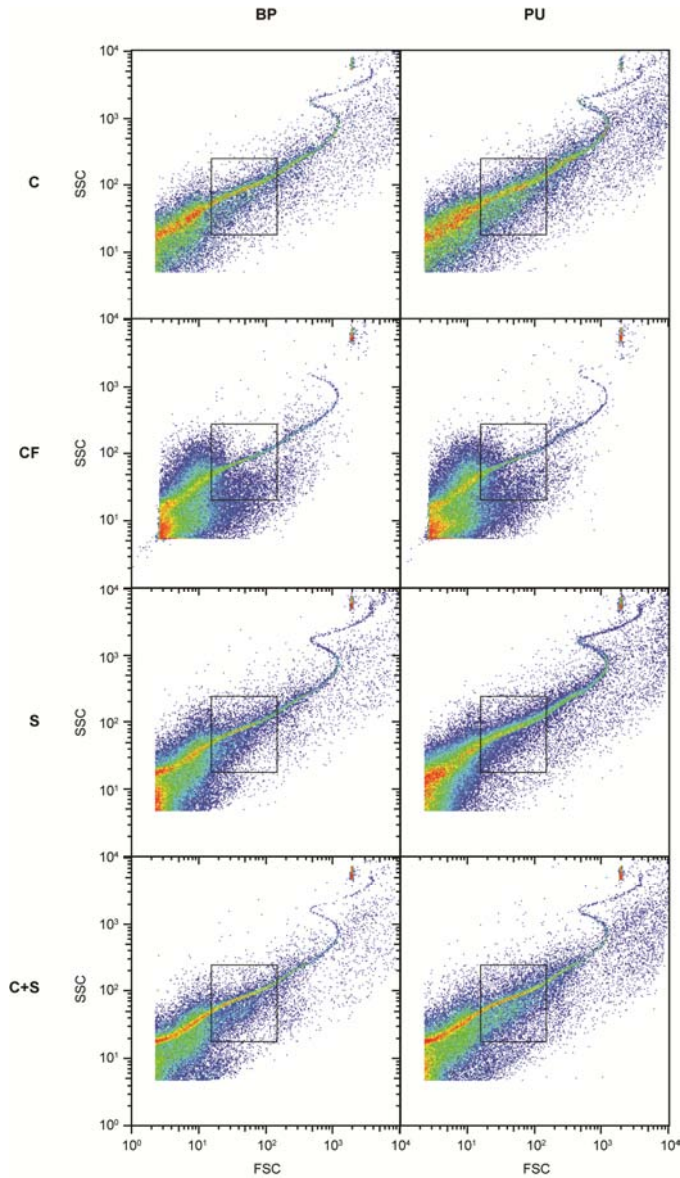
Figure 4.2 Effect of salad pre-treatments on flow cytometry scatter characteristics of background particles. Forward scatter (FSC) *vs.* side scatter (SSC) plots show background particles present in samples homogenized in BP (BagPage F) and PU (BagFilter Pull-Up) blender bags after C (centrifugation), CF (centrifugal filtration), S (second dilution) and C+S (centrifugation, second dilution). Polygonal regions depict the position of bacterial clusters.

homogenized in PU bags, which might lead to increased cell retention in centrifugal filters. Additionally, decrease in bacterial recovery in PU-CF samples may explain the aforementioned high percentage of background particles found in this sample, even when the absolute count was not the highest.

Table 4.2 Total *Escherichia coli* O157:H7 counts (log cell/g) in inoculated pasta salad assessed by flow cytometry after different salad pre-treatments.

Pre-treatment	SYBR + PI	SYTO 9 + PI	SYTO BC + PI
BP bag			
C	8.74±0.14	8.66±0.10	8.78±0.12
CF	8.36±0.15	8.33±0.15	8.31±0.20
S	8.93±0.15	8.87±0.08	8.88±0.16
C+S	8.82±0.15	8.76±0.10	8.79±0.15
PU bag			
C	8.69±0.21	8.78±0.06	8.77±0.15
CF	7.94±0.17	7.98±0.08	7.99±0.07
S	8.80±0.11	8.84±0.04	8.93±0.11
C+S	8.77±0.12	8.83±0.22	8.76±0.16

Mean ± standard deviation; n = 3.
BP: BagPage F bag; PU: BagFilter Pull-Up bag.
C: centrifugation; CF: centrifugal filtration; S: second dilution; C+S: centrifugation, second dilution.

The initial *E. coli* O157:H7 count obtained by plating (8.54±0.14 log CFU/g) was taken as the reference to assess the validity of total cell flow cytometry counts (Figure 4.3). For most pre-treatments, flow cytometry counts were significantly higher than plate counts. This finding suggests that the sample contained cells with intact membranes which were unable to grow on solid medium, the so-called VBNC cells, and is consistent with the idea of culturable cells being a subpopulation of cells with intact membranes (Nebe-von-Caron *et al.*, 1998; Joux and Lebaron, 2000; Davey *et al.*, 2004; Berney *et al.*, 2006). Injury may also be a cause for the VBNC state (Mackey, 2000), and injured cells were indeed detected by flow cytometry in untreated samples, which served as inocula for

salad samples, although in a low percentage (3.39±2.02%). Untreated samples also contained a low percentage of dead cells (1.24±0.50%), and so did sterilized salad samples. Pre-treatments including the CF (centrifugal filtration) step gave flow cytometry counts lower than plate counts. Despite these general trends, biological significance of the differences between plate and flow cytometry counts was remarkable for the dilution/wash step S (*ca.* 0.4 log CFU/g), regardless the blender bag; and, especially, for PU-CF (*ca.* -0.7 log CFU/g). An additional explanation for total cell counts obtained after S being especially higher than initial plate counts may be the presence of a high percentage of background particles and background fluorescence, which may lead to mistakenly scoring background particles as cells (Comas-Riu and Rius, 2009). Conversely, only a *ca.* 0.2 log CFU/g difference was found for CF, regardless the blender bag, and for BP-CF (negative difference).
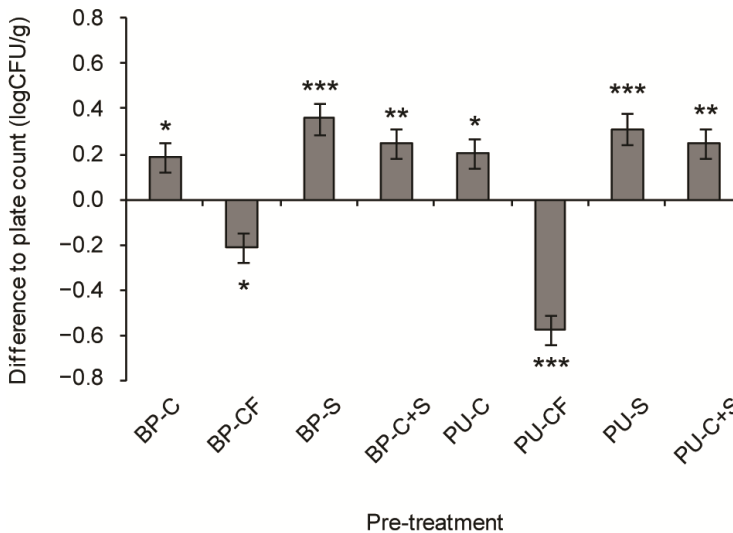
Figure 4.3 Effect of salad pre-treatments on difference between flow cytometry total *Escherichia coli* O157:H7 counts and initial plate counts (8.54±0.14 log CFU/g). BP: BagPage F bag; PU: BagFilter Pull-Up bag; C: centrifugation; CF: centrifugal filtration; S: second dilution; C+S: centrifugation, second dilution. Significance at $p < 0.05$, $p < 0.01$, and $p < 0.001$ are indicated as *, **, and ***, respectively. Error bars indicate standard error.

3.3. Performance of *Escherichia coli* O157:H7 membrane integrity assays in pasta salad treated by centrifugal filtration

Centrifugal filtration was selected for further assays based on the impact on background particles: concentration equivalent to that of 100-time diluted samples, percentage lower than percentage of cells in BP bags, and lower density in the scatter range of cells.

Two distinct populations were observed in control samples containing dual-stained mixtures of untreated and heat-killed cells (Figure 4.4A). Untreated cells, i.e. cells with intact membranes, were those showing high green fluorescence and low red fluorescence, due to presence of SYBR Green I, SYTO 9 or SYTO BC, and absence of PI inside the cell. Heat-killed cells, i.e. cells with damaged membranes, emitted high red fluorescence and low green fluorescence, due to a combined mechanism (Stocks, 2004): (i) PI displaces the nucleic acid-bound green-fluorescent dyes due to a higher affinity for the target, and (ii) the green-fluorescent dye enhances PI fluorescence emission through the FRET (Förster resonant energy transfer) phenomenon. Moreover, a gate could be set to encompass injured cells, i.e. cells with partially damaged membrane, which were expected to show both high green and red fluorescence, conceivably because intracellular PI concentration in such cells is insufficient to significantly displace the green-fluorescent dye molecules (Barbesti *et al.*, 2000). For inoculated salad samples, good discrimination between cell populations with different membrane integrity states was obtained when using any of the dye combinations (Figure 4.4B). Moreover, percentage of injured cells increased in salad samples, compared with control samples. The observed membrane injury may have arisen from exposing cells to cold and acid in salads, since the membrane is the main target for such stresses (Cotter and Hill, 2003; Sutherland, 2005). Cells with partially damaged membranes have also been detected by flow cytometry after exposure of Gram-negative and Gram-positive bacteria to stresses, such as bacteriocin leucocin B-TA11a (Swarts *et al.*, 1998), glycerol

(Saegeman *et al.*, 2007), irradiation (Berney *et al.*, 2007), supercritical CO_2 (Tamburini *et al.*, 2013), or in fecal bacteria (Ben-Amor *et al.*, 2005).
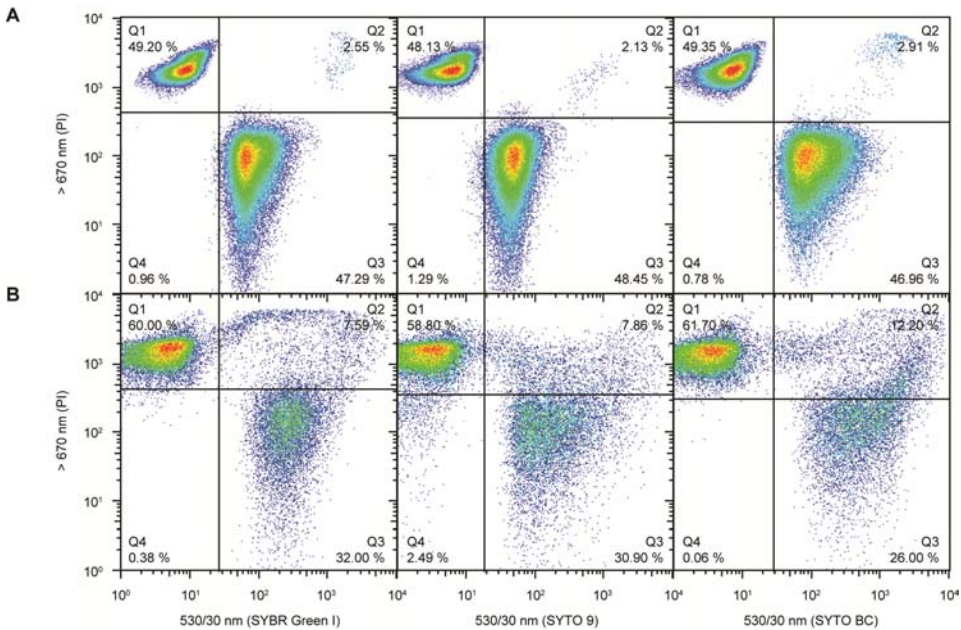
Figure 4.4 Flow cytometry assessment of *Escherichia coli* O157:H7 membrane integrity. (A) Control: heat-killed and healthy cells. (B) Inoculated pasta salad stored at 4°C for 14 days. Salad pre-treatment consisted in coarse filtration in BP (BagPage F) blender bags and CF (centrifugal filtration). Q1: dead cells, Q2: injured cells; Q3: healthy cells, Q4: negative.

The effect of the blender bag and counting method on healthy, injured, and dead cell counts was assessed independently for flow cytometry data, and for flow cytometry and plating data (Table 4.3). For all cell populations, fits of the flow cytometry data ANOVA models were better than those of the models including plating data (data not shown). In both cases, two-way ANOVA showed that the interaction between blender bag and counting method did not have a significant effect on healthy, injured and dead cell counts ($ps > 0.05$), and was thus removed from the statistical analyses.

Table 4.3 Physiological state assessment of *Escherichia coli* O157:H7 inoculated into 14-day refrigerated pasta salad assessed by flow cytometry after centrifugal filtration (log cell/g) and by plating (log CFU/g).

Blender bag	Method	Healthy	Injured	Dead
BP	Plating	7.07±0.24	8.21±0.29	8.09±0.20
	SYBR + PI	7.80±0.41	7.51±0.58	7.85±0.45
	SYTO 9 + PI	7.80±0.46	7.40±0.53	7.86±0.39
	SYTO BC + PI	7.72±0.50	7.52±0.55	7.86±0.34
PU	Plating	7.49±0.48	7.81±0.36	8.30±0.20
	SYBR + PI	7.11±0.56	7.34±0.40	7.55±0.28
	SYTO 9 + PI	7.21±0.61	7.23±0.41	7.64±0.26
	SYTO BC + PI	7.04±0.63	7.33±0.43	7.66±0.24

Mean ± standard deviation; n = 3.
BP: BagPage F bag; PU: BagFilter Pull-Up bag.

No significant differences were found among dye combinations for healthy, $F_{(2, 14)} = 0.10$, $p = 0.9050$, injured, $F_{(2, 14)} = 0.12$, $p = 0.8902$, and dead, $F_{(2, 14)} = 0.05$, $p = 0.9491$, cell counts. When flow cytometry and plating methods were compared, no significant differences were found for healthy cell counts $F_{(3, 19)} = 0.21$, $p = 0.8916$. On the contrary, the counting method did have a significant effect on injured, $F_{(3, 19)} = 3.39$, $p = 0.0393$, and dead, $F_{(3, 19)} = 3.44$, $p = 0.0375$, cell counts. In particular, injured cell plate counts (8.01±0.37 log cell/g) were higher than flow cytometry counts obtained with SYTO 9 + PI (7.32±0.43 log cell/g). A similar trend was observed for SYTO BC + PI (7.38±0.63 log cell/g) and SYBR Green I + PI (7.46±0.58 log cell/g) although differences were not significant. For dead cell counts, plating (8.19±0.21 log cell/g) gave higher counts than flow cytometry counts obtained with SYBR Green I + PI (7.71±0.37 log cell/g), SYTO 9 + PI (7.75±0.32 log cell/g), and SYTO BC + PI (7.76±0.28 log cell/g). These findings suggest that injured and dead cells are more prone to be miscounted than healthy cells, a fact that can be explained by the similarity between fluorescence intensity of some injured or dead cells and background particles, which leads to errors in data analysis. Moreover, since detection of

cells by these flow cytometry assays are based on the presence of nucleic acids, lower dead cell flow cytometry counts may also arise from cell lysis, as well as loss of cell nucleoid (ghost cells) (Joux *et al.*, 1997; Nebe-von-Caron *et al.*, 1998).

Nevertheless, the hypothesis of some cells being lost during centrifugal filtration cannot be ruled out, since a significant effect on healthy cell flow cytometry counts, which are not affected by background fluorescence, was found for the blender bag factor, $F(1, 14) = 7.98$, $p = 0.0135$, with BP bag (7.78±0.40 log cell/g) giving higher counts than PU bag (7.12±0.53 log cell/g). Conversely, the blender bag did not have an impact on injured, $F(1, 14) = 0.67$, $p = 0.4259$, and dead, $F(1, 14) = 2.70$, $p = 0.1229$, cell flow cytometry counts, although the same trend was evident. This may imply that, in these cases, the background fluorescence effect is more important than the decreased recovery associated with the centrifugal filtration step. Similarly, when flow cytometry and plating were compared, the blender bag had no significant effect on injured, $F(1, 19) = 1.80$, $p = 0.1950$, and dead, $F(1, 19) = 1.08$, $p = 0.3114$, cell counts. Neither was the difference for healthy cell counts, $F(1, 19) = 3.26$, $p = 0.0869$, although differences between flow cytometry and plate counts were positive when using BP bag, and negative with PU bag. Therefore, lack of significance in this case would be due to inclusion of plating data in the statistical model.

Furthermore, cell populations were expressed as percentages to correct for cell loss in flow cytometry samples. The proportion of injured cells found with flow cytometry (22.52±16.83%) was lower than with plating (37.67±21.33%), whereas the proportion of healthy cells with flow cytometry (26.58±16.41%) was higher than with plating (9.36±8.95%). An explanation for these differences may be the bias in flow cytometry injured and dead cell counts due to background fluorescence. Thus, loss of injured cells in flow cytometry data analysis may result in the lower proportion of these cells compared with that of healthy cells. Moreover, discrepancy between results obtained by flow

cytometry and plating is usually found, since physiological parameters measured by these techniques are different (Raybourne and Tortorello, 2003; Nebe-von-Caron *et al.*, 2000). Intact cell membrane being a requisite for reproductive growth (Mackey, 2000) may explain the concordance between percentages of dead cells revealed by flow cytometry (50.91±28.82%) and plating (52.97±18.86%). However, since the bias in flow cytometry counting also affects dead cells, it would be expected that the proportion was also lower than with plating. Dead cells present in inocula and sterilized salad samples, which cannot be excluded from flow cytometry data analysis in this study, may contribute to increase the proportion of dead cells detected by flow cytometry.

The different dye combinations were compared to select at least one giving the best resolution of cells from background particles and therefore fewer false-positive cell events, the highest total cell counts, and the best resolution of cell populations with different membrane integrity states. Nevertheless, no significant differences were found among dye combinations for the concentration of background particles, and total, healthy, injured and dead cell counts. These results are consistent with those of Lebaron *et al.* (2001), who found comparable total cell counts using SYBR Green I, SYBR Green II and SYTO 13 in aquatic systems. However, during flow cytometry data analysis, SYBR Green I and SYTO BC gave better resolution of healthy cells from background particles than SYTO 9 (data not shown). In spite of all being green-fluorescent cyanine dyes that stain both DNA and RNA, SYBR Green I has an especially high binding affinity for DNA, which makes it suitable for nucleic acid quantification, and a higher quantum yield than SYTO 9 when bound to DNA (0.8 *vs.* 0.6); whereas SYTO BC is claimed to be a mixture of the best SYTO dyes for bacterial detection (Haugland, 2010). Nevertheless, it was not possible to fully take advantage of these facts, since dead cells could not be gated in green fluorescence plots, due to loss of such fluorescence in the presence of PI, and consequent overlapping with background particles. Neither were red fluorescence plots used to

gate all the cells, since this fluorescence was rather high for background parti-cles and healthy cells. Nonspecific staining has been mainly linked to the pres-ence of protein and fat in food matrices such as milk (Gunasekera *et al.*, 2000), yoghurt, whey protein isolates and protein microbeads (Doherty *et al.*, 2010), surimi-based products (Endo *et al.*, 2001), and non-dairy probiotic drinks (Maukonen *et al.*, 2006). It was observed that all the cells could be fairly distin-guished in uncompensated yellow-orange fluorescence plots, probably because this channel receives a part of the fluorescence from SYBR Green I-, SYTO 9- and SYTO BC-stained healthy cells and the orange fluorescence component emitted by PI-stained cells (Barbesti *et al.*, 2000; Gunasekera *et al.*, 2003; Saegeman *et al.*, 2007).

4. Conclusions

The present study compared pre-treatments based on coarse filtration of salad homogenate and a dilution/wash step prior to fluorescent staining for flow cytometry analysis. After coarse filtration, *ca.* 8 log background particles/mL were released. Interestingly, the sample pre-treatment consisting of coarse filtration in a 63-μm filter blender bag and centrifugal filtration through a 5-μm filter was superior to simple sample washing and/or dilution, since it effec-tively reduced both the concentration (*ca.* 7 log event/mL) and percentage (*ca.* 50% from total events) of background particles. Although recovery of *E. coli* O157:H7 cells from salad samples was also reduced after centrifugal filtration, only a *ca.* 0.2 log CFU/g difference was found compared with plate counts. Cell loss equally affected healthy, injured, and dead cells. However, injured and, especially, dead cell counts were additionally influenced by the presence of background fluorescence. This interference was slightly higher for injured cells when using SYTO 9. Therefore, the proposed pre-treatment performed optimally in the detection and quantification of healthy and injured cells pre-sent in either SYBR Green I + PI- or SYTO BC + PI-stained samples. When using

the blender bag containing a 50-μm nonwoven filter for coarse filtration, worse results were obtained in terms of background particle concentration and relative frequency, as well as cell recovery. This highlights the importance of carefully selecting filter materials and formats for the preparation of flow cytometry samples.

In short, the proposed flow cytometry sample pre-treatment based on centrifugal filtration has proven suitable for the flow cytometry detection of *E. coli* O157:H7 in a complex food matrix and the assessment of its membrane integrity, which is a good estimator of cell viability. The next step should be using a fluorescently labeled antibody to selectively detect the pathogen in non-sterilized samples. In addition, the proposed protocol could be combined with other fluorochromes to obtain a complete picture of the physiological state of bacterial cells found in food samples.

5. References

Barbesti, S., S. Citterio, M. Labra, M.D. Baroni, M.G. Neri, and S. Sgorbati. 2000. Two and three-color fluorescence flow cytometric analysis of immunoidentified viable bacteria. *Cytometry Part A*. 40:214–218.

Ben-Amor, K., H. Heilig, H. Smidt, E.E. Vaughan, T. Abee, and W.M. de Vos. 2005. Genetic diversity of viable, injured, and dead fecal bacteria assessed by fluorescence-activated cell sorting and 16S rRNA gene analysis. *Applied and Environmental Microbiology*. 71:4679–4689.

Berger, C.N., S. V Sodha, R.K. Shaw, P.M. Griffin, D. Pink, P. Hand, and G. Frankel. 2010. Fresh fruit and vegetables as vehicles for the transmission of human pathogens. *Environmental Microbiology*. 12:2385–2397.

Berney, M., H.-U. Weilenmann, and T. Egli. 2006. Flow-cytometric study of vital cellular functions in *Escherichia coli* during solar disinfection (SODIS). *Microbiology*. 152:1719–1729.

Berney, M., F. Hammes, F. Bosshard, H.-U. Weilenmann, and T. Egli. 2007. Assessment and interpretation of bacterial viability by using the LIVE/DEAD BacLight kit in combination with flow cytometry. *Applied and Environmental Microbiology*. 73:3283–3290.

Breeuwer, P., and T. Abee. 2000. Assessment of viability of microorganisms employing fluorescence techniques. *International Journal of Food Microbiology*. 55:193–200.

Buchanan, R.L., and M.P. Doyle. 1997. Foodborne disease significance of *Escherichia coli* O157:H7 and other enterohemorrhagic *E. coli*. *Food Technology*. 51:69–76.

Buzatu, D.A., W.M. Cooper, C. Summage-West, J.B. Sutherland, A.J. Williams, D.A. Bass, L.L. Smith, R.S. Woodruff, J.M. Christman, S. Reid, R.K. Tucker, C.J. Haney, A. Ahmed, F. Rafii, and J.G. Wilkes. 2013. Photobleaching with phloxine B sensitizer to reduce food matrix interference for detection of

Escherichia coli serotype O157:H7 in fresh spinach by flow cytometry. *Food Microbiology*. 36:416–425.

Cao-Hoang, L., P.A. Marechal, M. Lê-Thanh, P. Gervais, and Y. Waché. 2008. Fluorescent probes to evaluate the physiological state and activity of microbial biocatalysts: a guide for prokaryotic and eukaryotic investigation. *Biotechnology Journal*. 3:890–903.

Comas-Riu, J., and N. Rius. 2009. Flow cytometry applications in the food industry. *Journal of Industrial Microbiology & Biotechnology*. 36:999–1011.

Cotter, P.D., and C. Hill. 2003. Surviving the acid test: responses of Gram-positive bacteria to low pH. *Microbiology and Molecular Biology Reviews*. 67:429–453.

Davey, H.M. 2011. Life, death and in-between: meanings and methods in microbiology. *Applied and Environmental Microbiology*. 77:5571–5576.

Davey, H.M., D.B. Kell, D.H. Weichart, and A.S. Kaprelyants. 2004. Estimation of microbial viability using flow cytometry. *Current Protocols in Cytometry*. 29:11.3.1–11.3.21.

Delaquis, P., S. Bach, and L.D. Dinu. 2007. Behavior of *Escherichia coli* O157:H7 in leafy vegetables. *Journal of Food Protection*. 70:1966–1974.

Dinu, L.D., and S. Bach. 2011. Induction of viable but nonculturable *Escherichia coli* O157:H7 in the phyllosphere of lettuce: a food safety risk factor. *Applied and Environmental Microbiology*. 77:8295–8302.

Doherty, S.B., L. Wang, R.P. Ross, C. Stanton, G.F. Fitzgerald, and A. Brodkorb. 2010. Use of viability staining in combination with flow cytometry for rapid viability assessment of *Lactobacillus rhamnosus* GG in complex protein matrices. *Journal of Microbiological Methods*. 82:301–310.

EFSA Panel on Biological Hazards. 2013. Scientific opinion on the risk posed by pathogens in food of non-animal origin. Part 1 (outbreak data analysis and risk ranking of food/pathogen combinations). *EFSA Journal*. 11:3025–3163.

Endo, H., Y. Nagano, H. Ren, and T. Hayashi. 2001. Rapid enumeration of bacteria grown on surimi-based products by flow cytometry. *Fisheries Science*. 67:969–974.

European Food Safety Authority, and European Centre for Disease Prevention and Control. 2013. The European Union summary report on trends and sources of zoonoses, zoonotic agents and food-borne outbreaks in 2011. *EFSA Journal*. 11:3129–3379.

Givan, A.L. 2001. Cells from without: leukocytes, surface proteins, and the strategy of gating. *In* Flow cytometry. First principles. Wiley-Liss, New York, NY. 81–113.

Gunasekera, T.S., P. V Attfield, and D.A. Veal. 2000. A flow cytometry method for rapid detection and enumeration of total bacteria in milk. *Applied and Environmental Microbiology*. 66:1228–1232.

Gunasekera, T.S., D.A. Veal, and P. V Attfield. 2003. Potential for broad applications of flow cytometry and fluorescence techniques in microbiological and somatic cell analyses of milk. *International Journal of Food Microbiology*. 85:269–279.

Haugland, R.P. 2010. Nucleic acid detection and genomics technology. *In* The Molecular Probes handbook. A guide to fluorescent probes and labelling technologies. M.T.Z. Spence, editor. Invitrogen, Carlsbad, CA. 302–360.

Heard, G. 1999. Microbial safety of ready-to-eat salads and minimally processed vegetables and fruits. *Food Australia*. 51:414–420.

Hothorn, T., F. Bretz, and P. Westfall. 2008. Simultaneous inference in general parametric models. *Biometrical Journal*. 50:346–363.

Hutten, I.M. 2007. Introduction to nonwoven filter media. *In* Handbook of nonwoven filter media. I.M. Hutten, editor. Elsevier, Oxford. 1–28.

Jaykus, L.-A. 2003. Challenges to developing real-time methods to detect pathogens in foods. *ASM News*. 69:341–347.

Joux, F., and P. Lebaron. 2000. Use of fluorescent probes to assess physiological functions of bacteria at single-cell level. *Microbes and Infection*. 2:1523–1535.

Joux, F., P. Lebaron, and T. Marc. 1997. Succession of cellular states in a *Salmonella typhimurium* population during starvation in artificial seawater microcosms. *FEMS Microbiology Ecology*. 22:65–76.

Lebaron, P., P. Servais, H. Agogué, C. Courties, and F. Joux. 2001. Does the high nucleic acid content of individual bacterial cells allow us to discriminate between active cells and inactive cells in aquatic systems? *Applied and Environmental Microbiology*. 67:1775–1782.

Leistner, L. 2000. Basic aspects of food preservation by hurdle technology. *International Journal of Food Microbiology*. 55:181–186.

Little, C.L., and I.A. Gillespie. 2008. Prepared salads and public health. *Journal of Applied Microbiology*. 105:1729–1743.

Liu, Y., C. Wang, G. Tyrrell, and X.F. Li. 2010. Production of Shiga-like toxins in viable but nonculturable *Escherichia coli* O157:H7. *Water Research*. 44:711–718.

Luo, Y., Q. He, and J.L. McEvoy. 2010. Effect of storage temperature and duration on the behavior of *Escherichia coli* O157:H7 on packaged fresh-cut salad containing romaine and iceberg lettuce. *Journal of Food Science*. 75:390–397.

Mackey, B.M. 2000. Injured bacteria. *In* Microbiological safety and quality of food. B.M. Lund, T. Baird-Parker, and G.W. Gould, editors. Springer-Verlag, Gaithersburg, MD. 315–341.

Maukonen, J., H.-L. Alakomi, L. Nohynek, K. Hallamaa, J.M. Leppämäki, and M. Saarela. 2006. Suitability of the fluorescent techniques for the enumeration of probiotic bacteria in commercial non-dairy drinks and in pharmaceutical products. *Food Research International*. 39:22–32.

McCarthy, J., R. Holbrook, and P.J. Stephens. 1998. An improved direct plate method for the enumeration of stressed *Escherichia coli* O157:H7 from food. *Journal of Food Protection.* 61:1093–1097.

Müller, S., and G. Nebe-von-Caron. 2010. Functional single-cell analyses: flow cytometry and cell sorting of microbial populations and communities. *FEMS Microbiology Reviews.* 34:554–587.

Nebe-von-Caron, G. 2009. Standardization in microbial cytometry. *Cytometry Part A.* 75:86–89.

Nebe-von-Caron, G., P.J. Stephens, and R.A. Badley. 1998. Assessment of bacterial viability status by flow cytometry and single cell sorting. *Journal of Applied Microbiology.* 84:988–998.

Nebe-von-Caron, G., P.J. Stephens, C.J. Hewitt, J.R. Powell, and R.A. Badley. 2000. Analysis of bacterial function by multi-colour fluorescence flow cytometry and single cell sorting. *Journal of Microbiological Methods.* 42:97–114.

Oliver, J.D. 2010. Recent findings on the viable but nonculturable state in pathogenic bacteria. *FEMS Microbiology Reviews.* 34:415–425.

Park, S.-H., S. Ryu, and D.H. Kang. 2011. Improved selective and differential medium for isolation of *Escherichia coli* O157:H7. *Journal of Clinical Microbiology.* 49:405–408.

Payne, M.J., and R.G. Kroll. 1991. Methods for the separation and concentration of bacteria from foods. *Trends in Food Science & Technology.* 2:315–319.

Purchas, D.B., and K. Sutherland. 2001. An introduction to filter media. *In* Handbook of filter media. D.B. Purchas and K. Sutherland, editors. Elsevier, Oxford. 1–34.

R Core Team. 2013. R: a language and environment for statistical computing. R Foundation for Statistical Computing, Vienna.

Raybourne, R.B., and M. Lou Tortorello. 2003. Microscopy techniques: DEFT and flow cytometry. *In* Detecting pathogens in food. T. McMeekin, editor. Woodhead Publishing, Cambridge. 186–216.

Robinson, A.L., and J.L. McKillip. 2010. Biology of *Escherichia coli* O157:H7 in human health and food safety with emphasis on sublethal injury and detection. *In* Current research, technology and education topics in applied microbiology and microbial biotechnology. A. Méndez-Vilas, editor. Formatex, Badajoz. 1096–1105.

Saegeman, V.S., R. De Vos, N.D. Tebaldi, J.M. van der Wolf, J.H. Bergervoet, J. Verhaegen, D. Lismont, B. Verduyckt, and N.L. Ectors. 2007. Flow cytometric viability assessment and transmission electron microscopic morphological study of bacteria in glycerol. *Microscopy and Microanalysis.* 13:18–29.

Shapiro, H.M. 2003. How flow cytometers work. *In* Practical flow cytometry. John Wiley & Sons, Hoboken, NJ. 101–224.

Sharpe, J., and S. Wulff. 2006. Small-particle analysis. *In* Guide to flow cytometry. S. Wulff, editor. Dako, Carpinteria, CA. 69–75.

Stevens, K.A., and L.-A. Jaykus. 2004. Bacterial separation and concentration from complex sample matrices: a review. *Critical Reviews in Microbiology.* 30:7–24.

Stocks, S.M. 2004. Mechanism and use of the commercially available viability stain, *Bac*Light. *Cytometry Part A.* 61:189–195.

Sutherland, J.P. 2005. Pathogen resistance and adaptation to low temperature. *In* Understanding pathogen behaviour: virulence, stress response and resistance. M. Griffiths, editor. Woodhead Publishing, Cambridge. 507–523.

Sutherland, K. 2008. Filter media. *In* Filters and filtration handbook. K. Sutherland, editor. Elsevier, Oxford, UK. 41–95.

Svarovsky, L. 2001. Centrifugal filtration. *In* Solid-liquid separation. L. Svarovsky, editor. Elsevier, Oxford. 432–441.

Swarts, A.J., J.W. Hastings, R.F. Roberts, and A. von Holy. 1998. Flow cytometry demonstrates bacteriocin-induced injury to *Listeria monocytogenes.* *Current Microbiology.* 36:266–270.

Tamburini, S., A. Ballarini, G. Ferrentino, A. Moro, P. Foladori, S. Spilimbergo, and O. Jousson. 2013. Comparison of quantitative PCR and flow cytometry as cellular viability methods to study bacterial membrane permeabilization following supercritical CO_2 treatment. *Microbiology.* 159:1056–1066.

Tortorello, M. L., D.S. Stewart, and R.B. Raybourne. 1997. Quantitative analysis and isolation of *Escherichia coli* O157:H7 in a food matrix using flow cytometry and cell sorting. *FEMS Immunology and Medical Microbiology.* 19:267–274.

Wesche, A.M., J.B. Gurtler, B.P. Marks, and E.T. Ryser. 2009. Stress, sublethal injury, resuscitation, and virulence of bacterial foodborne pathogens. *Journal of Food Protection.* 72:1121–1138.

Wilkes, J.G., R.K. Tucker, J.A. Montgomery, W.M. Cooper, J.B. Sutherland, and D.A. Buzatu. 2012. Reduction of food matrix interference by a combination of sample preparation and multi-dimensional gating techniques to facilitate rapid, high sensitivity analysis for *Escherichia coli* serotype O157 by flow cytometry. *Food Microbiology.* 30:281–288.

Yamaguchi, N., H. Ohba, and M. Nasu. 2006. Simple detection of small amounts of *Pseudomonas* cells in milk by using a microfluidic device. *Letters in Applied Microbiology.* 43:631–636.

Yoshitomi, K.J., R. Zapata, K.C. Jinneman, S.D. Weagant, and W. Fedio. 2012. Recovery of *E. coli* O157 strains after exposure to acidification at pH 2. *Letters in Applied Microbiology.* 54:499–503.

Zhao, L., and K.R. Matthews. 2000. Influence of starvation, temperature, and pH on culturability of *Escherichia coli* O157: H7. *Journal of Food Safety.* 20:193–208.

Chapter 5. Improvement of a protocol for flow cytometry immunodetection and membrane integrity assessment of *Escherichia coli* O157:H7

Abstract

Flow cytometry has been widely used in bacterial research to rapidly assess the physiological state of individual cells, with membrane integrity being one of the most popular parameters due to its essential role in survival. Staining with propidium iodide (PI) and SYBR Green I reveals the presence of cells with damaged membranes, considered as dead, and cells with intact membranes. Intermediate cellular states, which are attributed to partial membrane damage typical of injured cells, can also be differentiated after extensive optimization of several protocol factors. This study presents the development of a flow cytometry sample preparation protocol for the enterohemorrhagic foodborne pathogen *Escherichia coli* O157:H7 to differentiate the aforementioned three cell populations, and assess the compatibility with an R-phycoerythrin-labeled antibody (Ab-RPE). Different SYBR Green I-to-PI ratios were compared for cell suspensions stained both in Tris buffered saline with BSA (TBS-BSA) or Tris with BSA (Tris-BSA). Cell population separation by green fluorescence was the limiting element to achieve an orthogonal distribution for cells with intact and damaged membranes in the green *vs.* red fluorescence plot, which would allow to properly visualize cells with partially damaged membranes in a problem sample. This was only possible when using Tris-BSA, probably due to enhancement of intact membrane permeability to SYBR Green I. Thus, staining with $1:10^6$ SYBR Green I and 10 μM PI in Tris-BSA was the combination which gave the desired fluorescence pattern. Addition of 1 μg/mL Ab-RPE did not have a remarkable impact in population resolution compared with staining only with SYBR Green I and PI, and allowed clear recognition of *E. coli* O157:H7. The proposed protocol is simple, rapid, and permits specific detection of *E. coli* O157:H7 as well as visualization of three different membrane integrity states, namely intact, partially damaged and damaged, unlike other protocols also consisting of double staining with membrane integrity indicator dyes.

1. Introduction

The cytoplasmic membrane is a cellular structure central to the survival of bacteria. It is involved in a variety of functions, which range from the obvious retention of the cytoplasm and cellular components to the selective transport of molecules, the location of energy metabolic processes, and the recognition of environmental signals (Denich *et al.*, 2003; Trevors, 2003). Consequently, most methods to assess the physiological state of bacterial cells beyond culturability are based on fluorescent dyes acting as membrane integrity indicators (Müller and Nebe-von-Caron, 2010). Cell-associated fluorescence can then be detected by flow cytometry, a technique capable of analyzing multiple parameters of thousands of cells in few seconds (Ueckert *et al.*, 1995). Additionally, flow cytometry combined with fluorescently labeled antibodies allows the detection of specific bacteria present in clinical, food, or environmental samples (Yamaguchi *et al.*, 2003; Schellenberg *et al.*, 2006; Vital *et al.*, 2007; Rodriguez and Thornton, 2008).

Propidium iodide (PI) is one of the most popular dyes to detect membrane damage. Due to its large molecular weight (668.4) and hydrophilic nature, this red-fluorescent nucleic acid dye can only penetrate and stain cells with permeabilized membranes, which are therefore considered as dead (Manini and Danovaro, 2006; Sträuber and Müller, 2010). Moreover, to simultaneously detect those cells with intact membranes, PI is usually combined with a membrane-permeable green-fluorescent nucleic acid dye, such as SYTO 9 in the LIVE/DEAD *Bac*Light Bacterial Viability kit, or SYBR Green I in the so-called nucleic acid double-staining (NADS) assay (Barbesti *et al.*, 2000; Grégori *et al.*, 2001; Stocks, 2004). In these assays, cells with intact membranes are expected to emit high green fluorescence and very low red fluorescence. Cells with damaged membranes are expected to emit high red fluorescence and very low green fluorescence due to a combined mechanism consisting in (i) displace-

ment of nucleic acid-bound SYTO 9 due to the higher nucleic acid affinity of PI, and (ii) enhancement of PI fluorescence emission due to energy transfer from SYTO 9 with the concomitant quenching of SYTO 9 fluorescence (Förster Resonance Energy Transfer –FRET– phenomenon) (Stocks, 2004). An analogous staining mechanism was proposed for the NADS assay, since SYBR Green I has a fluorescence emission spectrum compatible with the FRET phenomenon in the presence of PI (Barbesti *et al.*, 2000; Grégori *et al.*, 2001), and might be displaced by PI as suggested by Manini and Danovaro (2006). Additionally, for both assays, intermediate cellular states have been reported with cells displaying both high green and red fluorescences (Barbesti *et al.*, 2000; Grégori *et al.*, 2001; Ziglio *et al.*, 2002; Saegeman *et al.*, 2007). Such fluorescence pattern is attributed to the presence of insufficient intracellular PI to efficiently reduce the green fluorescence emission, conceivably indicating that those cells have a partially damaged membrane (Barbesti *et al.*, 2000). However, several experimental factors have a remarkable impact on the reliable detection of this third cell population by the aforementioned assays. Dye concentrations and ratio are critical factors which, if not carefully adjusted, can result in cells with intact or damaged membranes misleadingly showing high green and red fluorescences, and thus in the inability to differentiate cells with partially damaged membranes. The practical approach proposed by Barbesti *et al.* (2000) is a valuable tool to find the optimum PI (saturating) concentration and consists in assessing the effect on population resolution of a range of PI concentrations in combination with a set SYBR Green I concentration. Composition of the staining medium may also influence cell fluorescence patterns. For example, buffers containing phosphate are not recommended by the manufacturer when using the LIVE/DEAD *Bac*Light kit, since this compound has been shown to reduce the staining efficiency; whereas Tris is the buffering agent recommended when using SYBR Green I. The optical configuration of the flow cytometer also seems to determine population resolution. Thus, Falcioni *et al.* (2008) did not consider the detection of cells with partially damaged mem-

branes, since the clear differentiation of this population was hindered by the inability of the flow cytometer used in their study to fully compensate the green and red fluorescence spillovers.

In this study, we sought to adapt the NADS assay for the enterohemorrhagic foodborne pathogen *Escherichia coli* O157:H7 with the purpose of differentiating three cell populations based on their membrane integrity state. This implied achieving an orthogonal distribution for populations of cells with intact (green fluorescence) and damaged (red fluorescence) membranes. Moreover, this adaptation constitutes a preliminary protocol to simultaneously detect *E. coli* O157:H7 and assess its membrane integrity in food samples, and so we also tested the compatibility of the selected nucleic acid dyes with a fluorescently labeled antibody. The NADS assay was selected against the LIVE/DEAD *Bac*Light kit, since SYBR Green I has very high nucleic acid affinity, which makes it suitable for nucleic acid quantification, as opposed to SYTO 9 (Haugland, 2010), and thus it would be less affected by the presence of interfering particles from the food matrix. Antibodies are also susceptible to nonspecific binding, thus a high ionic strength Tris buffered saline (TBS) was tested for immunostaining, based on reduction of this interference by ionic interactions (Clark, 1991; Diamandis *et al.*, 1996; Miller and Levinson, 1996). A fluorescently labeled primary antibody against *E. coli* O157:H7 surface epitopes was selected to avoid extensive sample processing and preserve the bacterial physiological state (Müller and Nebe-von-Caron, 2010).

2. Materials and Methods

2.1. Bacterial strain and culture conditions

Escherichia coli O157:H7 CECT 5947, provided by the Spanish Type Culture Collection (Colección Española de Cultivos Tipo, CECT, Paterna, Spain), was used for all the experiments. A lyophilized culture was reconstituted and cultured

for stock preparation. The stock was stored at –65°C in cryovials containing beads (AES Chemunex, Bruz, France). Pre-cultures were prepared by transferring one bead from the stock to a 100-mL Erlenmeyer flask containing 20 mL of tryptone soya broth (TSB; Oxoid, Basingstoke, UK), and then incubated overnight at 37°C in a shaking water bath at 86 rpm. To obtain stationary phase cultures, 50 μL of the overnight culture were inoculated into 20 mL of TSB and incubated at 37°C for 20 h. Growth time to reach stationary phase was previously determined by measuring the optical density at 600 nm (Bioscreen C; Oy Growth Curves AB, Helsinki, Finland).

2.2. General protocol for sample preparation

Stationary phase cultures were used to prepare *E. coli* O157:H7 suspensions for flow cytometry analysis. Untreated or heat-killed cells (80°C/30 min) were pelleted (13,000 × g, 30 s, 20°C), and then resuspended and diluted in filtered (0.22 μm, polyethersulfone; Millipore, Cork, Ireland) saline solution (pH 7.4): Tris buffered saline with bovine serum albumin (TBS-BSA; 20 mM Tris, 500 mM NaCl, 0.1% BSA) (Clark, 1991); Tris with BSA (Tris-BSA; 20 mM Tris, 0.1% BSA); 150 NaCl; or 500 mM NaCl. Untreated and heat-killed cell suspensions served as controls for cells with intact and damaged membranes, respectively. For fluorescent staining, cell suspensions were mixed with dye stock solutions and incubated at room temperature for 30 min in the dark. For flow cytometry *E. coli* O157:H7 detection, a goat polyclonal anti-*E. coli* O157:H7 antibody (BacTrace, KPL, Gaithersburg, MD, USA) conjugated to R-phycoerythrin (Ab-RPE; AntibodyBCN, Barcelona, Spain) was used. Cytoplasmic membrane integrity was assessed by using propidium iodide (PI; Invitrogen, Eugene, OR, USA) and SYBR Green I (Invitrogen). For three-color samples, selective labeling with Ab-RPE was performed before addition of nucleic acid dyes.

2.3. Protocol optimization

Several factors were optimized to make cells with intact and damaged membranes approach the expected fluorescence pattern.

In the first step, the suitability of Ab-RPE concentrations from 0.06 to 4.00 µg/mL was assessed in TBS-BSA, a buffer commonly used in immunological assays (Murano and Hudnall, 2001). For that purpose, a two-fold serial dilution of Ab-RPE was prepared in TBS-BSA, and untreated cells were added to reach *ca.* 7.5 log colony-forming unit (CFU)/mL. Immunostaining was also tested for heat-killed cells to confirm that they retained the capacity to be labeled.

In the second step, the effect of PI concentration on the resolution of cells with intact and damaged membranes was assessed according to the procedure used by Barbesti *et al.* (2000). A two-fold serial dilution of PI was prepared in TBS-BSA to obtain concentrations from 0.3 to 20.0 µM. Then, untreated and heat-killed cell mixtures (1:1) were added to reach *ca.* 7.5 log CFU/mL, and stained with a fixed SYBR Green I concentration (1:10^6 final dilution of the stock solution, previously adjusted by using unstained untreated cells as the reference to set the voltage amplifications).This staining procedure implied the presence of different amounts of dimethyl sulfoxide (DMSO), which came from PI and SYBR Green I stock solutions. However, the DMSO concentration in the samples did not exceed the maximum 0.3% v/v proposed by the manufacturer. Since results obtained with TBS-BSA were not satisfactory, the same procedure was repeated using Tris-BSA. Staining was also performed in 150 and 500 mM NaCl to determine the role of the solution components in the fluorescence patterns displayed by the cells. In these cases, only a 10.0 µM PI concentration was used.

In the third step, the effect of Ab-RPE labeling on the fluorescence pattern of SYBR Green I + PI-stained cells achieved in the second step was assessed.

Moreover, different cell concentrations were also analyzed to assess the flexibility of the previously selected dye concentrations. Thus, untreated and heat-killed cell mixtures (1:1) were diluted in Tris-BSA at *ca.* 5, 6 and 7.5 log CFU/mL, and stained with 1.00 µg/mL Ab-RPE, 10.0 µM PI and $1:10^6$ SYBR Green I.

Finally, in the attempt to improve population resolution when analyzing cell concentrations lower than 7.5 log CFU/mL, a range of SYBR Green I concentrations was tested. Untreated and heat-killed cells were diluted to *ca.* 4, 5, 6 and 7 log CFU/mL in Tris-BSA and stained with SYBR Green I concentrations ranging from $1:10^{10}$ to $1:10^6$ final dilution of the stock solution.

2.4. Flow cytometry and data analysis

Samples were analyzed with a FACScalibur flow cytometer (BD, Franklin Lakes, NJ, USA) equipped with a 15-mW 488-nm air-cooled argon-ion laser. Data were acquired for forward scatter (FSC), side scatter (SSC), green fluorescence (FL1), yellow-orange fluorescence (FL2) and red fluorescence (FL3) parameters. Band-pass filters for SYBR Green I and Ab-RPE light emission were 530/30 (FL1) and 545/82 (FL2), respectively, whereas long-pass filter for PI light emission was 670 nm (FL3). Voltage amplification was applied at logarithmic scale. Filtered double-distilled water was used as sheath fluid and sample flow rate was kept at 12 µL/min. CellQuest Pro software (version 4.0.2; BD) was used for acquisition of multiparametric data. When analyzing samples containing 7.5 log CFU/mL, data from 20,000 cells gated in the FSC *vs.* SSC plot were acquired. For samples containing lower cell concentrations, data were acquired for 30 s with a threshold set on the SSC parameter. Unstained and single-stained compensation controls always accompanied acquisition of samples.

FlowJo software (version 7.6.1; Tree Star, Ashland, OR, USA) was used for data compensation and analysis. Compensation settings were determined by using

unstained untreated cells as the negative control and positive controls as follows: single-stained heat-killed cells for SYBR Green I and PI; and single-stained untreated cells for Ab-RPE. To detect interferences and find the best gating strategy, raw data were first evaluated by displaying all parameter combinations in bivariate plots. For samples stained with Ab-RPE or Ab-RPE + SYBR Green I + PI, cells were gated in the FL2 *vs.* FSC plot (Figure 5.1A and 5.1C). For SYBR Green I-stained samples, cells were first gated in the FSC *vs.* SSC plot, and a second gate was set in the FL1 *vs.* FSC plot (Figure 5.1D). For SYBR Green I + PI-stained samples, cells were gated in the FSC *vs.* SSC plot (Figure 5.1B). Gated cells from samples stained with SYBR Green I + PI or Ab-RPE + SYBR Green I + PI were displayed according to their green and red fluorescences, and regions were set to discriminate bacterial populations with different degrees of membrane integrity (Figure 5.1B and 5.1C):

(i) *healthy cells*: cells with intact membranes (SYBR Green I$^+$/PI$^-$ or Ab-RPE$^+$/SYBR Green I$^+$/PI$^-$);

(ii) *injured cells*: cells with partially damaged membranes (SYBR Green I$^+$/PI$^+$ or Ab-RPE$^+$/SYBR Green I$^+$/PI$^+$);

(iii) *dead cells*: cells with damaged membranes (SYBR Green I$^-$/PI$^+$ or Ab-RPE$^+$/SYBR Green I$^-$/PI$^+$).

2.5. Flow cytometry statistics

Several statistics were obtained from gated cells using the FlowJo software, which reflected the effect of the different protocol factors. Relative green, yellow-orange and red fluorescence intensities were expressed as medians (median fluorescence intensity, MFI) in arbitrary units (a.u.). Dispersion of fluorescence distributions was expressed as the robust coefficient of variation (rCV), since this statistic is better suited to compare skewed distributions and to deal with logarithmic values than the coefficient of variation (Shapiro, 2003). The probability binning metric $T(\chi)$ was used to compare the green or
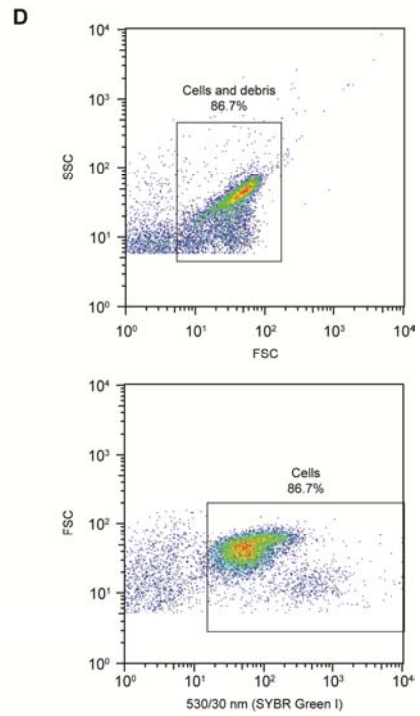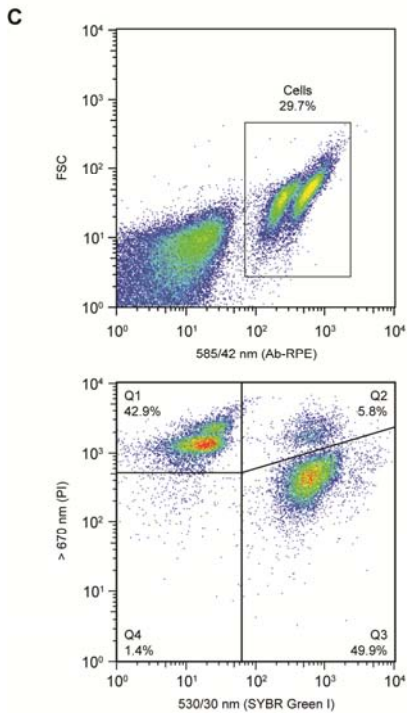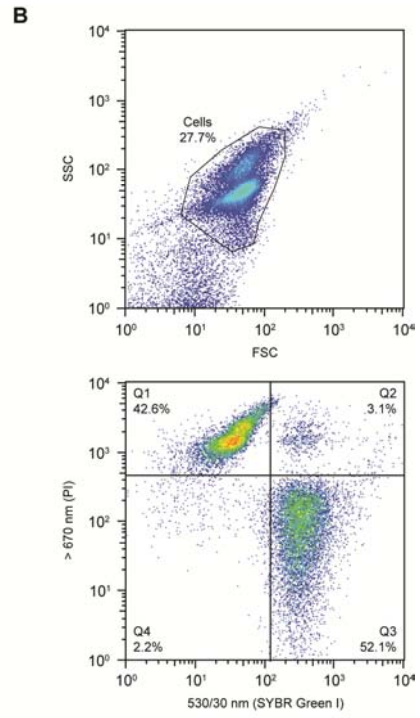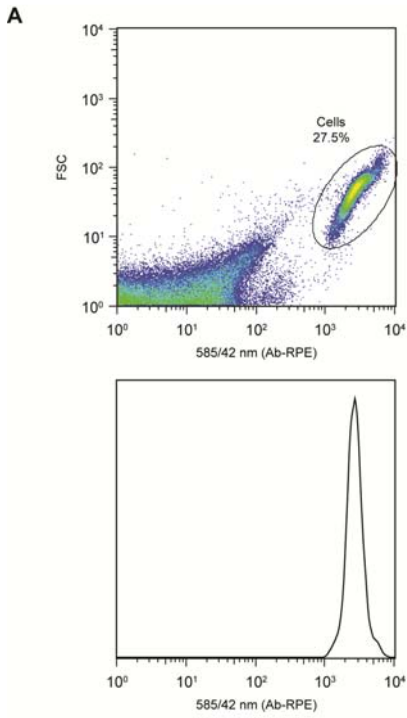
Figure 5.1 Gating strategy and gate boundaries for *Escherichia coli* O157:H7 stained in Tris-BSA. (A) Healthy cells, *ca.* 7.5 log CFU/mL, 1.00 µg/mL Ab-RPE. (B) Healthy and dead cells (1:1), *ca.* 7.5 log CFU/mL, 1:10^6 SYBR Green I and 10.0 µM PI. (C) Healthy and dead cells (1:1), *ca.* 7.5 log CFU/mL, 1.00 µg/mL Ab-RPE, 1:10^6 SYBR Green I and 10.0 µM PI. (D) Healthy cells, *ca.* 6 log CFU/mL, 1:10^6 SYBR Green I. Q1: dead; Q2: injured; Q3: healthy; Q4: negative.

red fluorescence distributions of healthy and dead cell populations, and thus to assess the similarity or dissimilarity between them (Roederer *et al.*, 2001). T(χ) estimates the probability that a test and a control distribution are different, and increases with the separation between them. The healthy cell population was considered the control distribution for the probability binning comparison algorithm. Finally, the correlation between the flow cytometry count and the expected plate count was evaluated by performing a linear regression analysis, where the cell event count in 30 s was used as the flow cytometry count.

3. Results and discussion

3.1. Effect of Ab-RPE concentration

To optimize the immunostaining protocol, several antibody conjugate concentrations were tested with healthy cells suspended in TBS-BSA at *ca.* 7.5 CFU/mL, as well as with TBS-BSA alone to account for background fluorescence. Yellow-orange fluorescence intensity of RPE-labeled *E. coli* O157:H7 and background control increased with Ab-RPE concentration (Figure 5.2A). However, the difference between RPE-labeled cells and background fluorescence intensities and thus the separation between them increased with Ab-RPE concentration. By using 1.00 µg/mL, Ab-RPE positive cells gave an on-scale distinct peak in the yellow-orange fluorescence intensity histogram (Figure 5.2B). Therefore, it was selected as the optimum final concentration. After immunostaining with this concentration, dead cells also showed a distinct fluorescence signal, which suggests that epitopes for the antibody used in this study were retained in cells with damaged membranes. Using the same antibody, conjugated to fluorescein isothiocyanate, Hussein *et al.* (2002) found that *E. coli* O157:H7 was also stained after heat or formalin treatment.
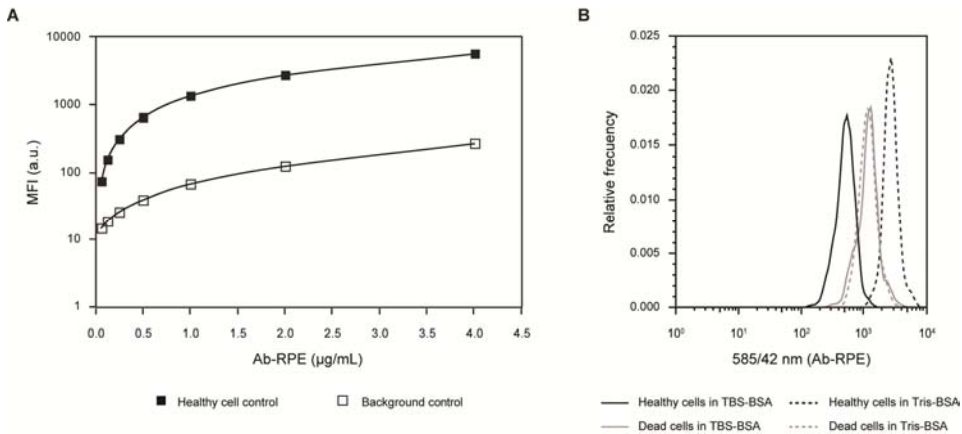
Figure 5.2   Titration of antibody anti-*Escherichia coli* O157:H7 conjugated to R-phycoerythrin (Ab-RPE). (A) Median fluorescence intensity (MFI) of healthy cells and Ab-RPE background control at varying Ab-RPE concentrations. (B) Histogram overlay of healthy and dead cells suspended in TBS-BSA and Tris-BSA and incubated with 1.00 µg/mL Ab-RPE.

3.2. Effect of PI concentration and staining medium

Before assessing the compatibility of Ab-RPE with the membrane integrity indicators SYBR Green I and PI, a range of PI concentrations was tested with a set SYBR Green I concentration to maximize the separation between the healthy and dead cell populations. Red fluorescence intensity of dead cells stained in TBS-BSA sharply increased from 0.3 to 2.5 µM PI, and steadily rose from 2.5 to 20.0 µM PI (Figure 5.3A); whereas green fluorescence intensity declined with increasing PI concentration, due to FRET from SYBR Green I to PI and displacement of nucleic acid-bound SYBR Green I molecules by PI (Barbesti *et al.*, 2000; Manini and Danovaro, 2006). For healthy cells, red fluorescence intensity steadily rose with PI concentration; whereas green fluorescence intensity remained nearly constant (Figure 5.3B). Faint red fluorescence emission in PI-stained viable cells is a phenomenon previously reported for Gram negative and Gram positive bacteria in the exponential and stationary growth phases, and may be due to the presence of transport proteins, as well as the

transient disturbance of the cell envelope integrity during cell growth and division (Herrero *et al.*, 2006; Shi *et al.*, 2007; Sträuber and Müller, 2010). This phenomenon did not prevent the separation of dead and healthy cell populations, as shown by the high $T(\chi)$ values obtained for the red fluorescence parameter at the various PI concentrations (Figure 5.3C). However, $T(\chi)$ values were notably lower for green fluorescence intensity and complete separation of dead and healthy cell populations was not achieved at any of the tested PI concentrations (Figure 5.3D).

Considering that results obtained when using TBS-BSA were not completely favorable, Tris-BSA was tested as an alternative staining medium. Dead cells in Tris-BSA emitted higher red fluorescence intensities than those in TBS-BSA (Figure 5.3A). This may be due to the high NaCl content in TBS-BSA, since increasing concentrations of this compound have been shown to reduce PI fluorescence intensity (Martens *et al.*, 1981). In contrast to TBS-BSA, the lowest PI concentration was sufficient to brightly stain dead cells in Tris-BSA and achieve a stable staining equilibrium. Additionally, the trend in green fluorescence intensity of healthy cells was also different in Tris-BSA, with higher fluorescence values than cells in TBS-BSA and increasing intensities with PI concentration (Figure 5.3B). This resulted in higher $T(\chi)$ values for green fluorescence in Tris-BSA compared with TBS-BSA at PI concentrations from 2.5 μM (Figure 5.3C). At lower PI concentrations, green fluorescence intensity of dead cells was higher than that of healthy cells, due to inefficient FRET and SYBR Green I displacement by PI, and hence the observed decrease in $T(\chi)$ values. Similarly to TBS-BSA samples, resolution of healthy and dead cell populations by red fluorescence was high in Tris-BSA.

Figure 5.3 Effect of propidium iodide (PI) concentration and staining solution on fluorescence intensity and resolution of healthy and dead *Escherichia coli* O157:H7 cell mixtures (1:1) stained with 1:10^6 SYBR Green I and a range of PI concentrations. (A) Median fluorescence intensity (MFI) of dead cells. (B) MFI of healthy cells. (C) Probability binning metric [T(χ)]. (D) SYBR Green I *vs.* PI plots with polygonal regions depicting the position of dead cell clusters.

Staining with 10.0 µM PI in Tris-BSA was chosen, since this combination gave optimal resolution for both green [T(χ) = 2,609] and red [T(χ) = 2,723] fluorescences, and thus allowed to properly set a gate for injured cells (double positive cells) in SYBR Green I *vs.* PI cytograms (Figure 5.3D). According to the goal of the present study, this achievement prevailed over obtaining low red background fluorescence for healthy cells. Additionally, Ab-RPE labeling of healthy and dead cells was not adversely affected by incubation in Tris-BSA compared with TBS-BSA (Figure 5.2B). On the contrary, orange-yellow fluorescence intensity of Ab-RPE-labeled healthy cells was higher when using Tris-BSA than with TBS-BSA, whereas no difference was found between fluorescence intensities of dead cells suspended in TBS-BSA and in Tris-BSA. Differences in fluorescence levels of cells may be due to the fact that epitopes can be partially masked, more exposed or altered depending on the characteristics of the environment where the antigen-antibody reaction takes place (Miller and Levinson, 1996; McCarthy and Culloty, 2011).

To ascertain the role of NaCl and Tris in the observed differences in green fluorescence emitted by SYBR Green I + PI-stained healthy cells in TBS-BSA and in Tris-BSA, 500 mM NaCl was tested at 10.0 µM PI, as well as 150 mM NaCl, which was considered the control staining solution due to its physiological ionic strength. As expected, the staining solution neither had a remarkable impact on dead cell green and red fluorescence intensities nor on distribution of such intensities (Figure 5.4A). In contrast, this factor did have an impact on healthy cell fluorescence emission, especially on green fluorescence (Figure 5.4B). When Tris was present in the staining solution (TBS-BSA and Tris-BSA), green fluorescence values tended to be higher than with NaCl alone. Moreover, the highest NaCl concentration (TBS-BSA and 500 mM NaCl) made green fluorescence distributions appear wider than with 150 mM NaCl or Tris-BSA (Figure 5.4B and 5.4D). These facts strongly affected resolution of healthy and dead cell populations by green fluorescence, with Tris-BSA showing the highest T(χ)

value, and with 500 mM NaCl and TBS-BSA showing much lower $T(\chi)$ values than 150 mM NaCl or Tris-BSA (Figure 5.4C and 5.4D). Increased green fluorescence in healthy cells suspended in a Tris-containing staining solution, which conceivably indicates enhanced SYBR Green I uptake in such cells, may be explained by the fact that Tris is a monovalent cation which, at high concentrations, acts as an outer membrane permeability-increasing agent (Vaara, 1992). It does so by binding to outer membrane lipopolysaccharides, replacing the stabilizer Ca^{2+} and Mg^{2+} cations, and thus reducing the interaction between lipopolysaccharide molecules. This outer membrane permeabilizing mechanism has also been reported for high concentrations of Na^+ (Vaara, 1992), and may explain the increase in green fluorescence intensity of some healthy cells in 500 mM NaCl compared with 150 mM NaCl. However, the presence of 500 mM NaCl in TBS-BSA may exert a competitive effect with Tris –as described by Vaara (1992) for several cationic permeabilizing agents– since, as mentioned above, green fluorescence intensity of healthy cells in TBS-BSA was lower than that of healthy cells in Tris-BSA. These findings support the outer membrane integrity dependent staining mechanism for SYBR Green I previously reported by Berney *et al.* (2007). Furthermore, the observed green fluorescence intensity increase with PI concentration for healthy cells in Tris-BSA, may be due to the presence of increasing amounts of DMSO from the PI stock solution, since this solvent is known to enhance the permeability of lipid membranes to hydrophobic molecules (Gurtovenko and Anwar, 2007; Nebe-von-Caron, 2009), and thus it can modulate SYBR Green I uptake. However, further experimentation would be necessary to support this hypothesis, as this effect was not observed in TBS-BSA. Regarding the red fluorescence intensity, healthy cells in Tris-BSA showed slightly higher background fluorescence values than those in the rest of staining media. Red fluorescence distributions were wider for 150 mM NaCl and Tris-BSA compared with 500 mM NaCl and TBS-BSA. Overall, healthy cells showed higher rCV values than dead cells, due to the individual heterogeneity in dye uptake for cells with intact membranes (Berney *et al.*, 2007).

A

B

C

■ 150 mM NaCl   □ Tris-BSA   ▨ 500 mM NaCl   ▨ TBS-BSA

D
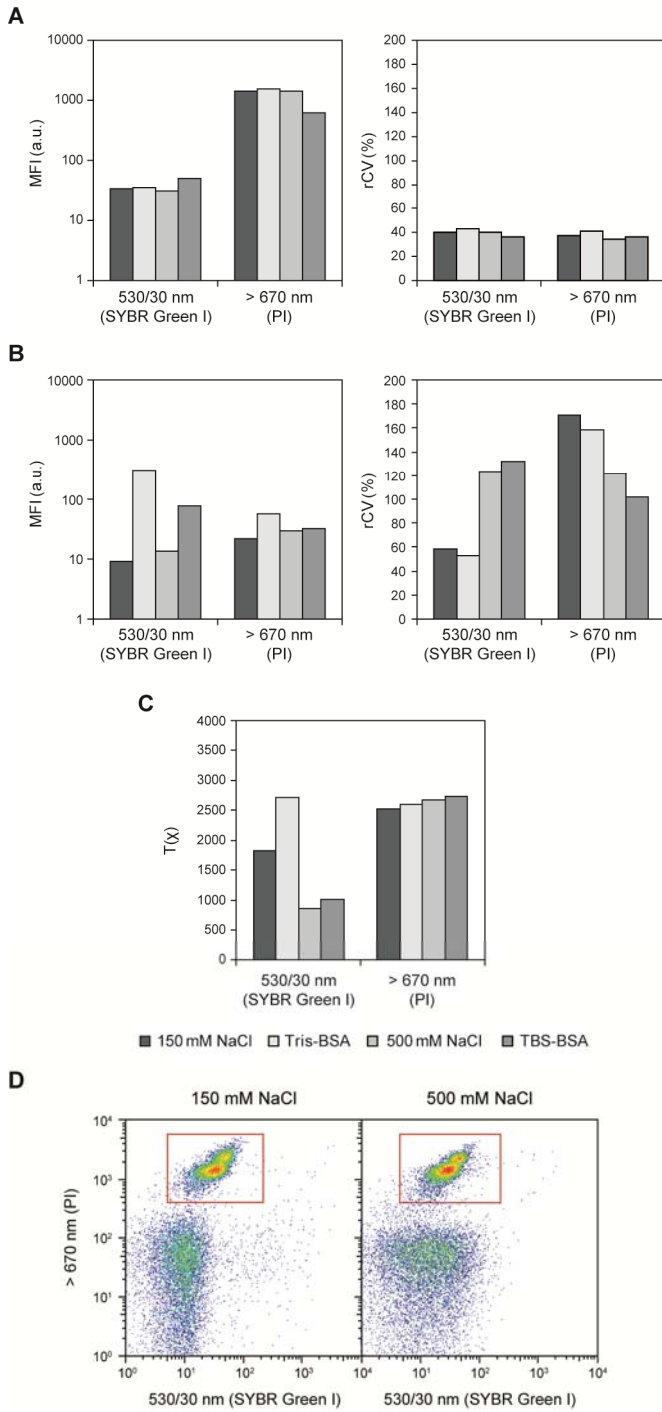
Figure 5.4 Effect of NaCl and Tris as staining solution constituents on fluorescence intensity and distribution, and resolution of healthy and dead *Escherichia coli* O157:H7 cell mixtures (1:1) suspended in 150 mM NaCl, Tris-BSA, 500 mM NaCl and TBS-BSA, and stained with 1:10^6 SYBR Green I and 10.0 μM PI. (A) Median fluorescence intensity (MFI) and robust coefficient of variation (rCV) of dead cells. (B) MFI and rCV of healthy cells. (C) Probability binning metric [T(χ)]. (D) SYBR Green I *vs.* PI plots with polygonal regions depicting the position of dead cell clusters.

3.3. Dye compatibility of 3-color flow cytometry assay

Next step in the optimization of the flow cytometry assay for simultaneous immunodetection and membrane integrity assessment of *E. coli* O157:H7 was the evaluation of the effect of Ab-RPE on the resolution of cells into healthy and dead populations obtained in previous steps. When healthy and dead cell mixtures at *ca.* 7.5 log CFU/mL were stained with 1.00 μg/mL Ab-RPE, $1:10^6$ SYBR Green I, and 10.0 μM PI in Tris-BSA, only a minimal reduction in population resolution for both red [$T(\chi) = 2,714$ *vs.* $T(\chi) = 2,723$] and green [$T(\chi) = 2,428$ *vs.* $T(\chi) = 2,609$] fluorescences was observed when compared with the corresponding SYBR Green I + PI-stained sample (Figure 5.3C and 5.5A). However, this reduction was remarkably pronounced with decreasing cell concentration (Figure 5.5A and 5.5B). Red fluorescence intensity of healthy cells at concentrations lower than 7.5 log CFU/mL appeared abnormally high, with fluorescence levels similar to those of dead cells. This artifact had been previously observed in samples stained with PI and high SYTO 9 concentrations (unpublished data), and was attributed to the unsuccessful compensation of the spillover of SYTO 9 fluorescence into the red fluorescence photodetector. In the present study, spillover occurred with SYBR Green I and Ab-RPE. For SYBR Green I, red background fluorescence after compensation increased with decreasing cell concentration and reached 130±81 a.u. For Ab-RPE, red background fluorescence was 552±372 a.u. and no apparent relation with cell concentration was observed. Judging by the lower red fluorescence of healthy cells compared with dead cells when stained with SYBR Green I + PI, the SYBR Green I spillover was adequately compensated at *ca.* 7.5 log CFU/mL (Figure 5.3B and 5.3D). However, compensation was not so successful for Ab-RPE.

Figure 5.5 Effect of antibody anti-*Escherichia coli* O157:H7 conjugated to R-phycoerythrin (Ab-RPE) on population resolution according to membrane integrity state. Healthy and dead cell mixtures (1:1) at different concentrations suspended in Tris-BSA and stained with 1.00 µg/mL Ab-RPE, 1:10^6 SYBR Green I and 10.0 µM PI. (A) Probability binning metric [T(χ)]. (B) SYBR Green I *vs.* PI plots of immunoidentified cells with polygonal regions depicting the position of dead cell clusters.

3.4. Effect of SYBR Green I concentration and cell concentration

Grégori *et al.* (2001) observed that compensation of SYBR Green I fluorescence spillover was not successful when staining diluted samples, and therefore proposed adapting the dye concentration to cell concentration. Thus, in the present study, SYBR Green I concentrations lower than $1:10^6$ were tested in a range of cell concentrations to reduce the fluorescence spillover into the red fluorescence photodetector. However, the desired SYBR Green I concentration also had to make cells in different concentrations emit a clearly distinct green fluorescence signal. This implied exceeding a green fluorescence intensity of 10 a.u., since this was the value below which 99% of background particles were found. When using $1:10^{10}$ SYBR Green I, fluorescence intensity of dead cells was too low to differentiate them from background particles (Figure 5.6A). Moreover, this concentration gave markedly higher rCVs and poor correlation between the theoretical cell concentration and flow cytometry cell counts (events with green fluorescence intensity above 15 a.u.). For the rest of SYBR Green I concentrations, increasing cell concentration led to a small decrease in fluorescence intensity, which could be attributed to changes in the equilibrium between the unbound and nucleic acid-bound dye molecules due to the presence of more binding sites (Givan, 2001; Brotherick, 2006). However, this fact did not affect discrimination of the cell clusters. Therefore, fairly strong correlations between the theoretical cell concentration and flow cytometry cell counts were found for these dye concentrations. The lowest rCVs were obtained with $1:10^6$ SYBR Green I. Fluorescence intensities of healthy cells were lower than those from dead cells (Figure 5.6B). Consequently, $1:10^9$ and $1:10^8$ SYBR Green I were not enough to stain healthy cells. Moreover, these dye concentrations gave poor correlation between the theoretical cell concentration and flow cytometry cell counts. Again, green fluorescence intensity variability was higher for healthy cells than for dead cells, with $1:10^6$ SYBR Green I generally showing the highest values. As mentioned above, reduced SYBR Green I uptake in cells with intact membranes has been attributed to the presence of

the outer membrane in Gram negative bacteria, which acts as a barrier to hydrophobic compounds (Berney *et al.*, 2007; Hammes *et al.*, 2012). Ethylene diamine tetraacetic acid (EDTA) may be used to disrupt the outer membrane, and thus enhance SYBR Green I uptake in healthy cells (Vaara, 1992). However, its use in the assessment of cell physiology is controversial, since EDTA treatments need extensive optimization to minimize adverse effects on cell functionality (Shapiro, 2000; Doherty *et al.*, 2010; Sträuber and Müller, 2010).

From these results, it was obvious that $1:10^6$ SYBR Green I was the concentration that gave clearly distinct healthy cell populations and a strong correlation between the theoretical cell concentration and flow cytometry cell counts. Thus, these facts prevailed over achieving lower green fluorescence intensity for dead cells, considering that this parameter is significantly reduced when PI is present in such cells, and lower SYBR Green I fluorescence spillover into the red fluorescence photodetector. Reduction of Ab-RPE concentration would have probably improved population resolution in Ab-RPE + SYBR Green I + PI-stained samples containing cell concentrations lower than *ca.* 7.5 log CFU/mL. However, this option was not further tested since extensive nonspecific binding may occur in more complex sample matrices, such as food (Comas-Riu and Rius, 2009; Müller and Nebe-von-Caron, 2010). Moreover, gates for cells with intact, partially damaged, or damaged membranes could be set adequately for samples at *ca.* 7.5 log CFU/mL.

4. Conclusions

The goal of the present study was to develop a sample preparation protocol to detect *E. coli* O157:H7 by using a RPE-labeled antibody, and assess three membrane integrity states with the nucleic acid dyes PI and SYBR Green I. Thus, we evaluated the contribution of dye concentrations and ratio, staining medium and cell concentration to the achievement of the desired fluorescence pattern and resolution for populations of cells with intact and damaged membranes,

A

B

(MFI (a.u.), rCV (%), and Cell count (event/30 s) plots versus Cell concentration (log CFU/mL))

Panel A, bottom plot legend:
+ $r^2 = 0.8426$
□ $r^2 = 0.9996$
◇ $r^2 = 0.9977$
△ $r^2 = 0.9776$
○ $r^2 = 0.9891$

Panel B, bottom plot legend:
+ $r^2 = 0.9017$
□ $r^2 = 0.9444$
◇ $r^2 = 0.6156$
△ $r^2 = 0.9825$
○ $r^2 = 0.9989$

+ 1:10^{10} SYBR   □ 1:10^9 SYBR   ◇ 1:10^8 SYBR   △ 1:10^7 SYBR   ○ 1:10^6 SYBR
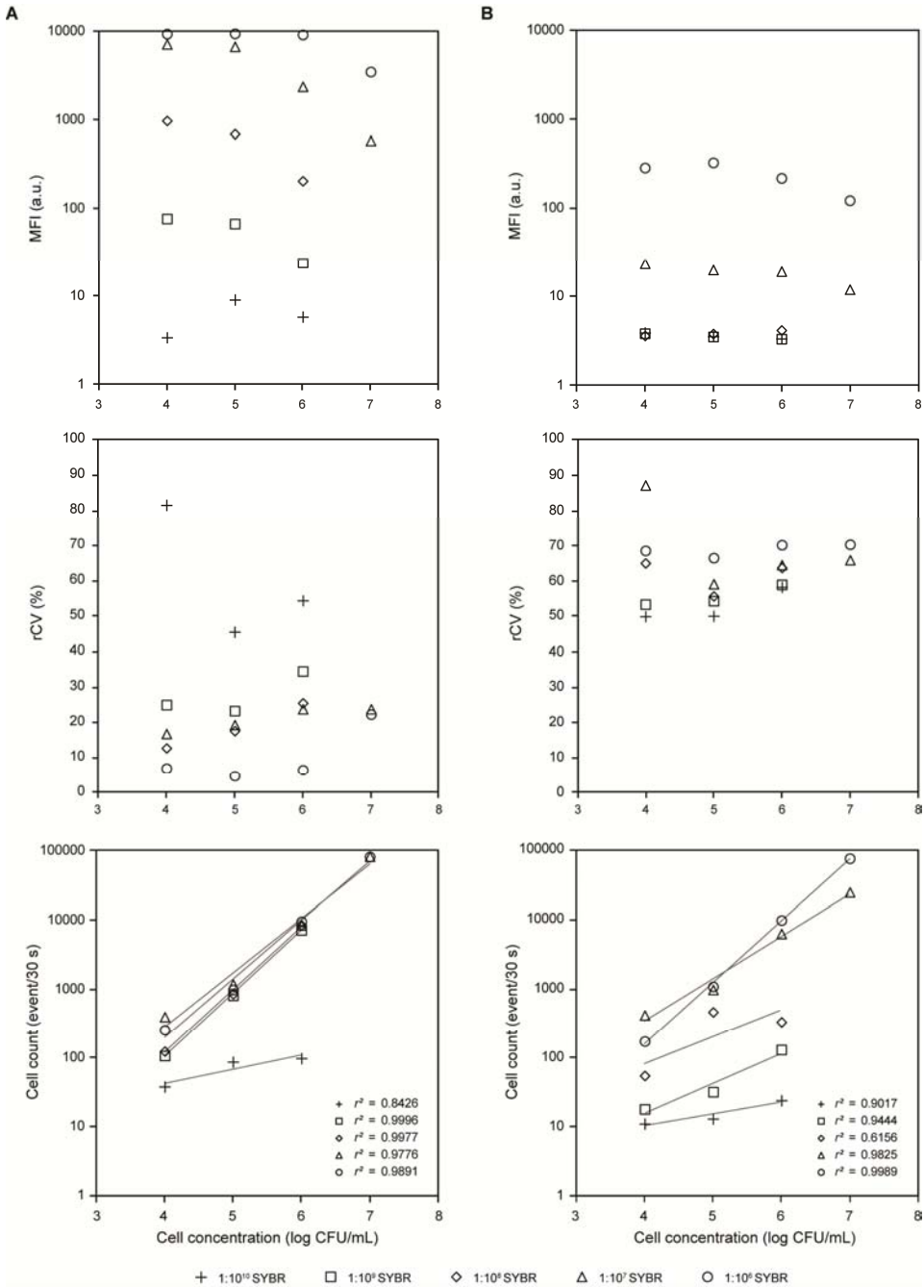
Figure 5.6 Effect of SYBR Green I and *Escherichia coli* O157:H7 concentration on fluorescence intensity and distribution, and accuracy of flow cytometry counts. Healthy and dead cells at varying concentrations suspended in Tris-BSA and stained with a range of SYBR Green I concentrations. Median fluorescence intensity (MFI), robust coefficient of variation (rCV) and linear regression analysis of flow cytometry cell counts and theoretical cell concentrations for dead (A) and healthy (B) cells.

considered as healthy and dead cells, respectively. This was possible when staining *ca.* 7.5 log CFU/mL *E. coli* O157:H7 with 1.00 μg/mL Ab-RPE, $1:10^6$ SYBR Green I, and 10.0 μM PI in Tris-BSA. Population resolution was remarkably reduced for cell concentrations lower than 7.5 log CFU/mL, and so was the ability to detect injured cells.

We observed that the composition of the staining medium was at least as important as the dye concentrations and ratio in the appearance of the expected orthogonal distribution of the cell populations in the green *vs.* red fluorescence plot. Unlike TBS-BSA, Tris-BSA allowed an optimal population separation by green fluorescence, due to enhanced SYBR Green I uptake in healthy cells. This fact was attributed to the ability of Tris to act as an outer membrane permeability-increasing agent (with no apparent change in cytoplasmic membrane permeability) in the absence of the competitive effect exerted by the high NaCl concentration of TBS-BSA. Even the use of physiological salt solution (150 mM NaCl) was found to be unsuitable to our purpose, since green fluorescence level of healthy cells was similar to that of dead cells, and this prevented visualization of injured cells. Moreover, by using Tris-BSA, no EDTA treatment is necessary to improve permeability of healthy cells to SYBR Green I, and thus the risk of damaging the cytoplasmic membrane and consequently altering the analysis outcome is avoided.

Further work needs to be done to validate the proposed protocol in food samples, where nonspecific binding of dyes with food particles can occur and result in changes in the fluorescence patterns of cell populations. Moreover, it would be necessary to establish whether reducing the Ab-RPE concentration, and thus fluorescence spillover, would allow better population resolution in samples with a variety of *E. coli* O157:H7 concentrations without increasing the detection limit of the assay.

5. References

Barbesti, S., S. Citterio, M. Labra, M.D. Baroni, M.G. Neri, and S. Sgorbati. 2000. Two and three-color fluorescence flow cytometric analysis of immunoidentified viable bacteria. *Cytometry Part A*. 40:214–218.

Berney, M., F. Hammes, F. Bosshard, H.-U. Weilenmann, and T. Egli. 2007. Assessment and interpretation of bacterial viability by using the LIVE/DEAD BacLight kit in combination with flow cytometry. *Applied and Environmental Microbiology*. 73:3283–3290.

Brotherick, I. 2006. Basic DNA measurement by flow cytometry. *In* Guide to flow cytometry. S. Wulff, editor. Dako, Carpinteria, CA. 99–106.

Clark, M.W. 1991. Immunogold labeling of yeast ultrathin sections. *Methods in Enzymology*. 194:608–626.

Comas-Riu, J., and N. Rius. 2009. Flow cytometry applications in the food industry. *Journal of industrial Microbiology & Biotechnology*. 36:999–1011.

Denich, T.J., L.A. Beaudette, H. Lee, and J.T. Trevors. 2003. Effect of selected environmental and physico-chemical factors on bacterial cytoplasmic membranes. *Journal of Microbiological Methods*. 52:149–182.

Diamandis, E.P., T.K. Christopoulos, and M.J. Khosravi. 1996. Development of in-house immunoassays. *In* Immunoassay. E.P. Diamandis and T.K. Christopoulos, editors. Academic Press, Burlington, VT. 555–568.

Doherty, S.B., L. Wang, R.P. Ross, C. Stanton, G.F. Fitzgerald, and A. Brodkorb. 2010. Use of viability staining in combination with flow cytometry for rapid viability assessment of *Lactobacillus rhamnosus* GG in complex protein matrices. *Journal of Microbiological Methods*. 82:301–310.

Falcioni, T., S. Papa, and J.M. Gasol. 2008. Evaluating the flow-cytometric nucleic acid double-staining protocol in realistic situations of planktonic bacterial death. *Applied and Environmental Microbiology*. 74:1767–1779.

Givan, A.L. 2001. Cells from within: DNA in life and death. *In* Flow cytometry. First principles. Wiley-Liss, New York, NY. 123–158.

Grégori, G., S. Citterio, A. Ghiani, M. Labra, S. Sgorbati, and S. Brown. 2001. Resolution of viable and membrane-compromised bacteria in freshwater and marine waters based on analytical flow cytometry and nucleic acid double staining. *Applied and Environmental Microbiology.* 10:4662–4670.

Gurtovenko, A.A., and J. Anwar. 2007. Modulating the structure and properties of cell membranes: the molecular mechanism of action of dimethyl sulfoxide. *The Journal of Physical Chemistry B.* 111:10453–10460.

Hammes, F., T. Broger, H.-U. Weilenmann, M. Vital, J. Helbing, U. Bosshart, P. Huber, R.P. Odermatt, and B. Sonnleitner. 2012. Development and laboratory-scale testing of a fully automated online flow cytometer for drinking water analysis. *Cytometry Part A.* 81:508–516.

Haugland, R.P. 2010. Nucleic acid detection and genomics technology. *In* The Molecular Probes handbook. A guide to fluorescent probes and labelling technologies. M.T.Z. Spence, editor. Invitrogen, Carlsbad, CA. 302–360.

Herrero, M., C. Quirós, L.A. García, and M. Díaz. 2006. Use of flow cytometry to follow the physiological states of microorganisms in cider fermentation processes. *Applied and Environmental Microbiology.* 72:6725–6733.

Hussein, H.S., B.H. Thran, and D. Redelman. 2002. Detection of *Escherichia coli* O157:H7 in bovine rumen fluid and feces by flow cytometry. *Food Control.* 13:387–391.

Manini, E., and R. Danovaro. 2006. Synoptic determination of living/dead and active/dormant bacterial fractions in marine sediments. *FEMS Microbiology Ecology.* 55:416–423.

Martens, A.C.M., G.J. van den Engh, and A. Hagenbeek. 1981. The fluorescence intensity of propidium iodide bound to DNA depends on the concentration of sodium chloride. *Cytometry.* 2:24–25.

McCarthy, M., and S.C. Culloty. 2011. Optimization of two immunofluorescent antibodies for the detection of *Escherichia coli* using immunofluorescent microscopy and flow cytometry. *Current Microbiology.* 62:402–408.

Miller, J.J., and S.S. Levinson. 1996. Interferences in immunoassays. *In* Immunoassay. E.P. Diamandis and T.K. Christopoulos, editors. Academic Press, Burlington, VT. 165–190.

Müller, S., and G. Nebe-von-Caron. 2010. Functional single-cell analyses: flow cytometry and cell sorting of microbial populations and communities. *FEMS Microbiology Reviews*. 34:554–587.

Murano, E.A., and J.A. Hudnall. 2001. Media, reagents, and stains. *In* Compendium of methods for the microbiological examination of foods. F.P. Downes and K. Ito, editors. American Public Health Association, Washington, DC. 601–648.

Nebe-von-Caron, G. 2009. Standardization in microbial cytometry. *Cytometry Part A*. 75:86–89.

Rodriguez, S.B., and R.J. Thornton. 2008. Use of flow cytometry with fluorescent antibodies in real-time monitoring of simultaneously inoculated alcoholic-malolactic fermentation of Chardonnay. *Letters in Applied Microbiology*. 46:38–42.

Roederer, M., A. Treister, W. Moore, and L.A. Herzenberg. 2001. Probability binning comparison: a metric for quantitating univariate distribution differences. *Cytometry*. 45:37–46.

Saegeman, V.S., R. De Vos, N.D. Tebaldi, J.M. van der Wolf, J.H. Bergervoet, J. Verhaegen, D. Lismont, B. Verduyckt, and N.L. Ectors. 2007. Flow cytometric viability assessment and transmission electron microscopic morphological study of bacteria in glycerol. *Microscopy and Microanalysis*. 13:18–29.

Schellenberg, J., W. Smoragiewicz, and B. Karska-Wysocki. 2006. A rapid method combining immunofluorescence and flow cytometry for improved understanding of competitive interactions between lactic acid bacteria (LAB) and methicillin-resistant *S. aureus* (MRSA) in mixed culture. *Journal of Microbiological Methods*. 65:1–9.

Shapiro, H.M. 2000. Microbial analysis at the single-cell level: tasks and techniques. *Journal of Microbiological Methods*. 42:3–16.

Shapiro, H.M. 2003. Data analysis. *In* Practical flow cytometry. John Wiley & Sons, Hoboken, NJ. 225–256.

Shi, L., S. Günther, T. Hübschmann, L.Y. Wick, H. Harms, and S. Müller. 2007. Limits of propidium iodide as a cell viability indicator for environmental bacteria. *Cytometry Part A*. 71:592–598.

Stocks, S.M. 2004. Mechanism and use of the commercially available viability stain, *Bac*Light. *Cytometry Part A*. 61:189–195.

Sträuber, H., and S. Müller. 2010. Viability states of bacteria. Specific mechanisms of selected probes. *Cytometry Part A*. 77:623–634.

Trevors, J.T. 2003. Fluorescent probes for bacterial cytoplasmic membrane research. *Journal of Biochemical and Biophysical Methods*. 57:87–103.

Ueckert, J., P. Breeuwer, T. Abee, P.J. Stephens, G. Nebe-von-Caron, and P.F. ter Steeg. 1995. Flow cytometry applications in physiological study and detection of foodborne microorganisms. *International Journal of Food Microbiology*. 28:317–326.

Vaara, M. 1992. Agents that increase the permeability of the outer membrane. *Microbiological Reviews*. 56:395–411.

Vital, M., H.P. Füchslin, F. Hammes, and T. Egli. 2007. Growth of *Vibrio cholerae* O1 Ogawa Eltor in freshwater. *Microbiology*. 153:1993–2001.

Yamaguchi, N., M. Sasada, M. Yamanaka, and M. Nasu. 2003. Rapid detection of respiring *Escherichia coli* O157:H7 in apple juice, milk, and ground beef by flow cytometry. *Cytometry Part A*. 54:27–35.

Ziglio, G., G. Andreottola, S. Barbesti, G. Boschetti, L. Bruni, P. Foladori, and R. Villa. 2002. Assessment of activated sludge viability with flow cytometry. *Water Research*. 36:460–468.

Chapter 6. Flow cytometry immunodetection and membrane integrity assessment of *Escherichia coli* O157:H7 in ready-to-eat pasta salad during refrigerated storage[1]

Abstract

Over the past years, products of non-animal origin have been increasingly linked to foodborne diseases caused by the enterohemorrhagic pathogen *Escherichia coli* O157:H7. Contaminated fresh produce and derived ready-to-eat (RTE) meals are of major concern, since no further or only minimal processing is applied. In this study, flow cytometry was evaluated as a rapid technique to detect *E. coli* O157:H7 by immunofluorescence, using polyclonal antibodies conjugated to R-phycoerythrin, in refrigerated RTE pasta salad containing acetic acid and benzoic acid. Signal filtering strategies were applied during sample analysis to reduce the limit of detection of the technique to 5 log CFU/g. Simultaneously with pathogen detection, physiological state was assessed by staining with the membrane integrity indicators propidium iodide and SYBR Green I. Fine tuning of dye concentrations and ratios allowed discrimination of not only cells with intact or damaged membranes, but also of cells with partially damaged membranes, which were considered injured cells. Then, changes in membrane integrity of inoculated *E. coli* O157:H7 cells were monitored throughout 14-day refrigerated storage. Most cells were injured at the beginning of refrigeration, but showed an intact membrane at the end. This suggests that injured *E. coli* O157:H7 cells underwent a membrane repair during exposure to refrigeration and acid stresses, and survived in RTE pasta salad. This highlights the importance of the implementation of control measures to limit the presence of this pathogen in non-animal origin food products. Additionally, the proposed immunodetection and membrane integrity three-color assay in food is a good tool to monitor the effect of a number of food-related treatments on *E. coli* O157:H7 cell membrane.

---

1. Introduction

Over the past years, consumer demand for convenience food has resulted in a fast growth of the chilled ready-to-eat (RTE) meal market (Quested *et al.*, 2010). Ingredients of non-animal origin, which are usually present in these meals (e.g. vegetable salads, salad meals), have been increasingly recognized as important vectors in foodborne diseases associated with bacteria, such as *Escherichia coli* O157:H7 (Little and Gillespie, 2008; Frankel *et al.*, 2009; Berger *et al.*, 2010; EFSA Panel on Biological Hazards, 2013). This pathogen is an important etiologic agent of hemorrhagic enteritis in humans, which is caused by a Shiga-like toxin, also known as verotoxin. Young children, the elderly, and other individuals with weakened immune system may also develop kidney failure (Beauchamp and Sofos, 2010; Robinson and McKillip, 2010). Owing to its zoonotic character, infections caused by *E. coli* O157:H7 are more frequently related with products of animal origin (e.g. cattle and small ruminants). However, *E. coli* O157:H7 contamination of non-host environments, such as fresh produce and derived RTE meals, can occur at any stage from pre-harvest to post-harvest operations (Greig and Ravel, 2009; Berger *et al.*, 2010; Erickson, 2010; Bautista-De León *et al.*, 2013). Indeed, this pathogen can adhere to and survive in crops, which may be contaminated with animal feces or fecal water, and cross-contamination from products of animal origin can occur during food preparation (Little and Gillespie, 2008; Frankel *et al.*, 2009). Minimal or non-existent further processing of contaminated products prior to consumption and/or inability of chemical treatments to eliminate surface contamination may then lead to the dissemination of the disease (Berger *et al.*, 2010; Erickson, 2010).

Refrigeration is the primary preservation means in RTE vegetable salads and salad meals (Little and Gillespie, 2008), and is usually combined with weak organic acids (e.g. acetic acid, benzoic acid). Low temperature reduces cell mem-

brane fluidity, which results in hampered functionality, namely leakage of intracellular components, disruption of active transport, and inactivation of membrane-bound redox enzymes. It also reduces transcription and translation efficiencies, and enzyme reaction rates. Globally, this leads to restriction of cellular activity, and thus, to growth arrest and establishment of the survival phase (Phadtare, 2004; Sutherland, 2005; Cavicchioli *et al.*, 2009). Decrease of intracellular pH due to exposure to weak organic acids interferes with essential metabolic processes, such as the synthesis of ATP, RNA and proteins. It also causes structural damage to the cell membrane, DNA and proteins (Brul and Coote, 1999; Cotter and Hill, 2003; Davidson *et al.*, 2013). Exposure of bacterial cells to cold and acid triggers adaptive responses in which metabolic changes take place to counteract the detrimental effects of such stresses (Phadtare, 2004; McClure, 2005). Cytoplasmic membrane intactness is crucial to sustain metabolic activity under these conditions and permit cell survival. Membrane integrity is therefore accepted as a good viability predictor. This physiological parameter has been widely assessed using propidium iodide (PI) (Endo *et al.*, 2001; Ananta *et al.*, 2005; Hayouni *et al.*, 2008; Tong *et al.*, 2009), which is a membrane-impermeant red-fluorescent nucleic acid dye that is therefore excluded by cells with intact membranes but stains permeabilized cells. In order to simultaneously analyze cells with intact and damaged membranes, PI has been combined with membrane-permeant green-fluorescent nucleic acid dyes, such as SYBR Green I (Barbesti *et al.*, 2000; Berney *et al.*, 2007, 2008). Several techniques can be used to analyze fluorescently stained cells. In particular, flow cytometry allows analyzing thousands of cells in few seconds and obtaining quantitative information on heterogeneity of population physiology (Breeuwer and Abee, 2000; Shapiro, 2000). Moreover, a fluorescently labeled antibody has been used for rapid flow cytometry detection of *E. coli* O157:H7 in foods, such as beef, milk, and juice (Tortorello *et al.*, 1997; Yamaguchi *et al.*, 2003). A known constraint of pathogen analysis by flow cytometry is the high limit of detection (LOD), which makes necessary the implementation of strate-

gies reducing the amount of interfering food matrix particles (Wilkes *et al.*, 2012). Thus, in the first stage of this study, we evaluated the feasibility of a sample preparation and analysis protocol for flow cytometry, based on fine-tuning of staining and signal filtering strategies, to detect *E. coli* O157:H7 in inoculated RTE pasta salad and simultaneously assess its membrane integrity. Then, changes in membrane integrity and culturability of *E. coli* O157:H7 were monitored during refrigerated storage to gain insight on the phenotypic response of this pathogen to cold and acid in RTE salad.

2. Materials and methods

2.1. Bacterial strain and culture conditions

Escherichia coli O157:H7 CECT 5947, provided by the Spanish Type Culture Collection (Colección Española de Cultivos Tipo, CECT), was used for all experiments. A lyophilized culture was reconstituted and cultured for stock culture preparation. The stock culture was stored at –65°C in cryovials containing beads (AES Chemunex, Bruz, France). Pre-cultures were prepared by transferring one bead from the stock culture to a 100 mL Erlenmeyer flask containing 20 mL of tryptone soya broth (TSB; Oxoid, Basingstoke, UK), and then, incubated overnight at 37°C in a shaking water bath at 86 rpm. To obtain stationary phase cultures, 50 µL of the overnight culture were inoculated into 20 mL of TSB and incubated at 37°C for 20 h. Growth time to reach stationary phase was previously determined by measuring the optical density at 600 nm (Bioscreen C; Oy Growth Curves AB, Helsinki, Finland).

2.2. Control and inoculum preparation

Flow cytometry controls (instrument set up, compensation and gating) consisted in bacterial suspensions containing untreated cells and/or heat-killed cells (80°C/30 min). Inocula for RTE pasta salad contained only untreated cells. To obtain these suspensions, cells from stationary phase cultures were pelleted

(13,000 × g, 30 s, 20°C), resuspended and diluted in filtered (0.22 µm, polyethersulfone; Merck Millipore, Cork, Ireland) Tris buffer with bovine serum albumin (Tris-BSA; 20 mM Tris, 0.1% BSA, pH 7.4; Sigma-Aldrich Chemie, Buchs, Switzerland) to reach the concentrations specified in next sections.

2.3. Ready-to-eat pasta salad sample preparation

Non-pasteurized RTE pasta salad (Central de Cocinados Catar, Mollet del Vallès, Spain) contained cooked fusilli, green and red pepper, onion, water, sunflower oil, vinegar, salt, sodium benzoate, garlic powder, basil, parsley, and xanthan gum. Salad samples (25 g) were inoculated with 2.5 mL of healthy *E. coli* O157:H7 suspensions to obtain final pathogen concentrations from 3 to 7 log colony-forming unit (CFU)/g. The same volume of Tris-BSA was added to non-inoculated (blank) samples. After inoculation, samples were vacuum-packaged in low porosity filter blender bags (63 µm, BagPage F; Interscience, Saint-Nom-la-Bretêche, France), and stored at 4°C during salad shelf-life (14 days). At designated time points after inoculation, samples were diluted in 225 mL buffered peptone water (Oxoid) and blended for 30 s (Pulsifier, Microgen Bioproducts, Camberley, UK).

2.4. Labeling, staining and flow cytometer

For *E. coli* O157:H7 detection in flow cytometry samples, a goat polyclonal anti-*E. coli* O157:H7 antibody (BacTrace, KPL, Gaithersbourg, MD, USA) was conjugated to R-phycoerythrin (Ab-RPE; AntibodyBCN, Barcelona, Spain). This antibody is adsorbed against non-O157:H7 *E. coli* serotypes during purification to minimize cross-reactivity, and has been previously used in other work with optimum results (Tortorello and Stewart, 1994; Hussein *et al.*, 2002; Yamaguchi *et al.*, 2003; Shriver-Lake *et al.*, 2007). Using RPE, which is a phycobiliprotein emitting yellow-orange fluorescence, signal from conjugated antibodies could be collected by a detector different from those used for membrane integrity indicators. Saturating staining concentrations, at 4 to 6 log colony-forming

unit (CFU)/mL, were determined by titration of the antibody conjugate. From these assays, 0.015 µg/mL and 1.000 µg/mL Ab-RPE were used for validation of flow cytometry set ups. To selectively label *E. coli* O157:H7 cells, samples, protected from light, were incubated at 20°C for 30 min after addition of Ab-RPE.

Cytoplasmic membrane integrity was assessed using 10 µM propidium iodide (PI; Invitrogen, Eugene, OR, USA), which stains permeabilized cells. In order to simultaneously analyze cells with intact membranes, PI was combined with SYBR Green I ($1{:}10^6$ final dilution of the stock solution; Invitrogen), which also stains cells with intact membranes. Thus, cells with intact membranes display very low red fluorescence and high green fluorescence, whereas cells with damaged membranes emit high red fluorescence and very low green fluorescence (Stocks, 2004). The latter is due to a combined mechanism occurring when SYBR Green I and PI are inside a cell at the same time: (i) displacement of SYBR Green I from its binding to nucleic acids due to a stronger nucleic acid affinity of PI, which causes a decrease in green fluorescence, and (ii) PI fluorescence enhancement by energy transfer from SYBR Green I (Förster resonant energy transfer –FRET– phenomenon). Cells with partially damaged membranes emit both high green and red fluorescence, since intracellular PI is insufficient to significantly displace SYBR Green I (Barbesti *et al.*, 2000). Dye concentrations were selected from preliminary work (unpublished data) as those giving adequate cell fluorescence profiles. Cells were incubated with nucleic acid dyes at 20°C for 30 min, protected from light. For three-color samples, selective labeling with Ab-RPE was performed before addition of nucleic acid dyes. A microsphere standard (Invitrogen) was used according to manufacturer's instructions when calculation of cell concentration was necessary. This calibrated suspension contained 10^8 polysterene microspheres/mL with a 6.0-µm diameter and green and red fluorescence emission.

Samples were analyzed with a FACScalibur flow cytometer (BD, Franklin Lakes, NJ, USA) equipped with a 15-mW 488-nm air-cooled argon-ion laser. Data were acquired for forward scatter (FSC), side scatter (SSC), green fluorescence, yellow-orange fluorescence and red fluorescence parameters. Band-pass filters for SYBR Green I and Ab-RPE light emission were 530/30 (FL1) and 545/82 (FL2), respectively, whereas long-pass filter for PI light emission was 670 nm (FL3). Voltage amplification was applied at logarithmic scale. Filtered double-distilled water was used as sheath fluid. CellQuest Pro software (version 4.0.2; BD) was used for data acquisition.

2.5. Optimization of flow cytometer set up for reduced interfering particle data acquisition

To operate below the maximum data acquisition rate established by the manufacturer (2,000 event/s), the sample flow rate was kept at the lowest possible value (12 µL/s) and different cell concentrations were tested. Moreover, the effect of different threshold strategies on the LOD and the limit of quantification (LOQ) of flow cytometry assay was evaluated for control and salad samples. These parameters were established based on calculation of signal-to-noise ratios (S:N), which account for false positive events in blank replicates (noise). Results above the LOD were assigned for S:N > 3, whereas the LOQ was set at S:N > 10. The best threshold strategies were then selected for subsequent data acquisition.

For controls, healthy cell suspensions in the range of 3 to 7 log colony-forming unit (CFU)/mL and a negative control (blank) were stained with SYBR Green I. For each suspension, data were acquired for 30 s with SSC set as the primary threshold at values of 0, 50, 150 and 200.

For salads, samples were homogenized at day 1 and then allowed to stand for 5 min. Two-mL aliquots were clarified (5,000 × g, 10 min, 20°C) by means of a

centrifugal filter device (5 μm, polyvinylidene difluoride, Ultrafree-CL; Millipore) and the pellets were washed with 1 mL of Tris-BSA. Unfiltered sample volume due to filter clogging was quantified and a correction was applied when calculating cell concentration. Ab-RPE (0.015 μg/mL or 1.000 μg/mL) was added to non-inoculated and inoculated samples. After labeling, cells were stained with SYBR Green I and PI, and the microsphere standard was added. Data from each sample were acquired for 30 s with SSC as the primary trigger parameter and FL2 (yellow-orange fluorescence) as the secondary threshold at values of 0, 150 and 200.

2.6. Validation of correlation between plating and flow cytometry

Control and salad samples were also plated to assess the linearity and accuracy of the flow cytometry procedure. After blending in buffered peptone water, salad samples were allowed to stand at 20°C for 1 h (recovery step), and then serially diluted in peptone physiological salt solution (1 g/L neutralized bacteriological peptone [Oxoid] and 8.5 g/L NaCl, in water). Appropriate dilutions of control samples were spiral-plated (Eddy Jet; IUL, Barcelona, Spain) on the nonselective medium tryptone soya agar supplemented with 0.6% (w/v) yeast extract (TSAYE; Oxoid), whereas salad sample dilutions were plated on sorbitol MacConkey (SMAC) agar (Oxoid), a selective medium for *E. coli* O157:H7. Plates were incubated at 37°C for 24 h.

2.7. Evaluation of the ability of flow cytometry set up to discriminate between membrane integrity states

Healthy and heat-killed cell controls containing 5 log CFU/mL were mixed at different healthy-to-dead ratios (0:100, 25:75, 50:50, 75:25 and 100:0), labeled with 0.015 μg/mL or 1.000 μg/mL Ab-RPE, stained with PI and SYBR Green I, and analyzed by flow cytometry. The correlation between cell counts and the

corresponding percentage of healthy and dead cells in the sample was assessed.

2.8. Monitoring of cell membrane integrity and plate counts throughout salad shelf life

Flow cytometry, plate count and pH analyses were carried out at days 1, 3, 7 and 14 after inoculation of salad at 6 log CFU/g *E. coli* O157:H7. To detect the pathogen by flow cytometry, 0.015 μg/mL Ab-RPE was used in combination with PI and SYBR Green I. Controls at 5 log CFU/mL were also prepared to set up the flow cytometer, compensate the spectral overlap and establish the analysis gates. Flow cytometry was used to estimate counts of:

(i)   *viable cells*: healthy cells + injured cells;

(ii) *healthy cells*: cells with intact membranes (SYBR Green I$^+$/PI$^-$/Ab-RPE$^+$);

(iii) *injured cells*: cells with partially damaged membranes (SYBR Green I$^+$/PI$^+$/Ab-RPE$^+$);

(iv) *dead cells*: cells with damaged membranes (SYBR Green I$^-$/PI$^+$/Ab-RPE$^+$).

Total viable counts of non-inoculated salad samples were obtained by plating on TSAYE, whereas inoculated samples were plated on SMAC agar and a double-layer medium, which consisted of SMAC agar overlaid with TSAYE (thin agar layer –TAL– method). The top layer in TAL provides a suitable environment for sublethally injured cells to recover and regain culturability during the first hours of incubation, whereas selective agents in the bottom layer diffuse to the top layer, which avoids the growth of non-target bacteria and allows the development of typical colonies (Wu, 2008). Thus, both healthy and injured *E. coli* O157:H7 cells are able to grow on TAL, whereas only healthy cells grow on SMAC. Parallel plating on TAL and SMAC was used to estimate counts of:

(i)   *viable cells*: count on TAL;

(ii) *healthy cells*: count on SMAC;

(iii) *sublethally injured cells*: count on TAL – count on SMAC;

(iv) *dead cells*: initial count on TAL – count on TAL.

These counts were expressed as a percentage of the initial count on TAL.

Moreover, the effect of the recovery step on the detection of sublethally in-jured cells was assessed using TAL, SMAC agar and SMAC agar supplemented with cefixime tellurite (SMAC-CT; Oxoid), which differ in selectivity.

2.9. Analysis of flow cytometry data

FlowJo software (version 7.6.1; Tree Star, Ashland, OR, USA) was used for data compensation and analysis. Unstained untreated cells were used as a negative control in software compensation. Compensation settings were determined using positive controls: single-stained heat-killed cells for SYBR Green I and PI; and single-stained untreated cells for Ab-RPE. Three-color controls containing untreated and heat-killed cells (1:1) were used as a reference to define the re-gions encompassing cells with intact, partially damaged, and damaged mem-branes. Both compensation and gating controls always accompanied acquisi-tion of data from salad samples. This procedure was applied in order to cor-rectly visualize double positive cells, that is, cells with partially damaged membranes.

Raw data were first evaluated by displaying all parameter combinations in bivariate plots to detect interferences and find the best gating strategy. Micro-spheres were gated in the FSC *vs.* SSC plot. For cell analysis, a first gate was also placed in the FSC *vs.* SSC plot. A second gate was set in the FL1 *vs.* FSC plot for SYBR Green I-stained controls (threshold evaluation), whereas cells in three-color (gating) controls were gated in the FL2 *vs.* FSC plot. To exclude from analysis the high number of interfering events present in salad samples, non-*E. coli* O157:H7 (Ab-RPE–) events were gated in the FL2 *vs.* FL3 and the FL1 *vs.* FL2 plots. *Escherichia coli* O157:H7 events were then displayed according to

green and red fluorescence, and regions were set to discriminate cell populations with different membrane integrity states.

2.10. Statistical analysis

Counts were logarithmically transformed, except for the calculation of S:N values and cell percentages, and means and standard deviations of three biologically independent replicates were calculated. A two-tailed two-sample *t*-test was used to compare plate counts after the recovery step with those without recovery. Analysis of variance was used to compare signal threshold strategy, counting method, day and cell population groups. For this purpose, the General Linear Models procedure of SAS software (the SAS System for Windows, version 9.1; SAS Institute, Cary, NC, USA) was used. When the analysis was significant ($P < 0.05$), Tukey's test was used to separate means.

3. Results and discussion

3.1. Protocol validation for controls

3.1.1. Effect of signal triggering and cell concentration on accuracy of flow cytometry data

Signal filtering techniques were applied to decrease the amount of interfering events. In particular, only events exceeding a SSC level of 50, 150 and 200 were recorded. Data were also acquired without a threshold. To select the best signal triggering strategy, counts obtained from control samples with different cell concentrations were compared with those obtained from blank samples (S:N). Slightly higher S:N values were obtained for all cell concentrations when acquiring control sample data with a SSC trigger at a threshold value of 150, compared with 0, 50 and 200 (Figure 6.1A). Moreover, only with the 150 threshold, all cell concentrations (with 3 log CFU/mL being the lowest one) were above the LOD (S:N > 3). In other work, a 2-log CFU/mL LOD has been
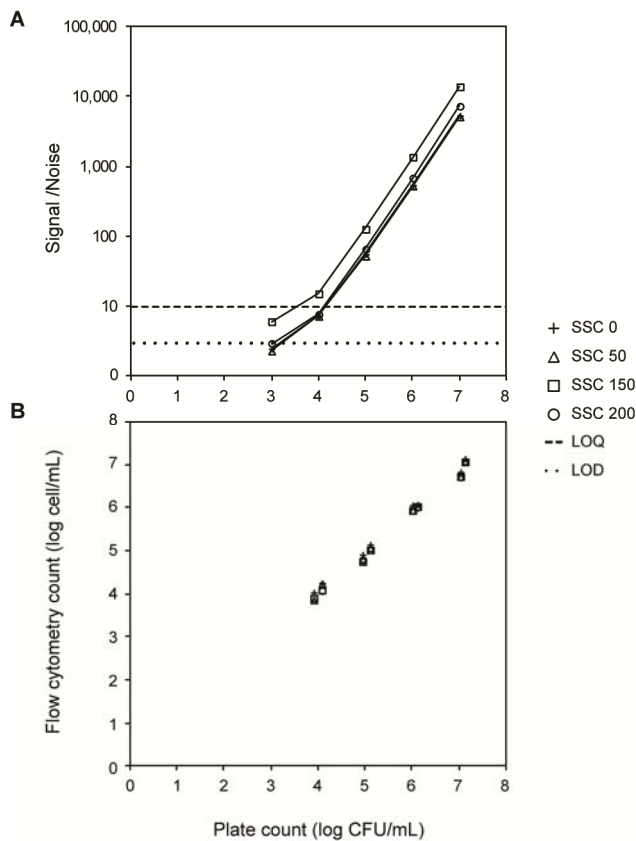
Figure 6.1 Protocol validation for controls. (A) Effect of inoculation level and signal triggering strategy on significance of flow cytometry *Escherichia coli* O157:H7 counts in controls stained with SYBR Green I. (B) Linear regression analysis of *E. coli* O157:H7 counts in controls, obtained by plating on SMAC agar and by flow cytometry in combination with SYBR Green I.

reported for pure cultures of immunolabeled *E. coli* O157:H7 (Yamaguchi *et al.*, 2003) and *S.* Typhimurium (Clarke and Pinder, 1998), which were also stained for viability assessment. McClelland and Pinder (1994) reported a LOD of 3 log CFU/mL for fluorescein isothiocyanate-antibody labeled *Salmonella* Typhimurium. However, no statements about the calculations applied to establish this parameter were included. Results above the LOQ (S:N > 10) were achieved from 4 log CFU/mL. Linear regression analyses of *E. coli* O157:H7

counts obtained by plate count and flow cytometry for each threshold value were then performed on this concentration range. Although standard curves were very similar, they gave slightly different regression statistics (Figure 6.1B). For the SSC threshold value (150) giving high S:N values, a strong positive correlation ($r = 0.9973$) was found between counts obtained by flow cytometry and plating, and fit of the model was also good ($r^2 = 0.9945$). Moreover, good accuracy between flow cytometry and plate counts was observed, as judged by the evaluation of the y-intercept (–0.2356-0.5623), which was not significantly different from 0 ($P = 0.3550$), and the slope (0.8823-1.0232), which was significantly different from 0 ($P < 0.001$). Data acquisition rate at a cell concentration of 5 log CFU/mL was 1,039±380 event/s, which did not differ significantly from the maximum acquisition rate (2,000 event/s) of the flow cytometer and the rate (1,000 event/s) proposed by Novo *et al.* (2000) for the analysis of bacterial cells by flow cytometry. This ensures the accuracy of the acquired data, since loss of information is avoided.

3.1.2. Performance of optimized staining protocol for immunodetection and membrane integrity three-color assay in pure culture

When untreated and heat-killed cell mixtures (1:1) were stained with SYBR Green I + PI and 1.000 µg/mL Ab-RPE, yellow-orange fluorescence cell emission was adequate to detect *E. coli* O157:H7 cells (Figure 6.2A). However, red fluorescence level of untreated cells was similar to that of dead cells, a fact that would have prevented the detection of true double positive cells (high green and high red fluorescences), considered as injured (partial membrane damage), in experimental samples. Conversely, 0.015 µg/mL Ab-RPE allowed good discrimination of Ab-RPE-labeled cells and proper spectral overlap compensation, that is, untreated cells displayed high green and low red fluorescences, whereas heat-killed cells emitted low green and high red fluorescences (Figure 6.2B). Moreover, such optimization allowed setting a gate for injured cells.

When combined with SYBR Green I, insufficient PI may make dead cells appear as double positive cells (Barbesti *et al.*, 2000). To rule out this artifact, performance of the optimized staining was further assessed by analysis of healthy and dead *E. coli* O157:H7 suspensions mixed at different ratios (Figure 6.2C). Correlation between cell concentration and proportion of healthy (r=0.9987) and dead (r=0.9996) cells was positive and strong, and good fits were obtained for the linear models (r^2=0.9974 for healthy cells and r^2=0.9992 for dead cells). Thus, variations in the proportion of cells with different membrane integrity did not distort the analysis outcome.

3.2. Protocol validation for ready-to-eat pasta salad samples

3.2.1. Effect of signal triggering, cell concentration and antibody concentration on accuracy of flow cytometry data

Food matrix interference is one of the main hurdles in the detection of bacterial pathogens by flow cytometry. In the present study, background reduction strategies were applied to increase the S:N ratio, and thus reduce the LOD of the assay compared with results obtained from non-optimized sample preparation and analysis procedures. Sample preparation included dilution, pulsification in 63 μm-filter bags, and centrifugal filtration (5 μm). For signal filtering during salad sample data acquisition, a primary trigger on SSC and a secondary trigger on yellow-orange fluorescence (FL2 trigger) were set at different threshold values. From Ab-RPE titration assays in suspensions from pure culture at 4-6 log CFU/mL (Figure 6.3A), 0.015 μg/mL and 1.000 μg/mL Ab-RPE were chosen to assess the effect of signal triggering on accuracy of flow cytometry data. Although 1.000 μg/mL Ab-RPE did not gave acceptable results in controls, it was used in salad samples to guarantee complete labeling of *E. coli* O157:H7 cells, considering food matrix nonspecific binding (Comas-Riu and Rius, 2009; Müller and Nebe-von-Caron, 2010). When *E. coli* O157:H7 cells in salad samples were labeled with either 0.015 μg/mL or 1.000 μg/mL Ab-RPE,
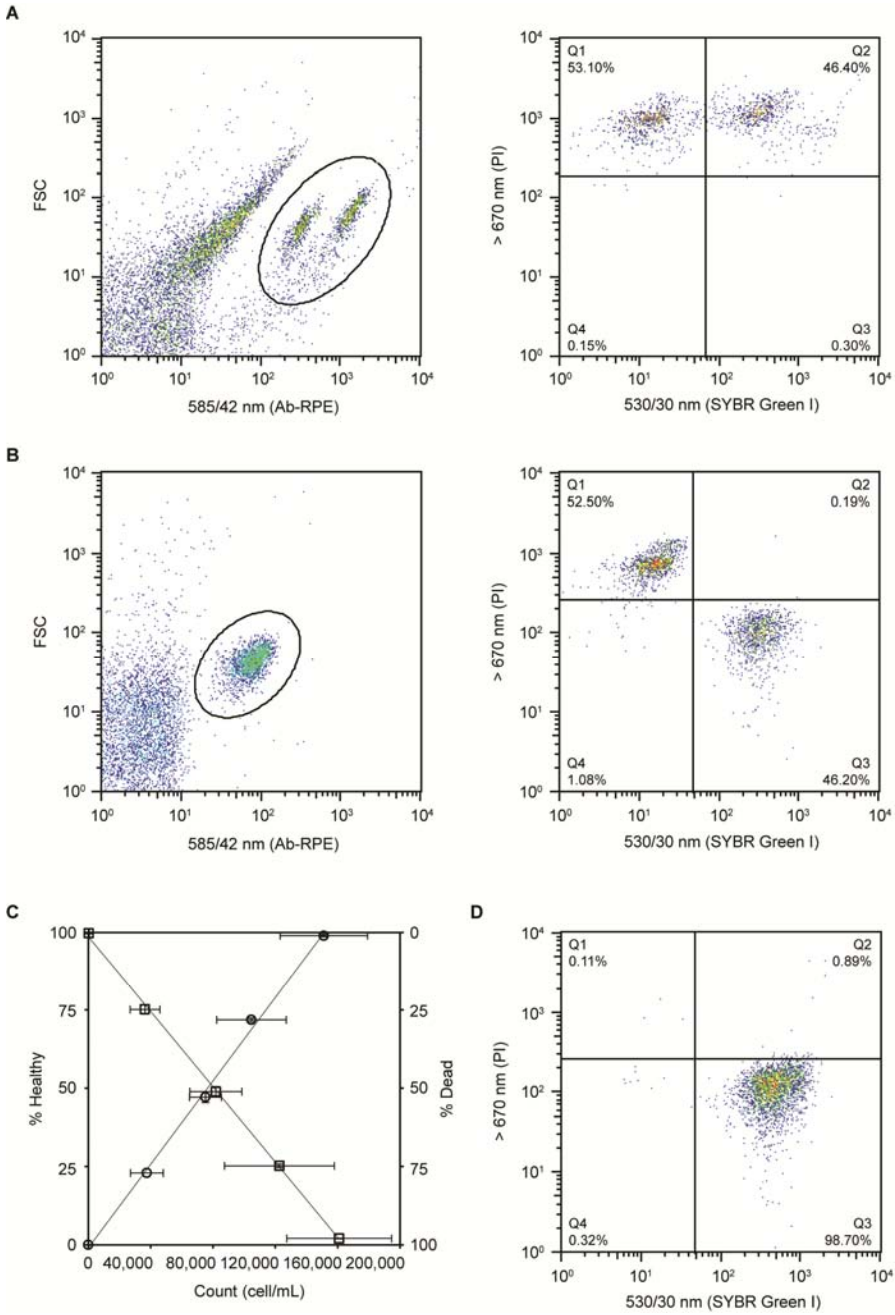
Figure 6.2 Discrimination of healthy and dead *Escherichia coli* O157:H7 by flow cytometry. Samples were stained with SYBR Green I + PI and labeled with (A) 1.000 μg/mL or (B, C and D) 0.015 μg/mL Ab-RPE. For A and B, left plots show gating of cells according to yellow-orange fluorescence (Ab-RPE) and forward scatter (FSC), whereas right plots show bivariate SYBR Green I *vs.* PI plot of immunoidentified healthy and dead cells (1:1). (C) Linear regression analysis of counts obtained from mixtures of healthy (○) and heat-killed (□) bacterial suspensions. (D) Membrane integrity assessment of inoculated cells. Q1: dead, Q2: injured, Q3: healthy, Q4: negative.

some signal triggering strategies allowed detection from 5 log CFU/g (Figure 6.4). A 4-log CFU/g LOD was reported for *E. coli* O157:H7 and *S.* Typhimurium in ground beef and egg samples, respectively; and the same pathogens were detected from 3 log CFU/mL in milk (McClelland and Pinder, 1994; Yamaguchi *et al.*, 2003). The somewhat higher LOD found in the present study is probably due to the presence of multiple ingredients, which may give a larger amount of particles in the size range of bacteria (Wilkes *et al.*, 2012). Moreover, centrifugation at speeds between 1,000 and 8,000 × *g* cause bacteria to sediment, but also food particles with equal or greater density (Stevens and Jaykus, 2004). When using 1.000 µg/mL Ab-RPE, LOQ rose to 7 log CFU/g, whereas 0.015 µg/mL Ab-RPE allowed quantification from 6 log CFU/g. This fact coincided with higher nonspecific background at the higher Ab-RPE concentration, as confirmed by the lower overlap ratio obtained from the titration assays (Figure 6.3B). Therefore, 6 log CFU/g was the chosen final pathogen concentration in salad samples to monitor changes in membrane integrity, whereas controls were prepared at 5 log CFU/mL to match the cell concentration in diluted salad samples. At 6 log CFU/g, a threshold value of 0 for the SSC trigger and of 150 for the FL2 trigger gave the highest S:N value when using 0.015 µg/mL Ab-RPE (Figure 6.4B). However, these conditions also gave the highest data acquisition rate (8,436±395 event/s). The lowest value for this parameter (3,341±1,962 event/s) was achieved with a SSC trigger at a threshold value of 200 and a FL2 trigger at 200. This signal triggering strategy also showed a high S:N value (Figure 6.4B). Moreover, a strong positive correlation (*r*=0.9935) between counts obtained by flow cytometry and plating method was found when using 0.015 µg/mL Ab-RPE. Fit of the linear model was also good (*r*²=0.9870). Conversely, at 1.000 µg/mL Ab-RPE concentration, worse correlation (*r*=0.8961) and linearity (*r*²=0.8030) were found. Furthermore, the linear regression model predicted higher flow cytometry counts compared to plate counts, as shown by a confidence interval of the y-intercept of –0.1124 to 4.3551 (*P*=0.0500), whereas the y-intercept (–1.9257-0.6561) of the model for 0.015 µg/mL Ab-RPE was not
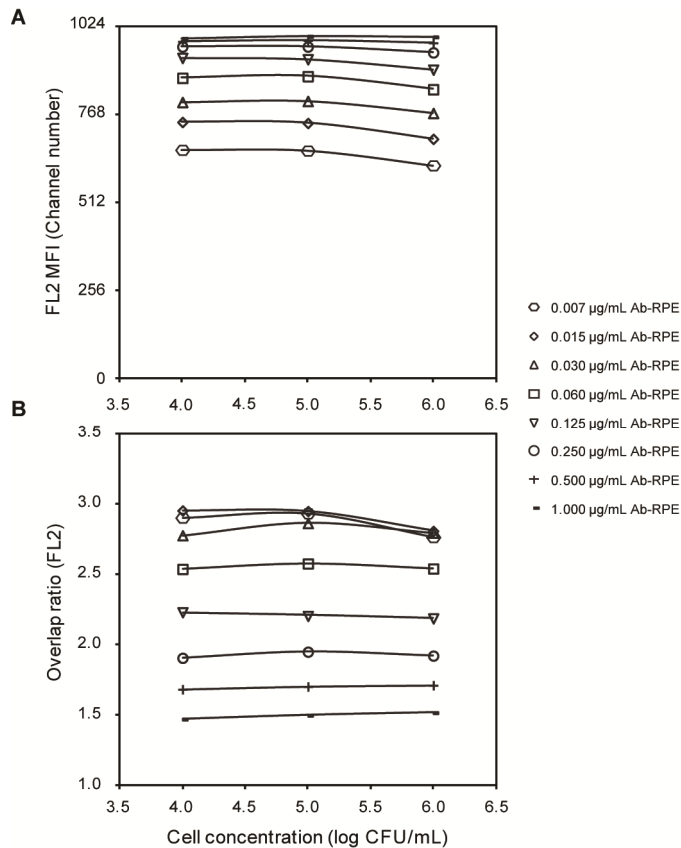
Figure 6.3 Titration of anti-*Escherichia coli* O157:H7 antibody conjugated to R-phycoerythrin (Ab-RPE). (A) Yellow-orange (FL2) median fluorescence intensity (MFI) of Ab-RPE positive events at varying Ab-RPE and cell concentrations. (B) Separation between Ab-RPE positive and Ab-RPE negative events at varying Ab-RPE and cell concentrations.

significantly different from 0 (P=0.2156) (Figure 6.5). This may be caused by an increased number of false positive counts, due to similarity in yellow-orange fluorescence emission between immunolabeled bacteria and food particles (Comas-Riu and Rius, 2009). Thus, the optimum conditions for further experiments with salad samples were 0.015 µg/mL Ab-RPE, and SSC and FL2 triggers at 200.
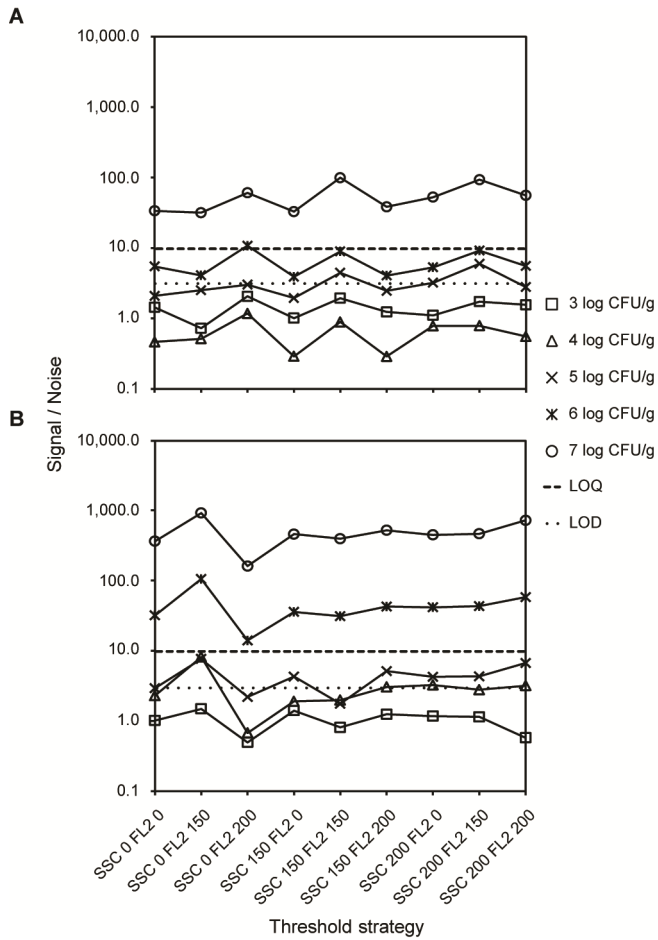
Figure 6.4 Effect of inoculation level and threshold strategy on significance of flow cytometry *Escherichia coli* O157:H7 counts in inoculated ready-to-eat pasta salad. Samples were labeled with (A) 1.000 μg/mL or (B) 0.015 μg/mL Ab-RPE and stained with SYBR Green I+ PI.
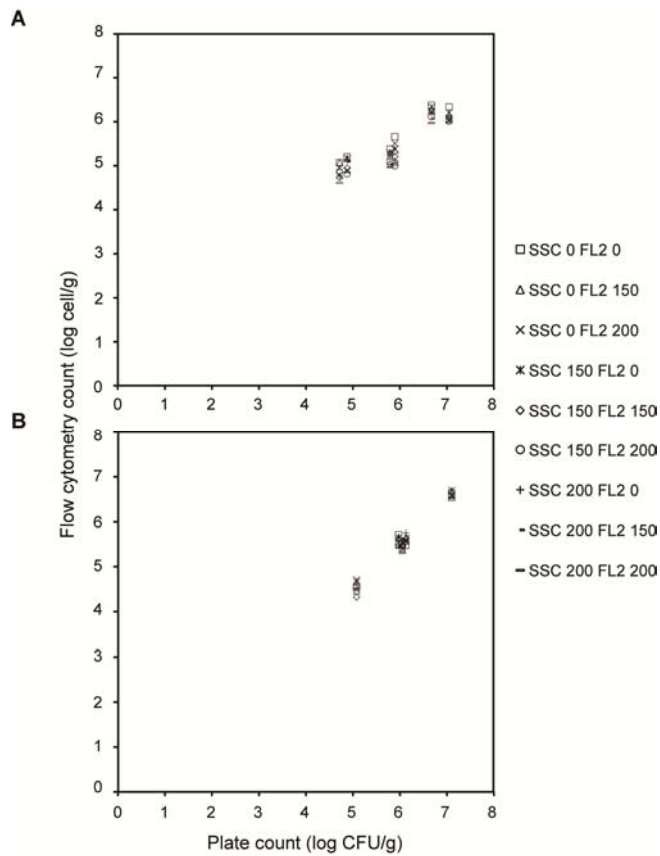
Figure 6.5 Linear regression analysis of *Escherichia coli* O157:H7 counts, in inoculated ready-to-eat pasta salads, obtained by plating on SMAC agar, and by flow cytometry in combination with SYBR Green I + PI and (A) 1.000 μg/mL or (B) 0.015 μg/mL Ab-RPE.

3.3. Changes in membrane integrity and culturability of *Escherichia coli* O157:H7 during refrigeration of inoculated ready-to-eat pasta salads

Sorbitol MacConkey agar is a widely used medium for the isolation of *E. coli* O157:H7 from foodstuffs. However, other *E. coli*, *Proteus* spp., and *Aeromonas* spp. give similar colorless colonies on this medium due to their inability to ferment sorbitol. To improve selectivity, SMAC is supplemented with cefixime and tellurite, which inhibit growth of *Proteus* spp. and *E. coli* other than O157, respectively (De Boer and Heuvelink, 2000). However, some Shiga-toxin producing *E. coli* lack resistance to this supplement (Orth *et al.*, 2007). Moreover, it has been shown to prevent recovery of injured cells (Park *et al.*, 2011; Yoshitomi *et al.*, 2012). Thus, the effect of CT supplementation as an additional selective agent for SMAC agar on recovery of the *E. coli* O157:H7 strain used in the present study was first evaluated, concomitantly with the effect of a recovery step (buffered peptone water, 20°C, 1 h) prior to plating. The TAL method was used to enumerate healthy and injured cells in salad samples. In this method, a thin layer of non-selective medium is overlaid onto prepoured selective medium. During the first hours of incubation, injured cells, if present, are able to recover and start growing on non-selective medium. Then, selective agents in the bottom layer diffuse to the top layer and react with bacteria (Wu *et al.*, 2001, 2008; Wu, 2008). Selective medium used alone is supposed to only support growth of healthy cells (Jasson *et al.*, 2007; Wesche *et al.*, 2009). No differences were found between counts on TAL and SMAC agar (Table 6.1). Conversely, counts on SMAC-CT agar were significantly lower than those obtained with TAL. The recovery step did not affect the results in any case ($P > 0.05$). Thus, since some cells were damaged in the presence of CT supplement, it was not further used. This did not influence the identification of typical *E. coli* O157:H7 colonies.

Table 6.1 Effect of recovery step (buffered peptone water, 20°C, 1 h) on *Escherichia coli* O157:H7 counts (log CFU/g) in inoculated ready-to-eat pasta salad.

Procedure	Time (day)	Thin agar layer	SMAC agar	SMAC–CT agar
No recovery	1	6.04±0.00[a,x]	6.07±0.04[a,x]	5.80±0.11[b,x]
	7	5.99±0.01[a,x]	6.00±0.02[a,x]	5.74±0.09[b,x]
	14	5.93±0.09[a,x]	5.72±0.08[a,y]	5.33±0.07[b,y]
Recovery	1	6.04±0.02[a,x]	6.03±0.00[a,x]	5.85±0.04[b,x]
	7	6.01±0.01[a,x]	6.06±0.04[a,x]	5.75±0.04[b,x]
	14	5.95±0.07[a,x]	5.93±0.10[a,x]	5.36±0.08[b,y]

Mean ± standard deviation; n = 3.
a–b: means within a row lacking a common letter differ significantly ($P < 0.05$).
x–y: for each procedure, means within a column lacking a common letter differ significantly ($P < 0.05$).

For non-inoculated salads, total viable counts on TSAYE (2.74±0.14 log CFU/g) and pH values (4.55±0.06) remained unchanged during the 14-day storage period. For inoculated salads, no changes were observed on *E. coli* O157:H7 plate counts and viable flow cytometry counts during refrigeration (Table 6.2). When bacteria are exposed to cold or acid stresses, cells respond by transiently modifying their physiology, which results in growth arrest to allow stress adaptation. *Escherichia coli* O157:H7 may then survive during extended periods of time (Panoff *et al.*, 1998; Ramos *et al.*, 2001; Sutherland, 2005; Gabriel and Nakano, 2010). Viable counts obtained by flow cytometry were lower than plate counts at days 1 and 7. Insufficient antibody concentration is not necessarily the cause for this result, since worse correlation results were obtained with 1.000 µg/mL Ab-RPE compared to 0.015 µg/mL. Instead, cells in certain physiological states may exhibit lower antibody binding due to changes in the number of exposed surface epitopes (Müller and Nebe-von-Caron, 2010). Moreover, a decrease in bacterial recovery may occur during centrifugal filtration, due to adsorption of cells to food particles (Stevens and Jaykus, 2004).

Table 6.2 *Escherichia coli* O157:H7 counts on inoculated ready-to-eat pasta salad assessed by plating and flow cytometry.

Time (day)	Thin agar layer (log CFU/g)	SMAC agar (log CFU/g)	Flow cytometry (log viable cell/g)
1	6.14±0.03[a,x]	6.14±0.09[a,x]	5.51±0.29[b,x]
3	6.09±0.06[a,x]	6.04±0.10[ab,x]	5.33±0.48[b,x]
7	6.16±0.06[a,x]	6.13±0.05[a,x]	5.40±0.36[b,x]
14	6.14±0.06[a,x]	6.10±0.07[a,x]	5.19±0.84[a,x]

Mean ± standard deviation; n = 3.
a–b: means within a row lacking a common letter differ significantly ($P < 0.05$).

x–y: means within a column lacking a common letter differ significantly ($P < 0.05$).

Parallel plating on TAL and SMAC agar did not show significant sublethal injury (Table 6.2). However, flow cytometry combined with membrane integrity indicators revealed that most *E. coli* O157:H7 cells were injured at day 1 (Table 6.3). Since inocula contained healthy cells (Figure 6.2D), injury might be conceivably caused by exposure to cold and acid, which mainly target cell membrane (Cotter and Hill, 2003; Sutherland, 2005). Upon cold exposure, membrane becomes less fluid due to a more ordered distribution of fatty acids from phospholipids. In such crystalline form, membrane fragility increases and minute breaks impair its selective barrier function (Phadtare, 2004; Sutherland, 2005; Cavicchioli *et al.*, 2009). This may allow the entrance of PI through damaged membranes. Conversely, plating gave a higher healthy cell percentage than flow cytometry. Thus, at the beginning, stress exposure may result in a large proportion of unadapted *E. coli* O157:H7 cells having partially damaged membranes. However, plate incubation, unlike flow cytometry, may promote and speed up membrane repair, as indicated by most cells being scored as healthy. Mismatch between results obtained by these methods evidenced the ability of flow cytometry to overcome the limitations of SMAC agar for injury estima-

tion, as it allows recovery of injured cells; and SMAC-CT agar, which damages healthy cells and thus overestimates injury caused by cold and acid stresses in salads. At day 14, flow cytometry showed that most *E. coli* O157:H7 cells were healthy. Thus, throughout the study, the percentage of injured cells decreased and that of healthy cells increased, whereas dead cell percentage remained constant. This was shown by a progressive decrease in red fluorescence of SYBR Green I-positive cells, which means that their membranes prevented the entrance of PI (Figure 6.6). Moreover, at day 14, the proportions of healthy and injured cells obtained by flow cytometry were not different from those obtained by plating. Coincidence between flow cytometry and plate healthy percentages at the end of the storage indicates that some cells may have repaired the membrane, conceivably by increasing fluidity through modification of fatty acid composition (homeoviscous adaptation) (Ramos *et al.*, 2001; Sutherland, 2005). Thus, partially damaged cells proved to be reversibly damaged cells.

Table 6.3 Physiological state progression of *Escherichia coli* O157:H7 inoculated into ready-to-eat pasta salad assessed by flow cytometry and plating.

Method	Time (day)	% Healthy cell	% Injured cell	% Dead cell
Flow cytometry	1	$4.70\pm2.38^{b,y}$	$89.26\pm2.35^{a,x}$	$6.03\pm4.17^{b,x}$
	3	$42.03\pm35.50^{a,xy}$	$49.43\pm35.87^{a,xy}$	$8.54\pm1.81^{a,x}$
	7	$61.59\pm27.80^{a,xy}$	$33.35\pm28.65^{a,xy}$	$5.05\pm1.10^{a,x}$
	14	$83.15\pm7.88^{a,x}$	$11.23\pm7.02^{b,y}$	$5.63\pm0.96^{b,x}$
Plating	1	$90.93\pm15.17^{a,x,*}$	$0.51\pm12.35^{b,x,*}$	$8.56\pm7.31^{b,x}$
	3	$72.10\pm13.19^{a,x}$	$9.46\pm11.08^{b,x}$	$18.44\pm13.71^{b,x}$
	7	$88.91\pm6.17^{a,x}$	$6.60\pm8.60^{b,x}$	$4.49\pm3.05^{b,x}$
	14	$83.34\pm15.38^{a,x}$	$7.68\pm14.67^{b,x}$	$8.98\pm1.98^{b,x}$

Mean ± standard deviation; n = 3.
a–b: means within a row lacking a common letter differ significantly ($P < 0.05$).
x–y: for each method, means within a column lacking a common letter differ significantly ($P < 0.05$).
* : means within the *plating* method differ significantly from their counterparts within the *flow cytometry* method ($P < 0.05$).
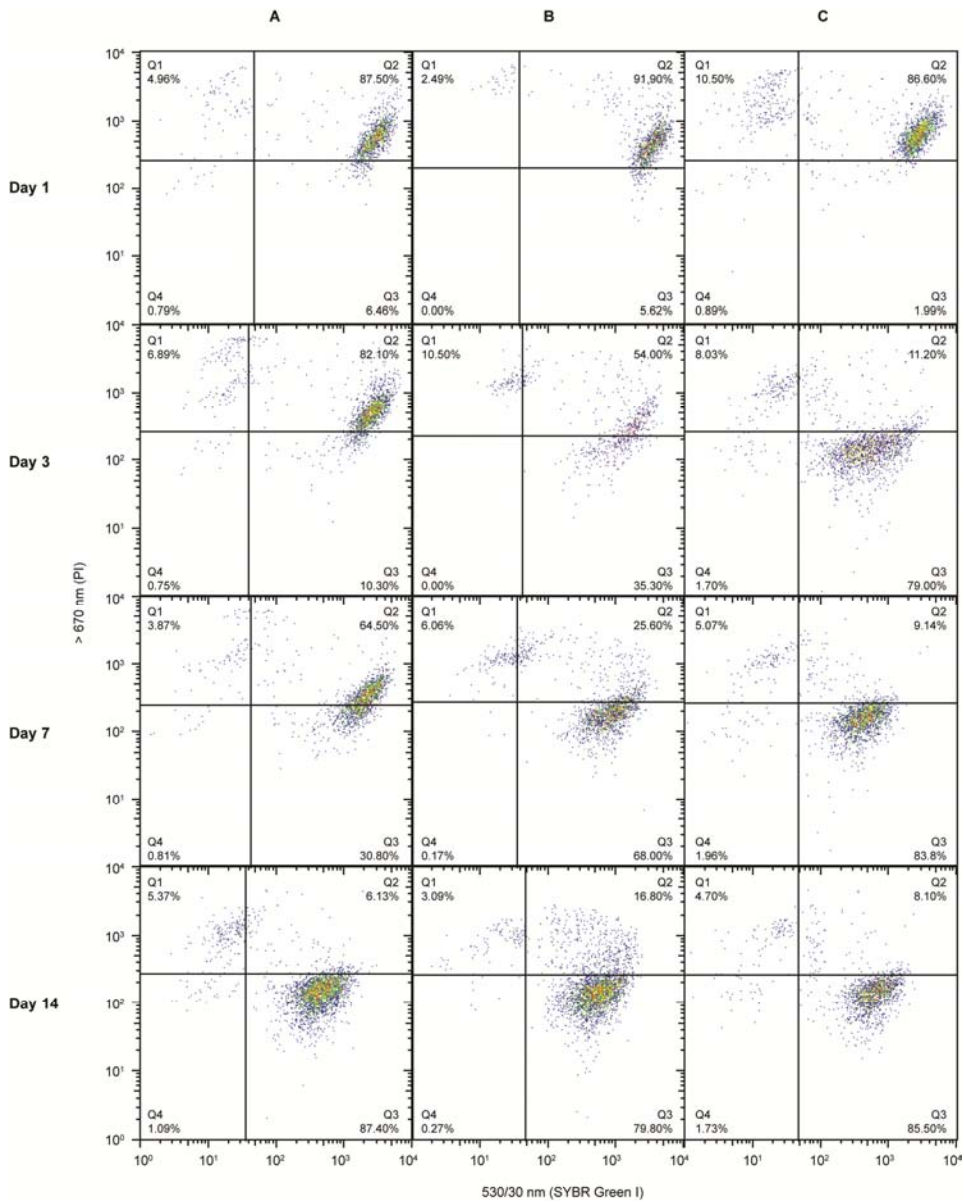
Figure 6.6 Flow cytometry membrane integrity assessment of immunoidentified *Escherichia coli* O157:H7 in inoculated ready-to-eat pasta salad stored at 4°C. Triplicate experiments are shown (A, B and C). Q1: dead cells, Q2: injured cells; Q3: healthy cells, Q4: negative.

Flow cytometry detection and quantification of healthy, injured and dead cell populations was influenced by storage time (Figure 6.7). At day 1, S:N values were above the LOD for all populations. From day 3, S:N values were higher for the healthy population. Conversely, some injured cells and, especially, dead cells were more prone to be miscounted. This coincided with an increasing proportion of healthy cells throughout the storage and a significantly lower contribution of background particles (identified in non-inoculated salads) to their gate (3.23 ± 0.69 log event/g) compared to injured (4.21 ± 0.61 log event/g) and dead cells (4.27 ± 0.65 log event/g) ($P < 0.05$). Higher contribution of background particles to injured and dead cell gates was due to similarity in fluorescence emission.
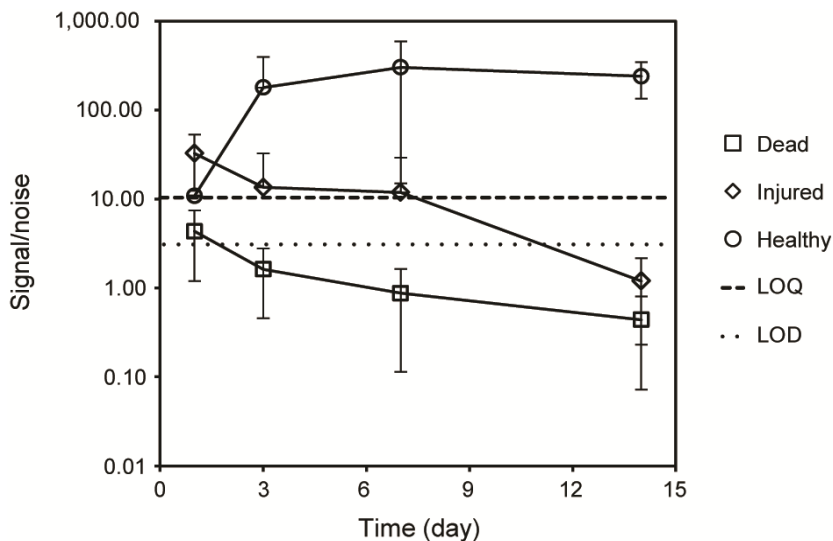

Figure 6.7 Effect of storage time at 4°C on flow cytometry detection and quantification of healthy, injured and dead *Escherichia coli* O157:H7 in inoculated ready-to-eat pasta salad.

4. Conclusions

The flow cytometry sample preparation and analysis protocol developed in this study gave reliable information on the *E. coli* O157:H7 load of inoculated RTE pasta salad in the range from 5 to 7 log CFU/g. This is still a rather high LOD, especially if the technique was intended for quality control purposes, since very low pathogen concentrations are usually found in naturally contaminated produce. Thus, including an enrichment step before flow cytometry analysis would be necessary for that purpose. Moreover, there would still be room for sensitivity improvement, based on other bacterial separation and concentration techniques, such as flotation, or coagulation and flocculation of proteins and fats present in food samples.

Besides from allowing detection and enumeration of *E. coli* O157:H7 in a food matrix, the proposed methodology provides an estimation of bacterial viability based on the assessment of single-cell membrane integrity. This approach revealed that injured *E. coli* O157:H7 cells undergo a progressive membrane repair during exposure to refrigeration and acid stresses, and survive in RTE pasta salad. This highlights the importance of the implementation of control measures to limit the presence of this pathogen in RTE meals. Moreover, simultaneous sample analysis by differential plating and flow cytometry showed that the latter is more sensitive to physiological changes. However, both give complementary information, since comparative results suggest that membrane damage in injured cells detected by flow cytometry does not prevent them from growing on SMAC. The proposed immunodetection and membrane integrity three-color assay in food is thus a good tool to monitor the effect of a number of food-related treatments on *E. coli* O157:H7 cell membrane.

5. References

Ananta, E., D. Voigt, M. Zenker, V. Heinz, and D. Knorr. 2005. Cellular injuries upon exposure of *Escherichia coli* and *Lactobacillus rhamnosus* to high-intensity ultrasound. *Journal of Applied Microbiology*. 99:271–278.

Barbesti, S., S. Citterio, M. Labra, M.D. Baroni, M.G. Neri, and S. Sgorbati. 2000. Two and three-color fluorescence flow cytometric analysis of immunoidentified viable bacteria. *Cytometry Part A*. 40:214–218.

Bautista-De León, H., C.A. Gómez-Aldapa, E. Rangel-Vargas, E. Vázquez-Barrios, and J. Castro-Rosas. 2013. Frequency of indicator bacteria, *Salmonella* and diarrhoeagenic *Escherichia coli* pathotypes on ready-to-eat cooked vegetable salads from Mexican restaurants. *Letters in Applied Microbiology*. 56:1–8.

Beauchamp, C.S., and J.N. Sofos. 2010. Diarrheagenic *Escherichia coli*. *In* Pathogens and toxins in food. Challenges and interventions. V.K. Juneja and J.N. Sofos, editors. ASM Press, Washington, DC. 71–94.

Berger, C.N., S. V Sodha, R.K. Shaw, P.M. Griffin, D. Pink, P. Hand, and G. Frankel. 2010. Fresh fruit and vegetables as vehicles for the transmission of human pathogens. *Environmental Microbiology*. 12:2385–2397.

Berney, M., F. Hammes, F. Bosshard, H.-U. Weilenmann, and T. Egli. 2007. Assessment and interpretation of bacterial viability by using the LIVE/DEAD BacLight kit in combination with flow cytometry. *Applied and Environmental Microbiology*. 73:3283–3290.

Berney, M., M. Vital, I. Hülshoff, H.-U. Weilenmann, T. Egli, and F. Hammes. 2008. Rapid, cultivation-independent assessment of microbial viability in drinking water. *Water Research*. 42:4010–4018.

De Boer, E., and A.E. Heuvelink. 2000. Methods for the detection and isolation of Shiga toxin-producing *Escherichia coli*. *Journal of Applied Microbiology*. 88:133–143.

Breeuwer, P., and T. Abee. 2000. Assessment of viability of microorganisms employing fluorescence techniques. *International Journal of Food Microbiology.* 55:193–200.

Brul, S., and P. Coote. 1999. Preservative agents in foods. Mode of action and microbial resistance mechanisms. *International Journal of Food Microbiology.* 50:1–17.

Cavicchioli, R., N. Saunders, and T. Thomas. 2009. Cold-shock response in microorganisms. *In* Extremophiles. C. Gerday and N. Glandsdorff, editors. Encyclopedia of Life Support Systems Publishers, Oxford. http://www.eolss.net.

Clarke, R.G., and A.C. Pinder. 1998. Improved detection of bacteria by flow cytometry using a combination of antibody and viability markers. *Journal of Applied Microbiology.* 84:577–584.

Comas-Riu, J., and N. Rius. 2009. Flow cytometry applications in the food industry. *Journal of Industrial Microbiology & Biotechnology.* 36:999–1011.

Cotter, P.D., and C. Hill. 2003. Surviving the acid test: responses of Gram-positive bacteria to low pH. *Microbiology and Molecular Biology Reviews.* 67:429–453.

Davidson, M.P., T.M. Taylor, and S.E. Schmidt. 2013. Chemical preservatives and natural antimicrobial compounds. *In* Food microbiology: fundamentals and frontiers. M.P. Doyle and R.L. Buchanan, editors. ASM Press, Washington, DC. 765–781.

EFSA Panel on Biological Hazards. 2013. Scientific opinion on the risk posed by pathogens in food of non-animal origin. Part 1 (outbreak data analysis and risk ranking of food/pathogen combinations). *EFSA Journal.* 11:3025–3163.

Endo, H., Y. Nagano, H. Ren, and T. Hayashi. 2001. Rapid enumeration of bacteria grown on surimi-based products by flow cytometry. *Fisheries Science.* 67:969–974.

Erickson, M.C. 2010. Microbial risks associated with cabbage, carrots, celery, onions, and deli salads made with these produce items. *Comprehensive Reviews in Food Science and Food Safety*. 9:602–619.

Frankel, G., R.K. Shaw, D. Pink, C.N. Berger, and P. Hand. 2009. Fresh produce as a potential vector for bacterial human pathogens. *Microbial Biotechnology*. 2:595–597.

Gabriel, A.A., and H. Nakano. 2010. Influences of simultaneous physicochemical stress exposures on injury and subsequent responses of *E. coli* O157:H7 to resuscitative and inactivative challenges. *International Journal of Food Microbiology*. 139:182–192.

Greig, J.D., and A. Ravel. 2009. Analysis of foodborne outbreak data reported internationally for source attribution. *International Journal of Food Microbiology*. 130:77–87.

Hayouni, E.A., M. Bouix, M. Abedrabba, J.-Y. Leveau, and M. Hamdi. 2008. Mechanism of action of *Melaleuca armillaris* (Sol. Ex Gaertu) Sm. essential oil on six LAB strains as assessed by multiparametric flow cytometry and automated microtiter-based assay. *Food Chemistry*. 111:707–718.

Hussein, H.S., B.H. Thran, and D. Redelman. 2002. Detection of *Escherichia coli* O157:H7 in bovine rumen fluid and feces by flow cytometry. *Food Control*. 13:387–391.

Jasson, V., M. Uyttendaele, A. Rajkovic, and J. Debevere. 2007. Establishment of procedures provoking sub-lethal injury of *Listeria monocytogenes*, *Campylobacter jejuni* and *Escherichia coli* O157 to serve method performance testing. *International Journal of Food Microbiology*. 118:241–249.

Little, C.L., and I.A. Gillespie. 2008. Prepared salads and public health. *Journal of Applied Microbiology*. 105:1729–1743.

McClelland, R.G., and A.C. Pinder. 1994. Detection of *Salmonella typhimurium* in dairy products with flow cytometry and monoclonal antibodies. *Applied and Environmental Microbiology*. 60:4255–4262.

McClure, P. 2005. *Escherichia coli*: virulence, stress response, and resistance. *In* Understanding pathogen behaviour: virulence, stress response and resistance. M. Griffiths, editor. Woodhead Publishing, Cambridge. 240–278.

Müller, S., and G. Nebe-von-Caron. 2010. Functional single-cell analyses: flow cytometry and cell sorting of microbial populations and communities. *FEMS Microbiology Reviews*. 34:554–587.

Novo, D.J., N.G. Perlmutter, R.H. Hunt, and H.M. Shapiro. 2000. Multiparameter flow cytometric analysis of antibiotic effects on membrane potential, membrane permeability, and bacterial counts of *Staphylococcus aureus* and *Micrococcus luteus*. *Antimicrobial Agents and Chemotherapy*. 44:827–834.

Orth, D., K. Grif, M.P. Dierich, and R. Würzner. 2007. Variability in tellurite resistance and the *ter* gene cluster among Shiga toxin-producing *Escherichia coli* isolated from humans, animals and food. *Research in Microbiology*. 158:105–111.

Panoff, J.-M., B. Thammavongs, M. Guéguen, and P. Boutibonnes. 1998. Cold stress responses in mesophilic bacteria. *Cryobiology*. 36:75–83.

Park, S.-H., S. Ryu, and D.H. Kang. 2011. Improved selective and differential medium for isolation of *Escherichia coli* O157:H7. *Journal of Clinical Microbiology*. 49:405–408.

Phadtare, S. 2004. Recent developments in bacterial cold-shock response. *Current Issues in Molecular Biology*. 6:125–136.

Quested, T.E., P.E. Cook, L.G.M. Gorris, and M.B. Cole. 2010. Trends in technology, trade and consumption likely to impact on microbial food safety. *International Journal of Food Microbiology*. 139:29–42.

Ramos, J.L., M.-T. Gallegos, S. Marqués, M.-I. Ramos-González, M. Espinosa-Urgel, and A. Segura. 2001. Responses of Gram-negative bacteria to certain environmental stressors. *Current Opinion in Microbiology*. 4:166–171.

Robinson, A.L., and J.L. McKillip. 2010. Biology of *Escherichia coli* O157:H7 in human health and food safety with emphasis on sublethal injury and detection. *In* Current research, technology and education topics in applied microbiology and microbial biotechnology. A. Méndez-Vilas, editor. Formatex, Badajoz. 1096–1105.

Shapiro, H.M. 2000. Microbial analysis at the single-cell level: tasks and techniques. *Journal of Microbiological Methods.* 42:3–16.

Shriver-Lake, L.C., S. Turner, and C.R. Taitt. 2007. Rapid detection of *Escherichia coli* O157:H7 spiked into food matrices. *Analytica Chimica Acta.* 584:66–71.

Stevens, K.A., and L.-A. Jaykus. 2004. Bacterial separation and concentration from complex sample matrices: a review. *Critical Reviews in Microbiology.* 30:7–24.

Stocks, S.M. 2004. Mechanism and use of the commercially available viability stain, *Bac*Light. *Cytometry Part A.* 61:189–195.

Sutherland, J.P. 2005. Pathogen resistance and adaptation to low temperature. *In* Understanding pathogen behaviour: virulence, stress response and resistance. M. Griffiths, editor. Woodhead Publishing, Cambridge. 507–523.

Tong, S., A.P. Bos, and S. Brul. 2009. Assessing freeze-thaw and high pressure low temperature induced damage to *Bacillus subtilis* cells with flow cytometry. *Innovative Food Science & Emerging Technologies.* 10:9–15.

Tortorello, M.L., and D.S. Stewart. 1994. Antibody-direct epifluorescent filter technique for rapid, direct enumeration of *Escherichia coli* O157:H7 in beef. *Applied and Environmental Microbiology.* 60:3553–3559.

Tortorello, M.L., D.S. Stewart, and R.B. Raybourne. 1997. Quantitative analysis and isolation of *Escherichia coli* O157:H7 in a food matrix using flow cytometry and cell sorting. *FEMS Immunology and Medical Microbiology.* 19:267–274.

Wesche, A.M., J.B. Gurtler, B.P. Marks, and E.T. Ryser. 2009. Stress, sublethal injury, resuscitation, and virulence of bacterial foodborne pathogens. *Journal of Food Protection*. 72:1121–1138.

Wilkes, J.G., R.K. Tucker, J.A. Montgomery, W.M. Cooper, J.B. Sutherland, and D.A. Buzatu. 2012. Reduction of food matrix interference by a combination of sample preparation and multi-dimensional gating techniques to facilitate rapid, high sensitivity analysis for *Escherichia coli* serotype O157 by flow cytometry. *Food Microbiology*. 30:281–288.

Wu, V.C.H. 2008. A review of microbial injury and recovery methods in food. *Food Microbiology*. 25:735–744.

Wu, V.C.H., D.Y.C. Fung, D.H. Kang, and L.K. Thompson. 2001. Evaluation of thin agar layer method for recovery of acid-injured foodborne pathogens. *Journal of Food Protection*. 64:1067–1071.

Wu, V.C.H., X. Qiu, and Y.H. Peggy Hsieh. 2008. Evaluation of *Escherichia coli* O157:H7 in apple juice with *Cornus* fruit (*Cornus officinalis Sieb. et Zucc.*) extract by conventional media and thin agar layer method. *Food Microbiology*. 25:190–195.

Yamaguchi, N., M. Sasada, M. Yamanaka, and M. Nasu. 2003. Rapid detection of respiring *Escherichia coli* O157:H7 in apple juice, milk, and ground beef by flow cytometry. *Cytometry Part A*. 54:27–35.

Yoshitomi, K.J., R. Zapata, K.C. Jinneman, S.D. Weagant, and W. Fedio. 2012. Recovery of *E. coli* O157 strains after exposure to acidification at pH 2. *Letters in Applied Microbiology*. 54:499–503.

Chapter 7. General discussion

1. Introduction

Uptake of the membrane-impermeant nucleic acid dye PI is widely accepted as an indication of cell death (Manini and Danovaro, 2006; Sträuber and Müller, 2010). Moreover, combination of PI with membrane-permeant nucleic acid dyes, such as SYTO 9, SYTO BC and SYBR Green I, allows simultaneous detection of cells with intact and damaged membranes (Bunthof *et al.*, 2001; Ben-Amor *et al.*, 2005; Tamburini *et al.*, 2014). Reports on the detection of an intermediate cell population, attributed to cells with partially damaged membranes (Barbesti *et al.*, 2000; Ben-Amor *et al.*, 2005; Saegeman *et al.*, 2007) prompted us to optimize these assays with the purpose of reliably detecting injured bacterial pathogens in food.

2. Protocol optimization

2.1. Enhancement of separation between populations of cells with intact and damaged membranes

Optimal resolution of populations of cells with intact and damaged membranes is a requisite for the reliable detection of cells with partially damaged membranes, and we found it to be related to dye concentration, dye ratio, composition of the staining medium, cell concentration, and dye combination.

Preliminary work with *E. coli* O157:H7 suspensions using SYTO 9 and PI at the concentrations recommended by the manufacturer (5 and 30 μM, respectively) gave healthy cells with higher red fluorescence than dead cells, a fact that was attributed to the inability to fully compensate the contribution of SYTO 9 fluorescence emission to the red fluorescence PMT due to a too high fluorescence intensity. According to this, concentrations of green-fluorescent dyes used in this thesis (SYTO 9, SYTO BC, SYTO 24 and SYBR Green I) were reduced, so that, being unstained cells the reference to set photodetector gains, single-stained

cells gave fluorescence peaks clearly separated from unstained cells and from background particles. Next step in optimization of staining with membrane integrity indicators consisted in finding the concentration ratio giving the maximum resolution of cell populations according to their green fluorescence. This can be achieved at saturating PI concentrations, which ensure the displacement of green-fluorescent dyes bound to nucleic acids in dead cells and therefore the desired decrease in green fluorescence (Barbesti *et al.*, 2000).

In **experiment 1**, these practical approaches were followed to optimize SYTO 9 + PI, SYTO BC + PI and SYTO 24 + PI staining of *E. coli* O157:H7, *S.* Enteritidis and *L. monocytogenes* suspended in potassium citrate solution. Reduction of green-fluorescent dye concentrations allowed optimum fluorescence compensation, with the consequent decrease in red fluorescence of dual-stained healthy cells and improved separation from dead cells for this fluorescence parameter. Resolution of healthy and dead cells by their green fluorescence increased with PI concentration. Conversely, red fluorescence resolution decreased with increasing PI concentration, due to increased background fluorescence in healthy cells. Despite this fact, optimum PI concentrations, i.e. those allowing the establishment of a gate for injured cells, could be selected for the three pathogens.

Since the ultimate goal of this thesis was to detect specific injured pathogen cells in RTE pasta salad, in **experiment 3**, optimization was also carried out for *E. coli* O157:H7 suspensions in buffers commonly used in immunoassays (TBS-BSA and Tris-BSA) and stained with the high-affinity nucleic acid dye SYBR Green I, PI, and a RPE-labeled antibody. Effect of PI concentration on population resolution of SYBR Green I + PI-stained *E. coli* O157:H7 cells suspended in Tris-BSA was similar to that of SYTO 9 + PI-stained cells on potassium citrate in **experiment 1**, and therefore, a gate for injured cells could be set. However, green fluorescence resolution was not possible at any of the tested PI concen-

trations when cells were stained in high ionic strength TBS-BSA, which was initially considered a good option. This effect was further studied and attributed to the low SYBR Green I permeability of cells with intact membranes, which indeed showed lower fluorescence intensity than dead cells. SYBR Green I uptake was increased in the presence of Tris, since this compound acts as an outer membrane permeability-increasing agent when used at high concentrations (Vaara, 1992), and therefore improved green fluorescence resolution. However, a high NaCl concentration in TBS-BSA would interfere with the permeabilizing effect of Tris and result in lower SYBR Green I uptake. Similarly, in **experiment 1**, healthy populations of stress-exposed Gram-negative pathogens (*E. coli* O157:H7 and *S.* Enteritidis) showed increased green fluorescence compared with their counterparts in control samples. This corroborates the role of the outer membrane in the staining efficiency of membrane-permeant nucleic acid dyes, which is in agreement with previous reports by Berney *et al.* (2007, 2008). In **experiment 4**, the suitability of the selected PI concentration was further confirmed, since variations in the proportion of healthy and dead cells did not affect the accuracy of the results.

Nucleic acid-bound dye molecules are in equilibrium with unbound dye molecules in solution (Givan, 2001; Brotherick, 2006). Therefore, a change in cell concentration also changes fluorescence intensity of these cells. In **experiment 1**, **2**, and **3**, staining was optimized for samples with high cell concentrations (*ca.* 7.5 log CFU/mL), but an implicit goal in **experiment 4** was to accurately analyze lower cell concentrations in food. Thus, in **experiment 3**, the selected staining conditions, i.e. staining medium, and SYBR Green I, PI and Ab-RPE concentrations, were evaluated in samples containing down to 5 log CFU/mL. Cell concentration decrease worsened population resolution according to their red fluorescence, which was attributed to the unsuccessful compensation of SYBR Green I and/or Ab-RPE fluorescence. However, SYBR Green I concentration could not be reduced, since this led to a decrease in sensitivity

due to insufficient fluorescence intensity, especially in healthy cells. Conversely, reduction of Ab-RPE concentration (from 1.000 µg/mL to 0.015 µg/mL) successfully improved population resolution without an impact on sensitivity, even in salad samples (**experiment 4**).

In **experiment 1** and **2**, several combinations of PI with green-fluorescent cyanine dyes were compared to select at least one giving the best resolution of cells from background signals and of populations with different membrane integrity states. SYTO 9 + PI, SYTO 24 + PI, and SYTO BC + PI were tested in stress-exposed bacterial suspensions (**experiment 1**), whereas SYBR Green I + PI was compared with SYTO 9 + PI and SYTO BC + PI for optimization of protocols for food analysis (**experiment 2**) since that combination was expected to offer better discrimination of cells from food particles due to the high nucleic acid affinity of SYBR Green I. In general, differences among dye combinations were minimal, probably because they belong to a common chemical family (Haugland, 2010). From results of **experiment 1**, SYTO 24 + PI was ruled out for further evaluation, considering that injured cell counts tended to be higher than with SYTO 9 + PI and SYTO BC + PI. This result may have arisen from an artifact since these cells showed atypically high red fluorescence. In the case of results from salad samples, cell counts obtained by using SYBR Green I + PI, SYTO 9 + PI and SYTO BC + PI were not significantly different, but SYTO 9 + PI was also ruled out since discrimination of dead and injured cells from background particles was slightly worse.

2.2. Reduction of interferences in flow cytometry analysis

Two different approaches were evaluated with the purpose of decreasing interference caused by background signals in the detection of bacterial cells in salad samples and therefore improve the LOD of the assay: firstly, the presence of food particles was reduced using a range of sample pre-treatments based on filtration and centrifugation (**experiment 2**), and secondly, acquisition of data

arising from background signals was also reduced by applying several combinations of threshold levels to SSC, which the flow cytometer used in this thesis measures with higher sensitivity than FSC, and yellow-orange fluorescence, which was associated with the specific detection of Ab-RPE-labeled *E. coli* O157:H7 cells (**experiment 4**)*.

Experiment 2 compared eight salad sample pre-treatments based on coarse filtration of homogenates (50-μm and 63-μm filter blender bags) and a dilution/wash step (centrifugal filtration through a 5-μm filter, conventional centrifugation, conventional centrifugation and second dilution, second dilution) prior to fluorescent staining. After coarse filtration, *ca.* 8 log background particles/mL were released. Interestingly, the sample pre-treatment consisting of coarse filtration in a 63-μm filter blender bag and centrifugal filtration through a 5-μm filter was superior to simple sample washing and/or dilution, since it effectively reduced both the concentration (*ca.* 7 log event/mL) and percentage (*ca.* 50% from total events) of background particles. Although recovery of *E. coli* O157:H7 cells from salad samples was also reduced after centrifugal filtration, probably as a result of filter clogging and cell adsorption to the filter and retained food particles (Payne and Kroll, 1991; Jaykus, 2003), only a *ca.* 0.2 log CFU/g difference was found compared with plate counts. Cell loss equally affected healthy, injured and dead cells, but injured and, especially, dead cell counts were additionally influenced by the presence of background particles due to their similar fluorescence intensities. Globally, sample pre-treatment based on centrifugal filtration proved suitable for the flow cytometry detection of *E. coli* O157:H7 in a complex food matrix and the assessment of its membrane integrity, and was therefore used in **experiment 4**. When using the blender bag containing a 50-μm nonwoven filter for coarse filtration, worse results were obtained in terms of background particle concentration and relative frequency, as well as cell recovery. A possible explanation for increased background particle count might be the migration of filter parti-

cles to the filtrate, which can occur with nonwoven filter media (Purchas and Sutherland, 2001; Sutherland, 2008). This highlights the importance of carefully selecting filter materials and formats for the preparation of flow cytometry samples.

In **experiment 4**, several signal filtering strategies were applied during analysis of control suspensions and salad samples and subsequently compared based on their ability to improve the data acquisition speed, which results in narrow fluorescence distributions, as well as the signal-to-noise ratio (S:N), which in turn improves the LOD and limit of quantification (LOQ) of the assay. The selected signal filtering strategy for control suspensions, a 150 threshold value for SSC, gave a 3-log CFU/mL LOD, which is in accordance with previous results reported by McClelland and Pinder (1994) for FITC-antibody labeled *S.* Typhimurium in pure culture. In other work, a 2-log CFU/mL LOD was reported for immunolabeled *E. coli* O157:H7 (Yamaguchi *et al.*, 2003) and *S.* Typhimurium (Clarke and Pinder, 1998). No statements about the calculations applied to establish this parameter were included in these studies. In the case of salad samples, a 200 threshold value for SSC and yellow-orange fluorescence was selected, since it gave the lowest acquisition rate and a S:N value similar to strategies including a 150 threshold for SSC. Salad samples incorporated interfering particles and therefore the LOD and the LOQ increased to 5 log CFU/g and 6 log CFU/g, respectively. This LOD coincided with that reported by Tortorello *et al.* (1997) for *E. coli* O157:H7 in ground beef, whereas a 4-log CFU/g LOD was reported by Seo *et al.* (1998) and Yamaguchi *et al.* (2003) for the same pathogen in the same food matrix. In this thesis, use of 1.000 µg/mL Ab-RPE increased the LOD of the assay to 7 log CFU/g due to high non-specific binding. In short, sample pre-treatment based on centrifugal filtration, interfering signal filtering and optimized staining (0.015 µg/mL Ab-RPE, 1:10^6 SYBR Green I, and 10 µM PI) allowed specific detection and quantification of 6 log CFU/g *E. coli* O157:H7 in salad samples for the monitoring of its membrane integrity

state during refrigerated storage. Again, it was observed that dead and injured cells were more prone to be miscounted than healthy cells since contribution of background particles to their gates was higher.

3. Performance of optimized protocols

3.1. Detection of injured cells after stress exposure

Upon application of optimized flow cytometry protocols, injured cells were detected both in bacterial suspensions exposed to a range of food-related stresses (freezing, refrigeration, heat, potassium sorbate + refrigeration, vinegar + refrigeration, and citric acid + refrigeration) (**experiment 1**) and in refrigerated pasta salad containing a vinaigrette dressing (**experiment 2** and **4**). Thus, the observed membrane injury was conceivably caused by exposure to these stresses, whose primary target is the cell membrane (Abee and Wouters, 1999; Cotter and Hill, 2003; Sutherland, 2005; Davidson *et al.*, 2013).

In **experiment 4**, *E. coli* O157:H7 membrane integrity was monitored during 14-day refrigerated storage of inoculated salads. Throughout this period, the percentage of injured cells decreased and that of healthy cells increased, whereas dead cell percentage remained constant. These results show that cells with partially damaged membranes were reversibly damaged and therefore this pathogen was capable of repairing its membrane during exposure to refrigeration and acid in pasta salad. This highlights the importance of implementing control measures to limit the presence of *E. coli* O157:H7 in RTE meals.

3.2. Comparison of flow cytometry and plating data

Plating is the standard technique to validate flow cytometry assays, although, as previously mentioned, physiological parameters measured by these techniques are different (Nebe-von-Caron *et al.*, 2000; Raybourne and Tortorello, 2003). Comparison between methods was done for bacteria exposed to stresses

(**experiment 1**, **2** and **4**), whereas untreated cells were used to evaluate the accuracy of flow cytometry counts by linear regression analysis (**experiment 4**).

When comparing flow cytometry total counts (i.e. the result of adding up healthy, injured and dead counts) with the count on nonselective medium before stress exposure, two relationships were found. As previously stated, in **experiment 2**, flow cytometry total counts were lower than plate counts for salad samples pretreated by centrifugal filtration, which was probably the cause of this reduced cell recovery. When pre-treatments other than centrifugal filtration were applied to salad samples, flow cytometry total counts higher than plate counts were observed. This finding suggests that the sample contained cells with intact membranes which were unable to grow on solid medium, the so-called VBNC cells, and is consistent with the idea of culturable cells being a subpopulation of cells with intact membranes (Nebe-von-Caron *et al.*, 1998; Joux and Lebaron, 2000; Davey *et al.*, 2004; Berney *et al.*, 2006). Injury may also be a cause for the VBNC state (Mackey, 2000), and injured cells were indeed detected by flow cytometry in the inocula for salad samples, although in a low percentage (3.39±2.02%). Dead cells present in the inocula (1.24±0.50%) and sterilized salad samples may have also contributed to flow cytometry total counts being higher than plate counts. An additional explanation for this fact may be the presence of high percentages of background particles and background fluorescence, which may lead to mistakenly scoring background particles as cells (Comas-Riu and Rius, 2009).

In **experiment 2** and **4**, healthy, injured and dead cell populations were expressed as percentages to correct for the discrepancy between flow cytometry total counts and plate counts. Concordance between percentages of dead cells is consistent with the idea that an intact cell membrane is a requisite for reproductive growth (Mackey, 2000), and implies that, in this thesis, PI was a

good indicator of cell death. As a result, concordance was also observed between percentages of viable cells obtained by flow cytometry (i.e. the result of adding up the percentages of healthy and injured cells) and plating (i.e. the percentage of cells grown on nonselective medium after stress exposure). Conversely, the monitoring of membrane integrity and culturability of *E. coli* O157:H7 during refrigerated storage of salad samples revealed that, for the percentages of healthy and injured cells, the relationship between flow cytometry and plating methods was not constant but varied with time. This corroborated that each method reports on injury of a different nature. In the case of the differential plating method, the proportions of healthy and injured cells are additionally affected by the choice of selective media. Thus, in **experiment 4**, it was observed that flow cytometry in combination with membrane integrity indicators was more sensitive for injury detection than the differential plating method including SMAC as the selective medium.

In **experiment 4**, optimized flow cytometry protocols for control suspensions and salad samples were validated against plating for *E. coli* O157:H7 enumeration. Based on the LOQ, linear regression of plate and flow cytometry counts was analyzed in the range of 4 to 7 log CFU/mL and 5 to 7 log CFU/g for control and salad samples, respectively. Strong positive correlation (r = 0.9973), good fit of the linear model (r^2 = 0.9945) and accuracy (y-intercept, P = 0.3550) were found for control samples. Only a minimal decrease in these parameters was observed for salad samples when using 0.015 μg/mL Ab-RPE (r = 0.9935; r^2 = 0.9870; y-intercept, P = 0.2156). However, use of 1.000 μg/mL Ab-RPE led to a pronounced decrease in these parameters (r = 0.8961; r^2 = 0.8030; y-intercept, P = 0.0500). This may be caused by an increased number of false positive counts, due to similarity in yellow-orange fluorescence emission between immunolabeled bacteria and food particles (Comas-Riu and Rius, 2009).

4. References

Abee, T., and J.A. Wouters. 1999. Microbial stress response in minimal processing. *International Journal of Food Microbiology*. 50:65–91.

Barbesti, S., S. Citterio, M. Labra, M.D. Baroni, M.G. Neri, and S. Sgorbati. 2000. Two and three-color fluorescence flow cytometric analysis of immunoidentified viable bacteria. *Cytometry Part A*. 40:214–218.

Ben-Amor, K., H. Heilig, H. Smidt, E.E. Vaughan, T. Abee, and W.M. de Vos. 2005. Genetic diversity of viable, injured, and dead fecal bacteria assessed by fluorescence-activated cell sorting and 16S rRNA gene analysis. *Applied and Environmental Microbiology*. 71:4679–4689.

Berney, M., H.-U. Weilenmann, and T. Egli. 2006. Flow-cytometric study of vital cellular functions in *Escherichia coli* during solar disinfection (SODIS). *Microbiology*. 152:1719–1729.

Berney, M., F. Hammes, F. Bosshard, H.-U. Weilenmann, and T. Egli. 2007. Assessment and interpretation of bacterial viability by using the LIVE/DEAD BacLight kit in combination with flow cytometry. *Applied and Environmental Microbiology*. 73:3283–3290.

Berney, M., M. Vital, I. Hülshoff, H.-U. Weilenmann, T. Egli, and F. Hammes. 2008. Rapid, cultivation-independent assessment of microbial viability in drinking water. *Water Research*. 42:4010–4018.

Brotherick, I. 2006. Basic DNA measurement by flow cytometry. *In* Guide to flow cytometry. S. Wulff, editor. Dako, Carpinteria, CA. 99–106.

Bunthof, C.J., S. van Schalkwijk, W. Meijer, T. Abee, and J. Hugenholtz. 2001. Fluorescent method for monitoring cheese starter permeabilization and lysis. *Applied and Environmental Microbiology*. 67:4264–4271.

Clarke, R.G., and A.C. Pinder. 1998. Improved detection of bacteria by flow cytometry using a combination of antibody and viability markers. *Journal of Applied Microbiology*. 84:577–584.

Comas-Riu, J., and N. Rius. 2009. Flow cytometry applications in the food industry. *Journal of Industrial Microbiology & Biotechnology*. 36:999–1011.

Cotter, P.D., and C. Hill. 2003. Surviving the acid test: responses of Gram-positive bacteria to low pH. *Microbiology and Molecular Biology Reviews*. 67:429–453.

Davey, H.M., D.B. Kell, D.H. Weichart, and A.S. Kaprelyants. 2004. Estimation of microbial viability using flow cytometry. *Current Protocols in Cytometry*. 29:11.3.1–11.3.21.

Davidson, M.P., T.M. Taylor, and S.E. Schmidt. 2013. Chemical preservatives and natural antimicrobial compounds. *In* Food microbiology: fundamentals and frontiers. M.P. Doyle and R.L. Buchanan, editors. ASM Press, Washington, DC. 765–781.

Givan, A.L. 2001. Cells from within: DNA in life and death. *In* Flow cytometry. First principles. Wiley-Liss, New York, NY. 123–158.

Haugland, R.P. 2010. Nucleic acid detection and genomics technology. *In* The Molecular Probes handbook. A guide to fluorescent probes and labelling technologies. M.T.Z. Spence, editor. Invitrogen, Carlsbad, CA. 302–360.

Jaykus, L.-A. 2003. Challenges to developing real-time methods to detect pathogens in foods. *ASM News*. 69:341–347.

Joux, F., and P. Lebaron. 2000. Use of fluorescent probes to assess physiological functions of bacteria at single-cell level. *Microbes and Infection*. 2:1523–1535.

Mackey, B.M. 2000. Injured bacteria. *In* Microbiological safety and quality of food. B.M. Lund, T. Baird-Parker, and G.W. Gould, editors. Springer-Verlag, Gaithersburg, MD. 315–341.

Manini, E., and R. Danovaro. 2006. Synoptic determination of living/dead and active/dormant bacterial fractions in marine sediments. *FEMS Microbiology Ecology*. 55:416–423.

McClelland, R.G., and A.C. Pinder. 1994. Detection of *Salmonella typhimurium* in dairy products with flow cytometry and monoclonal antibodies. *Applied and Environmental Microbiology*. 60:4255–4262.

Nebe-von-Caron, G., P.J. Stephens, and R.A. Badley. 1998. Assessment of bacterial viability status by flow cytometry and single cell sorting. *Journal of Applied Microbiology*. 84:988–998.

Nebe-von-Caron, G., P.J. Stephens, C.J. Hewitt, J.R. Powell, and R.A. Badley. 2000. Analysis of bacterial function by multi-colour fluorescence flow cytometry and single cell sorting. *Journal of Microbiological Methods*. 42:97–114.

Payne, M.J., and R.G. Kroll. 1991. Methods for the separation and concentration of bacteria from foods. *Trends in Food Science & Technology*. 2:315–319.

Purchas, D.B., and K. Sutherland. 2001. An introduction to filter media. *In* Handbook of filter media. D.B. Purchas and K. Sutherland, editors. Elsevier, Oxford. 1–34.

Raybourne, R.B., and M.L. Tortorello. 2003. Microscopy techniques: DEFT and flow cytometry. *In* Detecting pathogens in food. T. McMeekin, editor. Woodhead Publishing, Cambridge. 186–216.

Saegeman, V.S., R. De Vos, N.D. Tebaldi, J.M. van der Wolf, J.H. Bergervoet, J. Verhaegen, D. Lismont, B. Verduyckt, and N.L. Ectors. 2007. Flow cytometric viability assessment and transmission electron microscopic morphological study of bacteria in glycerol. *Microscopy and Microanalysis*. 13:18–29.

Seo, K.H., R.E. Brackett, J.F. Frank, and S. Hilliard. 1998. Immunomagnetic separation and flow cytometry for rapid detection of *Escherichia coli* O157:H7. *Journal of Food Protection*. 61:812–816.

Sträuber, H., and S. Müller. 2010. Viability states of bacteria. Specific mechanisms of selected probes. *Cytometry Part A*. 77:623–634.

Sutherland, J.P. 2005. Pathogen resistance and adaptation to low temperature. *In* Understanding pathogen behaviour: virulence, stress response and

resistance. M. Griffiths, editor. Woodhead Publishing, Cambridge. 507–523.

Sutherland, K. 2008. Filter media. *In* Filters and filtration handbook. K. Sutherland, editor. Elsevier, Oxford. 41–95.

Tamburini, S., P. Foladori, G. Ferrentino, S. Spilimbergo, and O. Jousson. 2014. Accurate flow cytometric monitoring of *Escherichia coli* subpopulations on solid food treated with high pressure carbon dioxide. *Journal of Applied Microbiology*. 117:440–450.

Tortorello, M.L., D.S. Stewart, and R.B. Raybourne. 1997. Quantitative analysis and isolation of *Escherichia coli* O157:H7 in a food matrix using flow cytometry and cell sorting. *FEMS Immunology and Medical Microbiology*. 19:267–274.

Vaara, M. 1992. Agents that increase the permeability of the outer membrane. *Microbiological Reviews*. 56:395–411.

Yamaguchi, N., M. Sasada, M. Yamanaka, and M. Nasu. 2003. Rapid detection of respiring *Escherichia coli* O157:H7 in apple juice, milk, and ground beef by flow cytometry. *Cytometry Part A*. 54:27–35.

Chapter 8. Conclusions

1. Detection of injured cells using membrane integrity assays is possible when the green-fluorescent nucleic acid dye concentration is adjusted to reduce fluorescence intensity and allow optimum fluorescence spillover compensation, and a saturating propidium iodide concentration is selected, which optimally decreases green fluorescence in dead cells without significantly increasing red background fluorescence in healthy cells.

2. Use of Tris buffer in membrane integrity assays improves SYBR Green I uptake by destabilizing the outer membrane.

3. Use of SYTO 24 in combination with propidium iodide is not suitable to assess membrane integrity, since injured cells are overestimated. Conversely, SYTO 9, SYTO BC and SYBR Green I are more suitable alternatives, since they give cell fluorescence patterns compatible with injured cell detection.

4. Sample pre-treatment based on centrifugal filtration, in contrast to conventional centrifugation and/or dilution, proved suitable for the flow cytometry detection of *Escherichia coli* O157:H7 and the assessment of its membrane integrity in ready-to-eat pasta salad. Moreover, filter materials and formats of blender bags need to be carefully selected since some may introduce further interference.

5. Centrifugal filtration, interfering signal filtering and optimized staining (0.015 µg/mL R-phycoerythrin-labeled antibody, $1:10^6$ SYBR Green I, and 10 µM propidium iodide) allowed specific detection and quantification of 6 log CFU/g *Escherichia coli* O157:H7 in salad samples for the monitoring of its membrane integrity state during refrigerated storage.

6. Injured *Escherichia coli* O157:H7 cells undergo a progressive membrane repair during storage under refrigeration and acid conditions, and survive in pasta salad. This highlights the importance of the implementation of control measures to limit the presence of this pathogen in ready-to-eat meals.

7. Plating is a suitable technique to validate the accuracy of flow cytometry counts when analyzing untreated cells. However, discrepancies may appear with stress-exposed cells, since these techniques report on different physiological attributes.